A model of complex plaque formation:7,8-Dihydroneopterin protects human monocyte-derived macrophages from oxidised low density lipoprotein-induced death

---

A thesis

submitted in partial fulfilment

of the requirements for the Degree

of

Doctor of Philosophy

in Biochemistry

at the

University of Canterbury

New Zealand

Zunika Amit

2008

Table of Contents

List of Figures

List of Tables

Abbreviations

6-PTPS	6-Pyruvol tetrahydropterin synthase
7β-OH	7 β-Hydroxycholesterol
7-KC	7-Ketocholesterol
7,8-NP	7,8-Dihydroneopterin
7-KCacLDL	7-KC acetylated LDL
7-OH	7-Hydroxycholesterol
7-OOH	7-Hydroperoxycholesterol
13-HPODE	13-Hydroperoxy linoleate
25-OHC	25-Hydroxycholesterol
$\Delta\psi_m$	Mitochondrial membrane potential
AAPH	2,2'-Azobis (2-amidino propane) dihydrochloride
ABC	ATP binding cassette
ABC1	ATP binding cassette transporter-1
ACAT	Acyl coenzyme A:cholesterol acyltransferase
acLDL	Acetylated LDL
AIF	Apoptosis inducing factor
anti-hsp65	Anti-heat shock protein 65
ANOVA	Analysis of variance
AP-1	Activator protein-1
Apaf-1	Apoptotic activating factor-1
AP-1 CAT	Activation protein-1 chloramphenicol acetyltransferase
APCs	Antigen presenting cells
apoB100	Apolipoprotein B100
ATP	Adenosine triphosphate
BCA	Bicinchoninic acid
BH_4	5,6,7,8-tetrahydrobiopterin
BHT	Butylated hydroxytoluene
BSA	Bovine serum albumin
BSO	DL-Buthionine-[S,R]-Sulfoximine
BSTFA	N,O-bis(Trimethylsilyl)trifluoroacetamide
cAMP	Cyclic adenine monophosphate
CARD	Caspase recruitment domain

CCR2	Monocyte chemotactic protein receptor
Cp	Ceruloplasmin
$cPLA_2$	Cytosolic phospholipase A_2
CRP	C-reactive protein
$CuCl_2$	Copper chloride
DAPI	4’6-Diamidino-2-phenylindole
DC	Dendritic cells
DED	Death-effector domain
DEM	Diethyl maleate
DEVD	Asp-Glu-Val-Asp
DHAA	Dehydroascorbic acid
DHE	Dihydroethidium
DIC	Differential interference contrast
DiI	1,1'-Dioctadecyl-3,3,3',3'-tetramethylindocarbocyanine perchlorate
DMSO	Dimethyl sulphoxide
DNA	Deoxyribonucleic acid
DTT	1,4-Dithiothreitol
EDTA	Ethylenediaminetetraacetic acid
EGTA	Ethlylene glycol-bis(2-aminoethylether)-N,N,N’,N’-tetracetic acid
ELISA	Enzyme-linked immunosorbant assay
EPR	Electron paramagnetic resonance
ETYA	5,8,11,14-Eicosatetraynoic acid
FADD	Fas-associated death domain
Fas	Fibroblast associated cell surface
FCS	Foetal calf serum
FLIP	FLICE-inhibitory protein
FITC	Fluorescein isothiocyanate
GAPDH	Glyceraldehydes-3-phosphate dehydrogenase
GC	Gas chromatography
GCS	γ-Glutamylcysteine synthethase
GH	Growth hormone
GM-CSF	Granulocyte-macrophage colony stimulating factor
GSH	Glutathione
GTP	Guanosine triphosphate
GTP-CH	GTP cyclohydrolase 1

HASMC	Human aortic smooth muscle cells
HBSS	Hanks' balanced salt solution
HCAECs	Human coronary artery endothelial cells
HCl	Hydrochloric acid
HDL	High density lipoprotein
HEK293	Human epithelial kidney cell line
Hep-2	Human larynx carcinoma epithelial
HIHS	Heat-Inactivated Human Serum
HIV	Human immunodeficiency virus
HMDMs	Human monocyte derived macrophages
HNE	4-Hydroxynonenal
HOCl	Hypochlorite
HPLC	High performance liquid chromatography
IAP	Inhibitors of apoptosis
ICPMS	Inductively coupled plasma mass spectroscopy
IFN-γ	Interferon-γ
IL-1β	Interleukin-1 β
IL-4	Interleukin-4
iNOS	Inducible nitric oxide synthase
JNKs	c-Jun NH2-terminal kinases
LPDS	Lipoprotein Deficient Serum
LPL	Lipoprotein lipase
LOs	Lipoxygenase
LOX-1	Lectin-like oxidised LDL receptor
LPS	Lipopolysaccharide
LysoPtdCho	Lysophosphatidylcholine
LXRα	Liver x receptor α
MAPKS	Mitogen-activated protein kinases
MARCO	Macrophage receptor with collagenous structure
MBB	Monobromobimane
M-CSF	Macrophage colony stimulating factor
MCP-1	Monocyte chemotactic protein
MDA	Malondialdehyde
MFI	Mean fluorescence intensity
MGC	Multinucleated giant cells

MHC	Major histocompatibility complex
mmLDL	Minimally modified LDL
MMP-1	Matrix metalloproteinase-1
MMP-9	Matrix metalloproteinase-9
MnSOD	Manganese superoxide dismutase
MOPS	4-Morpholine-propanesulfonic acid
MPO	Myeloperoxidase
MPT	Mitochondrial permeability transition
mPTP	Mitochondrial permeability transition pore
MTT	3-[4,5-Dimethylthiazol-2-yl]-2,5-diphenyl-tetrazolium bromide
NAC	N-acetylcysteine
$NaHCO_3$	Sodium hydrogen carbonate
NF-κβ	Nuclear factor-κβ
nLDL	Native LDL
NH_2TP	7,8-Dihydroneopterin triphosphate
$^{\bullet}NO$	Nitrogen monoxide
NO_2^-	Nitrite
$O_2^{\bullet-}$	Superoxide anion
oxLDL	Oxidised LDL
ORO	Oil red-O
PBS	Phosphate Buffered Saline
PDGF	Platelet-derived growth factor
PDTC	Pyrrolidine dithiocarbamate
PECAM	Platelet endothelial cell adhesion molecule-1
PI	Propidium iodide
PKC	Protein kinase C
PMA	Phorbol 12-myristate 13-acetate
PPARγ	Peroxisome proliferator-activated receptor-γ
PS	Phosphatidylserine
PUFA	Polyunsaturated fatty acids
REM	Relative electrophoretic mobility
RNS	Reactive nitrogen species
ROS	Reactive oxygen species
RO-H_2O	Reverse osmosis- water
RPMI	Roswell Park Memorial Institute 1640

SAPK	Stress-activated protein kinase
SD	Standard deviation of the mean
SDS	Sodium dodecyl sulphate
SFM	Serum-free media
SMCs	Smooth muscle cells
SOD	Superoxide dismutase
SRs	Scavenger receptors
SRA	Scavenger receptors class A
SR-B	Scavenger receptors class B
SR-D	Scavenger receptors class D
SR-E	Scavenger receptors class E
SR-G	Scavenger receptors class G
SR-PSOX	Scavenger receptor that binds PS and oxLDL
TBA	2-Thiobarbituric acid
TBARS	Thiobarbituric acid reactive substances
tBid	Truncated form of Bid
TCA	Trichloroacetic acid
TFA	Trifluoroacetic acid
TIMP-1	Tissue inhibitor of metalloproteinase-1
TMP	1,1,3,3-Tetramethoxypropane
TMS	Trimethylsilyl
TNF- α	Tumor necrosis factor-α
TNFR	Tumor necrosis factor receptor
TRADD	TNF receptor-associated death domain
TRAIL	TNF-related apoptosis-inducing ligand
TRAP	Tartrate-resistant acid phosphatase
VLA-4	Very late antigen 4
VSMCs	Vascular smooth muscle cells

Abstract

Plasma neopterin is an excellent marker of inflammation and is found in elevated levels in plasma of patients with cardiovascular disease. Neopterin originates as the oxidation product of 7,8-dihydroneopterin (7,8-NP), which is secreted by human macrophages when stimulated with interferon-γ during inflammation. 7,8-NP has been shown to be a very efficient free radical scavenger and a potent antioxidant which can protect macrophages from a range of oxidative stresses. The uptake of oxidised low density lipoprotein (oxLDL) by macrophages which lead to the formation of foam cells is a hallmark of early atherosclerotic lesions. OxLDL-induced cell death is also considered to be an important process in the formation of necrotic lipid rich plaques and in atherosclerotic plaque destabilisation. This thesis examined the extent of oxLDL-induced damaged to HMDMs and whether 7,8-NP can inhibit oxLDL-mediated cell death in HMDMs.

Foam cells had previously been defined as cholesteryl ester (CE) macrophages that stained positive with oil red-O. This thesis shows that the foamy appearance and presence of lipid droplets stained with oil red-O was not dependent on accumulation of CE which raises the suitability of using oil-red-O staining to identify the foam cells. In addition, HPLC but not GC analysis showed an increased in CE levels of the macrophages when the macrophages were incubated with oxLDL. The HPLC approach spared the samples of lengthy manipulations that might cause ex vivo oxidation. It also avoided subjecting the samples to high temperature treatment that could alter the lipid composition and therefore quantification of the lipid contents.

Previous studies showed that 7,8-NP is a potent antioxidant and cytoprotective agent. Exposure of HMDMs to 1 mg/ml oxLDL caused 50% loss of cell viability as measured by the MTT reduction and trypan blue exclusion assays. The development of apoptotic features including caspase-3 activity, cytochrome *c* release from mitochondria and phophatidyserine (PS) exposure was examined. OxLDL did not cause caspase-3 activation as shown by Western Blot analysis and did not cause DEVD-AMC cleavage in HMDMs. However, cytochrome *c* release and phosphatidylserine exposure were observed when HMDMs were incubated with oxLDL as shown by Western Blot analysis and Annexin V-FITC staining respectively.

Dihydroethidium (DHE) staining showed that oxLDL treatment caused mitochondrial superoxide generation in HMDMs. OxLDL-induced oxidative stress appeared to cause a rapid loss of HMDMs' intracellular glutathione (GSH) as analysed by HPLC technique. Incubation of HMDMs' with buthionine sulfoximine (BSO) and diethyl

maleate (DEM) caused similar loss in GSH as incubation with oxLDL but did not result in HMDMs' death. This showed that oxLDL-induced decrease in GSH alone was not sufficient to cause cell death.

The loss of cell viability by oxLDL was inhibited by 7,8-NP in the concentration range of 50 to 200 μM. HMDMs' GSH loss caused by oxLDL was similarly inhibited by 7,8-NP supporting the idea that preventing the cellular GSH loss will protect the HMDMs from death. Incubation of HMDMs with 7,8-NP showed reduction in DHE fluorescence intensity staining suggesting that 7,8-NP inhibited or scavenged oxLDL-dependent generation of superoxide. 7,8-NP also effectively inhibited oxLDL-induced PS externalisation to the outer membrane but failed to inhibit the oxLDL-induced release of cytochrome *c* from mitochondria to the cytosol. The labelling of oxLDL with DiI showed that 7,8-NP significantly inhibited the uptake of oxLDL. However, the inhibitory effect was only measured at non-toxic concentration of oxLDL. The ability of 7,8-NP to inhibit oxLDL uptake raised the possibility that 7,8-NP protective effect against oxLDL involved modulation of the scavenger receptors' expression in particular SRA and CD36. The Western Blot analysis showed that incubation of HMDMs with 7,8-NP did not affect HMDMs' SRA protein expression. In 50% of the experiments, it was demonstrated that certain isoforms of CD36 protein were significantly down regulated by 7,8-NP suggesting that various factors might interact with 7,8-NP or CD36.

The ability of 7,8-NP to protect HMDMs from oxLDL-induced death provides further evidence that this antioxidant is secreted by HMDMs to protect them against the oxidative damage in the highly oxidative environment of atherosclerotic plaque.

1 Introduction

1.1 Overview

Atherosclerosis is a chronic inflammatory disease affecting the arterial blood vessels. It has been well demonstrated that low density lipoproteins (LDL) are involved in the pathogenesis of atherosclerosis. LDL is thought to become atherogenic after undergoing oxidative (and possibly other) modifications. The oxidized LDL (oxLDL) is taken up by macrophages in unregulated manners which cause their transformation into foam cells (Libby *et al*., 2002).

Macrophages appear to survive in the inflammatory environment suggesting they are able to neutralise the reactive oxygen species and other damaging biomolecules that they are exposed to. Synthesis of antioxidant, 7,8-dihydroneopterin (7,8-NP) by macrophages themselves, may be part of this protective mechanism. This laboratory and others had shown that 7,8-NP is a potent antioxidant that can protect cells from a range of oxidative stresses (Baier-Bitterlich *et al*., 1995; Baird, 2003; Bratslavska *et al*., 2007; Duggan *et al*., 2002; Gieseg *et al*., 2001; Kojima *et al*., 1993). 7,8-NP had also been detected in the atherosclerotic plaque (Frostegard *et al*., 1999; Geng *et al*., 1995; Shen, 1994) which further supports its involvement in protecting the macrophages and LDL from oxidative damage during the inflammatory response.

The lack of *in vitro* studies using appropriate cell models, have hindered the understanding of the role of the macrophage foam cell in atherosclerosis. This thesis will therefore, examine the possibility of developing macrophage foam cells by exposure of human monocyte-derived macrophages (HMDMs) to sub-toxic level of oxLDL. Since the mechanisms of oxLDL-induced death in macrophages are still controversial, this thesis will also explore the mechanisms of oxLDL-mediated cell death in HMDMs. Finally, this thesis will determine the role of 7,8-NP on oxLDL-induced death in HMDMs.

1.2 Atherosclerosis

Atherosclerosis and its complication such as cardiovascular disease, heart infarction, and stroke are the leading causes of death in the developed countries (Halliwell & Gutteridge, 2007). The predispose risk factors include hyperlipidemia, hypertension, diabetes, smoking and obesity. Other factors such as the individual genetic makeup and infection also play an additional role in atherosclerosis (Scott, 2004; Wu & Wu, 2006). Atherosclerosis is a chronic inflammatory condition (Berliner *et al*., 1995) characterised by

the accumulation of lipids and fibrous elements in the large arteries (Lusis, 2000). Fully developed atherosclerotic plaques contain numerous lipid-laden macrophages, smooth muscle cells, and T cells (Carpenter *et al.*, 1995a). Plaques can cause complication by limiting blood flow to a region of an organ such as the heart or brain.

1.2.1 Development of Atherosclerosis

1.2.1.1 Lesion Initiation

The hypothesis that an injury to the endothelium might precipitate the atherosclerosis process is supported by many observations (Ross, 1993). The arterial lesion normally begins at the dysfunction endothelium, typically in the vicinity of branch points and areas of major curvature. In the tubular regions of arteries, where blood flow is uniform and laminar, the endothelial cells (ECs) are ellipsoid in shape and aligned in the direction of flow, whereas in regions of disturbed flow, this orderly pattern is disrupted. The turbulent blood flow in this areas can cause mechanical damage to the endothelium (Gimbrone, 1999). Besides that, damaged endothelium can also be caused by infection of the vessel wall (e.g. by herpes viruses, cytomegalovirus and *Chlamydia*) and exposure to blood-borne toxins, including both xenobiotics (e.g. from cigarette smoking) and elevated levels of normal metabolites such as glucose, LDL or homocysteine (Halliwell & Gutteridge, 2007).

Manifestation of the endothelial injury increases permeability and trapping of LDL in the artery (Lusis, 2000). The accumulation of LDL would lead to chronic inflammation, a feature commonly associated with atherosclerosis (Pentikainen *et al.*, 2000) since LDL entering the vessel wall undergoes modification (will be discussed in section 1.2.2.2) and produces a number of pro-inflammatory molecules. Once LDL is trapped in the artery, monocyte recruitment from the circulation will follow. This is aided by endothelial expression of various adhesion molecules (Figure 1.1). Entry into the arterial intima initially requires a weak and rolling interactions between L-selectin on the monocytes and endothelial-associated P- and E-selectin (Dong *et al.*, 1998). The firm adhesion of monocytes to endothelial cells is mediated by the monocytic integrin very late antigen (VLA-4), which interacts with endothelial vascular cell adhesion molecule-1 (VCAM-1) on the endothelium and the connecting segment-1 (CS-1) domain of fibronectin (Shih *et al.*, 1999). Firm attachment to endothelial cells is followed by migration of the monocytes into the intima through endothelial tight junctions. Platelet endothelial cell adhesion molecule-1 (PECAM) is responsible in assisting the monocyte-endothelial interactions required for this movement (Scott, 2004). OxLDL is directly chemotactic to monocytes probably because it contains lysophosphatidylcholine (lysoPtdCho), which directly attracts

the monocytes. It indirectly causes migration of monocytes because it induces the production of monocyte chemotactic protein-1 (MCP-1) and such like by endothelial cells (Steinberg *et al*., 1989). Mice deficient in MCP-1 or MCP receptor (CCR2) had significantly reduced atherosclerotic lesions, suggesting a MCP-1/CCR2 interaction is absolutely required for monocyte recruitment in atherosclerosis (Boring *et al*., 1998; Gu *et al*., 1998).

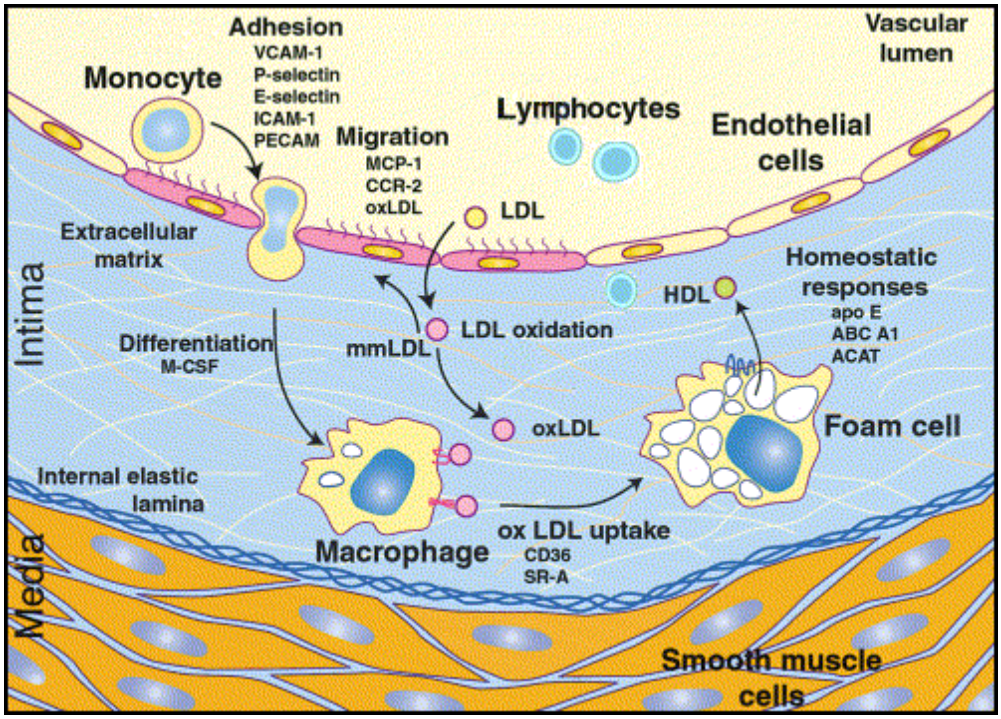

Figure 1.1 Initiating events in the development of a fatty streak lesion.
LDL is trapped in the sub-endothelial space, where it undergoes oxidation. Monocytes attach to endothelial cells and migrate into the intima through tight junctions. This process involves an intimate interaction with the junctional adhesion molecule PECAM and the release of spare membrane from cellular invaginations. Monocytes become activated, and express the scavenger receptors CD36 and SR-A, which promote the uptake of oxLDL. Homeostatic responses facilitate reverse cholesterol transport through HDL. Adapted from Glass and Witzum, (2001).

T-lymphocytes recruitment is also vital to atherosclerosis particularly during early stage of the atherosclerotic development. It has been shown that the $RAG^{-/-}$ mice deficient in this cell type exhibiting retarded lesion development compared to controls (Song *et al*., 2001). T-lymphocytes enter the vessel wall by binding to adhesion molecules such as VCAM-1, being attracted by cytokines. Once there, lymphocytes can respond to antigens (e.g. from bacteria and viruses) to produce antibodies. In the intima, the cytokine macrophage colony stimulating factor (M-CSF) and interferon-γ (IFN-γ) stimulate the proliferation and differentiation of monocytes into macrophages (Glass & Witztum, 2001). Mice deficient in M-CSF has been shown to be relatively resistant to the development of

atherosclerotic lesions (Smith *et al*., 1995) pointing to macrophage critical role in atherosclerosis.

1.2.1.2 Foam Cell Formation

As LDL circulates in blood or after it infiltrates the arterial wall, it is modified via enzymatic or nonenzymatic mechanisms and the nature of modification is generally described as being oxidative in nature. Even though oxidised LDL was not observed in plasma, autoantibodies to oxLDL have been detected in the plasma of patients with coronary artery disease (Salonen *et al*., 1992; Shaw *et al*., 2001). LDL oxidation will be discussed in more detailed in section 1.2.2.2. The rapid unregulated uptake of the oxLDL particles by macrophages is mediated by a group of receptors known as scavenger receptors (will be discussed in section 1.3) that recognize a wide array of ligands. OxLDL can also enter the cell using non-receptor mechanisms. For example aldehydes and oxysterols can partition from the lipid phase of oxLDL into the cell's plasma membrane (Brown *et al*., 1997; Gotoh *et al*., 1993). OxLDL can also be taken up by non-specific receptor-mediated endocytosis, especially in aggregated form (Brown *et al*., 1997).

OxLDL brought into macrophages consists of free cholesterol and cholesterol esters that are hydrolysed in lysosomes. The free cholesterol undergoes esterification catalysed by acyl coenzyme A:cholesterol acyltransferase. (ACAT). The free cholesterol is also stored in the lipid droplets that characterise foam cells. Cholesterol esters within these lipid droplets can in turn be hydrolysed by cholesteryl ester hydrolase (acid lipase) generating free cholesterol and fatty acids, for incorporation into membranes and transport out of the cells.

Mechanism mediating excess cholesterol efflux is critical for maintenance of cholesterol homeostasis in the macrophage since the build up of excess cholesterol is cytotoxic to the cells (Warner *et al*., 1995). Therefore, in the presence of an appropriate extracellular acceptor mainly high density lipoprotein (HDL), excess cholesterol can be exported from the cell via the plasma membrane through a process called reverse cholesterol transport (Jessup & Kritharides, 2000) which is found to be impaired in foam cells (Yancey & St Clair, 1992). However, in the absence of extracellular acceptors, excess free cholesterol in the cytosol undergoes re-esterification to detoxify the excess cholesterol and store it as cholesterol ester in the cytosol. This leads to intracytoplasmic accumulation of cholesterol ester as membrane-free lipid droplets and transforming macrophages into foam cells (van Reyk & Jessup, 1999). The formation of foam cells has been cited as a key process in plaque development (Steinberg *et al*., 1989). The cluster of

foam cells lead to the development of fatty streak. Thereafter, continued cell influx and proliferation leads to more advanced lesions, distinguished by their fibrous character and ultimately to the fibrous plaque.

1.2.1.3 Lesion Progression and Immunologic Response

The immigration of smooth muscle cells (SMCs) from the medial layer of the artery wall into the intima characterised the transition of fatty streaks to the more complex lesion (Figure 1.2). Cytokines and growth factors secreted by macrophages and T cells are important for SMC migration and proliferation. Intimal SMCs may take up oxLDL and develop into foam like appearance as well. SMCs also synthesise extracellular matrix proteins composing primarily of type I collagen and other components for example proteoglycans, elastin, glycoproteins fibrin and other forms of collagen. These components lead to the development of the fibrous cap (Jang *et al*., 1993; Stary *et al*., 1995). Fibrous cap separates the thrombogenic lipid core contents from the blood in the lumen.

The interactions between monocytes/macrophages and T cells greatly influenced this phase of lesion. This result in a broad range of cellular and humoral responses and the acquisition of many features of a chronic inflammatory state. Macrophages, ECs and SMCs are activated based on their expression of MHC class II molecules and numerous inflammatory products, such as TNFα, IL-6 and MCP-1 (Figure 1.2) (Hansson, 2001). Bacterial and viral antigens, heat shock protein and neoepitopes (antigenic epitopes resulting from the formation of adducts between oxidised lipids in oxLDL and apoB or arterial wall components) have been cited as important antigens responsible for immune activation in atherosclerotic lesions (Glass & Witztum, 2001).

The activated lesional T cells express Th1 (inflammatory) and Th2 (helper) T cell. The Th1 cells secrete pro-inflammatory cytokines, interferon-γ (IFNγ), tumour necrosis factor-α (TNF- α) as well as IL-2. The Th2 cell secretes the B cells stimulating factor, interleukin-4 (IL-4), as well as the haematopoiesis-regulating IL-3 and IL-5 and the cytokine-secretion-regulating IL-10 and IL-13 (Frostegard *et al*., 1999). Many proinflammatory genes, including those encoding TNF-α, IL-2, and IL-6, are regulated by the c-Jun NH2-terminal kinases (JNKs, stress-activated protein kinases) pathway (Tedgui & Mallat, 2006). For instance, TNF-α is strongly proinflammatory, increasing oxidative stress via promotion of phagocyte reactive oxygen species (ROS) production. Increase in mitochondrial ROS production due to TNF-α can lead to activation of nuclear genes, in part via JNK. JNK phosphorylates the transcription factor c-Jun and increases activator

protein-1 (AP-1) transcriptional activity which ultimately can trigger cell death (Halliwell & Gutteridge, 2007; Izadi *et al*., 2007).

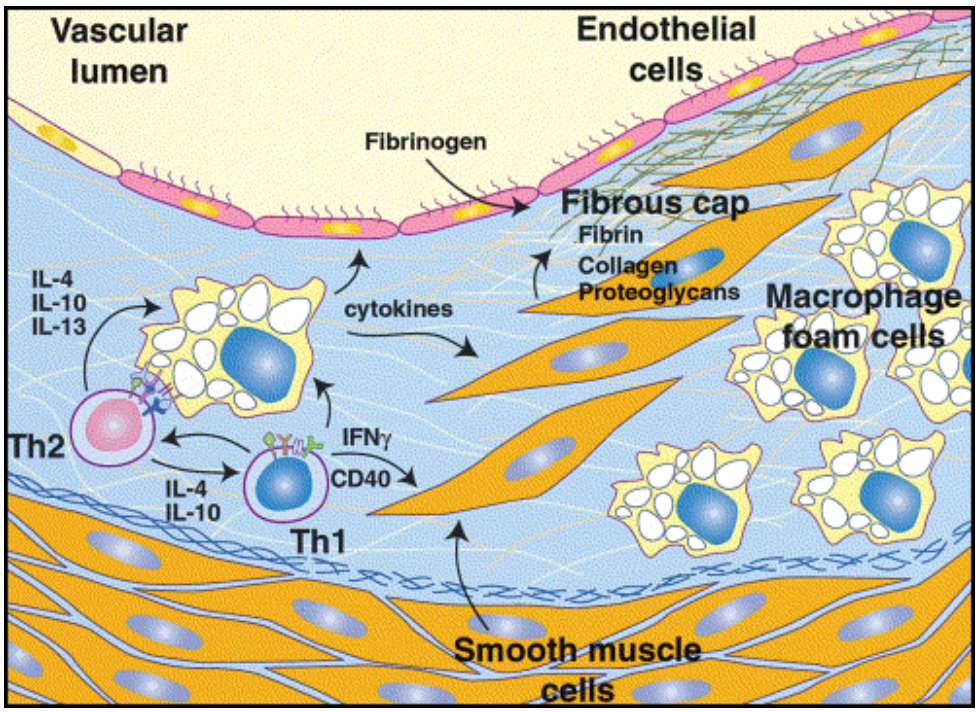

Figure 1.2 Lesion Progression
Macrophages signal the recruitment and activation of T-lymphocytes. Interactions between macrophage foam cells, Th1 and Th2 and also SMCs cells establish a chronic inflammatory process. Adapted from Glass and Witzum, (2001).

Immune responses appear to have complex effects on lesion development by exerting both atherogenic and antiatherogenic. For example, IFN-γ secreted by Th1 has potentially antiatherogenic effects; reduces scavenger receptor expression on macrophages (Geng & Hansson, 1992), inhibits the production of matrix by SMCs (Amento *et al*., 1991), and inhibits SMCs proliferation (Hansson *et al*., 1989b). These effects may inhibit the progression of fatty streaks into fibrofatty plaques (Hansson *et al*., 1989b). On the other hand, the same effects could cause destabilisation of the fibrous cap causing plaque to be prone to rupture. IFN-γ also stimulates macrophages production of proinflammatory cytokines (such as TNF- α and interleukin-1 β (IL-1β)) (Libby & Hansson, 1991) and increases expression of MHC class II molecules (Whitman *et al*., 2000). Thus, the net effect of IFN-γ on atherosclerosis may depend on the balance between its anti- and pro-atherogenic actions in the different stages of lesion development (Hansson *et al*., 1989b). However, Gupta *et al.,* (1997) demonstrated that the net effect of IFN-γ is atherogenic

since the lesions in apoE-deficient mice lacking the IFN-γ were less cellular and had decrease collagen content.

IL-4 secreted by Th2 cells appear to be antagonist of IFN-γ but at the same time a potent inducer of 15-LO, which promotes LDL oxidation whereby, IL-10 has potent deactivating properties in macrophages, interfering with the development and stability of atherosclerotic plaque (Mallat *et al*., 1999; Oslund *et al*., 1999) Interaction of CD40 expressed by T cells, macrophages, ECs and SMCs with its receptor results in the production of inflammatory cytokines, matrix-degrading proteases and adhesion molecules (Mach *et al*., 1998). The balance between pro-inflammatory and anti-inflammatory cytokines may be decisive for the progression of the lesion

1.2.1.4 Plaque Rupture and Thrombosis

A stable plaque normally has a thick fibrous cap (protecting lipid core from contact with the blood), large amount of SMCs and low levels of inflammatory cells (Libby, 1995). Vulnerable plaques generally have abundant foam cells, T lymphocytes, debris cells and increased number of inflammatory cells (Scott, 2004). They also have a large soft lipid core (necrotic core) with thin fibrous caps (Libby, *et al*., 2002). The fibrous caps of ruptured atherosclerotic plaques have more macrophages than those of non-ruptured atherosclerotic plaques which certainly implicated macrophages in plaque rupture (Libby, 2002). Plaque ruptures generally occur at the shoulder region of plaque (Bjorkerud & Bjorkerud, 1996a). It is noteworthy that apoptotic macrophages and SMCs have been identified in the shoulder region and fibrous cap of the plaque (Bjorkerud & Bjorkerud, 1996a; Kolodgie *et al*., 2000). Macrophage foam cells that die and are not phagocytosed can spill lipid into the extracellular environment and so contribute to the lipid core of the plaque, whilst death of SMC erodes the fibrous cap. The release of oxidised and insoluble lipid from necrotic core cells contributes to the formation of 'gruel' characteristics of advanced lesion (Figure 1.3) (Glass & Witztum, 2001). This oxidised lipid will be pro-inflammatory and cytotoxic so promoting further destabilisation of the plaque. Apoptosis of SMCs and macrophages therefore, influence plaque stability and increase the potential for thrombosis (Bjorkerud & Bjorkerud, 1996a; Kolodgie *et al*., 2000).

Activated T cells secrete IFN-γ which in combination with other stimuli induces macrophages to secrete matrix metalloproteinase-1 (MMP-1) (Anderson *et al*., 2002) (Figure 1.3). MMP-1 degrades extracellular matrix proteins, thereby thinning the fibrous cap and making it more susceptible to rupture (Galis *et al*., 1994). The stability of atherosclerotic lesions may also be influenced by calcification and neovascularisation (i.e.

formation of microvessel) (Dickson & Gotlieb, 2003; Stary *et al*., 1995). Intimal calcification is an active process in which pericyte-like cells secrete a matrix scaffold, which subsequently becomes calcified, akin to bone formation. The process is regulated by oxysterols and cytokines. Neovascularisation may provide a conduit for entry of inflammatory cells and it is prevalent in human atherosclerotic lesions (Falk, 2006). These vessels are also prone to rupture. These intra-plaque haemorrhages are often absorbed into the existing plaque.

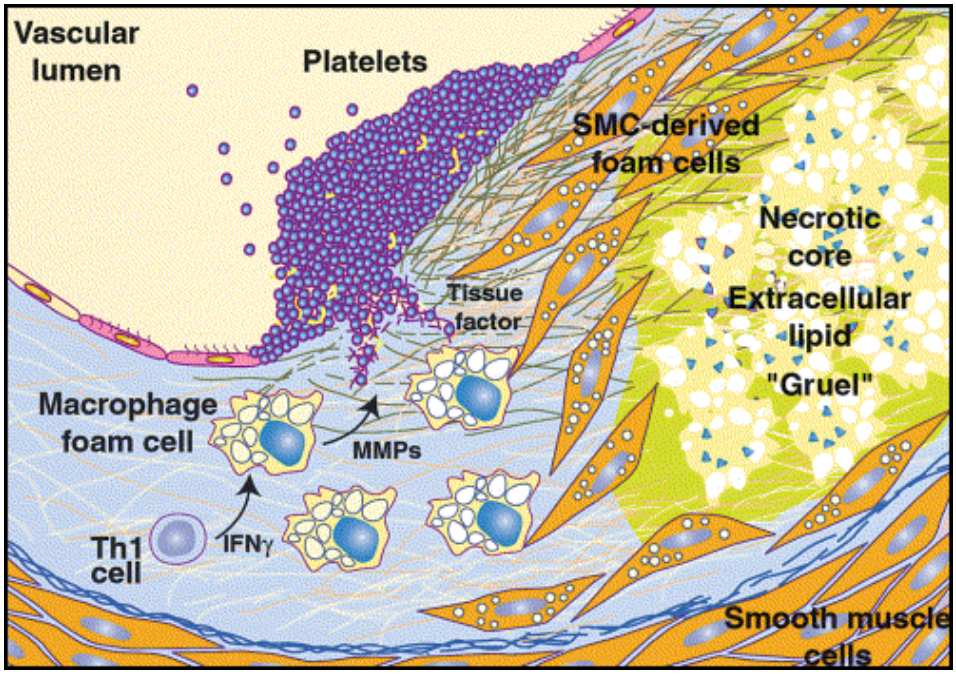

Figure 1.3 Plaque rupture and thrombosis
Necrosis of macrophage and SMCs–derived foam cells leads to the formation of a necrotic core and accumulation of extracellular cholesterol. Macrophage secretion of matrix metalloproteinases and neovascularization contribute to plaque weakness and susceptibility to rupture. Plaque rupture exposes blood components to tissue factor, initiating coagulation, the recruitment of platelets, and the formation of a thrombus. Adapted from Glass and Witzum, (2001).

The presence of tissue factor is vital for the initiation of the coagulation cascade (Wilcox *et al*., 1989). The production of tissue factor by ECs and macrophages is enhanced partly by oxLDL. If the plaque rupture, blood will be in contact with the highly thrombogenic material (especially lipid and collagen) of the core and a blood thrombus will form (Dickson & Gotlieb, 2003). A small thrombus will contribute to rapid progression of the plaque. Like intra-plaque haemorrhage, this thrombus is often absorbed into the existing plaque and once a certain size is exceeded, the thrombus can block arteries, resulting in events such as coronary infarcts (heart attacks) cerebral infarcts (stroke) and death (Jang *et al*., 1993).

1.2.2 Low Density Lipoproteins

Electron microscopy studies show that the earliest atherosclerotic lesion, the fatty streak, consists mainly lipid-laden macrophages, which imply lipoprotein uptake by these cells in the initiation of atherosclerosis. Studies done by Henriksen and colleagues, (Henriksen *et al*., 1983; Henriksen *et al*., 1981) first showed that native LDL is incapable of promoting foam cell formation unless it is oxidatively modified (oxLDL) to a form recognised by scavenger receptors on the macrophages. Initially uptake of oxLDL is part of defence mechanisms to protect the vascular wall. However, oxLDL imposes an oxidative stress on the macrophages that eventually causes death to the macrophages and also leads to loss of endothelial integrity. The later property leads to fatty streak formation due to lipid infiltration and subsequently the fatty streak progresses to more advanced lesions. Therefore, in 1989, Steinberg and his colleagues had put forward the 'oxidative modification hypothesis' that states oxidation of LDL is a key process in plaque development (Figure 1.4). As such, a key feature of the oxidative modification hypothesis is that it no longer presupposed the loss of endothelial cells as an initiating event in atherogenesis (Jessup *et al*., 2004) as stated by response-to-injury hypothesis of atherogenesis (Ross, 1986).

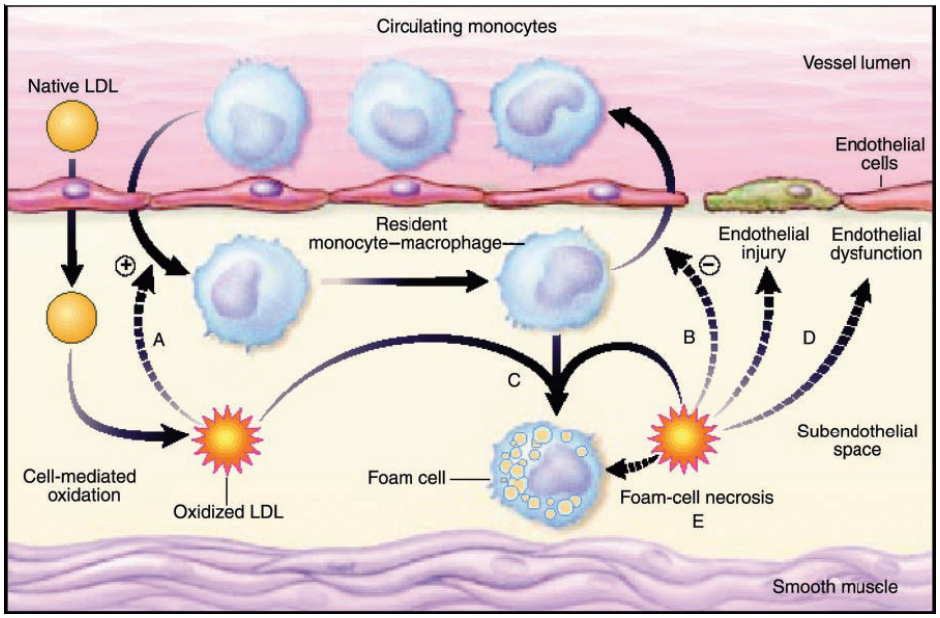

Figure 1.4 Oxidative modification hypothesis of atherosclerosis.
LDL becomes entrapped in the subendothelial space where it is subject to oxidative modification by resident vascular cells such as SMCs, endothelial cells, and macrophages. Oxidized LDL stimulates monocyte chemotaxis (*A*), prevents monocyte egress (*B*), and supports foam cell formation (*C*). Once formed, oxidized LDL also results in endothelial dysfunction and injury (*D*), and foam cells become necrotic due to the accumulation of oxidized LDL (*E*). Adapted from Diaz *et al.,* (1997).

1.2.2.1 LDL Compositions

LDL is part of a lipoprotein system for the controlled transport and metabolism of lipids in the bloodstream. It is the main carrier of cholesterol delivering it to the peripheral cells. The serum LDL concentration of normolipidemic persons ranges from 130 to 260 mg/100ml of human plasma and typically, this LDL carries about 60% of the total plasma cholesterol. The endogenous and exogenous pathways of cholesterol are highly regulated so that the serum cholesterol level in normolipidemic persons is maintained constant and in a narrow range of 160 and 200 mg/100 ml (Mathews & van Holde, 1996).

LDL has a spherical shape, diameter of 19-25 nm, relative molecular mass between 1.8 and 2.8 million. The density range of LDL is 1.090-1.063 g/ml. The major LDL's protein is apolipoprotein B100 (apoB100), which has a β structure with small fractions of α-helices. ApoB100 has 4536 amino acids and a M_r of 512,000. Each LDL molecule has an average of 170 molecule of triglycerides, 600 molecules of cholesterol and 1600 molecules of cholesterol ester (mostly cholesterol linoleate) forming an inner core. The core is surrounded by a phospholipid monolayer containing about 700 phospholipid molecules (mainly phosphatidylcholine) with their polar head groups oriented towards the aqueous phase. ApoB100 protein is embedded in the outer layer. Lipids are therefore, abundant in LDL and almost half are fatty acids. Of the fatty acids, half are polyunsaturated fatty acids (PUFA) making LDL highly susceptible to free radical mediate oxidation. The fatty acid content contents vary considerably among individuals. For instance, linoleic acid content varied from 1200 to 2400 nmol/mg LDL protein. Variation in the PUFA content will most likely affect the oxidation behaviour of different LDL samples (Esterbauer *et al*., 1992). The range of lipophilic antioxidants also varies with donor. On average, each molecule of LDL has 6 α-tocopherol molecules and the rest for example γ-tocopherol, ubiquinol-10, carotenoids (more than 20 different carotenoids have been reported) and retinoids present at less than one mole per molecule of LDL. Antioxidants are present in both core and phospholipid coat (Esterbauer *et al*., 1992). Since the structure of LDL is quite fluid the lipid soluble antioxidants can freely move between the core and the phospholipids coat (Schuster *et al*., 1995).

The uptake of LDL by cells occurs via receptor-mediated pathway and by nonspecific endocytosis. LDL interacts with the LDL receptor based on ionic interactions between clusters of amino acids and the acidic amino acids of the receptor. Most of these sites are on apoB, although some weak binding sites are found on phospholipids (Pifat *et al*., 1992). The oxidation of LDL results in the chemical modification of certain moieties

of apoB by lipid peroxidation products; with the ε-amino groups of lysine residues being particularly susceptible (Steinbrecher, 1987). Particles modified in this way no longer bind to the LDL receptor but to the scavenger receptor (Esterbauer *et al*., 1993).

1.2.2.2 LDL Oxidation

In vitro, LDL oxidation can be initiated by incubating LDL with macrophages, endothelial cells, SMCs, and lymphocytes or in cell free systems utilising a variety of pro-oxidants. Even though there is convincing evidence that oxLDL exists in atherosclerotic lesions, the precise location of LDL oxidation, how and to what extent LDL becomes oxidised during atherogenesis is still a matter of speculation (Esterbauer *et al*., 1993).

Oxidation of LDL possesses the general lipid peroxidation chain reaction and three consecutive time phases, the lag phase, propagation phase and decomposition phase (Figure 1.5). It begins when an initiating radical abstracts a hydrogen atom from one of the PUFAs contained in the LDL lipids. The exact identity of the initiating radical both *in vivo* and *in vitro* situation is still unknown, even though intensive research into this key step had been carried out.

Once formed, the carbon-centred PUFA radical reacts extremely quickly with molecular oxygen yielding a lipid peroxyl radical which in turn abstracts a hydrogen atom from an adjacent PUFA, yielding a lipid hydroperoxide and a new PUFA radical. It is the later reaction, termed propagation that generates lipid peroxidation chain. The antioxidants in LDL slow down the propagation by scavenging and neutralising the peroxyl radical and thereby inhibit lipid peroxidation. If no chain termination took place, a single initiating event could convert all LDL PUFAs into lipid hydroperoxides. The precise length of the chain, i.e. the number of PUFAs oxidised per one initiating radical depends on many factors especially on the antioxidants. The antioxidants of LDL slow down the chain propagation by very efficiently scavenging lipid peroxyl radicals and thereby inhibit lipid peroxidation. If no recycling (e.g., by ascorbate) takes place the antioxidants are consumed in the sequence α-tocopherol, ubiquinol-10, vitamin E, oxycarotenoids and β–carotene. It is not until the LDL has lost its antioxidants compounds that the propagation phase commences.

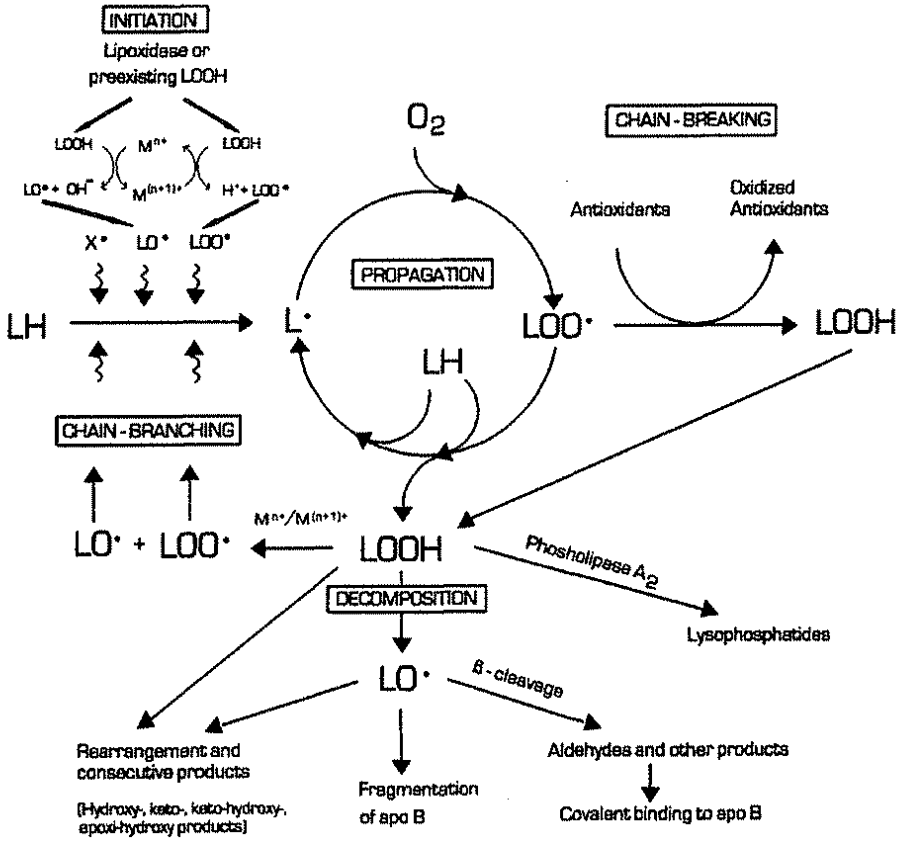

Figure 1.5 Scheme showing the major events occurring during LDL oxidation.
LH is a lipid containing a PUFA. $X^{\bullet}$ is any reactive radical able to abstract a hydrogen atom form LH; $L^{\bullet}$ is a carbon-centred lipid radical; $LOO^{\bullet}$ and $LO^{\bullet}$ are lipid peroxyl radicals and lipid alkoxyl radicals;LOOH are lipid hydroperoxides; in their decomposition to $LO^{\bullet}$ and $LOO^{\bullet}$ metal ions in both valency states (e.g. Cu^{2+}/ Cu^{+} or Fe^{3+}/Fe^{2+}) can take part, but the reaction with Cu^{+} or Fe^{2+} is thermodynamically favoured. Adapted from Esterbauer *et al.,* (1992).

Besides PUFAs, the lysine residues of apoB100 of LDL are also subject to oxidative modification during the propagation phase (Akeson *et al*., 1991; Gieseg & Cato, 2003; Giessauf *et al*., 1995; Knott *et al*., 2002). The modified apoB100 has a greater net negative charge and is no longer recognised by the LDL receptor, but becomes recognised by scavenger receptor and is taken up rapidly be macrophages (Haberland *et al*., 1984). In addition, the cholesterol associated with LDL is oxidised predominantly to oxysterols at the seventh position. 7-Hydroperoxycholesterol (7-OOH) is present in fairly large amounts in LDL during its early stages of oxidation, but there are only traces of it present in atherosclerotic lesions (Brown *et al*., 1997; Jessup & Kritharides, 2000; Upston *et al*., 2002). It has also been reported that protein hydroperoxides, produced secondarily to lipid peroxidation, are a major product in LDL oxidised by copper, peroxyl radicals and cells (Gieseg, *et al*., 2003; Firth, *et al*., 2006 Firth, *et al*., 2007). Aggregation also starts to

appear when all antioxidants are depleted and increase as lipid peroxidation proceeds (Meyer *et al*., 1995).

When most of the PUFAs (about 70-80%) are oxidised, decomposition becomes dominant and the lipid hydroperoxide concentration starts to fall. The lipid hydroperoxides break down to a wide range of products, including stable end-products such as aldehydes (including malonaldehyde (MDA) and 4-hydroxynonenal (HNE)), hydrocarbon gases, epoxides, and alcohols (Esterbauer *et al*., 1995). This decomposition can occur spontaneously but is accelerated in the presence of transition metals, resulting in the initial formation of lipid peroxyl and lipid alkoxyl radicals (Cheeseman & Slater, 1993). Jessup *et al.* (1990) and Garner *et al*., (1997b) clearly showed that as with the copper ions, macrophages also first deplete LDL from α-tocopherol, before lipid peroxidation. Moreover, only when the lipid hydroperoxides decompose that LDL is highly taken up by macrophages (leading to foam cell development). This stage also suggests that decomposition of the lipid hydroperoxides is a necessary prerequisite to generate the characteristic epitopes on apoB100 recognised by scavenger receptor.

This sequence of events of LDL oxidation has been demonstrated for oxidation of LDL initiated by macrophages and copper ions and is probably common to all process of LDL oxidation regardless of the method of initiation. An LDL that has reached the end point of decomposition always has more or less similar chemical and biological properties (Esterbauer *et al*., 1992). The time and change in the composition and functional properties of LDL exposed to copper ions as pro-oxidant was intensively studied by Esterbauer and colleagues (Esterbauer *et al*., 1989; Esterbauer *et al*., 1991; Esterbauer *et al*., 1992) (Figure 1.6) and by others (Heinecke *et al*., 1984; Jessup *et al*., 1990; Steinbrecher *et al*., 1990). Most investigators followed LDL oxidation by measuring the consumption of α-tocopherol and lipid oxide/hydroperoxide formation (Esterbauer *et al*., 1992; Jessup *et al*., 1990). The time course of oxidation can be followed by measuring the formation of conjugated dienes at 234 nm (Esterbauer *et al*., 1989), formation of lipid hydroperoxides (Esterbauer *et al*., 1989), or production of thiobarbituric acid reactive material (TBARS) (Esterbauer *et al*., 1989; Steinbrecher *et al*., 1984) and fluorescence at 430 nm with excitation at 360 nm (Esterbauer *et al*., 1989),. LDL that has undergone extensive oxidation also has an increased relative electrophoretic mobility (REM) on native gel electrophoresis (Esterbauer *et al*., 1992; Gieseg & Cato, 2003). A combination of these procedures is necessary since none of these methods by itself alone gives a full picture of the stage of oxidation.

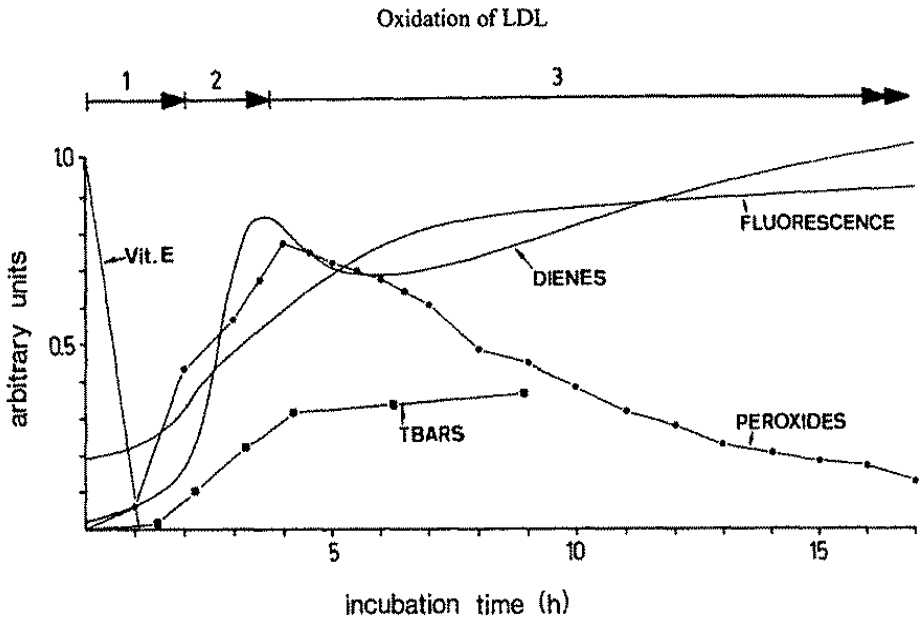

Figure 1.6 Kinetics of Cu^{2+} stimulated oxidation of LDL.
LDL is measured by consumption of vitamin E, change of 430 nm fluorescence, lipid hydroperoxides, conjugated dienes and TBARS. The numbers 1, 2, 3 on top give the length of the lag, propagation, and decomposition phases. Adapted from Esterbauer *et al.,* (1992).

1.2.2.3 Mechanisms of LDL Oxidation

Surprisingly, there are still uncertainties (and considerable disagreement) about the mechanism of LDL oxidation *in vivo*. The cellular sources of free radical and how exactly LDL is oxidised *in vivo* is still controversial. Speculation on the mechanisms of LDL oxidation by cells in the presence of metal ions is doubtful since there are multiple mechanisms exist *in vivo* for binding free transition metal ions, rendering them redox-inactive. However several convincing evidence has been presented for a role of metal ion-mediated oxygen-radical formation. For example gruel samples from advanced human atherosclerotic lesions had been shown to contain redox active iron and copper detectable in the bleomycin and phenanthroline assays respectively. Consistent with the presence of these ions, gruel samples were shown to be capable of stimulating lipid peroxidation and generating $OH^{\bullet}$ (Smith *et al*., 1992). Recently this data was backed up by the detection of redox active iron and copper by electron paramagnetic resonance (EPR) spectroscopy and their measurement by inductively coupled plasma mass spectroscopy (ICPMS) showed their elevated levels in lesion versus healthy controls (Stadler *et al*., 2004).

The finding that the copper-containing acute plasma protein ceruloplasmin (Cp) which has been studied for years as antioxidant could act as potent oxidant of LDL had also created an interesting concept in redox metal-dependent oxidation of LDL (Ehrenwald

et al., 1994; Ehrenwald & Fox, 1996). The study found that LDL exposed to Cp exhibited many characteristics of LDL oxidised in the presence of free cupric ion. Copper was shown to be a potent mediator of LDL oxidation due to its ability to bind histidine residues on the apoB100 (Roland *et al*., 2001; Wagner & Heinecke, 1997). The binding permits both LDL-mediated reduction of copper to its redox active form and site-specific damage to LDL. Cp can become more catalytically active under acidic conditions (Lamb and Leake, 1994a) and the acidic condition of atherosclerotic plaque provides such a conducive environment for this kind of reaction to occur (Lamb & Leake, 1994b).

The studies of Cp in cell-mediated LDL oxidation also suggest that other protein-bound redox-active transition metals might participate in the extracellular oxidation events. Under physiological conditions globin degradation such as hemin (Camejo *et al*., 1998) and iron binding proteins such as transferrin (Lamb & Leake, 1994b) and ferritin (Abdalla *et al*., 1992) may catalyse the oxidation reactions. Superoxide radicals and an acidic pH were suggested to provide conditions that promote iron release from ferritin and transferrin (Abdalla *et al*., 1992; Lamb & Leake, 1994b) whereas hemin exhibits pro-oxidant activity even at neutral pH and in the presence of human serum (Camejo *et al*., 1998; Tribble *et al*., 1996).

Although these studies support the potential for metal-mediated LDL oxidation, they fail to confirm the significance of such reactions in humans. For example, copper levels are significantly elevated in people afflicted with Wilson's disease but this increase fails to correlate with atherosclerosis (Heinecke, 1999). Further an autopsy on patients with hemochromatosis, a genetic disorder with iron overload in plasma and tissue levels, showed no association with an increased prevalence of coronary artery disease (Miller & Hutchins, 1994).

One of the cell-derived factors that may participate in LDL oxidation of LDL is lipoxygenase (LOs). They are non-heme iron-containing enzymes found in various cells that catalyse the insertion of molecular oxygen into PUFAs, giving rise to a family of biologically active lipids (Jessup *et al*., 2004). In monocyte-macrophage systems, substantial evidence links 15-LO to LDL oxidation. LO could oxidise cellular fatty acid, cholesteryl ester or phospholipid substrates, and the hydroperoxide products could be transferred to LDL making LDL more susceptible to oxidation. LO products could also participate in signal transduction pathways regulating other monocyte-macrophage functions involved in oxidation (Chisolm *et al*., 1999).

Another cell-derived factor that may participate in LDL oxidation of LDL is myeloperoxidase (MPO). MPO is a heme-containing protein released by activated

neutrophils and monocytes during inflammation and present in some tissue macrophages such as those in vascular lesions (Heinecke, 2002). MPO can amplify the oxidising potential of hydrogen peroxide (H_2O_2), the dismutation product of superoxide anion ($O_2^{\bullet-}$), by using it as a co-substrate to generate a variety of oxidants including diffusible radical species (Heinecke *et al*., 1993; Savenkova *et al*., 1994), reactive halogens (Hazen & Heinecke, 1997), aldehydes (Febbraio *et al*., 2000) and nitrating agents (Carr *et al*., 2000; Podrez *et al*., 1999).

MPO-mediated oxidation reactions occur in the absence of free transition metal ions and are resistant to inhibition by chelators. MPO can catalyse the two-electron oxidation of chloride forming the powerful oxidant, hypochlorous acid (HOCl). Exposure of LDL to HOCl results in chlorination and oxidation of protein and lipid constituents of LDL, induces LDL aggregation, and converts the lipoprotein into a high uptake form for macrophages (Hazell & Stocker, 1993; Hazen & Heinecke, 1997). MPO-generated aldehydes can then modify nucleophilic targets on LDL protein and lipids (Hazen & Heinecke, 1997). MPO also catalyses the one-electron oxidation of L-tyrosine, generating the tyrosyl radical (Savenkova *et al*., 1994) which can initiate LDL lipid peroxidation and dityrosine cross-linking of proteins (Heinecke *et al*., 1993).

Nitric oxide itself is unable to oxidise LDL, however, MPO can use H_2O_2 and nitrite (NO_2^-), a major end product of nitric oxide (nitrogen monoxide, $^{\bullet}NO$) metabolism, to generate a peroxynitrite. The later has been shown to be capable of nitrating aromatic compounds and tyrosine residues of the apoB100 of LDL, besides promoting lipid peroxidation *in vitro* (Hazen *et al*., 1999). In addition, HOCl can react with NO_2^- to form a nitrating and chlorinating intermediate. Recent studies demonstrate that exposure of LDL to NO_2^- and either elutriated human monocytes or isolated MPO and H_2O_2 sources, results in LDL lipid peroxidation and protein nitration. Moreover, LDL modified by MPO-generated nitrating intermediates is rendered a ligand for high affinity binding and foam cell formation. Another intriguing characteristic of MPO is its ability to induce LDL modification even in the presence of blood serum that normally blocked copper-catalysed LDL oxidation (Podrez *et al*., 1999). Thus it is possible that MPO secreted from inflammatory cells in atherosclerotic lesions could oxidise LDL and thereby modify various proteins in the lesions.

Due to the complexity of lesions, it is therefore difficult to ascertain which pro-oxidants is the most important initiator of LDL oxidation. Probably they are all important in different regions and/or at different stages of the lesion. Regardless of which

mechanism(s) are involved in LDL modification *in vivo*, the end product is still a heterogeneous population of LDL that is oxidised to varying degrees.

1.2.2.4 Proatherogenic (Proinflammatory) Effect of OxLDL

LDL oxidation is a progressive process leading to formation of a continuum of oxLDL (from mildly to extensively oxLDL) (Salvayre *et al*., 2002). OxLDL contains a complex, variable, and incompletely characterised mixture of toxic oxidation products. Thus oxLDL are heterogeneous in their composition, metabolism and biological properties. Table 1.1 summarises briefly the differences between native LDL and oxLDL. A substantial body of evidence suggest that most if not all of the atherogenic effects of oxLDL are derived from the oxidised lipid components (Parthasarathy *et al*., 1999). The active lipid include both esterified and unesterified peroxidised lipids, lysoPtdCho, cholesterol oxidation products (also termed oxysterols), aldehydes derived from breakdown of both esterified and unesterified oxidised fatty acids, and proteolipids that may have peroxidised lipids bound to fragmented apoB100. Every single aspect of atherogenesis is likely to be affected by one or more of these components (Salvayre *et al*., 2002).

Different types of modified LDL can be developed depending on the condition of oxidation which includes type and concentration of radical or oxidant, the level of endogenous (e.g. α-tocopherol, carotenoid) or added antioxidants (e.g. ascorbic acid and uric acid) and modification of apoB 100. For example, a novel method for production of lipid hydroperoxide- or oxysterol-rich LDL was developed by Gerry *et al.,* (2008). LDL was dialysed against MOPS buffer containing Cu^{2+} ions for 24 hours at either 4 °C to form hydroperoxide-rich LDL or 37 °C to form oxysterol-rich LDL. Carpenter *et al.,* (2003) demonstrated that three species of oxLDL (moderately, mildly and very mildly oxLDL) can be differentiated according to the conditions of incubation. Incubation of LDL with Cu^{2+} ions in PBS (pH 7.4); Fe^{2+} in saline and Fe^{2+} in PBS (pH 5.5) at 37 °C for 15 hours produced; moderately, mildly and very mildly oxLDL respectively. After 15 hours oxidation, mildly oxLDL consistently contained higher levels of hydroperoxides, lower levels of oxysterols, lower levels of MDA and lower REM than did moderately oxLDL. Hydroperoxide levels in very mildly oxLDL were only slightly above native LDL whilst REM, TBARS and 7β-hydroxycholesterol (7β–OH) in mildly oxLDL were similar to native LDL. While very mildly oxLDL was non-toxic to HMDMs, mildly oxLDL induced more death and apoptosis in HMDMs than moderately oxLDL as measured by LDH release and nucleosome ELISA respectively (Carpenter *et al*., 2003). This was in

agreement with Siow *et al.,* (1999) where their moderately oxLDL (which contains the peak level of lipid hydroperoxides) but not highly oxLDL caused SMCs apoptosis within 6 hours. However, later finding shows that J774, mouse and human macrophages are more susceptible to apoptosis by a highly oxLDL species rich in oxysterols than do moderately oxLDL (Harris *et al*., 2006).

Table 1.1 Lipids and proteins of native LDL and oxLDL adapted from Parthasarathy *et al.,* (1999)

Native LDL	OxLDL
Presence of intact, single apoB100. Non-antigenic in the same species.	Proteolysed, fragmented, oxidised, cross-linked apolipoprotein with a different amino acid composition. The protein is also covalently modified by lipid peroxidation products that include intact core aldehydes derived from esterified lipid. New functional groups (protein carbonyls, sulfonic acids, carboxylic acids, etc) might be present on the protein. Chlorination and nitration might occur. Highly antigenic.
Contains abundant amounts of PUFA and antioxidants.	PUFA and antioxidants are depleted.
Free of lipid peroxides and their degradation products such as aldehydes and ketones.	Contain massive amounts of lipid peroxides and their degradation products.
Very low levels of oxidised cholesterol.	Increased amounts of oxidised cholesterol product. May also contain large amounts of cholesterol ester core aldehydes.
No unusual lipids.	Chlorinated and nitrated lipid species might be present.
May contain very low levels of lysoPtdCho.	Contained increased levels of lysoPtdCho. Might also contain oxidatively tailored phospholipids, which are intact phospholipids with fragmented fatty acid chain.

Boullier and colleagues (2006) shows that very mildly oxidised or minimally modified LDL (mmLDL) binds to native LDL receptors but not to scavenger receptors. It contains early lipid peroxidation products but in contrast to oxLDL or mildly oxLDL, it does not contain any measurable TBARS or EO6-reactive phospholipid oxidation products above those noted in native LDL. Table 1.1 summarises the biological properties of extensively oxidised LDL.

OxLDL is known to induce chemoattractant cytokines like P-selectin, GRO, VCAM-1 and MCP-1 that recruit monocytes and T cells to the intima (Berliner & Heinecke, 1996) which is an early event in atherogenesis. LysoPtdCho, 13-hydroperoxy linoleate (13-HPODE) and a number of products derived from oxidised PtdCho are suggested to induce the adhesion and chemotactic recruitment of monocytes by activating the EC adhesion molecules and specific chemotactic factors. these lysoPtdCho are also direct chemotaxins for monocytes and T-lymphocytes (Parthasarathy *et al*., 1999). The monocytes in the intima will be subjected to various actions mediated by oxidised components of LDL. For example, monocyte differentiation is promoted by the oxLDL-induced release of endothelial-derived M-CSF (Rajavashisth *et al*., 1990).

OxLDL also adversely affects plaque stability. It promotes a net increase in macrophage-mediated matrix degradation by down-regulating the tissue inhibitor of metalloproteinase-1 (TIMP-1) but upregulating matrix metalloproteinase-9 (MMP-9) (Xu *et al*., 1998). Thrombus formation can be aggravated by oxLDL since oxLDL stimulates the production of tissue factor (Berliner *et al*., 1995) and promotes platelet aggregation (Volf *et al*., 2000). Components of oxLDL have also been suggested to affect vascular endothelium- dependent relaxation and promote pro-coagulatory responses from both the endothelium and the platelets. Hydroperoxides are more potent toxins in oxLDL than are the more advanced oxidation products such as aldehydes and oxysterols (Carpenter *et al*., 2003). However, Leake and colleagues (Harris *et al*., 2006) claimed that even though moderately oxLDL containing the maximum level of lipid hydroperoxides that induce apoptosis, LDL species most toxic towards macrophages is highly oxidised LDL rich in 7-ketocholesterol (7-KC). Quantitation by gas chromatography indicated that 7-KC was the major oxysterol present (Zhang *et al*., 1990). 7-KC has been shown to modify lipid raft domains in THP-1 cells causing an increase in cytosolic calcium and activation of calcium dependent proteases (Berthier *et al*., 2004). It also initiates oxidative stress in mouse macrophage J774A.1 through the activation of NADPH oxidase; a possible source of oxLDL induced oxidative stress (Leonarduzzi, *et al*., 2006). 7-KC is a major contributor to the inhibition of cholesterol export from oxidised LDL-loaded macrophages (Gelissen *et al*., 1996). Besides 7-KC, 7β-hydroperoxycholesterol and 7β-OH are also cytotoxic. These oxysterols are reported to destabilise macrophage lysosomes, leading to leakage of lysosomal contents and subsequent induction of apoptosis or necrosis (Yuan *et al*., 2000). OxLDL uptake leads to expansion of an acidic endolysosomal compartment that leads to inactivation of lysosomal cysteine proteases and dysfunction of other lysosomal proteins required for processing and recycling of the hybrid lysosomes (Lougheed *et al*., 1999).

Although most of the atherogenic effects of oxLDL are attributed to its oxidised lipid components, other components of oxLDL also play a role. The oxLDL's protein moiety appears to stimulate IL-1 production (Lipton *et al*., 1995) and respiratory burst activity in macrophages (Nguyen-Khoa *et al*., 1999). OxLDL have been demonstrated to ultimately increase secondary messengers, cyclic adenine monophosphate (cAMP) (Parhami *et al*., 1993) and activate various cytokines and signal transduction pathways (Berliner & Heinecke, 1996). Signal transduction occurs through the oxLDL-mediated activation of protein kinase C (PKC) (Li *et al*., 1998), nuclear factor-κβ (NF-κβ) (Parhami *et al*., 1993), AP-1 (Whatling *et al*., 2004) and PPARγ (Nagy *et al*., 1998).

1.3 Lipoproteins and Macrophage Scavenger Receptors

In vitro studies have shown that LDL can only induce cellular cholesterol accumulation when presented to macrophages in a modified form and required different routes of modified LDL uptake. This is because intracellular free cholesterol level regulates the level of LDL receptors forms on the plasma membranes. Brown and Goldstein first described this 'scavenging' activity of macrophages in 1979 when investigating the formation of lipid laden macrophages in atherosclerotic plaques (Brown *et al*., 1979). Subsequent cloning has revealed the receptors responsible are a broad family of transmembrane multidomain structures classified into six (or more) subgroups based on their proposed tertiary structures (Krieger & Herz, 1994). On the basis of functional studies and evidence for expression in the arterial intima, only some of the scavenger receptors (SRs) are good candidates for contributing to atherosclerotic foam cell formation. Class A receptors (SRA) were the first identified and originally found through their binding to acLDL. A second class of SR, SR class B (SR-B) has been identified as the oxLDL receptor. CD36 and SR-B1 belong to class B SR. In addition to SR-A and SR-B are CD68 (SR-D class), lectin-like oxidised LDL receptor (LOX-1, SR-E class) and SR that binds PS and oxLDL (SR-PSOX, SR-G class). In addition to these, endothelial cells express SREC and SR-F class (Greaves & Gordon, 2005).

SR-A recognises the oxidised apoprotein portion of the lipoprotein particle. The SR-A was shown to be a trimeric Type II membrane protein with a broad range of polyanionic ligands. It has grown to include 4 members that share common collagen-like domains and a homotrimeric structure: SR-AI, SR-AII, SR-AIII and macrophage receptor with collagenous structure (MARCO). SRA-I, SR-AII and SR-AIII have 6 similar structural domains: cytoplasmic, transmembrane, spacer, α-helical coiled, collagenous, and a type specific carboxyl terminus. SR-AI has cysteine linked C terminal extension of 110

amino acids, a highly conserved protein motif found in many other immunological proteins. SR-AII has a short carboxyl-terminal domain that is relatively nonconserved between species. SR-AIII is located within the endoplasmic reticulum and is not accessible to extracellular ligands, thus, making its function difficult to define (Gough *et al*, 1998) MARCO is a structurally related molecule expressed by murine macrophages and has similar structures as the SR-AI but differs in having a longer extracellular domain and completely lacking an alpha-helical coiled domain. MARCO has been demonstrated to bind bacteria but not acLDL or oxLDL.

Studies from (Kunjathoor *et al*, 2002; Suzuki, *et al*, 1997) suggested that SR-AI and SR-AII account for the majority (~80%) of macrophages uptake of acLDL but have a lower affinity for oxLDL. SR-AI and SR-II recognise the modified apoB protein component of oxLDL (Lougheed & Steinbrecher, 1996; Zhang *et al*., 1993) In addition, both SR-AI and SR-AII also bind apoptotic cells, bacterial surface lipids (endotoxin and lipoteichoic acid), anionic phospholipids, proteins modified by advanced glycation and β-amyloid fibrils (Moore & Freeman, 2006).

SR-A deficient macrophages are less prone to foam cell formation when treated with modified LDL and results from genetically modified mice suggest that macrophage SR-A is probably pro-atherognenic (Babaev *et al*., 2000; Sakaguchi *et al*., 1998; Suzuki *et al*., 1997). However, another report on a different atherosclerosis-prone genetic background suggested that they had no decrease in atherosclerosis (de Winther *et al*., 1999) and macrophage over expression of SR-A had no effect on atherosclerosis (Herijgers *et al*., 2000; Van Eck *et al*., 2000). Recently it was reported that JNK2-dependent phosphorylation of SR-A is critical for uptake of oxidised LDL and formation of foam cells *in vitro*, potentially contributing to decreased atherosclerosis in JNK2-deficient mice (Ricci *et al*., 2004). Ligand binding to SR-A induces focal adhesion complexes and adhesion (Post *et al*., 2002) that see the potential for modified lipoproteins to induce signalling through binding to SR-A.

Immunofluorescent staining of murine macrophages demonstrated that SR-As were distributed at the membrane closest to the adherence surface to tissue culture plate suggesting that SR-As play a role in the adhesion of macrophages to tissue culture plate (Lougheed & Steinbrecher, 1996). This led to a suggestion that SR-A may play a role in retention of macrophages at sites of inflammation, as it appears that the contribution of SR-A to cell adhesion is more in activated than resident macrophages.

SR-B was established with the identification of CD36 as a receptor for oxLDL. Unlike the SR-A family, CD36 is a type III (multiple transmembrane domains) receptor

that traverses the membrane twice to form a heavily glycosylated extracellular loop with 2 short intracellular tails. SR-B has 2 additional members with similar structure: SR-BI and lysosomal integral membrane protein-II. CD36 and SR-BI appear to play quite distinct roles in lipid metabolism and atherosclerosis. While CD36 has been shown to specifically bind oxLDL (Endemann *et al*, 1993), SR-B1 has a high affinity for native LDL (Acton *et al*., 1994).

The very first observations showing the capacity of CD36 to bind and endocytose oxLDL came from the work of Endemann *et al.,* (1993). They showed that CD36 bind specifically oxLDL by using a human epithelial kidney cell line (HEK293) transfected with CD36. CD36 binds to the oxidised phospholipids and protein moieties of oxLDL (Boullier *et al*., 2000). It is highly regulated during monocyte differentiation. Devaraj, 2001 reported that human macrophage CD36 expression is upregulated by day 4 and is elevated about 5-fold in 8-10 days of culture. Another study reported that in human macrophages, CD36 expression was maximal after 10 days of culture (Nakagawa *et al*., 1998). This in contrast with Huh *et al.,* (1996), who showed that CD36 expression is up regulated and is maximal on day 4 (8- to 10-fold) and is reduced by day 8 of culture. The different types of serum and tissue culture plates used in culturing the cells might explain the discrepancy in their findings. It is also to be remembered that these studies were on mRNA levels rather than the actual receptor levels on the membrane.

A few studies then followed supporting the paradigm that CD36-mediated oxLDL uptake is required for the macrophage foam cell formation and atherosclerosis. CD36 contributes to 60% to 70% of cholesterol ester accumulation in macrophages exposed to LDL oxidized by Cu^{2+} and myeloperoxidase/peroxynitrite mechanism (Kunjathoor, *et al*., 2002; Febbraio, *et al*., 2000). An absence of CD36 on monocytes as observed in small population in the Japanese population, results in 40% less oxLDL binding to monocyte-derived macrophages and 40% less in accumulation of cholesterol ester when compared to cells derived from normal controls (Nakagawa *et al*., 1998). Moreover, studies performed in $apoE^{-/-}$ mice lacking CD36 showing marked reduction in atherosclerotic lesion area (Febbraio *et al*., 2000). In contrast, another study (Moore *et al*., 2005) reported that deletion of SR-A or CD36 does not ameliorate atherosclerosis in $apoE^{-/-}$ and the reason for this absence is presently unclear although they attributed this disparity to the difference in the genetic background of the mice. However, there are more continued supports on a role for CD36 in atherosclerosis specifically in the descending aorta. Transplantation of *Cd36*$^{-/-}$ bone marrow into *Apoe*$^{-/-}$ mice resulted in a large reduction in aortic en face lesion area in hypercholesterolemic mice, indicating that macrophage CD36 contributes to

lesion progression in the aortic tree (Febbraio *et al*., 2000). Moreover, treatment of *Apoe*$^{-/-}$ mice with a CD36 ligand derived from growth hormone–releasing peptide, EP80317 reduced aortic atherosclerotic lesion area by up to 50% (Marleau, *et al*., 2005). This ligand reduces oxLDL internalisation and up-regulate genes involving in regulating peripheral cholesterol trafficking. Altogether, these studies suggest that CD36 may differentially contribute to lesion development in the aortic sinus and the descending aorta. Whether this effect is attributable entirely to its lipid uptake function is not known.

SR-B1 can bind native and modified forms of LDL but does not lead to foam cell formation (Krieger & Kozarsky, 1999). It binds native HDL and mediates selective cholesterol uptake from HDL to cells (Krieger & Kozarsky, 1999). SR-B1 plays important role in reverse cholesterol transport due to its ability to facilitate cholesterol transfer from macrophages to HDL and mediate selective cholesterol delivery to liver and steroidogenic tissues without HDL degradation (Greaves & Gordon, 2005). SR-B1-deficient mice have dramatically increased atherosclerosis (Van Eck *et al*., 2004). Thus, macrophage SR-B1 expression is antiatherogenic; although promotion of cholesterol efflux to HDL may be one mechanism, the precise mechanism(s) remain unknown.

The class D SRs includes CD68 and macrosialin. Human macrophages CD68 and its murine homolog macrosialin are heavily glycosylated type I transmembrane proteins that are predominantly expressed in late endosomes and lysosomes of macrophages (Ramprasad *et al*., 1995). Based on their expression pattern, they are unlikely to play a major role in oxLDL internalisation (de Beer *et al*., 2003), but may contribute to oxLDL endolysosomal processing. Levels of microsialin are up regulated by oxLDL, and this receptor is expressed in macrophage foam cells in atherosclerotic plaques in Apoe$^{-/-}$ mice but further studies of its actual role remains to be determined.

The class E SRs, LOX-I is a lectin-like, type II transmembrane protein and is expressed on macrophages, endothelial and vascular SMCs. It binds to SR ligands, including oxLDL, advanced glycation end-products, apoptotic cells and bacteria (Moore & Freeman, 2006). Recently, LOX-1 scavenger receptor has been shown to directly bind phosphatidylserine (PS)-containing apoptotic bodies, in a Ca^{2+}-dependent manner (Murphy *et al*., 2006).

SRs expressed by endothelial cells, SREC-I, and SREC-II, are type I transmembrane receptors and classified as Class F SRs. These 2 receptors share 35% homology, and although both bind modified LDL, only SREC-I internalises these ligands for degradation. Studies in SrecI$^{-/-}$ macrophages demonstrated that this receptor accounts

for only 6% of total acetylated LDL degradation, suggesting that it plays a minor role in foam cell formation (Greaves & Gordon, 2005).

Finally the class G SRs, SR-PSOX, was identified by its ability to bind oxLDL (Shimaoka *et al*., 2000) and was subsequently shown to be identical to the membrane-bound CXC chemokine CXCL16 (Wuttge *et al*., 2004). This receptor is expressed in human and mouse atherosclerotic lesions, where it is present on endothelium, SMCs and macrophages. To date the contribution of SR-PSOX to macrophage oxLDL uptake, foam cell formation and atherosclerosis is unclear, however, one study suggests an association of a CXCL16 gene polymorphism with severity of coronary artery stenosis (Lundberg *et al*., 2005).

1.4 APOPTOSIS

Cells die in response to a variety of stimuli. Cell death commonly can occur by two mechanisms, necrosis and apoptosis, although, sometimes death by mechanisms with features of both pathways can also be seen (Halliwell & Gutteridge, 2007).

Necrotic death occurs when a cell is severely injured, for example by a physical blow or by oxygen deprivation. Necrosis is characterised by swelling of the internal organelles and cell, loss of integrity of mitochondrial, peroxisomal and lysosomal membranes and eventual rupture of the plasma membrane, releasing cell contents into the surrounding which may affect adjacent cells (Lelli *et al*., 1998). These effects occur because injury prevents the cell from maintaining its ion homeostasis. Another hallmark of necrosis is inflammation where cells of the immune system converge on the necrotic cells and ingest them. Inflammation helps to limit infection and clear away debris, but the activities and secretions of the white cells can also damage normal tissue in the vicinity, sometimes extensively (Duke *et al*., 1996).

In apoptosis, the earliest visible morphological changes are cell shrinkage and blebs forming on the surface membrane without the membrane losing its integrity (Haunstetter & Izumo, 1998). Internal organelles retain their structure, but the nucleus changes dramatically during apoptosis (Alcouffe *et al*., 1999). Most prominently, its usually dispersed chromatin condenses and becomes fragmented (Yuan *et al*., 2000). This is usually associated with DNA double-strand break in internucleosomal regions and when these fragments are separated by gel electrophoresis a ‘ladder’ pattern is seen. Other features of apoptosis are the collapse of cytoskeletal structure, nuclear fragmentation, and eventual break-up of the cell into apoptotic bodies, without rupture of organelle membranes (Haunstetter & Izumo, 1998). Certain modification in the plasma membrane

for instance, the redistribution of phosphatidylserine (PS) to the outer leaflet of plasma membrane enable the recognition of apoptotic bodies by phagocytic cells (van Engeland *et al*., 1998). Since the apoptotic bodies are surrounded by an intact plasma membrane, apoptosis usually occurs without leakage of cell content and usually without inflammation. If the apoptotic bodies are not phagocytosed, a process known as secondary necrosis will occur in which the membranes of apoptotic bodies lyse and the contents of the bodies are released (Skepper *et al*., 1999; Tabas, 2005).

1.4.1 Molecular Mechanism of Apoptosis

Apoptosis is a tightly regulated cell death program which involves the interplay of a multitude of factors. Apoptosis can be triggered by various stimuli from outside or inside the cell, e.g. by ligation of cell surface receptors, by DNA damage as a cause of defects in DNA repair mechanisms, treatment with cytotoxic drugs or irradiation, by a lack of survival signals, contradictory cell cycle signalling or by developmental death signals.

In most instances the initiation and regulation of apoptosis is highly controlled by a family of proteolytic enzymes called caspases. The caspases are a novel class of at least 14 cysteine proteases that could be described as 'the central executioners' of the apoptotic programme. Their name reflects the active cysteine group and the characteristic cleavage of their target at aspartate residues, hence the name 'cysteine-aspartyl-specific proteases', abbreviated to caspases (Chandra & Orennius, 2002; Hampton & Orennius, 1997).

In the cell, caspases are synthesised as inactive zymogens, the so called procaspases. Upon activation, the caspases cleave a variety of cellular proteins C-terminal to aspartate residues. Activation involves proteolytic conversion of a procaspase zymogen to the active form. This occurs rapidly after triggering of apoptosis, and is seen with a wide variety of apoptotic stimuli (Chandra & Orennius, 2002; Hampton & Orennius, 1997; Haunstetter & Izumo, 1998).

Functionally, caspases can be classified into two classes; (i) the initiator caspases that are characterised by long prodomains containing either death-effector domain (DED) domains (caspase-8 and caspase-10) or a caspase recruitment domain (CARD) (caspase-2, and caspase –9) and (ii) the executioner or effector caspases containing short prodomains (caspase-3, caspase-6 and caspase-7) (Grutter, 2000). They all exist as inactive zymogens in normal cells. Procaspase forms of the initiator caspases have some catalytic activity and their enforced localisation leads to autocatalytic processing and activation. Upon activation by a wide variety of apoptotic stimuli, the initiator caspases cleave and activate the effector caspases, which proteolytically degrade an array of structural and regulatory

proteins at Asp-Glu-Val-Asp (DEVD) or closely related sequences which put in motion the cellular events characteristic of apoptosis (Hampton *et al*., 2002).

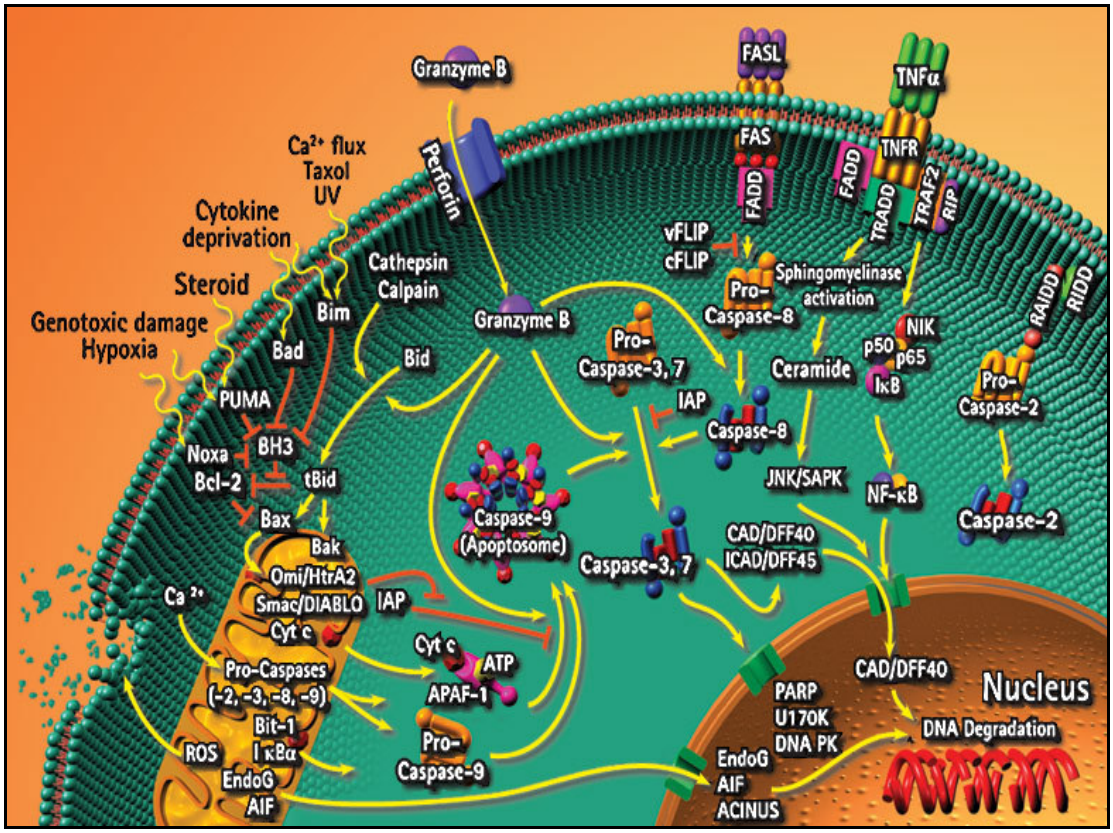

Figure 1.7 Some major apoptotic signalling pathways.
Refer to the text in section 1.4.1 for the description of the pathway. Figure was adapted from www.chemicon .com.

Until now two pathways leading to caspase activation have been described; the receptor mediated or extrinsic pathway and the intrinsic pathway (Figure 1.7) (Lawen, 2003; Lesauskaite *et al*., 2003). In the first pathway, the first step is the engagement of a receptor at cell surface. These receptors are called 'death receptors'. Death receptors belong to the tumour necrosis factor receptor (TNFR) gene superfamily, including TNFR-1, Fas/CD95 (fibroblast associated cell surface), and the TNF-related apoptosis-inducing ligand (TRAIL) receptors DR-4 and DR-5 (Ashkenazi, 2002). All members of the TNFR family consist of cysteine rich extracellular subdomains which allow them to recognise their ligands with specificity, resulting in the trimerisation and activation of the respective death receptor. The cytoplasmic 'tails' of these receptors recruit other proteins such as FADD (Fas-associated death domain) and TRADD (TNF receptor-associated death domain). These carry a DED that binds procaspase-8. The complex of Fas, FasL, FADD and procaspase-8 is called the DISC. The procaspase-8 molecules are brought into close proximity in the DISC, so they can transactivate one another. Active caspase-8 then can

directly cleave caspase-3 or other executioner caspases eventually leading to the apoptotic outcome (Ashkenazi, 2002; Halliwell & Gutteridge, 2007).

The intrinsic or mitochondrial pathway is activated by a variety of extracellular and intracellular stresses, including oxidative stress and treatment with cytotoxic drugs. In intrinsic pathway, the signal coming from the activated receptor does not generate a caspase signalling cascade strong enough for execution of cell death on its own. In this case the signal needs to be amplified via mitochondria-dependent apoptotic pathways. The link between the caspase signalling cascade and the mitochondria is provided by the Bcl-2 family member Bid. Bid is cleaved by caspase-8 and in its truncated form (tBid) translocates to the mitochondria where it acts in concert with the proapoptotic Bcl-2 family members Bax and Bak to induce the release of cytochrome *c* and other mitochondrial proapoptotic factors into the cytosol (Luo *et al*., 1998). Cytochrome *c* is a 14 kDa soluble protein attached to the inner membrane of the mitochondria. In its traditional role in the respiratory chain, cytochrome *c* shuttles electrons between complexes III and IV on the inner mitochondrial membrane. The resulting breakdown in electron flow generates reactive oxygen species, specifically superoxide and reduces the supply of adenosine triphosphate (ATP) (Cai & Jones, 1998; Stridth *et al*., 1998). Earlier data suggested that loss of mitochondrial membrane potential ($\Delta\psi_m$) and opening of the mitochondrial membrane permeability pore are necessary for cytochrome *c* release (Kluck *et al*., 1999; Liu *et al*., 1996), however, recent data suggest that both events are not needed (Ly *et al*., 2003; Stridth *et al*., 1998; Waterhouse *et al*., 2002).

Once in the cytosol, cytochrome *c* binds to the apoptotic activating factor-1 (Apaf-1). Binding of cytochrome *c* to Apaf-1 triggers the formation of the apoptosome (Aoshima *et al*., 1997), a complex containing Apaf-1, cytochrome *c*, dATP and procaspase–9 molecules. Binding leads to cleavage of procaspase-9, converting it to an active form which in turn cleaves and activates caspase-3 thereby setting in motion the events that lead to DNA fragmentation and cell death (Aoshima *et al*., 1997).

Besides cytochrome *c*, other molecules are also released from mitochondria, for example apoptosis inducing factor (AIF) and SMAC (alternative name DIABLO). SMAC is a protein that binds and inhibits endogenous caspase blockers (inhibitors of apoptosis, (IAP)) (Adam *et al*., 2000; Verhagen *et al*., 2000). AIF appears to induce an apoptosis-like cell death that is independent of caspases (Joza *et al*., 2001). It enters the nucleus and induces peripheral and ‘dot’ chromatin condensation and DNA fragmentation (Marzo *et al*., 2001).

Another way of triggering apoptosis is to introduce an agent that directly activates caspases and/or mitochondrial proapoptotic proteins. For example, tributylin targets mitochondria, causing swelling, and cytochrome *c* release. Finally, the cytotoxic T lymphocytes can deliver a pore-forming protein (perforin) and a set of proteolytic enzymes (granzymes) into their target cells. Granzymes B can directly activate the target cell's caspase and by doing so induce apoptosis. Granzyme B can also bypass caspases by directly cleaving ICAD, Bid and caspase-3. The ER stress response can also lead to apoptosis (Halliwell & Gutteridge, 2007).

1.4.2 Bcl-2, ROS and Redox Regulation of Apoptosis

The Bcl-2 family of proteins has a role in the regulation of apoptosis where it regulates the mitochondrial membrane potential, outer membrane permeability and hence the release of the proapoptotic factors. Bcl-2 family of proteins can be defined by the presence of conserved sequence motifs known as Bcl-2 homology domains (BH1 to BH4). It contains over 30 members. Some members including Bcl-2, Bcl-X_L, Bcl-w, and Bcl-B suppress apoptosis and they posses the domains BH1, BH2, BH3 ad BH4. The proapoptotic group of Bcl-2 members can be divided into two subgroups: the Bax-subfamily consists of Bax, Bak, and Bok that all possess the domains BH1, BH2 and BH3, whereas the BH3 only proteins (Bid, Bim, Bik, Bad, Bmf, Hrk, Noxa, Puma, Blk, BNIP3 and Spike) have only the short BH3 motif an interaction that is both necessary and sufficient for their killing action (Cory & Adams, 2005). The relative ratios of these pro- and anti-apoptotic members are more important to the survival of a cell than the expression of any member in particular (Carmody & Cotter, 2001).

Bax, Bcl-Xs, Bid, Bim and Bak occur as dimers or oligomers in the cytoplasm and form ion-conducting channels in the mitochondrial outer membrane (Kroemer & Reed, 2000). They also form pores in the membranes of the endoplasmic reticulum and nucleus. These pores probably induce mitochondrial membrane permeability and cytochrome *c* release from the mitochondria, intervene in Ca^{2+} signalling by inducing Ca^{2+} release from the endoplasmic reticulum and modulate nuclear membrane. Since, several other pro-apoptotic family members do not possess BH1 and BH2 domains that are essential for ion channel formation, thus it is unlikely that formation of ion channel is the only mechanism by which Bcl-2 family protein regulate apoptosis. The family's pro-apoptotic effect to some extent also depends on caspases. For example caspases 1 and 3 degrade Bcl-X_L and

Bcl-2, respectively, converting anti-apoptotic proteins into pro apoptotic mediators (Kirsch *et al*., 1999).

Bcl-2 also appears to functions as antioxidant. It was reported to prevent lipid peroxidation associated with apoptosis, suggesting that Bcl-2 may indirectly regulate antioxidant defences to prevent cell death (Hockenbery *et al*., 1993). There is also a strong link between Bcl-2 and the endogenous antioxidant GSH. Analysis of multiple lymphoid systems shows increased in Bcl-2 protein levels were related to increase in intracellular GSH levels. The resistance of cells to apoptosis-inducing stimuli conferred by elevated Bxl-2 expression is significantly decreased following depletion of intracellular GSH (Mirkovic *et al*., 1997). In addition, Domenicotti *et al.,* (2000) showed that glutathione depletion induces apoptosis through activation of PKC and dependent increase in AP-1 nuclear binding.

The role of ROS and redox in apoptosis is not clearly defined since it is difficult to distinguish whether oxidative events are a consequence of damage or cause of cell death. Even though many oxidants had been demonstrated to be potent inducers of apoptosis in a range of cell types, the studies failed to demonstrate whether ROS also serve as mediators of apoptosis. Besides that, many apoptotic agents, which are not oxidants, generate significant levels of intracellular ROS during the induction of apoptosis. Nevertheless, the ability of antioxidants to prevent apoptosis provides evidence for a role of ROS in apoptotic signal transduction (Carmody & Cotter, 2001).

The oxidation of the anionic phospholipid cardiolipin facilitates cytochrome *c* release from mitochondria (Kagan *et al*., 2004) and as a consequence disrupts the mitochondrial electron transport chain causing more superoxide formation. In contrast, caspases have exposed –SH groups in their active sites which are essential for activity and can readily be inactivated by H_2O_2, HOCl, $OH^{\bullet}$, $ONOO^-$ and other RS (Hampton *et al*., 2002; Hampton & Orennius, 1997). Thus, high levels of ROS can delay or halt apoptosis but often cell death continues by necrotic or intermediate pathway (Halliwell & Gutteridge, 2007). Reduction in GSH can also activate the sphingomyelinase enzyme to catalyse the formation of ceramide (Singh *et al*., 1998). Ceramide can trigger apoptosis in part by acting upon mitochondria and ceramide also contribute to apoptosis induced by cytokines and some other mediators in several cell types.

1.4.3 Apoptosis, Atherosclerosis and OxLDL

Several studies have identified apoptotic cells including endothelial cells, vascular SMCs, T-lymphocytes and macrophages in animal and human atherosclerotic lesions (Littlewood & Bennet, 2003). The distribution of apoptosis within the plaque as determined by *in situ* end-labelling techniques and *in situ* nick translation is heterogeneous, being more frequent in regions with a high density of macrophages (Liu *et al*., 2005; Tabas, 2005). Macrophage apoptosis has been proposed to be a mechanism by which lipids accumulate within the coronary vasculature and thereby contribute to plaque formation and progression. Apoptosis of macrophages could be beneficial for plaque stability if apoptotic bodies were removed since macrophage apoptosis probably limits the number of necrotic macrophages and thrombogenicity associated with necrotic cell death within lesions (Liu *et al*., 2005). Several studies showed that apoptotic bodies in the advanced atherosclerotic plaque are often not scavenged, therefore activating the coagulation cascade, potentially leading to plaque rupture and luminal thrombosis. Moreover, pathological studies of advanced lesions have revealed a strong correlation between macrophage apoptosis and large necrotic cores on the one hand and the incidence of plaque rupture and acute vascular events on the other (Tabas, 2005).

Two separate caspase-dependent apoptotic pathways have been implicated in oxLDL-induced apoptosis. The extrinsic pathway, mediated by Fas and/TNFR and downstream by caspase-8/caspase-3 was demonstrated in endothelial cells (Li *et al*., 2006; Sata & Walsh, 1998a; Sata & Walsh, 1998b) and macrophages (Li *et al*., 2006). In human coronary endothelial and SMCs, apoptotic signals mediated by both Fas and TNFR were observed (Napoli *et al*., 2000). Activation of apoptotic receptors was accompanied by an increase of proapoptotic and a decrease in antiapoptotic proteins of the Bcl-2 family and resulted in marked activation of caspases. Moreover, oxLDL also activated MAP and Jun kinases (oxidative stress proteins) and increased p53 and other transcription factors (ATF-2, ELK-1, CREB, AP-1) (Napoli *et al*., 2000). It was initially postulated that Bcl-2 inhibits apoptosis by preventing lipid oxidation (Harada *et al*., 1997). Recently Ermak *et al.,* (2008) showed that Bcl-2 plays a role in preventing the release of cytochrome *c* from the mitochondria to the cytosol.

The generation of ROS plays important role in oxLDL-mediated apoptosis, and antioxidants of various types including ebselen, rotenone and vitamin C have been shown to inhibit apoptosis (Coffey *et al*., 1995; Hsieh *et al*., 2001; Siow *et al*., 1999). In endothelial cells, oxLDL induces apoptosis via activation of CPP32-like protease and

appears to involve the elaboration of ROS (Dimmeler *et al*., 1997; Harada *et al*., 1997). Moreover, overexpression of Bcl-2 significantly suppressed the apoptotic cell death (Harada *et al*., 1997). In U937 cells, it was shown that oxLDL-induced apoptosis involved ROS generation. In association with generation of ROS generation there was mitochondrial Bax translocation with a disruption of mitochondrial membrane potential, cytosolic liberation of cytochrome *c* and subsequently activation of caspases-9 and -3 (Ermak *et al*., 2008). Bcl-2 overexpression prevented Bax translocation but failed to prevent ROS generation indicating that ROS is an upstream signal for inducing mitochondrial apoptotic damage (Ermak *et al*., 2008). OxLDL also promotes the over expression of Bax (Kataoka *et al*., 2001; Okura *et al*., 2000) and reduce Bcl-X_L (Siow *et al*., 1999), thereby promoting susceptibility to apoptosis (Kataoka *et al*., 2001).

Some studies observed caspase-3-dependent apoptosis caused by oxLDL (Chen *et al*., 2004; Dimmeler *et al*., 1997; Vindis *et al*., 2005), while others, Porn-Ares *et al.,* (2003) and Gieseg *et al.,* (2008b) reported that oxLDL induced apoptosis by caspase-3 independent pathway. Interestingly, oxLDL trigger caspase-3-dependent apoptosis in THP-1 cells but caspase-3-independent necrosis in U937 cells (Baird *et al*., 2004). OxLDL may activate a caspase-independent apoptotic pathway by the release of AIF from mitochondria (Zhang *et al*., 2004). While, Chen *et al.,* (2004) showed that oxLDL did not cause Bid truncation but activated caspase-3, Porn-Ares *et al.,* (2003) observed that oxLDL induced Bid truncation -without any caspase-3 activation. These discrepancies could be due to the variations in oxLDL preparation from laboratory to laboratory.

A sustained rise of cytosolic calcium also plays an important role in oxLDL-mediated apoptosis by activating Bid cleavage and cytochrome *c* release (Escargueil-Blanc *et al*., 1994; Vindis *et al*., 2005). OxLDL also triggers the over expression of the pro-apoptotic protein p53 (Napoli *et al*., 2000) through a mechanism involving the over expression of manganese superoxide dismutase (MnSOD), and the sphingomyelin–ceramide pathway activation (Kinscherf *et al*., 1998). Exposure of macrophages to oxLDL can increase TNF-α generation which is itself a pro-apoptotic mediator and further contribute to the oxidative burden on the cells by inducing mitochondrial generation of ROS (Jovinge *et al*., 1996). Furthermore, oxLDL decreases expression of the endogenous cellular caspases inhibitor, FLICE-inhibitory protein (FLIP) in human ECs and thereby increases the level of apoptosis (Sata & Walsh, 1998a).

Changes in gene expression induced by oxLDL are mediated through the activation/inhibition of transcription factors, such as ATF-2, ELK-1, CREB, AP-1 and NFκB. For instance, oxLDL and lysoPtCho elicit a dose- and time-dependent biphasic

effect on NFκB (activation by low concentrations of oxLDL and inhibition by higher concentrations) (Alcouffe *et al*., 1999; Sugiyama *et al*., 2004). NFκB regulates the expression of various genes involved in the balance between survival and apoptosis, such as A20, cMyb, cFLIP, Bfl-1/A1, c-IAP2, xIAP, TRAF1, and Bcl-xL (Auge *et al*., 2002). In endothelial cells, oxLDL-induced inhibition of NFκB reduces the expression of anti-apoptotic genes, thereby increasing the susceptibility of cells to apoptosis (Heermeier *et al*., 2001).

Oxysterols components oxLDL, have been demonstrated to largely account for the apoptotic activity of oxLDL in macrophages (Aupiex *et al*., 1995; Chisolm *et al*., 1994). Among the oxysterols, 7-KC which account for up to 30% of the total sterols in oxLDL (Brown *et al*., 1996) is the predominant one. 7-KC in the 10–25 μM range has been shown to induce apoptosis in macrophages, vascular endothelial cells, and SMCs (Lizard *et al*., 1999). Another oxysterol, 25-hydroxycholesterol (25-OHC), induces apoptosis in cultured monocyte-macrophages (Harada *et al*., 1997) and lymphoid cell lines in the range of 1–10 μM. Oxysterols induce the release of cytochrome *c* from mitochondria (Lizard *et al*., 1998), which is the hallmark of the mitochondrial apoptosis pathway. 7β-OH and 25-OHC caused apoptosis in U937 cells and HL60 cells (Aupiex *et al*., 1995), as did 7-KC (Lizard *et al*., 1998), which also induce apoptosis in bovine ECs and human ECs (Lizard *et al*., 2000). 2-Oxoaldehydes caused apoptosis in U937 cells and rabbit aortic SMCs were found not to undergo apoptosis with lysoPtCho .

A large and rapid decrease in glutathione level was observed during 7-KC- and oxLDL-induced apoptosis in U937 cells (Lizard *et al*., 1998; Baird *et al*., 2004; respectively). However, in oxLDL-induced apoptosis in THP-1, there was only a small decrease in glutathione level (Baird *et al*., 2004). While caspse-3 activation was seen in in THP1 cells, it was absent in U937 cells. It was postulated that the inhibition of caspase-3 activation seen here is probably due the glutathione loss where the rapid macrophage GSH loss caused by oxLDL have greatly increased the intracellular antioxidant stress, where caspase thiols can oxidized resulting in the loss of caspase activity (Baird *et al*., 2004).

Recently, Panini *et al*, (2001) and Rusinol *et al.,* (2004) demonstrated that the mechanism by which 25-OHC and 7-KC induce apoptosis involves an increase in cytosolic calcium and the subsequent activation of cytosolic phospholipase A_2 ($cPLA_2$). Their studies also show that macrophages treated with 5,8,11,14-eicosatetraynoic acid (ETYA), an inhibitor of arachidonic acid (AA) metabolism, are resistant to the induction of apoptosis by 25-OHC or 7-KC indicating that metabolism of $cPLA_2$-released AA may be required for

the induction of apoptosis by these oxysterols. Interestingly using P388D1 macrophage cell line and mouse peritoneal macrophages (MPMs), it was revealed that the loss of ACAT activity in macrophages, results in reduced induction of apoptosis in response to 7-KC or oxLDL implying a role for ACAT in 25-OHC- and 7-KC- induced apoptosis (Freeman *et al*., 2005).

MmLDL, generated by exposure of LDL to 15-LO expressing cells, is able to activate PI3K/Akt in macrophages (Rusiñol *et al*., 2004) a pathway known to promote cell survival. This mechanism is shown to be employed by macrophages for their survival at atherosclerotic lesions (Boullier *et al*., 2006). In addition, a moderate reduction in extracellular pH can also protect macrophages against oxLDL-induced apoptosis (Gerry and Leake, 2008).

Interestingly, receptors for oxLDL have recently been shown to affect cellular apoptotic responses to oxLDL differentially. LOX-1 expression was linked to apoptosis in ECs (Adam *et al*., 2000; Gu *et al*., 1998), SR-AII over expression in SMCs increased apoptosis (Lehtolainen *et al*., 2000) and CD36 was linked to apoptosis in a monocyte/macrophages and other cells (Asmis & Jelk, 2000; Rusinol *et al*., 2000) however, SR-AI expression was linked to anti-apoptotic influence in THP-1 cells (Liao *et al*., 2000). There is evidence that the surface of oxLDL particles and the surface of apoptotic cells have common epitopes and compete for receptor-mediated clearance by macrophages (Alcouffe *et al*., 1999; Bird *et al*., 1999).

1.5 Inflammation and Atherosclerosis

Macrophages and to a lesser extent T lymphocytes appear to be the dominant cells at the immediate site of plaque rupture or superficial erosion (Libby & Hansson, 1991; van der Wal *et al*., 1994). These sites moreover, were always characterised by abundant expression of HLA-DR antigens on both inflammatory cells and adjacent SMCs suggesting an active inflammatory reaction (van der Wal *et al*., 1994). The HLA-DR antigens are class II major histocompatibility complex (MHC) membrane bound glycoprotein that play important role in the regulation of immune response. The detection of inflammatory markers and antibodies in patients provides additional support for the inflammatory nature of the atherosclerotic lesion. Xu *et al.,* (1993) reported that there is a strong correlation between anti-heat shock protein 65 (anti-hsp65) antibodies and carotid atherosclerosis, suggesting that hsp65 might be involved in the pathogenesis of atherosclerosis. In addition, measurement of serum levels of C-reactive protein (CRP) (an important marker of inflammation) demonstrates subclinical inflammatory states, which may reflect vascular

inflammation (Wilson *et al*., 2006). CRP was also found abundant in early and late stages of atherosclerotic lesions (Patrick & Uzick, 2001). Liuzzo *et al.,* (1994) reported that, CRP and serum amyloid A protein levels were elevated in most of the patients with a diagnosis of unstable angina. Elevation of soluble CD40 ligand is associated with platelet activation and therefore, increased risk of cardiovascular events (Scott, 2004). The level of neopterin which is synthesised and released from IFN-γ activated macrophages is also significantly elevated in patients with vascular disease (Schumacher *et al*., 1992; Tatzber *et al*., 1991).

Various infectious agents have also been shown to initiate or promote inflammatory atherogenesis. *Chlamydia pneumonia, Helicobacter pylori* and cytomegalovirus have been identified in cardiovascular atheroma (Osterud & Bjorklid, 2003; Torgano *et al*., 1999). It is noteworthy that lipopolysaccharide (LPS) is capable of enhancing both cell- and copper-mediated LDL oxidation (Maziere *et al*., 1999).

1.5.1 Interferon-γ and Macrophages

Macrophages are extremely versatile cells involve in a number of complex functions in disease and health. The interaction between macrophages and lymphocytes within the atherosclerotic lesion microenvironment exemplifies a site where both innate and adaptive immunity contribute towards disease progression. T lymphocytes constitute a significant proportion of the cell population in the atherosclerotic plaque. Many of these T lymphocytes are in an activated state (Hansson *et al*., 1989a). There is evidence for local IFN-γ secretion both directly by immunohistochemistry (Hansson *et al*., 1989b) and indirectly by the induction of histocompatibility gene expression in surrounding cells (Carpenter *et al*., 1995b; Libby, 1995). In addition, both protein and mRNA for IFN-γ have been detected in atherosclerotic lesions from humans and mice (Hansson *et al*., 1989b; Zhou *et al*., 1998).

IFN-γ has a dimer structure, and is much more plurifunctional than the other interferons, carrying out antiviral, anticellular, antiparasitic and immunoregulatory activities. IFN-γ production is controlled by cytokines secreted by antigen presenting cells (APCs) most notably IL-12 and IL-18. These cytokines serve as a bridge to link infection with IFN-γ production in the innate immune response. Macrophage recognition of many pathogens induces secretion of IL-12 and chemokines. These chemokines attract NK cells to the site of inflammation, and IL-12 promotes IFN-γ synthesis in these cells. In macrophages, NK and T cells, the combination of IL-12 and IL-18 stimulation further increases IFN-γ production (Schroder *et al*., 2004).

IFN-γ is associated with both pro- and anti-atherogenic activities. IFN-γ proatherogenic activities include up regulation of antigen presenting components like MHCs, activation of macrophages, stimulation of respiratory burst (Hansson *et al*., 2006), and induction of ceruloplasmin synthesis (Mazumder *et al*., 1997). In addition, IFN-γ promotes T lymphocyte and monocyte recruitment by enhancing release of endothelial-derived T cell α-chemoattractant (Cole *et al*., 1998) and increasing expression of the VCAM, ICAM-1 and MCP-1 chemokines (Leon & Zuckerman, 2005). Conversely, IFN-γ inhibits induction of E-selectin, P-selectin, PECAM-1, MCP-1 receptor and CCR2 (Leon & Zuckerman, 2005). Its antiatherogenic effect extend to the ability of IFN-γ to inhibit 15-LO synthesis (Folcik *et al*., 1997).

The effect of IFN-γ on cholesterol and lipid trafficking is rather conflicting. For example SR-A and CD36 mRNA and protein expressions in human monocyte-derived macrophages and THP-1 cells macrophages are decreased by *in vitro* treatment with IFN-γ (Geng & Hansson, 1992; Grewal *et al*., 2001; Nakagawa *et al*., 1998). The same studies observed a decrease in intracellular cholesteryl ester accumulation and subsequently foam cell formation. In contrast to the down-regulation of SR-A and CD36, IFN-γ increased the expression of SR-PSOX in human monocytes and THP-1 cells, both at the protein and mRNA levels (Wuttge *et al*., 2004). A similar effect was observed in IFN-γ treated apoE knockout mice where increased macrophage expression of SR-PSOX was detected in macrophages localised at the atherosclerotic lesions (Wuttge *et al*., 2004). Up-regulation of this scavenger receptor would provide a mechanism for the continued uptake of oxLDL by macrophages while other scavenger receptors were down regulated by IFN-γ.

IFN-γ inhibits LDL receptor expression in murine and human macrophages (Garner *et al*., 1997a; LaMarre *et al*., 1993) and VLDL receptor expression in phorbol ester stimulated THP-1 and HL60 human macrophage cell (Kosaka *et al*., 2001). IFN-γ also reduces lipoprotein (a)/apoprotein (a) receptor expression by disrupting ligand-induced receptor recycling (Skiba *et al*., 1994). In addition, IFN-γ also decreases cholesterol efflux and ATP binding cassette transporter-1 (ABC1) expression in murine macrophages and macrophages derived foam cells and cholesterol efflux in THP-1 cells (Panousis & Zuckerman, 2000; Reiss *et al*., 2004).

Moreover, IFN-γ decreases synthesis of lipoprotein lipase (LPL) (Garner *et al*., 1997a; Jonasson *et al*., 1990), apoE (Garner *et al*., 1997a; Kalkan *et al*., 2005) and cholesterol 27-hydroxylase (Carpenter *et al*., 2001; Reiss *et al*., 2004). Decrease in LPL and apo E synthesis could result in reduced LDL and VLDL clearance from the circulation

or lesion while decrease synthesis of 27-hydroxylase could reduce clearance of cholesterol from foam cells as 27-hydroxylation represents the first step in extrahepatic cholesterol metabolism. Finally, IFN-γ stimulated increases in ACAT activity and expression in macrophages would be expected to promote cholesterol storage by increasing cholesterol ester content thereby promoting foam cell formation (Panousis & Zuckerman, 2000).

1.5.2 Neopterin and 7,8-Dihydroneopterin

In addition to the functions above, IFN-γ also upregulates the synthesis of 7,8-dihydroneopterin. All pteridines, including 7,8-NP and neopterin are synthesised *in vivo* from guanosine triphosphate (GTP) precursor, via GTP cyclohydrolase 1 (GTP-CH) (Figure 1.8). The main trigger of GTP-CH is IFN-γ.

The compound 7,8-dihydroneopterin triphosphate (NH_2TP) is on the biosynthetic pathway of 5,6,7,8-tetrahydrobiopterin (BH_4). The conversion of NH_2TP to BH_4 requires the sequential action of 6-pyruvol tetrahydropterin synthase (6-PTPS) and sepiapterin reductase (Wachter *et al*., 1992). BH_4 represents the electron donor in the hydroxylation of phenylalanine to tyrosine in the liver and of tyrosine to L-dopa and tryptophan in neuroendocrine tissue synthesising catecholamines or serotonin (Walter *et al*., 2001). BH_4 also serves as a cofactor for nitric oxide synthase (Walter *et al*., 2001).

In human and primate tissues or cell lines, activity of PTPS was found to be lower as compared to that of other mammals with lowest activities found in monocytes and macrophages (Werner *et al*., 1990). As a consequence, instead of synthesising BH_4, monocytes and macrophages accumulate NH_2TP, which, is then released as 7,8-NP due to the action of intracellular phosphatases. 7,8-NP diffuses out of the activated macrophages into the intracellular space and finally to the plasma. 7,8-NP can be oxidised to two different products depending on the oxidant. Firstly, some of the 7,8-NP is oxidised to the highly fluorescent neopterin (Hamerlinck, 1999). To date, the only mechanism known to generate neopterin from 7,8-NP is oxidation by hypohalous acids in particular HOCl, by the loss of hydrogen at carbon-7 and nitrogen-8 (Gieseg *et al*., 2001; Widner *et al*., 2000). The other product is 7,8-dihydroxanthopterin that comes about through the loss of the trihydroxylpropyl side chain at position 6 of 7,8-NP. The reaction may occur by a retro-aldol reaction initiated by the abstraction of a hydrogen atom from the middle carbon hyroxyl group on the 7,8-NP side chain. This may occur through the scavenging action of 7,8-NP of superoxide, peroxyl radicals and hydrogen peroxide (Gieseg *et al*., 2001; Murr

et al., 1994; Widner *et al*., 2000). The compound 7,8-dihydroxanthopterin is not fluorescent and is difficult to detect in plasma.

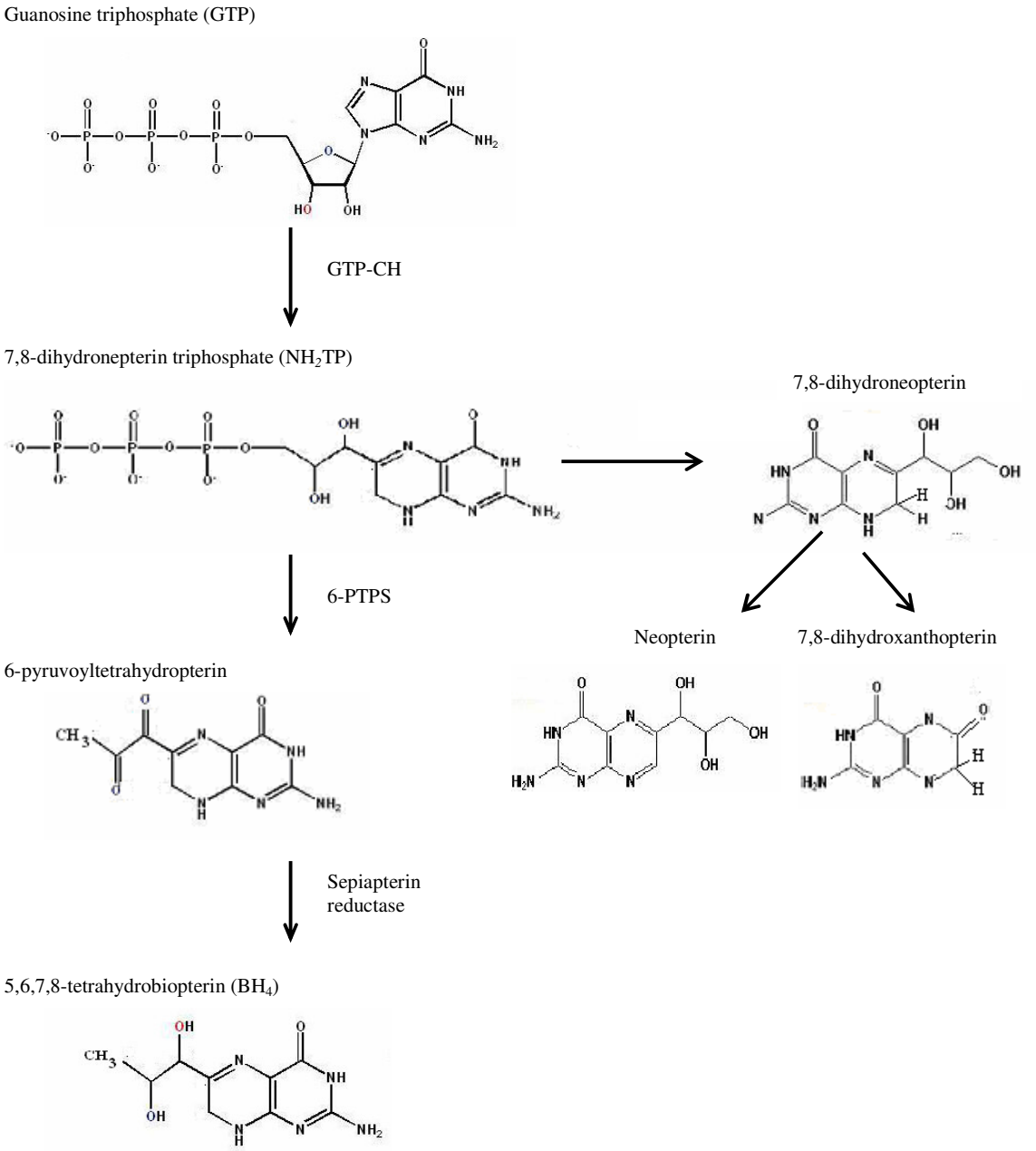

Figure 1.8 The biosynthesis and metabolism of 7,8-dihydroneopterin and neopterin.
Human monocytes/macrophages lack the enzyme 6-PTPTS that converts NH_2TP to 6-pyruvol tetrahydropterin. Monocytes and macrophages instead of synthesising BH_4 accumulate NH_2TP, which, after hydrolysis by phosphatases, is excreted as 7,8-dihydroneopterin or neopterin. Adapted from Hoffmann *et al.,* (2003) with modification.

1.5.3 Neopterin as a Marker of Inflammation

Due to its fluorescent nature, neopterin is easily measured in plasma and urine by HPLC (Rippin, 1992; Werner *et al*., 1987). Neopterin can also be measured using immuno-based methods such as radioimmunoassay or enzyme-linked immunosorbant assay (ELISA) (Wachter *et al*., 1989; Westermann *et al*., 2000). For healthy individuals, mean neopterin serum concentrations lie within 5.2 $\pm$ 2.7 nM and in urine range between 100 and 200 µmol/mol creatinine (Wachter *et al*., 1989). Only minimal data of other body fluids such as synovial fluid, saliva and cerebrospinal fluid from healthy controls are available due to the invasive techniques required to obtain these samples. Nevertheless, neopterin concentrations in these samples range between 1.0 and 9.0 nM (Hoffmann *et al*., 2003). In pus and plaque, neopterin concentrations were found to be up to 1.2 µM and 2.5 µM respectively (Firth et al., 2008; Gieseg, *et al*., 2008a, respectively).

Neopterin is constantly excreted via the kidneys, and the half-life of neopterin within the circulatory system was calculated to be approximately 90 min (Fuchs *et al*., 1994). The neopterin:7,8-NP ratio of 1:2 is nearly constant in urine, serum, or cerobrospinal fluid suggesting that neopterin is not further metabolised after production. Higher 7,8-NP to neopterin ratios exists in arterial as compared with venous blood. Since neopterin is stable in biological fluids, it has become a useful marker for infectious and inflammatory diseases. In certain countries, neopterin measurements are routinely used for blood and organ donor screenings. Using a cut-off limit of the 98th percentile of neopterin concentrations (=10nM), it is feasible to detect acute infections in blood donors with great sensitivity (Hoffmann *et al*., 2003).

The production of 7,8-NP and neopterin correlates closely with activation of immune response by IFN-γ involving cell-mediated (Th1) immunity (Schroecksnadel *et al*., 2004). An increased neopterin concentration in urine and serum is found in infections by viruses including human immunodeficiency virus (HIV), living bacteria, fungi and parasites. Increased in neopterin concentrations also reflect the severity of the diseases for example autoimmune diseases, malignant tumor diseases, allograft rejection and some neurodegenerative diseases (Fuchs *et al*., 1994; Hamerlinck, 1999; Hoffmann *et al*., 2003; Wirleitner *et al*., 2005).

Currently, plasma neopterin is not generally used in the management of cardiovascular diseases, however there is considerable amount of knowledge on its value. For example, higher serum concentrations of CRP and neopterin together with lower phospholipid concentrations are observed in patients with coronary heart disease (Rudzite

et al., 2003). The decrease of serum total phospholipids concentrations in coronary heart disease may depend on an impaired phosphatidylcholine biosynthesis and an increased phosphatidylcholine phagocytosis mediated by CRP (Rudzite *et al*., 2003). Serum neopterin concentration is increased in patients with unstable angina and acute myocardial infarction (Schumacher *et al*., 1992; Schumacher *et al*., 1997; Tatzber *et al*., 1991). There is a strong correlation between serum neopterin and the thrombolysis in myocardial infarction risk score in patients with unstable angina or acute myocardial infarction (Johnston, *et al*., 2006).

Some studies also demonstrate that neopterin production increased with increased production of reactive oxygen species and low serum concentrations of antioxidants like α-tocopherol (Schroecksnadel *et al*., 2004) and folic acid (Nathan, 1986). These evidence point to the ability of neopterin as a marker of oxidative stress caused by an activated immune system. Therefore, by measuring neopterin, not only the extent of cellular immune activation, but also the extent of tissue damage caused by reactive oxygen species can be estimated.

1.5.4 Physiological Role of Neopterin and 7,8-Dihydroneopterin

The physiological role of neopterin or 7,8-NP synthesis during inflammation is controversial. It has been suggested that they are synthesised as pro-oxidants, enhancing oxidant production and cell death in combination with TNF-γ. In contrast 7,8-NP has also been reported to act as antioxidant protecting biomolecules and macrophages from oxidants during inflammation (Gieseg, *et al*., 1995; Gieseg, *et al*, 2007; Gieseg, *et al*., 2008a,b). Numerous *in vitro* studies have provided evidence supporting these two functions as well as roles in apoptosis, signal transduction and gene expression.

1.5.4.1 Effects of Neopterin and 7,8-Dihydroneopterin on Cell Death

7,8-NP and neopterin are found to be very potent antioxidants at low concentration. The addition of 1.5 mg/ml of oxLDL caused 50% loss in cell viability in THP-1 and U937 cells as measured using MTT assay (Baird *et al*., 2004). In similar experiment, 90% loss of glutathione was observed in U937 cells but only 25% glutathione loss was observed in THP-1 cells (Baird *et al*., 2004). Two hundred micromolar of 7,8-NP restored the U937 cell viability to 90% of the untreated control cells (Baird *et al*., 2005). The addition of 7,8-NP also resulted in concentration dependent protection of the cellular thiol pool with 200 μM 7,8-NP reducing the oxLDL mediated loss to only 50% of the control U937 cells'

level. In contrast the THP-1 cells' viability and thiol loss could not be prevented by the addition of 7,8-NP (Baird *et al*., 2005). Interestingly, 200 μM 7,8-NP provides protection to both cell lines exposed to AAPH peroxyl radicals suggesting that the protection from oxLDL was not due to the scavenging of extracellular radicals or oxidants on the oxLDL (Baird *et al*., 2005). The preincubation of oxLDL with 7,8-NP did not reduce the cytotoxicity (Baird *et al*., 2005). This suggests that 7,8-NP may be acting in U937 cells by scavenging intracellular oxidants generated in the presence of oxLDL and consequently protecting the intracellular glutathione pool thus maintaining the redox state of the cell (Baird *et al*., 2005).

In erythrocytes, 7,8-NP at 50 μM reduced the H_2O_2- and AAPH-induced haemolysis by 39% and 100% of the control value after 12 hours incubation. (Gieseg *et al*., 2000b; Gieseg *et al*., 2001). One hundred μM 7,8-NP prevented hypochlorite (HOCl) haemolysis using a high HOCl concentration of 5 μmole/HOCl/10^7 RBC (Gieseg *et al*., 2001). HPLC-TBAR analysis and measurement of dienes failed to show any connection between 7,8-NP inhibition of H_2O_2- and AAPH-induced haemolysis and lipid peroxidation. However, protein bound DOPA (protein oxidation marker) formation was reduced when erythrocytes were pretreated with 7,8-NP before addition of AAPH. This lead to speculation that 7,8-NP inhibit erythrocyte haemolysis by preventing protein oxidation (Gieseg *et al*., 2000b; Gieseg *et al*., 2001).

The antioxidant effect of 7,8-NP and neopterin was also demonstrated by Baier-Bitterlich *et al.,* (1995). Lower concentrations of 7,8-NP and neopterin, which is up to concentrations of 300 μM and 1 mM respectively, inhibit TNF-α mediated apoptosis of U937. Interestingly another study (Kojima *et al*., 1993) reported a suppression of superoxide-generating NADPH-oxidase by neopterin in macrophages stimulated with PMA. Parallel with this, at lower concentrations, neopterin and 7,8-NP appeared to scavenge reactive oxygen intermediates and quench hydrogen peroxide induced chemiluminiscence.

In contrast, 7,8-NP exhibits a strong pro-oxidant activity at high concentrations. A concentration of 5 mM 7,8-NP superinduced TNF-α mediated apoptosis in U937 cells (Baier-Bitterlich *et al*., 1995). At 5 mM concentration, 7,8-NP also induced a maximum apoptotic effect on rat pheochromocytoma cell line PC12 (Enzinger *et al*., 2002), neuronal NT2/HNT cells (Spottl *et al*., 2000) and Jurkat cells (Enzinger *et al*., 2002; Spottl *et al*., 2000; Wirleitner *et al*., 1998; Wirleitner *et al*., 2001). In Jurkat cells, 7,8-NP was demonstrated to induce apoptosis by a Bcl-2 sensitive pathway (Enzinger *et al*., 2002). In rat alveolar epithelial cell line L2 cells, a strong proapoptotic effect of the pteridines were

discovered (Schobersberger *et al*., 1996). Neopterin or 7,8-NP with concentration as low as 10 μM induced apoptosis and also augments TNF-α/ IFN-γ-mediated apoptosis in L2 cells. The same study also revealed no involvement of NO production on neopterin-mediating apoptosis in L2 cells (Schobersberger *et al*., 1996). This was not the case in neopterin- and 7,8-NP-induced apoptosis in vascular smooth muscle cells (VSMC) where inhibition of iNOS results in a strong suppression of the proapoptotic effects of neopterin in VSMC and it was suggested that neopterin-induced iNOS gene expression in VSMC via activation of NF-κB (Hoffmann *et al*., 1998; Hoffmann *et al*., 1996).

High doses of 7,8-NP (5 mM) in the presence of TNF-α also enhanced the formation of ROS in U937 cells (Baier-Bitterlich *et al*., 1995). Later it was illustrated that neopterin enhances hydrogen peroxide effects only in the presence of iron chelator complexes. Antioxidants ranging form N-acetylcysteine (NAC) to pyrrolidine dithiocarbamate (PDTC), catalase and superoxide dismutase (SOD) have been demonstrated to significantly inhibit 7,8-NP-mediated apoptosis (Baier-Bitterlich *et al*., 1995; Baier-Bitterlich *et al*., 1996a; Enzinger *et al*., 2002; Hoffmann *et al*., 2003; Spottl *et al*., 2000). It therefore appears that the presence of excess 7,8-NP results in ROS generation, disrupting the oxidant/antioxidant balance and ultimately leading to cell death.

1.5.4.2 Effect of Neopterin and 7,8-Dihydroneopterin on Radical Formation

7,8-Dihydroneopterin rapidly reacts with free radical and oxidising species. The action can be either pro- or antioxidant depending on their concentrations. At micromolar concentrations, 7,8-NP scavenges luminol chemiluminescence of zymosan-activated human macrophages (Heales *et al*., 1988) and inhibits hydrogen-peroxide-induced luminol chemiluminescence (Shen, 1994). In splenic macrophages/PMA and xanthine/xanthine oxidase superoxide generation system, neopterin as low as 1 μM significantly suppresses the superoxide generation via the inhibition of NADPH-oxidase (Kojima *et al*., 1993). 7,8-NP (Gieseg *et al*., 1995; Oettl *et al*., 1997) and to a lesser extent neopterin (Oettl *et al*., 1997) acts a potent inhibitor of peroxyl radicals by effectively scavenging the radicals. Neopterin in contrast to 7,8-NP shows no reduction of the ESR signal except with superoxide radicals produced by xanthine oxidase. This effect is shown to be due to an inhibition of enzyme rather than to radical scavenging (Oettl *et al*., 1997; Oettl & Reibnegger, 1999). A spin trap study revealed a rate constant for the reaction between 7,8-NP and peroxyl radicals that is quite close to the rate constant for the reaction between

peroxyl radicals and α-tocopherol (Oettl *et al*., 1997) indicating that 7,8-NP is as efficient antioxidant as α-tocopherol.

7,8-NP's antioxidant capacities had been clearly demonstrated by it ability to inhibit LDL oxidation (Gieseg *et al*., 1995). Concentrations of 7,8-NP between 1 and 10 μM dramatically increases, in a dose dependent manner, the lag time of low density lipoprotein oxidation and diminishing the consumption of vitamin E, mediated by copper ions or the peroxyl radical generator 2,2'-azobis (2-amidino propane) dihydrochloride (AAPH). 7,8-NP also inhibits AAPH mediated oxidation of linoleate. 7,8-NP appeared to be acting as a potent chain breaking antioxidant which functions by scavenging lipid peroxyl radicals (Gieseg *et al*., 1995). Protein hydroperoxides and their decay product carbonyls make a large and significant contribution to the oxidative damage occurring on the LDL particle (Gieseg *et al*., 2003; Yan *et al*., 1997). 7,8-NP also appears to prevent copper- and AAPH-induced protein hydroperoxide formation on LDL by scavenging the lipid-derived radicals that are suggested to promote protein peroxidation (Gieseg *et al*., 2003). 7,8-NP has also been shown to decompose protein hydroperoxides on BSA, but it is 7,8-NP's scavenging activity that give more significant form of protection against the AAPH-mediated peroxidation of BSA (Duggan *et al*., 2001). Using THP-1 cells and HMDMs, oxLDL formation is totally inhibited by micromolar concentrations of 7,8-NP (Gieseg & Cato, 2003). As THP-1 cell mediated oxidation is independent of superoxide formation, it is likely that inhibition is due to scavenging the lipid peroxyl radicals in the LDL (Gieseg & Cato, 2003).

Nitric oxide and peroxynitrite have been implicated in modification of LDL within plaques. 7,8-NP appears to efficiently inhibit peroxynitrite-induced nitration of tyrosine by scavenging reactive nitrogen species (RNS) (Greilberger *et al*., 2004; Herpfer *et al*., 2002; Widner *et al*., 1998). The protective effect of 7,8-NP on both peroxynitrite and copper-mediated LDL oxidation was enhanced by preincubation before addition of oxidants which suggests that 7,8-NP might diffuse into the phospholipids layer of the LDL particle (Herpfer *et al*., 2002).

Conversely, the pteridines also exhibit pro-oxidant activities. Neopterin is capable of enhancing peroxynitrite as well as copper-mediated LDL oxidation (Herpfer *et al*., 2002) though the effect cannot be reproduced in our laboratory. Although 7,8-NP is clearly a potent radical scavenger, under certain circumstances it can also exhibit pro-oxidant activity. In copper-induced LDL oxidation, a prooxidative effect of 7,8-NP could be observed if the 7,8-NP was added late during the lag phase of oxidation (Herpfer *et al*., 2002). This is probably due to the ability of 7,8-NP to reduce copper to its redox active

form, with antioxidant activity then dominating reactions once the reduction was complete (Herpfer *et al*., 2002). The reaction also requires very high 7,8-NP concentrations. The same effect was reported in phosphate-buffered solution containing low levels of iron where 7,8-NP enhanced the rate of hydroxyl radical generation (Oettl *et al*., 1999). 7,8-NP also has been shown to reduce another transition metal, iron, to the redox active ferrous ion state (Wirleitner *et al*., 2005). 7,8-NP's strong reducing activity is also suggested to promote the oxidation of both minimally and moderately oxidized LDL in the presence or absence of copper ions (Greilberger *et al*., 2004).

Neopterin and high concentration of 7,8-NP intensify hydrogen peroxide- and chloramine T-mediated luminol-dependent chemiluminescence assay suggesting an enhancement of free radical formation (Murr *et al*., 1996; Weiss *et al*., 1993). Unlike 7,8-NP, the effects of neopterin were generally dependent on pH. For example, 3-Nitrotyrosine formation was promoted by neopterin only between pH 4 to pH 5.5 (Widner *et al*., 1998), while its enhancement of chloramine T- and hydrogen peroxide-induced chemiluminiscence and cytotoxicity required a neutral or slightly alkaline pH (Weiss *et al*., 1993). In addition hydrogen peroxide-induced chemiluminescence was shown to be dependent on the presence of iron chelator complexes (Murr *et al*., 1994).

A few enzymes that play an important role as a source of radicals are also affected by the pteridines. For example, in human neutrophils, it is suggested that by inhibiting myeloperoxidase, neopterin increases generation of singlet oxygen and hydroxyl radical and nitric oxide (Razumovitch *et al*., 2003). In a melanoma cell line, neopterin enhances UV-A irradiation-induced DNA synthesis, which is inhibited by addition of the antioxidant catalase (Kojima *et al*., 1995).

Moreover, neopterin can potentiate the toxicity of oxygen and chloride species originating from hydrogen peroxide and chloramines T against *Escherichia coli*, (Wede *et al*., 1999; Weiss *et al*., 1993). At high concentration, 7,8-NP behaved like a pro-oxidant and the most likely explanation is that in the presence of molecular oxygen, 7,8-NP is prone to auto-oxidation and capable to form hydroxyl radicals via generation of superoxide anion (Oettl *et al*., 1999).

1.5.4.3 Effect of Neopterin and 7,8-Dihydroneopterin on Gene Expression and Signal Transduction

Reactive oxygen intermediates play an important role in cellular metabolic events such as signal transduction and regulation of gene expression. Disruption of the cellular redox

balance can also be accounted for neopterin- and 7,8-NP mediated activation of various redox transcription factors. The transcription factor AP-1 (activator protein 1) is known to be able to sense the intracellular redox state and regulates the expression of multiple genes involved in stress response. It is a dimer of proteins of the *Fos* and *Jun* families, usually a c-*fos* /c-*jun* heterodimer. The activity of AP-1 is controlled both by regulating how much c-*fos* and c-*jun* the cell makes, and by phosphorylation of already-synthesised proteins (e.g. by mitogen-activated protein kinases (MAPKS)). Various ROS can alter both processes.(Halliwell & Gutteridge, 2007).

Along this line it was observed that incubation of cells with neopterin and to a greater extent 7,8-NP together with cGMP induces *c-fos* gene expression in a *c-fos*-CAT reporter transactivation system of NIH3T3 mouse fibroblasts (Uberall *et al*., 1994). In Jurkat cells, 7,8-NP clearly activates the redox-sensitive transcription factor activation protein-1 chloramphenicol acetyltransferase (AP-1-CAT) and amplifies TNF-α induced NF-κB activation (Baier-Bitterlich *et al*., 1997b). 7,8-NP was found to enhance apoptosis in rat PC12 cells by up regulating signalling cascades associated with MAPKS (Enzinger *et al*., 2001). Activation of p44/42 ERK was mediated by 7,8-NP alone, while strong activation of stress-activated protein kinase (SAPK) required co-incubation with TNF-α (Enzinger *et al*., 2002). Altogether these data suggests that neopterin and 7,8-NP may alter the gene expression by modulating the intracellular redox state. It should be noted that, to date, no specific pteridine receptor has been reported.

Neopterin enhances inducible nitric oxide synthase (iNOS) gene expression and subsequent nitric oxide release in rat vascular SMCs (Schobersberger *et al*., 1995). Neopterin also amplifies the secretion of TNF-α in peripheral blood mononuclear cells induced by LPS, IFN-γ, and IL-2 (Barak & Gruener, 1991). In VSMC, neopterin is a potent stimulus of TNF-α gene expression and TNF-α protein release. Coincubation of cells with both compounds resulted in at least additive effects on nitric oxide synthesis (Hoffmann *et al*., 1998). These data suggest that neopterin and tumor necrosis factor-alpha are closely associated with regard to synthesis and effects, respectively. In conjunction with this, pretreatment of cells with the antioxidant pyrrolidine dithiocarbamate completely suppressed the effects of neopterin on NF-κB translocation to the nucleus, iNOS gene expression and nitric oxide (Hoffmann *et al*., 1996). The interactions of both inflammatory mediators (neopterin and TNF-α) in vascular SMCs might contribute to the excessive release of nitric oxide during inflammation.

In transfected Jurkat cells, 7,8-NP induces trans-activation of the IFN-γ as well as the type I human T-cell leukaemia virus long terminal repeat sequence and HIV-1 promoter, which is further substantiated when 7,8-NP is given in combination with hydrogen peroxide (Baier-Bitterlich *et al*., 1996a; Baier-Bitterlich *et al*., 1997a). A time- and concentration-dependent effect of neopterin on ICAM-1 gene expression and protein synthesis in type II-like alveolar epithelial cells has been detected (Hoffmann *et al*., 1999) and as mentioned earlier increased production of ICAM-1 promote the recruitment of immune cells into the intima. Infectious diseases of the lungs (e.g. sarcoidosis, fibrosis, adult respiratory distress syndrome) are also associated with enhanced serum concentrations of neopterin and an increased production of ICAM-1 (Wirleitner *et al*., 2005).

The pteridines also affect second messengers. For example, both neopterin and 7,8-NP at micromolar concentrations induce an intracellular calcium influx in THP-1 cells (Woll *et al*., 1993) and effectively inhibits ATP-induced calcium release from alveolar epithelial cells (Hsieh *et al*., 2001). Neopterin was also demonstrated to cause cardiac contractile dysfunction in isolated perfused rat hearts (Balogh *et al*., 2005). These results imply the adverse clinical effect of neopterin since deposition of calcium represents a serious deterioration in patient prognosis due to the increasing complexity of the plaque tissue.

1.6 Research Programme

There are two major aims of this PhD project:

- to develop foam cell model by treating human monocyte-derived macrophages (HMDMs) with copper oxidised low density lipoprotein (oxLDL).
- to investigate the potential protective effect of 7,8-NP on oxLDL-induced damage to HMDMs and foam cells.

The formation of foam cells from monocyte-derived macrophages is believed to be the hallmark of the pathogenesis of atherosclerosis whereby; cytotoxic effect of oxLDL is detrimental to the atherosclerotic lesions. The role of 7,8-NP *in vivo* remains controversial but, given the oxidative stress that the cells encounter at and the inflammatory nature of the atherosclerosis plaque, the cells are likely to evolve some mechanisms to survive in these environments. Increasing number of studies have demonstrated an antioxidant ability of 7,8-NP *in vitro*, raising the possibility that macrophages may synthesize this 7,8-NP to protect themselves and/or other substrates from oxidative damage.

Chapter 3 will discuss the preliminary work done on optimising the factors needed for maximum growth of HMDMs. This chapter will clarify the effect of different media, percentage of heat inactivated human serum and tissue culture plates on the growth of HMDMs. The formation of foam cells is investigated in Chapter 4. The accumulation of cholesteryl ester in cells treated with oxLDL as compared to control cells (cells not treated with oxLDL) will be used to determine the formation of foam cells. The lipid contents (free and total cholesterol contents) are analysed by high performance liquid chromatography (HPLC) and gas chromatography (GC) methods. Oil rapid-O staining will also be used to show the accumulation of lipid in the cells. Attention will then turn to the effects of toxic concentration of oxLDL on cholesteryl ester loaded macrophages by looking at the cell viability and the secretion of 7,8-NP.

The mechanisms of oxLDL-induced damage on HMDMs will be discussed in detail in Chapter 5. Loss in cell viability and changes in morphology will be used to determine the cytotoxic effects of oxLDL. Effects of oxLDL on glutathione loss, caspase-3 activation, cytochrome *c* release, ROS generation and phosphatidylserine exposure will be examined. The efficacy of 7,8-NP to protect HMDMs from oxLDL-induced damaged will be conducted by adding 7,8-NP.

2 Materials and Methods

2.1 Materials

2.1.1 Reagents

All reagents used were of analytical grade or better. All solutions were prepared using ion-exchanged ultra filtered water, produced using a NANOpure ultrapure water system from Barnstead/Thermolyne (IA/USA).

β-mercaptoethanol	Sigma Chemical Co., St. Louis, USA
1,1'-dioctadecyl-3,3,3',3'-tetramethylindocarbocyanine perchlorate (DiI)	Aldrich Chemical Co., Wisconsin, USA
1,1,3,3-Tetramethoxypropane (TMP)	Sigma Chemical Co., Missouri, USA
1,4-Dithiothreitol (DTT)	Boehringer, Mannheim, Germany
3-[4,5-Dimethylthiazol-2-yl]-2,5-diphenyl-tetrazolium bromide (MTT)	Sigma-Aldrich Chemical Co., Missouri, USA
4’6-diamidino-2-phenylindole (DAPI)	Aldrich Chemical Co., Wisconsin, USA
4-morpholine-propanesulfonic acid (MOPS)	Sigma Chemical Co., Missouri, USA
7,8-Dihydroneopterin (7,8-NP)	Schircks Laboratory, Switzerland
Acetic acid	Merck Ltd, Poole, England
Acetone	Merck Ltd, Poole, England
Anchor non fat milk powder	Fonterra Brand New Zealand, Ltd, NZ
Annexin V Apoptosis Kit	Santa Cruz Biotechnology Inc., (USA)
Argon gas	BOC Gasses; Auckland, NZ
Ascorbic acid	Sigma Chemical Co., St. Louis, USA
Bicinchoninic acid (BCA) protein determination kit	Pierce, Illinois, USA
Bovine serum albumin (BSA)	Sigma Chemical Co., Missouri, USA
Bromophenol blue	Sigma Chemical Co., Missouri, USA
Butylated hydroxytoluene (BHT)	Sigma Chemical Co., Missouri, USA
Calcium chloride	BDH lab supplies Ltd., Poole, England
Chelex 100 resin	Bio-Rad Laboratories, California, USA
Chloroform	Merck Ltd and Asia Pacific Speciality Chemicals Ltd, Auckland, NZ
Cholestane	Sigma Chemical Co., Missouri, USA
Cholesterol	Sigma Chemical Co., Missouri, USA
Cholesteryl arachidonate	Sigma Chemical Co., Missouri, USA
Cholesteryl linoleate	Sigma Chemical Co., Missouri, USA
Cholesteryl palmitate	Sigma Chemical Co., Missouri, USA
Cholesteryl oleate	Sigma Chemical Co., Missouri, USA
Cholesterol reagent	Roche Diagnostics GmbH, Mannheim,Germany
Copper chloride	BDH lab supplies Ltd., Poole, England
Coumassie blue	Bio-Rad Laboratories, California, USA
Cytochrome C	Sigma Chemical Co., Missouri, USA
Deoxyribonucleic acid (DNA)	Sigma Chemical Co., Missouri, USA
Dialysis tubing	Biolab Scientific, Auckland, NZ
Di-ammonium hydrogen orthophosphate	BDH lab supplies Ltd., Poole, England
Diethyl ether	Merck Darmstadt, Germany
DL-Buthionine-[S,R]-Sulfoximine (BSO)	Sigma-Aldrich Chemical Co., Missouri, USA
Dimethyl sulphoxide (DMSO)	BDH lab supplies Ltd., Poole, England
Ethanol	BDH lab supplies Ltd., Poole, England

Ethyl acetate	Merck Darmstadt, Germany
Ethylenediaminetetraacetic acid (EDTA)	BDH lab supplies Ltd., Poole, England
Ethlylene glycol-bis(2-aminoethylether)-N,N,N',N'-tetracetic acid (EGTA)	Sigma Chemical Co., Missouri, USA
Glycerol	Sigma Chemical Co., Missouri, USA
Glutathione (reduced form)	Sigma Chemical Co., Missouri, USA
HEPES	Sigma Chemical Co., Missouri, USA
Hexane	Merck Darmstadt, Germany
Hydrochloric acid (HCl)	BDH lab supplies Ltd., Poole, England
Iodine	BDH lab supplies Ltd., Poole, England
Interferon-γ (IFN-γ)	Imukin®; Boehringer Ingelheim Pty Ltd, New South Wales, Australia
Isopropanol (2-propanol)	J.T. Baker, New Jersey, USA
Lymphoprep	Axis-Shield PoC AS, Oslo, Norway
Magnesium chloride	BDH lab supplies Ltd., Poole, England
Methanol	Merck Darmstadt, Germany
Molecular Weight Marker	Fermentas International Inc, Ontario, Canada
Monobromobimane	Sigma-Aldrich, Steinheim, Switzerland
Neopterin	Schircks Laboratory, Switzerland
Nitrogen gas	BOC Gasses, Auckland, NZ
N,O-bis(Trimethylsilyl)trifluoroacetamide (BSTFA)	Sigma Chemical Co., Missouri, USA
NuPAGE 4-12% Bis-Tris Gel, 1.0 mm x 10 well	Invitrogen, California, USA
Oil Red-O	Sigma Chemical Co., Missouri, USA
Paraformaldehyde	Merck Darmstadt, Germany
Phenol	Sigma Chemical Co., Missouri, USA
Ponceau S	Sigma Chemical Co., Missouri, USA
Potassium bromide	Merck Darmstadt, Germany
Potassium hydroxide	Merck Darmstadt, Germany
Potassium iodide	May & Barker Ltd, Dagenham, England
Pyridine	Sigma Chemical Co., Missouri, USA
Sodium azide	BDH lab supplies Ltd., Poole, England
Sodium chloride	BDH lab supplies Ltd., Poole, England
Sodium dihydrogen orthophosphate	Merck Darmstadt, Germany
Sodium dodecyl sulphate (SDS)	Sigma-Aldrich Chemical Co., Missouri, USA
Sodium hydrogen carbonate ($NaHCO_3$)	Merck, Darmstadt, Germany
Sodium hydroxide	Merck, Darmstadt, Germany
Sucrose	Chelsea Sugar Refinery, Auckland, NZ
Supersignal West Dura chemiluminescence	Pierce Biotechnology Inc., Illinois, USA
Thimerosal	Sigma Chemical Co., Missouri, USA
Trichloroacetic acid (TCA)	Sigma Chemical Co., Missouri, USA
Trifluoroacetic acid (TFA)	Sigma Chemical Co., Missouri, USA
Tris	Roche Diagnostics GmbH, Mannheim, Germany
Trypan blue solution (0.4%)	Sigma-Aldrich Chemical Co., Missouri, USA
Tween-20	Sigma-Aldrich Chemical Co., Missouri, USA.
Vetashield	Vector Laboratories Inc. California, USA

2.1.2 Antibodies

Donkey anti-goat IgG HRP-conjugated	Santa Cruz Biotechnology Inc., California, USA
Goat anti-mouse IgM HRP-conjugated	Santa Cruz Biotechnology Inc., California, USA
Goat anti-mouse IgG HRP-conjugated	Pierce Biotechnology Inc., Illinois, USA
Goat anti-rabbit IgG HRP-conjugated	Pierce Biotechnology Inc., Illinois, USA
Goat Polyclonal IgG to SR-A	Santa Cruz Biotechnology Inc., California, USA

Mouse IgG2a E-8 to Caspase-3	Santa Cruz Biotechnology Inc., California, USA
Mouse Monoclonal IgM to CD36 (SMϕ)	Santa Cruz Biotechnology Inc., California, USA
Mouse Monoclonal to β-Actin	Sigma-Aldrich Chemical Co., Missouri, USA
Rabbit Polyclonal IgG to Cytochrome c	Santa Cruz Biotechnology Inc., California, USA
Sheep Anti-mouse IgG HRP-conjugated	Amersham Biosciences, Buckinghamshire, England

2.1.3 Media

Hanks' balanced salt solution (HBSS)	Sigma-Aldrich Chemical Co., Missouri, USA.
Macrophage-SFM Medium	Gibco, New York, USA
Penicillin/streptomycin (100 units/ml penicillin G and 100µg/ml streptomycin, final concentration)	Gibco, New York, USA
Roswell Park Memorial Institute 1640 (RPMI)	Sigma-Aldrich Chemical Co., Missouri, USA
RPMI 1640, without phenol red	Sigma-Aldrich Chemical Co., Missouri, USA

2.1.4 General Solutions, Buffers and Media

2.1.4.1 Phosphate Buffered Saline (PBS)

Phosphate buffered saline (150 mM sodium chloride and 10 mM sodium dihydrogen orthophosphate, pH 7.4) was stirred with 1 g of washed Chelex 100 resin for at least four hours to remove contaminating metal ions before being vacuum filtered through a 0.45 µm membrane. PBS required for cell culture work, was autoclaved for 15 minutes, at 121 °C and 15 psi.

2.1.4.2 Roswell Park Memorial Institute (RPMI) Media (with or without phenol red)

The media was prepared as per the manufacturer's instructions. Powdered RPMI was dissolved in water, before adding sodium bicarbonate and adjusting the solution to pH 7.4 with 1 M HCl or 1 M NaOH. The media was sterilized using a peristaltic pump (CP-600, Life Technologies, Maryland, USA) and a 0.22 µm Millex®-GP_{50} filter (Sartorius AG, Goettingen, Germany) into sterile bottles and stored at 4 °C. RPMI 1640 containing phenol red was used to maintain the cells and supplemented with 100 units/ml penicillin G and 100 µg/ml streptomycin.

2.1.4.3 7,8-Dihydroneopterin Solution

A 2 mM stock of 7,8-dihydroneopterin (7,8-NP) was prepared fresh prior to each experiment. It was dissolved in degassed ice cold RPMI during a two to five minute

sonication. 7,8-NP was subsequently sterilized by filtration through a 0.22 µm membrane filter (Sartorius AG, Goettingen, Germany).

2.1.4.4 BSO Solution

A 5 mM stock of DL-buthionine-S-sulfoximine (BSO) solution was prepared prior to each experiment. BSO was dissolved in RPMI and sterilized by filtration through a 0.22 µm membrane filter.

2.1.4.5 4% Paraformaldehyde in PBS

Two grams of paraformaldehyde was added to 40 ml of PBS and heated on a heating block to dissolve. The temperature was not allowed to exceed 60 °C. A few drops of 10 M NaOH were gradually added to help paraformaldehyde to dissolve. Once the solution had cooled to room temperature, it was made up to 50 ml with nanopure water and the pH was adjusted to 7.4 with 11.44 M HCl. It was kept at 4 °C for 2-3 weeks.

2.2 Methods

2.2.1 LDL Preparation

2.2.1.1 Density Gradient Solutions for Ultracentrifugation

Density gradient solutions were prepared by dissolving required amount of NaCl in nanopure water. Firstly, a 10 mg/ml EDTA solution was prepared by dissolving EDTA in nanopure water and adjusting the pH to 7.4 with 10 M NaOH. Solutions A and B of density 1.0688 g/ml and 1.043g/ml were made up by adding 8 g and 5g NaCl respectively to 10 ml of 10 mg/ml EDTA solution and made up to 100 ml with nanopure water. Calculation to prepare solution A.

> The partial specific volume of NaCl is 0.14 ml/g. Therefore 8 g of NaCl will occupy 8 x 0.14 ml in solution or 1.12 ml. The 100 ml of solution will therefore contain 8 g of NaCl and 98.88 ml of water, giving a mass of 106.88 g. The density will therefore be 106.88/100 or 1.0688 g/ml.

Finally, solution C of density 1.0 g/ml was made up by adding 10 ml of 10 mg/ml EDTA solution to 90 ml of nanopure water.

2.2.1.2 Preparation of Dialysis Tubing

The dry dialysis membrane tubing (Medical International Ltd, London, England) with 14.4 mm flat width and molecular weight cut off, 14,000 Daltons, was pre-treated before use.

The dialysis tubing was first cut into 220 mm lengths. The tubes were boiled in a glass beaker containing solution of 5 % w/v $NaHCO_3$ and 1 mM EDTA. After 20 minutes of boiling, the tubes were washed with reverse osmosis- water (RO-H_2O) and boiled again in a glass beaker containing RO-H_2O. After 20 minutes the tubes were washed thoroughly with RO-H_2O and stored in solution of RO-H_2O:ethanol (50:50 v/v) at 4 °C. The tubes were washed thoroughly with RO-H_2O again before being used for dialysis.

2.2.1.3 Blood Collection for Isolation of Plasma

A written consent was first obtained from the healthy blood donors who were required to fast overnight. Blood was collected from donors by venipuncture using a 21 G x ¾ inch or 19 G needle attached to a 30 ml syringe. The blood was transferred into 50 ml centrifuge tubes containing 0.5 ml of 10% (w/v) EDTA (pH 7.4). Fifty ml of whole blood was placed into each tube. The tubes were centrifuged for 20 minutes at 4 °C in a swing-out rotor at 4,700 rpm with soft start using Multifuge 1 S-R centrifuge (Sorvall Heraeus, Kendor Laboratory Products GmBH, Germany). The maximum radius of the swing-out rotor was 18.7 cm. The resulting top yellow plasma was transferred to 50 ml round bottom centrifuge tubes and spun for 30 minutes at 11,000x g in a fixed angle rotor to remove any remaining trace of cells. Plasma from all donors was pooled and total volume was recorded. The pooling of plasma minimized inter-individual variation. The plasma was stored in 20 ml or 32 ml aliquots at –80 °C for a maximum of six months (Gieseg, *et al*., 1994).

2.2.1.4 Low Density Lipoprotein (LDL) Preparation Using Swing Out Bucket Rotor Method (SWT 4i)

A tube of plasma (20 ml) was thawed under running cold water (approximately 6 °C) and centrifuged at 4,700 rpm for ten minutes at 4 °C to remove any precipitated fibrinogen. The supernatant was decanted into a beaker placed on ice. Potassium bromide (410 mg/ml) was gradually added to the plasma while continuous stirring with a magnetic stirrer to produce a plasma density of 1.41 g/ml. The plasma was pipetted evenly between six Beckman ultracentrifuge tubes. 3 ml of solution A was gently layered onto the plasma by using syringe attached to 180° bend needle followed by 3 ml of solution B and finally solution C (see section 2.2.1.1).

The centrifuge tubes were then transferred to a Beckman SW41-Ti rotor and centrifuged at 40,000 rpm for 22 hours at 10°C using an Optima^{TM} L-90K Preparative Ultracentrifuge (Beckman Coulter, Inc., Fullerton, California). The top VLDL layer was

first discarded. An orange band of LDL in the density range of 1.019 g/ml to 1.063 g/ml was collected using 20 ml syringe attached to 90° bend needle. The HDL band which was the second yellow band from the bottom of the tube was collected using the same way. The LDL or HDL was transferred into treated dialysis tube, layered with argon gas and dialysed for 24 hours at 4 °C against four changes of degassed PBS containing Chelex 100 resin in order to remove all traces of EDTA. Freshly dialysed LDL or HDL was stored under argon and filter sterilized through a 0.22 µm membrane filter immediately prior to the start of an experiment.

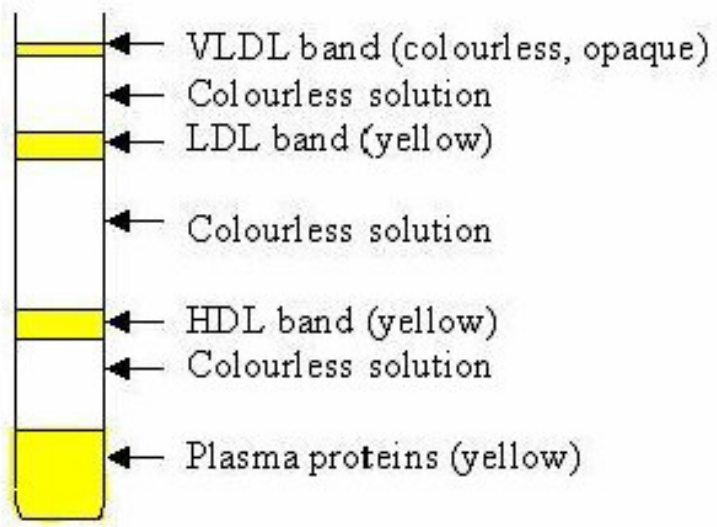

Figure 2.1 Location of lipoprotein fractions after centrifugation.

2.2.1.5 LDL Preparation Using Vertical Beckman NVT65 Rotor Method

This method is performed using a Beckman Near Vertical Rotor using the method of Chung *et al.* (1980) with modification described in Gieseg and Esterbaur (1994). The method was directly adapted from Dr. Wendy Jessup at The Heart Research Institute Ltd, Sydney for LDL preparation in a vertical rotor. The method involves setting up a one step gradient that, during centrifugation, redistributes to form a gradient that separates the lipoproteins.

Thirty two ml EDTA-plasma was thawed under running cold water, and centrifuged at 4,700 rpm for ten minutes at 4 °C to remove any precipitated fibrinogen. The supernatant was decanted into a beaker placed on ice and the plasma density was adjusted to a density of 1.24 by gradual addition of 382 mg/ml of solid KBr. The solution was gently stirred to prevent the formation of foam, which is the sign of LDL denaturation. Eight ml of degassed 1 mg/ml EDTA pH 7.4 solution was added to 8 centrifugation tubes

before under layering with 4 ml of KBr-plasma using a long luer-fitting needle attached to a 5 ml syringe. The tubes were transferred to NVT-65 rotor and centrifuged at 60,000 rpm for 2 h at 10 °C using slow acceleration/deceleration. An orange band of LDL was collected using the same method as above and dialysed.

2.2.1.6 Determination of Cholesterol Content of LDL

LDL concentration was determined as a function of cholesterol level using a cholesterol kit supplied by Roche Diagnostic. The cholesterol content of LDL was determined by incubating 10 µl of LDL with 1 ml of cholesterol reagent at room temperature. After incubation for ten minutes, the absorbance was measured at 500 nm against a blank containing only cholesterol reagent. An LDL concentration was calculated from this absorbance, based on an estimate of cholesterol accounting for 31.69% of the LDL particle by weight and LDL having a molecular weight of 2.5 MDa (Gieseg, *et al*., 1994).

Calculation of LDL concentration:

Molar cholesterol: Absorbance x 14.9 = mM cholesterol

Mass cholesterol: Concentration (M) x 386.64 g/mol (g/l)

Total mass LDL: 31.69% of LDL is cholesterol: g/l x 100/31.69 = g/l LDL (or mg/ml LDL concentration)

Concentration of LDL (M) = g/l LDL / 2.5 x 10^{6}

All the concentrations of oxLDL used in the experiments are based on the concentrations of the total mass of LDL, unless stated otherwise.

2.2.1.7 Preparation of Oxidised LDL

Copper chloride ($CuCl_2$) from a sterile 50 mM stock was added to filter sterilised 3 mg/ml of total mass LDL in a 25 ml cell culture flask at a final concentration of 300 to 400 μM. mixture was incubated for 15 hours at 37 °C. The LDL oxidation was carried out in the absence of any buffer. The presence of heavily oxidesed LDL was indicated by the changing of LDL colour to colourless. The copper ions were removed by mixing the oxidised LDL with 1 g Chelex 100 resin by placing the tube on a rotating turntable which inverts the tube 8 times in a minute. This was done at 4 °C for 2 hours. The Chelex 100 resin was allowed to settle down by centrifugation at 500x g for 2 minutes or left standing for 1 h before collecting the oxLDL from above it. OxLDL was concentrated using a Vivapore membrane concentrator (Millipore, MA, USA) to the concentration (usually between 10 to 12 mg/ml) necessary to allow a small volume of oxLDL to be added to the medium during experimentation. OxLDL was filter sterilised through a 0.22 μm membrane filter and stored at 4 °C.

2.2.2 Cell Culture

All cell manipulations were performed under aseptic conditions in a Class II biological safety cabinet (Clyde-Apex BH 200). All instruments and equipment were either sterile plastic ware (Falcon products, Bector Dickinson & Co.; Nunc products, Nalge Nunc International; Sarstedt products, NC, US; and Greiner products, Greiner Bio-one, Frickenhausen, Germany) or had been sterilized by autoclaving (15 minutes, 121°C and 15 psi). All media and solutions to be added to the cells were sterilised by autoclaving or by filtration through a 0.22 μm membrane filter. Cells were kept at 37 °C in a humidified incubator, with an atmosphere calibrated to 5% carbon dioxide: 95% air (Nuaire™ IR Autoflow). All equipments and the outside of bags and tissue culture dishes and flasks were sprayed with 70% (v/v) ethanol.

2.2.2.1 Human Monocyte-Derived Macrophages

Ethics approval for the use of human blood was granted by the Upper South B Committee (protocol number 98/07/069). The isolation procedure for HMDMs was adapted from Firth (2006). All the solutions for the preparation of human monocyte-derived macrophages were warmed to room temperature. All the operations were performed at room temperature. Once isolated, the cells were maintained in RPMI 1640 containing

phenol red supplemented with 10% (v/v) heat-inactivated human serum, 100 units/ml penicillin G and 100 µg/ml streptomycin.

2.2.2.2 Preparation of Human Monocyte-Derived Macrophages

Unlinked blood in a 600 ml autologous bag was obtained from haemochromatosis patients by the NZ Blood Bank (Riccarton Road, Christchurch). Written permission was given by the NZ Blood. Consent was verbally obtained from the donors by the nurse. There was no contact made between researcher and donor, nor was any identifying label on the blood bags so designating this blood as "unlinked". The blood bag was gently inverted several times to ensure even distribution of blood cells and then aseptically transferred to 50 ml centrifuge tubes. The tubes were centrifuged at 3000x g, with the brake off, for 30 minutes at room temperature.

The resulting buffy coat of white cells was removed using a mixing cannula attached to 10 ml syringe and mixed with Hanks' Balanced Salt Solution (HBSS) or PBS in a ratio of 15 ml buffy coat:20 ml buffer. Then this mixture was underlayed with 15 ml of Lymphoprep using a mixing cannula attached to 25 ml syringe. After centrifuging at room temperature at 1000x g for 30 minutes with the brake off, a white layer of monocytes/lymphocytes was visible approximately halfway down the centrifuge tube. This layer was transferred to new centrifuge tubes with a syringe and mixing cannula and washed four times in 45 ml HBSS or PBS by centrifugation at 500x g; the first wash was 15 minute centrifugation followed by 10 minutes centrifugation for the subsequent washing. Either HBSS or PBS could be used to suspend the cells from Lymphoprep or to wash the cells in the procedures above since preliminary works showed that both solutions did not affect the yield of the cells or interfere with their growth (data not shown).

After washing, the cells were resuspended in serum-free RPMI 1640 (warmed to room temperature), at a concentration of $5x10^6$ cells/ml, and then 7 ml per well was aliquoted into six well suspension plates (Falcon products, Bector Dickinson & Co.). The plates were incubated for approximately 40 hours to allow T cells death and platelets to adhere to the surface of the plates while the monocytes remain viable in suspension. The monocytes were subsequently resuspended in fresh RPMI 1640, supplemented with 10% heat-inactivated human serum, at a concentration of $5x10^6$ cells/ml and plated at 1 ml/well in 12 well adherent plates. Fresh medium (RPMI 1640 containing 10% heat-inactivated human serum) was renewed every three to four days and experiments were conducted once the majority of monocytes had matured to macrophages, usually 14 days after the initial isolation of the cells.

2.2.3 Preparation of Serum

2.2.3.1 Heat-Inactivated Human Serum (HIHS)

Unlinked blood from consenting haemochromatosis patients was collected into 600 ml dry bags by the NZ Blood Bank (Riccarton Road, Christchurch). The blood was left in upright position at 4 °C overnight to provide sufficient time for the serum to separate from the blood clot which developed. The bag was opened under sterile conditions and the serum was collected into 50 ml centrifuge tubes using a 20 ml syringe attached to a mixing cannula. The tubes were centrifuged at 1500 rpm for 15 minutes and the resulting serum was decanted into new centrifuge tubes. The serum was heat inactivated in a water bath at 56 °C for 30 minutes before being cooled to 4 ºC, and then transferred to –20 ºC and later to –80 ºC refrigerator for long term storage. Serum was stored for up to one year.

2.2.3.2 Lipoprotein Deficient Serum (LPDS)

Lipoprotein deficient serum (LPDS) was prepared from HIHS by adjusting the density of HIHS to 1.24 g/ml with KBr. The partial specific volume of KBR is 0.31 ml/g (refer to section 2.2.1.1 for the calculation of density). Twenty ml of HIHS was poured into a beaker placed on ice and 7.63 g KBr was added to it with gentle stirring. The resulting mixture was pipetted evenly between six Beckman ultracentrifuge tubes. Solution A was overlayed onto the serum till to the top of the tubes by using 180° bend needle attached to 10 ml syringe. The tubes were then transferred to a Beckman SW41-Ti rotor and centrifuged at 10 °C and 40,000 rpm for 20 hours. The upper layer solutions were removed leaving a light orange band of LPDS at the bottom of the tubes. This was collected using 20 ml syringe attached to 90° bend needle. This was transferred into treated dialysis tube and dialysed for 24 hours at 4 °C against four changes of degassed PBS containing Chelex 100 resin in order to remove all traces of EDTA. The LPDS was filter sterilized through a 0.22 µm membrane filter before addition to the media.

2.2.4 Determination of Protein Concentration

Protein concentration was determined using the bicinchoninic acid (BCA) protein determination kit from Sigma. The working reagent was freshly prepared by mixing Reagent A (sodium carbonate, sodium bicarbonate, BCA and sodium tartrate in 0.1 M sodium hydroxide) and Reagent B (4% $CuSO_4.5H_2O$) in a 50:1 ratio. The assay was carried out by mixing 50 µl with 1 ml of working reagent and incubated at 60 °C for 30 minutes with gentle shaking. The reaction was subsequently stopped by placing samples

on ice before reading the absorbance at 562 nm against a water blank. Protein concentration was determined from a standard curve prepared by the incubation of known concentrations of BSA (0-250 μg/ml) in 1 ml of working reagent.

2.2.5 Determination of Cellular DNA Content

2.2.5.1 Solutions for Determination of Cellular DNA Content

The buffer contained 100 mM NaCl, 10 mM EDTA and 10 mM Tris, pH 7. 4'6-diamidino-2-phenylindole (DAPI) stock was prepared by dissolving DAPI in water at 1 mg/ml before diluting further to 10 μg/ml in water. The assay used a final concentration of 100 ng /ml of DAPI, therefore 10 μl of 10 μg/ml stock was added to 1 ml of buffer. The stock solution was stored in dark at 4 °C and stable for 2 to 3 weeks. DNA from calf thymus (Sigma Chemical Co., product number D1501) was used as DNA standard and the concentration was adjusted to 20 μg/ml by measuring the absorbance at 260 nm. The DNA concentration was determined using the equation below:

[DNA] = A_{260} x 50 μg/ml x dilution factor.

2.2.5.2 Determination of Cellular DNA Content

This assay was based on the method described by Brunk *et al.* (1979). The fluorescent dye 4'6-diamidino-2-phenylindole (DAPI) complexes with DNA to give a product with fluorescence intensity about 20 times greater than that of the dye alone. In this assay, the fluorescence increase produced by the DNA was compared directly with the fluorescence increase produced by a calf thymus DNA standard. All measurements were performed in series using a single dye solution, thus providing an internal control.

After removal of the incubation medium the cells were washed twice in PBS and submerged in nanopure water. The cells were scraped and transferred into Eppendorf tubes. The cell lysate was sonicated for fifteen seconds to homogenise the cell lysates in order to alleviate the high noise levels in the fluorometer.

Firstly, the fluorescence of 3 ml buffer containing 100 ng/ml DAPI was measured using a fluorescence spectrophotometer (Cary Eclipse) at an excitation wavelength of 360 nm and emission wavelength of 450 nm and slit set to 10 nm. Then, one aliquot of 15 μl of the cellular homogenate was added to the same cuvette and the fluorescence was remeasured. Second, third, and fourth addition of homogenate followed this. Then four aliquots of 15 μl of a purified DNA standard (known concentration) were added to the

same cuvette sequentially. The slopes for the homogenate and DNA standards were determined using the software program, Prism (version 4.0; GraphPad Software, USA). A comparison of the slope for the homogenate with the slope for the DNA standard multiplied with the concentration of DNA standard yielded the DNA content of the homogenate. Example of calculation is shown in the Figure 2.2 adapted from Brunk *et al.* (1979).

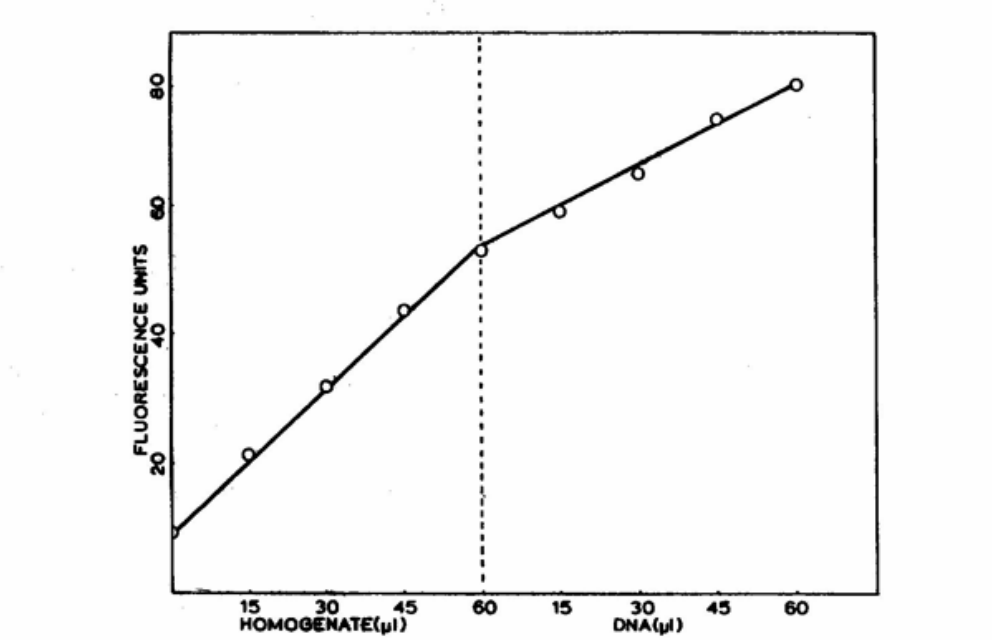

Figure 2.2 An example of graph showing the slope of homogenate and the standard DNA.
Comparing the slope of fluorescence enhancement for the homogenate with the slope for the DNA standard, the ratio is 1.76. This value times the DNA standard concentration (20 µg/ml) yields 35.2 µg/ml, the DNA concentration of the homogenate.

2.2.6 Cell Viability Analysis by Trypan Blue Exclusion Staining

Trypan blue exclusion staining monitors cell viability via analysis of membrane integrity (Moldeus, *et al*., 1978). Viable cells have intact membranes that are impermeable to the dye and, as a consequence, appear colourless when viewed under a microscope. In contrast, the membrane integrity of the dead cells has been breached and is no longer able to pump the dye out. Therefore, the dead cells will appear blue.

The incubation medium was removed and 200 µl of trypan blue was added directly to the adherent cells in the well. The dye was removed after 30 seconds and replaced with 1ml of warm PBS. An inverted microscope (40x magnification with a 10x eyepiece) was used to randomly examine five fields of view across each well. The proportion of viable cells was calculated by dividing the number of viable cells from all five fields of view by the total number of cells (both alive and dead) from all five fields of view.

2.2.7 Cell Viability Analysis by MTT Assay

2.2.7.1 Solutions for MTT Assay

MTT powder was dissolved in RPMI 1640 without phenol red to 5 mg/ml. The media was sterilised through a 0.2 µm filter and stored at –20 °C in the dark.
A 0.01 M HCl solution was made up from 11.44 M HCl and nanopure water. SDS was added to this solution and stirred slowly to a give a final concentration of 10% SDS.

2.2.7.2 MTT Assay

The reduction of 3-(4,5-dimethylthiazol-2-yl)-2,5-diphenyl tetrazolium bromide (MTT) is widely accepted as a reliable method to measure cell viability and the method is best described by Mosman (1983). This laboratory has previously shown this method agrees well with results obtained with trypan blue. The yellow tetrazolium MTT (3-(4, 5-dimethylthiazolyl-2)-2, 5-diphenyltetrazolium bromide) is reduced by metabolically active cells, in part by the action of dehydrogenase enzymes, to generate reducing equivalents such as NADH and NADPH. The resulting intracellular purple formazan can be solubilised and quantified by spectrophotometric means (Mosmann, 1983). As a result, the intensity of the colour provides an indication of both the concentration of cells and their metabolic activity.

After removal of the incubation medium, the adherent cells were washed three times in PBS. 900 µl of non-phenol red RPMI 1640 plus 100 µl of 5 mg/ml MTT was

added. Samples were then incubated at 37 °C in a humidified incubator for one to three hours allowing sufficient time for significant quantities of purple compound to form in the control wells. This range of time is due to the metabolic activity of HMDMs differing from one preparation to the next. The resulting purple insoluble MTT-formazan crystals were dissolved by mixing 1 ml of 10% (w/v) SDS (in 0.01 M HCl) in each well and incubating for a further 10 minutes in a humidified incubator. The absorbance was read at 570 nm, against a blank lacking cells but containing all other reagents.

2.2.8 Extraction of Lipids for Gas Chromatography Analysis

2.2.8.1 Extraction of Total Lipids

Total lipids were extracted according to the method of Brown *et al*. (1996) and Brown *et al.* (2000). Cells were seeded at 10 x 10^6 cells/3 ml/well in six well plate. After removal of the incubation medium the cells were washed three times in PBS and 1.2 ml of 0.2 M NaOH was added to each well. The plate was placed on ice and agitated for 30 min on an orbital shaker before the cells were scrapped off from the bottom of the wells. 100 µL of the cell lysate was removed for protein assay and 2 aliquots of 500 µl were put into two 15 ml black top centrifuge tubes. One aliquot was hydrolysed for determination of total cholesterol and the second one was analysed for free cholesterol. To each tube, 0.5 ml of ice cold PBS supplemented with 20 µM BHT and 2 mM EDTA were added. 20 µg cholestane standard (from stock 1 mg/ml) was added as an internal standard followed by 1.0 ml ice cold methanol. The tubes were vortexed gently and briefly before adding 5.0 ml ice-cold hexane. The tubes were vortexed vigorously for 60 seconds followed by centrifugation at 1000 rpm for 2 min. Four ml of upper phase hexane layer containing total lipids was removed and dried under nitrogen gas.

2.2.8.2 Alkaline Hydrolysis of Lipids for Total Cholesterol Derivitisation

The total lipids were hydrolysed under alkaline conditions to release sterols from the steryl esters by adding 0.5 ml of 15% KOH (v/v) in 100% methanol (water free). The tube was flushed with argon gas, capped tightly and heated at 65 °C for 30 minutes. After saponification, 1.0 ml of water was added and vortexed briefly before adding 5 ml of hexane. After vortex mixing for 1.0 minute the tube was centrifuged at 1000 rpm for 2 minutes to obtain complete phase separation. Four ml of the upper hexane layer containing total sterols was removed and dried under nitrogen gas.

2.2.9 Gas Chromatography Analysis

Sterols were derivitised to enhance volatilisation and hence their detection by Gas Phase Chromatography. Total lipids and total cholesterol were converted to their trimethylsilyl (TMS) derivatives by adding 100 µl of BSTFA and pyridine (50:50 v/v). After heating at 65 °C for 30 minutes under argon gas, the mixture was dried down under nitrogen. The residue was redissolved in 10 µl heptane and 2 µl was analysed by gas chromatography using a Hewlet-Packard 5890 Series II, equipped with a 25 m by 0.32 mm-inner-diameter capillary column coated with 0.25 µm of BPX70 (SGE International Pty. Ltd.), flame ionisation detector and HP 3366 series II integrator. The injector and detector temperatures were set at 250 °C. Thermal gradient analyses were performed using the following oven temperature profile: initial temperature of 200 °C; held for 1 minute then increased to the final temperature of 250 °C at 4 °C/minutes. Sample was analysed by split injection (30:1 ratio) using nitrogen gas as the carrier gas at a flow rate of 2.5 ml/min.

Free and total cholesterol were identified based on the cholesterol standard retention time and quantified by FID response relative to an internal standard (20 µg cholestane) added prior to lipid derivatisation. Their concentrations were calculated according to the formula shown below:

Cholesterol concentration in sample (µg) = (peak area of cholesterol/peak area of cholestane) x 20 µg cholestane
= A

Cholesterol concentration in each well (µg/well) = A x (total volume of hexane added/volume of hexane dried) x (total volume of cell lysate/volume of cell lysate extracted)

Protein concentration was determined as in section 2.2.4, calculated as total protein per well, and expressed as mg/ml. Therefore, the final concentration of cholesterol was in µg cholesterol per mg of protein. In some data the amount of cholesterol was based on the total DNA content of the samples.

2.2.10 Labelling of Lipoproteins (LDL and OxLDL) with DiI

1,1'-dioctadecyl-3,3,3',3'-tetramethylindocarbocyanine perchlorate (DiI) is a highly lipophilic molecule and it is extensively use in studies of receptor –mediated metabolism of LDL. The lipoproteins were labelled with the fluorescent probe DiI as described by Stephen and Yurachek (1993) and Devaraj *et al.* (2001). Purified LDL or oxLDL of

known concentration (mg protein/ml) was filter sterilised through a 0.22 µm membrane filter into a sterile flask and incubated with 50 µl of 3 mg/ml DiI in DMSO for each milligram of lipoprotein protein. The flask was covered with aluminium foil to prevent exposure to light. After incubating the mixture overnight at 37 °C, the labelled lipoprotein was reisolated by ultracentrifugation using the same procedure as LDL preparation, dialysed against 4 changes of PBS containing Chelex 100 resin and filter sterilised. DiI labelled LDL or oxLDL was kept at 4 °C in the dark and used immediately since DiI was not stable.

Measurement of DiI-oxLDL or Di-LDL uptake was according to the method of Stephan and Yurachek (1993). Cells were incubated at 4 °C and 37 °C to measure membrane bound and cell-associated DiI-oxLDL or DiI-LDL respectively. At the end of the incubation period, the medium was removed and cells were washed 3 times with warm PBS. Then 1.0 ml isopropanol was added to each well and plates were gently shaken on an orbital shaker (Bioline, Edwards Instrument Company, Australia) for 15 min. The cells were harvested and the cell lysates were transferred into Eppendorf tubes, centrifuged at 3000 rpm for 15 min. The supernatant was taken out for determination of fluorescence intensity using a fluorescence spectrophotometer (Cary Eclipse). The excitation and emission wavelengths were set at 520 and 580 nm, respectively. The cell pellets were dissolved in 2 M NaOH for protein determination.

Results were expressed as mean fluorescence intensity (MFI) per mg of cell protein. The difference in MFI between cell associated (37 °C) and membrane-bound (4 °C) DiI-oxLDL or DiI-LDL is directly proportional to the internalised DiI-oxLDL or DiI-LDL.

2.2.11 Rapid Oil red-O staining

The method was adapted from Davies *et al*. (2005). After incubation, the cells were washed 3 times with warm PBS and fixed in 4% paraformaldehyde for 20 minutes at room temperature. After removal of paraformaldehyde, the cells were stained for 15 minutes by adding 0.5 ml of 0.05% oil red-O (ORO) in isopropanol:water (3:2 v/v). Cells were washed twice in water and viewed *in situ* using an inverted microscope. The images were taken with Kodak Digital Camera and processed with Adobe Photoshop 8.0.

2.2.12 Staining of Cells for Phosphatidylserine Exposure for Apoptosis Analysis by Fluorescence Microscopy

Loss of plasma membrane asymmetry is one of the earliest features of apoptosis where the membrane phosphatidylserine (PS) is translocated from the inner to the outer leaflet of the plasma membrane thereby exposing the PS to the external cellular environment (van Engeland, *et al*., 1998). Annexin V has a high affinity binding to PS and when conjugated to flurochrome fluorescein isothiocyanate (FITC) serve as a sensitive marker for apoptosis that can be detected by flow cytometry or fluorescence microscopy. Cells with bound Annexin V-FITC will show green staining in the plasma membrane under the fluorescence microscope.

All the operations were carried out with minimum exposure to light since FITC was light sensitive and the procedures carried out as per the manufacturer's instructions. Cells were cultured at 5 x 10^6 cells/ml on sterile glass cover slips in 6 well plate. At the end of an incubation period, the cells were washed twice in warm RPMI and left in 0.5 ml of binding buffer (10 mM Hepes (pH 7.4/NaOH), 140 mM NaCl and 2.5 mM $CaCl_2$) for one minute. After removal of the binding buffer, 150 µl of binding buffer containing 1.5 µg/ml annexin V was added on the top of the cover slips and the cells were incubated in a humidified incubator for 15 minutes in the dark. After incubation, the coverslips were washed twice in binding buffer. Fifteen microlitres of binding buffer was placed on top of a glass slide and the coverslip was placed with the cells facing down on the glass slide.

Cells were examined using a Zeiss AxioImager.M1 epifluorescent microscope (Carl Zeiss (NZ) Ltd, Wellington, New Zealand), equipped for Differential Interference Contrast (DIC) condenser and fitted with an HBO 100 W mercury vapour lamp. Cells were viewed using 20x and 40x Plan-NEOFLUAR objectives. The fluorescent filter used for FITC was a Zeiss filter set 38 HE. The images were captured using a Zeiss AxioCam HRc CCD camera with AxioVision Rel. 4.5 software (1300 x 1030 pixel resolution) and processed with Adobe Photoshop 8.0.

2.2.13 Dihydroethidium (DHE) Staining for Detection of Superoxide Production - Analysis by Fluorescence Microscopy

DHE is a highly specific dye for super oxide anion ($O_2^{\bullet-}$) with low affinity for hydrogen peroxide. It is freely permeable to cells and oxidised to DNA-binding fluorophore, ethidium by $O_2^{\bullet-}$ (Burnaugh *et al*., 2006).

Cells were cultured at 5 x 10^6 cells/ml on sterile glass cover slips in 6 well plate. At the end of an incubation period, the cells were washed twice in warm PBS. Subsequently, 150 µl of 10 µM of DHE in PBS was added onto the top of the coverslips and the cells were incubated in a humidified incubator for 20 minutes in the dark. Cells were washed twice in warm PBS to wash off excess DHE. Fifteen microlitres of PBS was added on top of the glass slide and the coverslip was placed on a glass slide with the cells facing down.

Cells were examined using a Zeiss AxioImager.M1 epifluorescent microscope (Carl Zeiss (NZ) Ltd, Wellington, New Zealand), equipped for Differential Interference Contrast (DIC) condenser and fitted with an HBO 100 W mercury vapour lamp. Cells were viewed using 20x and 40x Plan-NEOFLUAR objectives. The fluorescent filter used for DHE was Zeiss filter set 00 for propidium iodide (PI). The images were captured using a Zeiss AxioCam HRc CCD camera with AxioVision Rel. 4.5 software (1300 x 1030 pixel resolution) and processed with Adobe Photoshop 8.0.

2.2.14 Detection of Cytochrome *c* Release by Histochemical Staining - Analysis by Fluorescence Microscopy

Cytochrome *c* is a water-soluble protein that either promotes cell survival or death depending upon its intracellular location. In healthy cells, it is a peripheral membrane protein of the mitochondria that transports electrons from the coenzyme QH_2 cytochrome c reductase complex to the cytochrome *c* oxidase complex. When proapoptotic stimuli induce permeabilisation of the mitochondria, allowing cytochrome *c* to be released to the cytosol where it causes the activation of caspase-9 so triggering apoptosis (Hajek, *et al*., 2001; Hampton, *et al*., 1998). The release of cytochrome *c* into the cytoplasm can be detected using fluorescence microscope or immnunoblotting.

Cells were cultured at 5x10^6 cells/ml on sterile glass coverslips in 6 well plate. At the end of an incubation period, the cells were washed twice in warm RPMI without phenol red. This was followed by fixation in 4% paraformaldehyde in PBS, pH 7.4 for 10 minutes with gentle rocking in an orbital shaker. After removal of the paraformaldehyde solution the cells were permeabilised with –20 °C methanol for 10 minutes placed in –20 °C freezer. Cells were then washed three times in PBS containing 1% BSA and 0.01% sodium azide (PBS-BSA) and then incubated with 5 µg/ml of anticytochrome *c* rabbit polyclonal raised against horse cytochrome *c* (diluted in PBS) for 1 hour at room temperature. This was followed by washing in PBS-BSA solution for

6 times and probing with secondary antibody, 1:200 dilution (diluted in PBS) goat-anti rabbit IgG-FITC for 1 hour at room temperature. This step was carried out in the dark since FITC is light sensitive. After incubation, the coverslips were washed 6 times in PBS-BSA solution before removal from the wells using fine forcep. Fifteen microlitres of Vetashield was placed on a glass slide and the coverslip was placed on the slide with the cells on it on facing down on to the pool of Vetashield. The edges of the coverslips were sealed with nail polish.

Cells were examined using a Zeiss AxioImager.M1 epifluorescent microscope (Carl Zeiss (NZ) Ltd, Wellington, New Zealand), equipped for Differential Interference Contrast (DIC) condenser and fitted with an HBO 100 W mercury vapour lamp. Cells were viewed using 20x and 40x Plan-NEOFLUAR objectives. The fluorescent filter used for FITC was Zeiss filter set 38 HE. The images were captured using a Zeiss AxioCam HRc CCD camera with AxioVision Rel. 4.5 software (1300 x 1030 pixel resolution) and processed with Adobe Photoshop 8.0.

2.2.15 Extraction of Cytosol and Organelle Fraction

The solutions were stored and the procedures were performed at 4 °C. At the end of an experimental incubation period, the media were collected so that any cells dislodged during the incubation period were recovered. The media were centrifuged for 5 minutes at 500 g and the resulting pellet was washed twice in PBS by centrifugation at 500x g for 5 minutes.

At the same time, the adherence cells were washed twice in ice cold PBS and harvested on ice with a cell scraper in ice cold lysis buffer (250 mM sucrose, 20mM HEPES-KOH pH 7.5, 10mM KCl, 1.5 mM EGTA, 1.5 mM EDTA, 1 mM $MgCl_2$, 1 mM dithiothreitol and protease inhibitor). The cell lysate was combined with the resulting pellet and allowed to swell on ice for 10 minutes. Cell lysate were then passed through a 23 G needle for 10 times to break open and homogenise the cells further. The cell homogenate were centrifuged at 23,000x g (~15,000 rpm) for 30 min at 4°C. The pellet was used as a mitochondrial fraction whereas the supernatant was used as a cytosolic fraction. The mitochondrial fraction (pellet) was resolved in lysis buffer.

2.2.16 SDS PAGE and Western Blot Analysis

2.2.16.1 Solutions for SDS-PAGE and Western Blot

Cracker buffer was prepared by first making up a stock of 0.5 M Tris-HCl in water and the pH was adjusted to 6.8 by adding 11.4 M HCl drop wise. Caution was taken, not to overshoot the pH as adding base will change the conductivity. Then, 0.125 M Tris-HCl, pH 6.8 (from 0.5 M stock), 1% SDS, 20% glycerol and 0.1% bromophenol blue was made up in 50 ml of water. Prior to the use, 1 ml of the above solution was transferred into a 1.5 ml Eppendorf tube and 20 µL of β-mercaptoethanol and 2 ul of 100 mg/ml EDTA were added. The final cracker buffer was therefore consisted of 0.125 M Tris-HCl, pH 6.8, 10% SDS, 20% glycerol, 0.1% bromophenol blue, 2% β-mercaptoethanol and 0.54 mM EDTA.

A 10 x stock MOPS consisted of 500 mM MOPS, 500 mM Tris base, 1% SDS, and 10 mM EDTA was prepared in water and pH adjusted to 7.7. This was made up to 1 x concentration by diluting it with water.

Transfer buffer consisted of 25 mM Tris, 200 mM glycine and 20% methanol in water and stored at 4 °C. Ponceau S stain consisted of 0.01% Ponceau S in 5% acetic acid

Washing Solution, TBS, consisted of 40 mM Tris-HCl, pH 7.5, 150 mM NaCl, 0.05% Tween-20, Thimerosal (contains Hg) was made in water. The blocking solution (TBSM) was 5% (w/v) of Anchor non-fat milk powder made in TBS.

2.2.16.2 SDS-Polyacrylamide Gel Electrophoresis

Cracker buffer was added to the sample and heated in a heating block at 95 ºC for 3 minutes. This was followed by centrifugation for 5 minutes at 15000 rpm to remove cell debris. Five µl/well of Fermentas prestained molecular weight marker mix (Fermentas International Inc, Ontario, Canada) and 5-25 µl/well (depending on protein content) of samples were loaded into the wells. The samples were run on a gradient polyacrylamide gel, 4-12%, (Bis-Tris Gel, Invitrogen, Carslband, CA, USA) in MOPS running buffer. The gel was electrophoresed at 200 V for approximately 60 minutes.

2.2.16.3 Sample Preparation

Samples for cytochrome c detection was prepared as above (see section 2.2.15). For caspase 3, CD36 and SR-A detection, the cells were harvested in lysis buffer (40 mM HEPES, 50 mM NaCl, 1 mM EDTA, 1 mM EGTA and protease inhibitor, pH 7.4). The protein content of the samples were determined by BCA protein determination assay in

order to have equal loading of protein onto the gels. Further confirmation of equal loading was obtained by reprobing the membrane with β-actin antibody (see section 2.2.16.5). Samples were resolved by SDS-PAGE electrophoresis as described in the previous section 2.2.16.2.

2.2.16.4 Western Blot Analysis

The protein on the SDS-PAGE gels after electrophoresis were electrophoretically transferred onto nitrocellulose membrane (Invitrogen, USA, 0.45 μm pore size). This was done overnight (approximately 15 hours) at 70 V, using a tank transfer electrophoresis unit (Hoeffer TE22) containing transfer buffer. The next day, to ensure that the transfer had been effective, the membrane was stained with Ponceau S stains for 1 minute and rinsed with dH_2O. Pink bands of proteins were visible with Ponceau S stain.

The following procedures were performed on a rocking platform mixer (Ratex Instruments, Australia). After rinsing with water, the membrane was blocked using 5% TBSM for 2 hours followed by three consecutive 5-minute washes in TBS. Then, the membranes were probed with mouse monoclonal IgM antibodies against CD36 (SMϕ) (SC-7309, Santa Cruz Biotechnology Inc, USA), mouse monoclonal IgM antibodies against caspase-3 (E-8) (SC-7272-Santa Cruz Biotechnology Inc, USA), rabbit polyclonal IgG antibodies against cytochrome *c* (H-104) (SC-7159, Santa Cruz Biotechnology Inc, USA), goat polyclonal antibodies against SR-A (I-20) (SC-20441, Santa Cruz Biotechnology Inc, USA) and mouse monoclonal antibodies against β-actin (A5316, Sigma-Aldrich Chemical Co., USA) for 1.5 hours. The primary antibodies of CD36 and cytochrome *c* were diluted to 1:500; SR-A and caspase-3, 1:1000; and β-actin, 1:10000 in 1% TBSM.

Subsequently, the membranes were washed for 5 lots of 5-minute washes in TBS followed by 1 hour incubation with secondary antibody. With the exception to β-actin, all the secondary antibodies were of 1:1000 dilution and β-actin antibody was 1:10000 dilution in 1% TBSM.

Binding to CD36, caspase-3, cytochrome *c*, SR-A and β-actin was detected by incubation with peroxidase-conjugated goat anti-mouse IgM (SC-2064, Santa Cruz Biotechnology Inc, USA), peroxidase-conjugated goat anti-mouse IgG (F_c) (31434, Pierce Biotechnology Inc, USA), peroxidase-conjugated goat anti-rabbit IgG (F_c) (31463, Pierce Biotechnology Inc, USA), peroxidase-conjugated donkey anti-goat IgG (SC-2020, Santa Cruz Biotechnology Inc, USA) and peroxidase-conjugated sheep anti-mouse IgG (RPN4401, Amersham Biosciences, England) respectively.

The membrane was again given five 5-minute washes in TBS and finally rinsed briefly with water before being visualised. The reprobing of the membrane with β-actin antibody was done after visualisation of the first desired protein. The membranes that need to be reprobed were kept in TBS at 4 ºC until reprobing. The membrane was directly incubated with the primary β-actin antibody without blocking and the rest of the procedures for WesternBlot analysis were then followed.

Table 2.1 Full description of the primary and secondary antibodies used for detection of CD36, Caspase-3, SR-A, β-actin and Cytochrome *c* by Western Blot analysis.

Ligand	Primary Ab	Dilution	Secondary Ab	Dilution
CD36	mouse monoclonal IgM antibodies against CD36 (SMϕ) (SC-7309, Santa Cruz Biotechnology Inc, USA)	1:500	peroxidase-conjugated goat anti-mouse IgM (SC-2064, Santa Cruz Biotechnology Inc, USA)	1:1000
Caspase-3	mouse monoclonal IgM antibodies against caspase-3 (E-8) (SC-7272-Santa Cruz Biotechnology Inc, USA)	1:1000	peroxidase-conjugated goat anti-mouse IgG (F_c) (31434, Pierce Biotechnology Inc, USA)	1:1000
SR-A	goat polyclonal antibodies against SR-A (I-20) (SC-20441, Santa Cruz Biotechnology Inc, USA)	1:1000	peroxidase-conjugated donkey anti-goat IgG (SC-2020, Santa Cruz Biotechnology Inc, USA)	1:1000
β-actin	mouse monoclonal antibodies against β-actin (A5316, Sigma-Aldrich Chemical Co., USA)	1:10000	peroxidase-conjugated sheep anti-mouse IgG (RPN4401, Amersham Biosciences, England)	1:10000
Cytochrome *c*	rabbit polyclonal IgG antibodies against cytochrome *c* (H-104) (SC-7159, Santa Cruz Biotechnology Inc, USA)	1:500	peroxidase-conjugated goat anti-rabbit IgG (F_c) (31463, Pierce Biotechnology Inc, USA)	1:1000

2.2.16.5 Visualization

Detection of signals was by "Supersignal West Dura chemiluminescence" substrates, which was mixed at 1:1 ratio and pipetted evenly on to the membrane. With the exception to detection of β-actin, the image was recorded over 15 minutes on a Syngene Chemigenius-2 bioimaging system using Genesnap software (Global, NZ). For β-actin detection, the exposure was only 2 minutes.

2.2.17 HPLC Analysis of Cholesteryl Esters

Cholesteryl esters detection was carried out by modifying the original method described by (Kritharides, *et al*., 1993). Lipids were initially extracted from 3 wells containing $5x10^6$ cells/ml and injected onto HPLC. However, only a very small peak of cholesterol peak was detected. Therefore, larger sample volumes were required where samples from 12 wells of 5 x 10^6 cells/ml in 12 well plate were pooled.

After removal of the incubation medium, the cells were washed twice in PBS. 0.5 ml of cold nanopure water was added to each well and the cells were harvested by scraping. Cell lysate from 12 wells were pooled, sonicated for 15 seconds and aliquoted into 1.5 ml into 3 separate 15 ml black top centrifuge tubes (the tube was too small for lipid extraction of a total of 4.5 ml cell lysate). The remaining cell lysate was used for DNA quantification. 20 µl of 20 mg/ml EDTA, 20 µl of 100 mg/ml BHT and 1 ml of ice cold methanol was added to the tubes and vortexed briefly. Then, 5 ml of hexane was added, vortexed vigorously for 1 min and centrifuged at 1000 rpm at 4 °C for 2 min to obtain complete phase separation. 4 ml of the hexane layers from each of the 3 black top centrifuge tubes was removed, pooled into one tapered glass test tube and dried under nitrogen gas.

The dried residue was redissolved in 100 µl of mobile phase, acetonitrile:isopropanol (30:70, v/v). Twenty µl of each sample was injected twice onto a Phenosphere reverse-phase C-18 column, 250 x 0.46 mm, and 5 µm particle size (Phenomenex; Auckland, NZ) and eluted isocratically at 1 ml/min with the column temperature maintained at 35 °C. Analysis of cholesterol and cholesteryl esters was performed by detecting 234 nm absorbance. Detection and quantification of sterols were carried out by comparison with the known concentration of standards (cholesterol, cholesteryl arachidonate, cholesteryl linoleate, cholesteryl palmitate and cholesteryl oleate made up in mobile phase). All samples were injected twice.

2.2.18 TBARS-HPLC Lipid Analysis Assay

2.2.18.1 Solutions for the TBARS-HPLC Lipid Analysis Assay

Malondialdehyde (MDA) standard was prepared on the day of analysis by diluting 6.07 M of 1,1,3,3-tetramethoxypropane (TMP) in 2:3 (v/v) ethanol:water, with subsequent dilution in water to the appropriate concentration.

The mobile phase consisted of 50 mM sodium dihydrogen phosphate with pH adjusted to 6.8 with 10 M sodium hydroxide and filtered through 0.45 µm filter. This was mixed with HPLC grade methanol in a ratio of 65:35 (v/v) before degassing by sonication.

A 42 mM of 2-thiobarbituric acid (TBA) was made up fresh on the day of analysis and dissolved in nanopure water by stirring on a hot plate ensuring the temperature did not exceed 55 °C.

2.2.18.2 TBARS-HPLC Lipid Analysis Assay

The TBARS assay provides means of quantifying general lipid peroxidation. The method used here is a modification of the method described by Draper *et al.* (1993). It relies on the ability of 2-thiobarbituric acid (TBA) and the malondialdehyde (MDA) lipid hydroperoxide break-down product to readily react, forming the pink TBA-MDA adduct being fluorometrically detectable via HPLC.

100 µl of samples were mixed with 50 µl of 150 mM phosphoric acid and any further oxidation was inhibited by the addition of 10 µl of 20 mg/ml BHT. After addition of 50 µl of 42 mM TBA reagent the tubes were mixed by inversion and placed in a heating block at 95 °C for 30 minutes with very gentle shaking. Samples were then cooled on ice and centrifuged at 4 °C for ten minutes at 15000 rpm. 100 µl of the resulting supernatant was transferred to autosampling vial and 20 µl was injected onto the HPLC (Shimadzu RF-10AXL, Shimadzu Corporation, Japan). The HPLC was equipped with a Phenosphere reverse phase C-18, 4.6 x 150 mm, 5 µm column (Phenomenex; Auckland, NZ), heated to 30 °C. TBARS were fluorometrically detected using excitation and emission wavelengths of 525 nm and 550 nm, respectively. The mobile phase was pumped through the system at a flow rate of 1 ml/minute.

TBARS concentrations in all samples were quantified by comparison with the peak areas of 0 µM and 1 µM MDA standards. Fresh MDA was prepared before each assay by hydrolysis of 1,1,3,3-tetramethoxypropane (TMP) in 2:3 (v/v) ethanol:water, with subsequent dilution in water to the appropriate concentration. Phosphoric acid and BHT were then added, as per the experimental samples.

2.2.19 Pterin HPLC Analysis Assay

2.2.19.1 Solutions for the Pterin HPLC Analysis Assay

Both neopterin and 7,8-NP are light sensitive. A stock of neopterin standard was prepared by sonicating neopterin in 10 mM phosphoric acid in the dark. By contrast, the 7,8-NP standard was prepared by sonication in degassed water in the dark.

The mobile phase was prepared on the day of analysis. It consisted of 20 mM ammonium phosphate and the pH was adjusted to pH 6 by addition of 10 M phosphoric acid. Five percent methanol (v/v) was added to the buffer and the mixture was filtered through 0.45 µm filters.

The acidic iodide solution was prepared by dissolving 2.7 g solid iodine and 5.4 g potassium iodide in 35 ml of nanopure water. 3.7 ml of 50% TCA was added and the final volume was made up to 50 ml.

2.2.19.2 Pterin HPLC Analysis Assay

This assay monitored pterin levels in the cell-conditioned medium, and in the cells themselves. When the latter was measured the cells were washed in PBS before hypotonic lysis in 0.5 ml of ice cold water. 135 µl sample (the cell conditioned medium and or cell lysate) was collected into microcentrifuge tubes and mixed with 13.5 µl of 50% TCA. The mixture was vortexed and centrifuged at 15000 rpm for 15 minutes. 100 µl of the resulting supernatant was transferred to autosampling vial and mixed with 5 µl of 2 M ammonium phosphate (pH 6).

When total neopterin which was the oxidation of all 7,8-NP to neopterin was to be measured, 10 µl of an acidic iodide solution, followed by 13.5 µl of 50% TCA were added to the samples. The mixture was vortexed and incubated in the dark for 20 minutes. Then, 10 µl of 0.6 M ascorbate was added to reduce the remaining iodine to iodide. The samples were centrifuged at 4 °C and 15000 rpm for ten minutes. 100 µl of the resulting supernatant was transferred to autosampling vial and mixed with 5 µl of 2 M ammonium phosphate (pH 6).

20 µl of this mixture was analysed by the HPLC (Shimadzu RF-10AXL, Shimadzu corporation, Japan) equipped with a reverse phase Develosil C18, 250 x 4.6 mm, 5 µm column (Nomura Chemicals; Japan) maintained at 35 °C. The mobile phase was pumped through the system at a flow rate of 1 ml/minute (Gieseg, *et al*., 2001). Neopterin was detected using a fluorescence detector set at an excitation and emission wavelengths of 353

nm and 438 nm, respectively. Neopterin concentrations in all samples were quantified by comparison with the peak areas of 5 µM and 10 µM neopterin standards.

2.2.20 Monobromobimane Glutathione (GSH) Measurement by HPLC Analysis

2.2.20.1 Solutions for GSH Assay

A 40 mM stock of monobromobimane (MBB) was prepared by dissolving 10.8 mg of MBB in 1.0 ml acetonitrile. The solution was stored in darkness at 4 °C and freshly made every 1-2 weeks.

Reduced glutathione of 10 mM stock was dissolved in PBS solution and freshly made prior to experiment. The stock solution was diluted with PBS to concentrations of 5 and 10 µM.

100% (w/v) TCA was made up in nanopure water by adding 10 g of TCA to 10 ml of nanopure water.

The mobile phase A consisted of 0.25% acetic acid and mobile phase B consisted of 100% acetonitrile.

2.2.20.2 GSH Measurement by HPLC Analysis

Monobromobimane (MBB) is a cell-permeable fluorescent dye that binds thiol groups, specifically glutathione (GSH). The assay utilises this property to measure GSH by HPLC after precipitating protein (Cotgreave, *et al.*, 1986). All the experiments were carried out under minimum exposure of light, as MBB is light sensitive.

After removal of the incubation medium, the cells were washed twice in PBS and submerged in 0.4 ml of PBS. Nine microlitres of 0.1 M NaOH were added to the wells to bring up the pH to 8 before the addition of 10 µl of 40 mM MBB. Following twenty minute incubation in the dark at room temperature, 20 µl of 100% (w/v) TCA was added to lyse the cells. The adherent cells were scraped, transferred into Eppendorf tubes and subsequently centrifuged at 10 000 rpm for 5 min.

100 µl of the resulting supernatant was transferred to autosampling vial and 20 µl was injected onto the HPLC (Shimadzu RF-10AXL, Shimadzu Corporation, Japan). The HPLC was equipped with a Phenosphere reverse phase C-18, 4.6 x 150 mm, 5 µm column (Phenomenex; Auckland, NZ), heated to 35 °C. GSH-MBB adducts were fluorometrically detected using excitation and emission wavelengths of 394 nm and 480 nm, respectively. The mobile phase was pumped through the column at a flow rate of 1.5 ml/minute and

with the following gradient; at 0 minute: A: B (90:10), at 10 minute: A:B (90:10), at 11 minute: A: B (0:100), at 15 minute: A: B (0:100), at 16 minute: A:B (90:10), and at 20 minute: A:B (90:10). GSH concentrations in all samples were quantified by comparison with the peak areas of 5 μM and 10 μM GSH standards.

2.2.21 Statistical Analysis

Results shown were obtained from single experiments, which was representative of at least three separate experiments. The means and standard deviation of the mean (SD) shown within each experiment were calculated from triplicate samples. Data were graphed and statistically analysed using the software program, GraphPad Prism version 4.0 for windows, GraphPad Software, San Diego California USA. Significance was confirmed by a one-way analysis of variance (ANOVA) followed by Tukey's multiple comparison test, * indicating a significant difference from the control value (* $p < 0.05$; ** $p < 0.01$; *** $p<0.001$).

3 Experimenting the Culture of Human Monocyte-derived Macrophages in Different Conditions

3.1 Introduction

This laboratory routinely uses RPMI to culture isolated blood human monocytes. RPMI-1640 was developed in 1966 by Moore and his co-workers at Roswell Park Memorial Institute (hence the acronym RPMI) (Sigma product information sheet). It is a media that utilizes a bicarbonate buffering system and contains amino acids, vitamins, cofactors, carbohydrates and salts necessary to support cell growth. While it was originally formulated to support lymphoblastoid in suspension culture, it has been proven to support a wide variety of anchorage-dependant cells (Sigma product information sheet). When culturing isolated human blood monocytes, the media are mostly supplemented with 5-30% heat inactivated human serum (HIHS) although mixtures of foetal calf serum (FCS) and HS or media containing FCS alone is also used (Garner *et al*., 1997a). However, serum contains extracellular cholesterol acceptors, high density lipoprotein (HDL), which could promote cholesterol efflux from the cells and consequently reduces cholesterol esterification (Innerarity, *et al*., 1986). One of the objectives of this research is to develop foam cell from HMDMs whose main characteristic is an accumulation of cellular cholesteryl ester. There is a concern that adding serum to the media may interfere with the study of characterising the foam cell formation. Therefore, the ability of blood monocytes to grow in RPMI supplemented with serum which is devoid of lipoprotein (called lipoprotein deficient serum, LPDS) will be explored in this section. LPDS lacks HDL. It is envisaged that if the cells could grow well in RPMI supplemented with LPDS, this culture condition will be used to culture the monocytes for developing foam cells.

Media that are free of serum are widely recognized to provide a more defined and controlled cell culture environment. Since serum is of animal-origin the use of serum-free media (SFM) will limit the potential of introducing adventitious agents into a cell culture system. In this study, Gibco BRL's macrophage SFM was used. This media was optimized to support the growth of monocytes and macrophages and does not require supplementation with serum (Gibco product information sheet). This feature should make SFM an ideal media to develop foam cell from isolated human blood monocytes. Therefore, the next objective of this section is to explore an alternative media to RPMI and serum to culture the human monocytes by using SFM.

The ability of the cell to grow in different conditions will be assessed by examining their morphology observed by inverted light microscope and measuring the cells' viability by MTT or trypan blue assay. This section will also investigate the effects of replacing HIHS with LPDS on the viability of HMDMs. In addition, observation was also made on the growth of macrophages in suspension well plate and the possibility of growing the cells back on to the adherence plate.

3.2 Results

3.2.1 Growth of HMDMs in the Macrophage-Serum Free Media

Isolated blood human monocyte were routinely cultured in RPMI supplemented with 10% HIHS. After 14 days in culture, the monocytes differentiated into macrophages with a morphology that resembles a 'fried-egg'. Some monocytes still remain small and round (Figure 3.1).

The ability of monocytes to grow in SFM was investigated by observing their growth under the inverted light microscope. The isolated monocytes (5×10^6 cells /ml) were seeded on to the adherent plate in SFM from day 1 of culture. Their morphology was compared to the cells isolated from the same donor but cultured in RPMI with 10% HIHS.

After 5 days of culture (day 5), some macrophages were seen in RPMI with 10% HIHS while cells cultured in SFM were all still monocyte like in appearance (Figure 3.1). After 3 further days (day 8), monocytes in SFM still had not differentiated into macrophages. In addition, the number of cells also seemed to be reduced. Only by day 14 were some macrophages like cells were observed in SFM while in RPMI containing 10% HIHS the cells were mainly macrophage appearance. However, the cells in SFM did not look 'healthy' and less homogenous macrophage culture was observed. This is because growing the cells in the SFM also induced morphological alteration in the HMDMs. A proportion of the cells displayed elongated cellular processes (dendritic look) that were not seen in cells grown in RPMI with 10% HIHS.

Lipid accumulation in cells cultured in SFM and RPMI containing 10% HIHS was examined microscopically following staining of cells with oil red-O (Figure 3.2). Oil red-O positive staining materials indicating the presence of lipid droplets were observed in cells cultured in both types of media. The results suggest that the cells can survive in both media but they differentiated faster in RPMI containing 10% HIHS than in SFM. Cellular accumulations of lipids was observed in cells grown in both media.

The rate of monocytes differentiation into macrophages was also determined for cells grown in RPMI with 10% HIHS by observing the change in their morphology. Monocytes were the small round cells while macrophage cells appear large and foamy. After 14 days in culture, 70% of the cells were macrophages (Figure 3.3) and this percentage varied from blood donor to blood donor.

3.2.2 Effect of oxLDL on Viability of HMDMs Cultured in SFM and RPMI Containing 10% HIHS

The effect of oxLDL on the viability of HMDMs cultured in RPMI containing 10% HIHS compared to HMDM cultured in SFM was examined. At the same time the cells were seeded at two different cell concentrations, 5 x 10^6 cells/ml and 3 x 10^6 cells/ml. This is to determine which concentration of cells at the time of seeding will give a better cell growth. After 14 days in culture, the cells were incubated with increasing concentrations of oxLDL for 10 days. The viability of the HMDMs was assessed using the trypan blue exclusion assay.

Figure 3.4a shows that cells plated at 5 x 10^6 cells/ml and grown in the RPMI containing 10% HIHS had a viability of more than 90% whereas, cells grown in SFM had lower viability around 80%. In addition, there was a large standard deviation (SD) in cell viability for the cells cultured in SFM both in controls and with oxLDL. The presence of sub cytotoxic concentrations of oxLDL did not significantly affect the cell viability of the cells either in SFM or RPMI containing 10% HIHS. Though a 10% loss in viability was observed in the SFM media at 200 μg/ml oxLDL but this was not significant. This experiment was repeated but using another HMDMs preparation from different donor and the cells were plated at lower cell concentration of 3 x 10^6 cells/ml. The cell viability of the cells was a mean of 90% and 45% for the cells grown in RPMI and SFM respectively (Figure 3.4b). Even though the presence of oxLDL did not significantly affect the cell viability, there was a very large variation (as measured by the Standard Deviation (SD)) for each concentration of oxLDL in both media at this lower cell concentration (Figure 3.4b) when compared to Figure 3.4a. The large variation probably reflects the irregularity in the number of cells in the well because even though the same concentration of cells was seeded onto each well, not all of them survived. The most likely explanation for this is probably because the cells need to be in close contact with each other in order to grow well and this was achieved when they were seeded at higher density number. This is supported by the trypan blue assay result showing that cells plated at higher cell concentration, 5 x

10^6 cells/ml had higher viability than cells plated at 3 x 10^6 cells/ml indicating that having more cells present will increase the number of viable cells. In addition, higher percentage of cell viability when cells cultured in RPMI with 10% HIHS reflects the preference of the cells towards this media for growth than SFM.

The following three consecutive attempts to culture HMDMs in SFM were met with failure indicating the lack of reliability of SFM media for culturing. Cells isolated from the same donor did not grow in SFM but survived in RPMI containing 10% HIHS (data not shown). This result led to the investigation of the effect of changing the media from RPMI with 10% HIHS to SFM on healthy cells that were already cultured in RPMI with 10% HIHS. Figure 3.5 shows that after 2 days in SFM the cells viability dropped to 60% and stayed constant until 6 days in SFM. This suggests that there were some factors in RPMI with 10% HIHS that was missing in SFM and caused a drop in the cell viability.

The manufacturer, Gibco BRL, will not disclose the compositions of the SFM making it difficult to identify what is missing within the media for macrophages. A suggestion was proposed by Dr. Keri Carpenter of Cambridge University (personal communication) to include granulocyte-macrophage colony stimulating factor (GM-CSF) to the SFM when culturing the cells. There was a striking effect of the presence of GM-CSF in SFM on the growth of the cells (Figures 3.6 and 3.7). At day 5 of culture, most of the cells grown in SFM supplemented with GM-CSF (Figure 3.6b) had differentiated into macrophages and some had elongated cellular processes or taken on the appearance of dendritic cells. By day 14, all the cells appeared as normal looking macrophages (fried egg-like morphology) (Figure 3.7b). It is not known whether the disappearance of the elongated processes was due to these cells changing their shaped to fried egg-like macrophage morphology or that elongated cells simply die. Moreover, cells cultured in SFM only displayed elongated processes at day 14 (Figure 3.1), but cells grown in SFM with GM-CSF had significant proportion of cells with elongated processes as early as day 5 (Figure 3.6b). In addition, it appears that the differentiation of monocytes into macrophages when they were cultured in SFM with GM-CSF occurred faster than what had been observed in cells grown in RPMI with 10% HIHS (Figure 3.1). In these experiments, few cells grown in SFM without GM-CSF survived until day 14 of culture. Therefore, the presence of GM-CSF is important in stimulating the growth of monocytes and their differentiation into macrophages in SFM media.

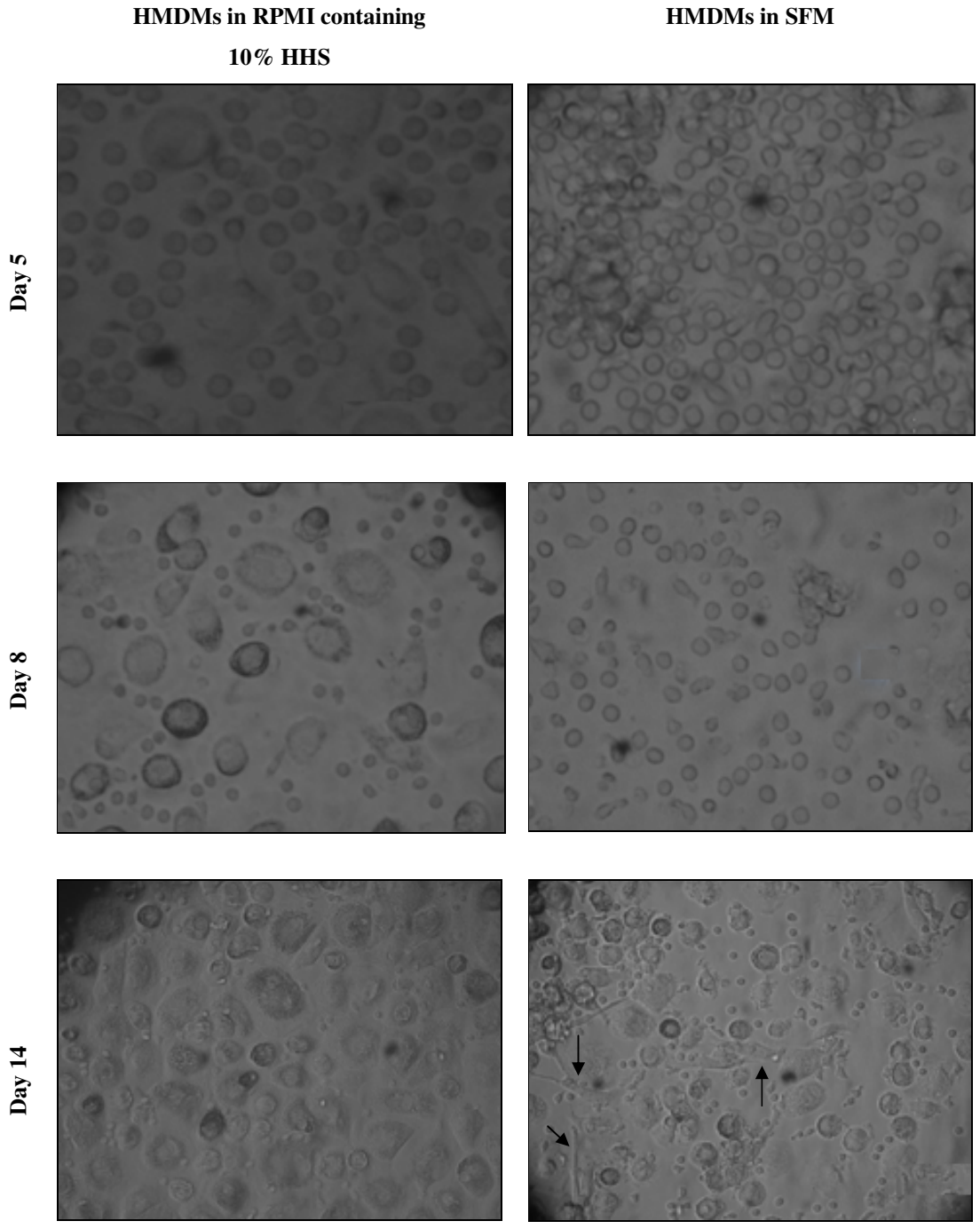

Figure 3.1 Comparison between the growth of HMDMs in RPMI containing 10% HIHS and SFM.

HMDMs (5 x 10^6 cell/ml) were cultured in RPMI containing 10% HIHS or SFM in 12 well plates. Cells were viewed *in situ* in tissue culture wells using an inverted microscope. Macrophage cells appear large and foamy while monocytes were the small round cells. The arrows point to cells having elongated cellular processes or taken on the appearance of dendritic cells. Original magnification of the microscope was 40x and the pictures were taken using a digital camera.

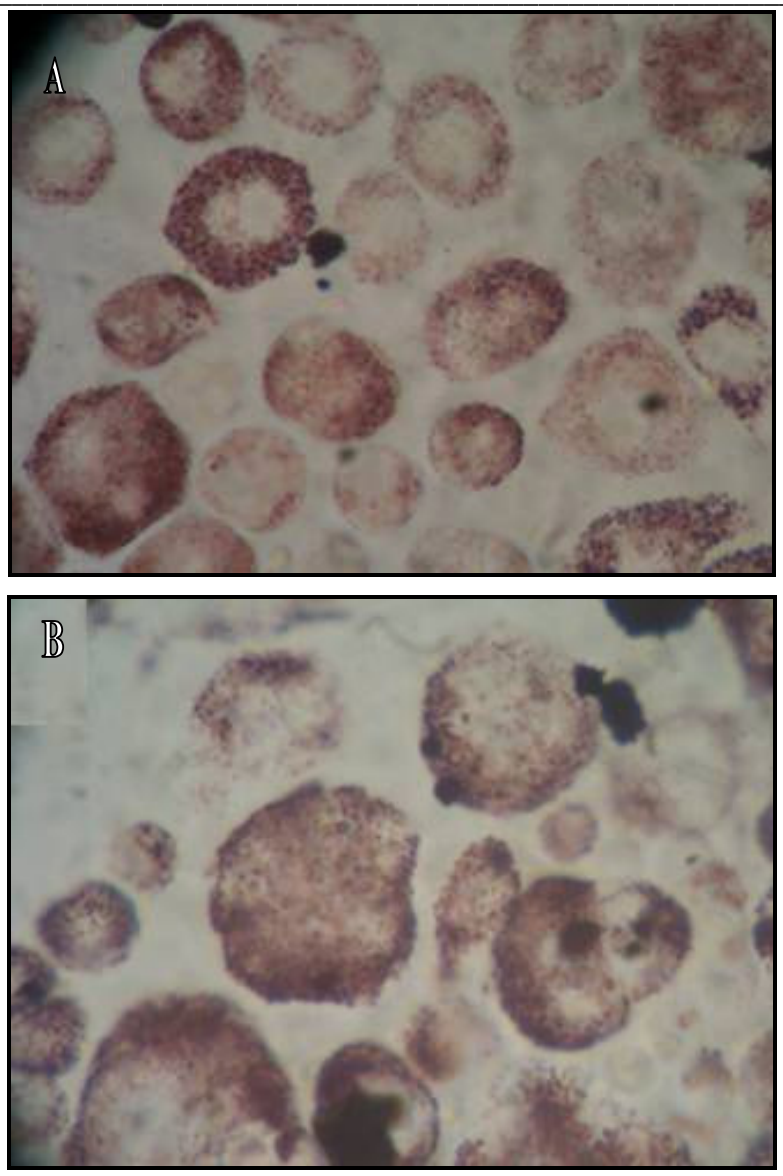

Figure 3.2 Culture of HMDMs in RPMI and SFM produces oil red-O positive, lipid loaded cells.

HMDMs (5 x 10^6 cell/ml) were cultured in RPMI containing 10% HIHS (a) or SFM (b) in 12 well plates for 14 days. Cells were stained with oil red-O stain as described in chapter 2 and viewed *in situ* in tissue culture wells using an inverted microscope. Original magnification was 40x and the pictures were taken using a digital camera.

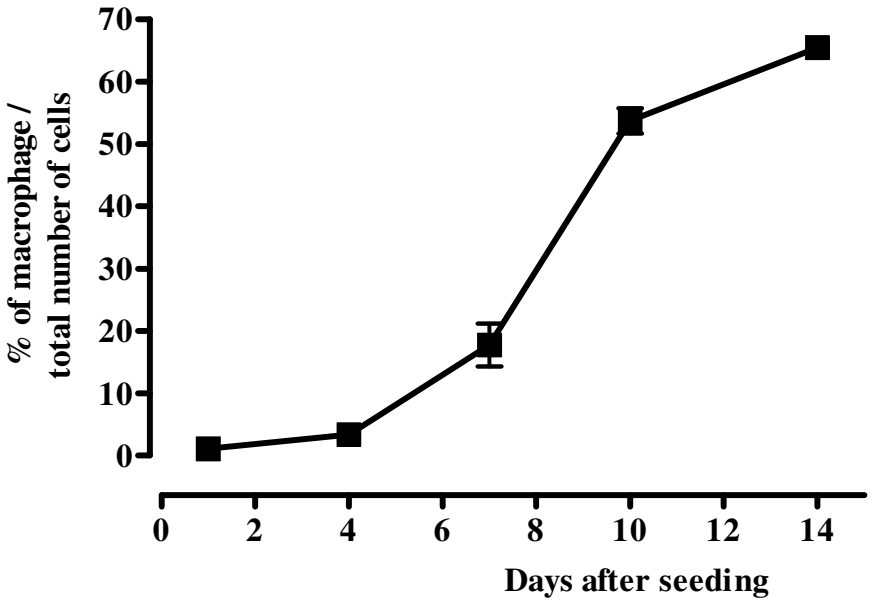

Figure 3.3 Number of monocytes and macrophages over 14 days culture in RPMI with 10% HIHS

HMDMs (5 x 10^6 cell/ml) were cultured in RPMI containing 10 % HIHS. The number of monocytes and macrophages were counted on the day of seeding (day 0), days 4, 7, 10 and 14 after seeding. The cell number was counted in 3 wells and at least from 5 views. Results are displayed as mean ± SD of triplicates from a single experiment representative of three separate experiments.

(a)

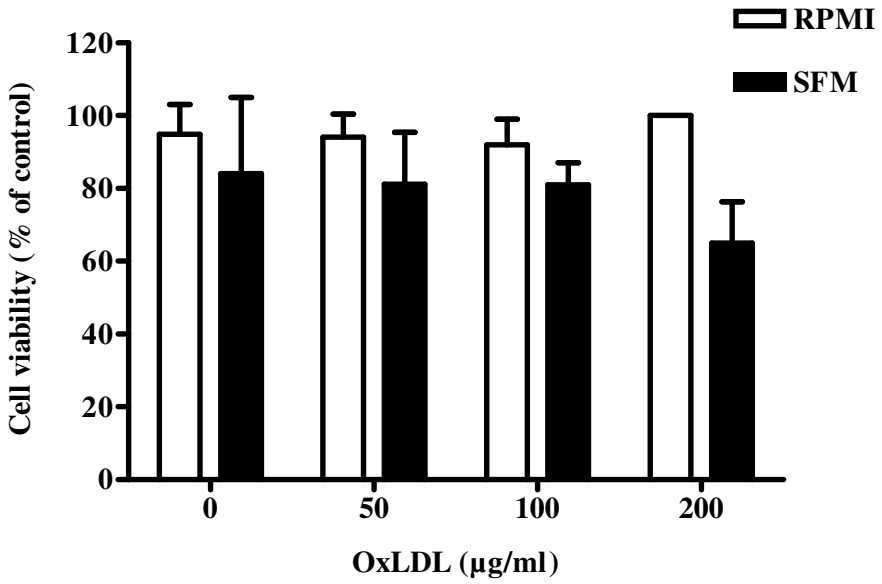

(b)

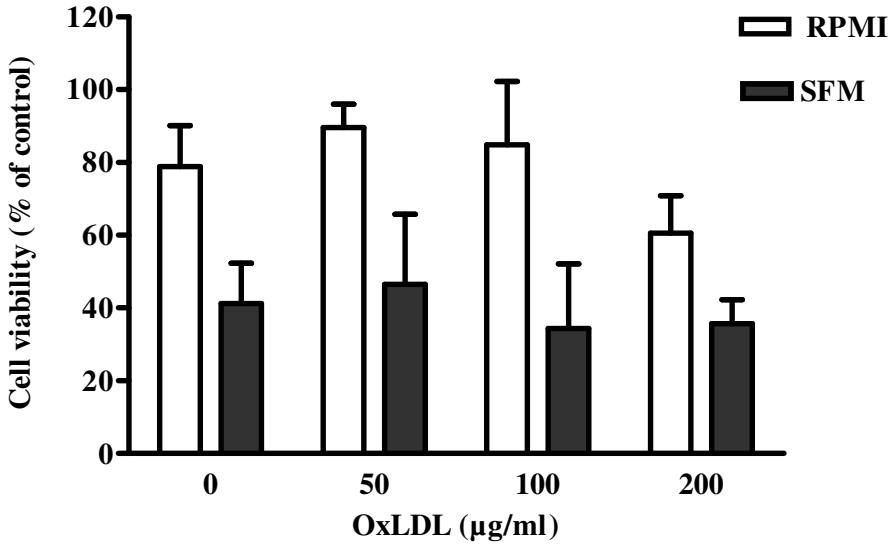

Figure 3.4 Effect of oxLDL on viability of HMDMs grown in SFM and RPMI containing 10% HIHS.

HMDMs were plated at $5x10^6$ cells/ml (a) and $3x10^6$ cells/ml (b) in SFM and RPMI containing 10% HIHS. After 14 days the cells were incubated with increasing concentrations of oxLDL for 10 days. The cell viability was assessed via trypan blue exclusion staining. Results are displayed as mean ± SEM of triplicates from a single experiment representative of three separate experiments.

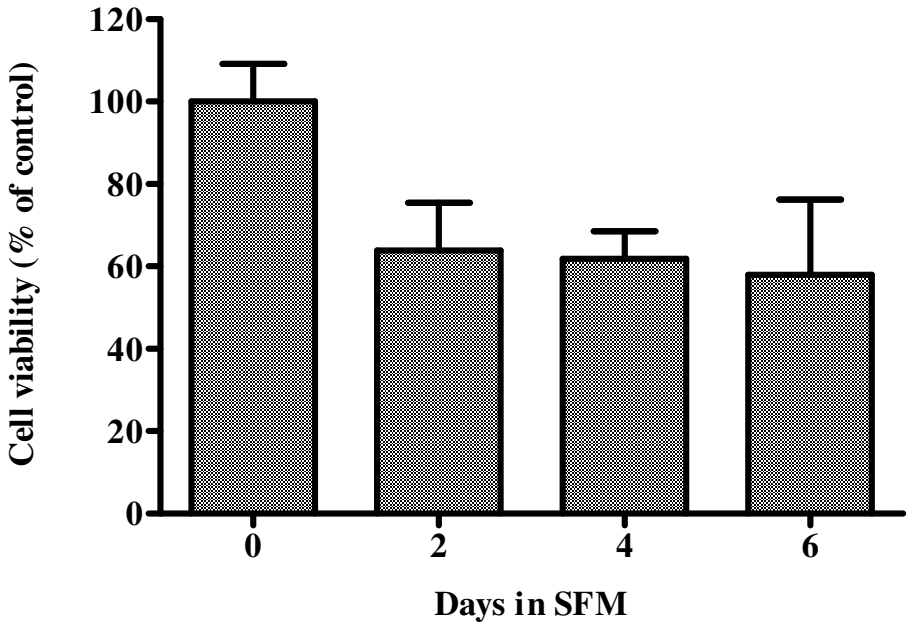

Figure 3.5 Effect of changing the media from RPMI containing 10% HIHS to SFM on the viability of HMDMs

Cells were cultured at 5 x 10^6 cells/ml in 12 well plate in RPMI containing 10% HIHS. After 14 days, the medium was changed to SFM. The cells were further cultured in SFM for the indicated days. Data shown are the mean $\pm$ SD of triplicate from a single experiment.

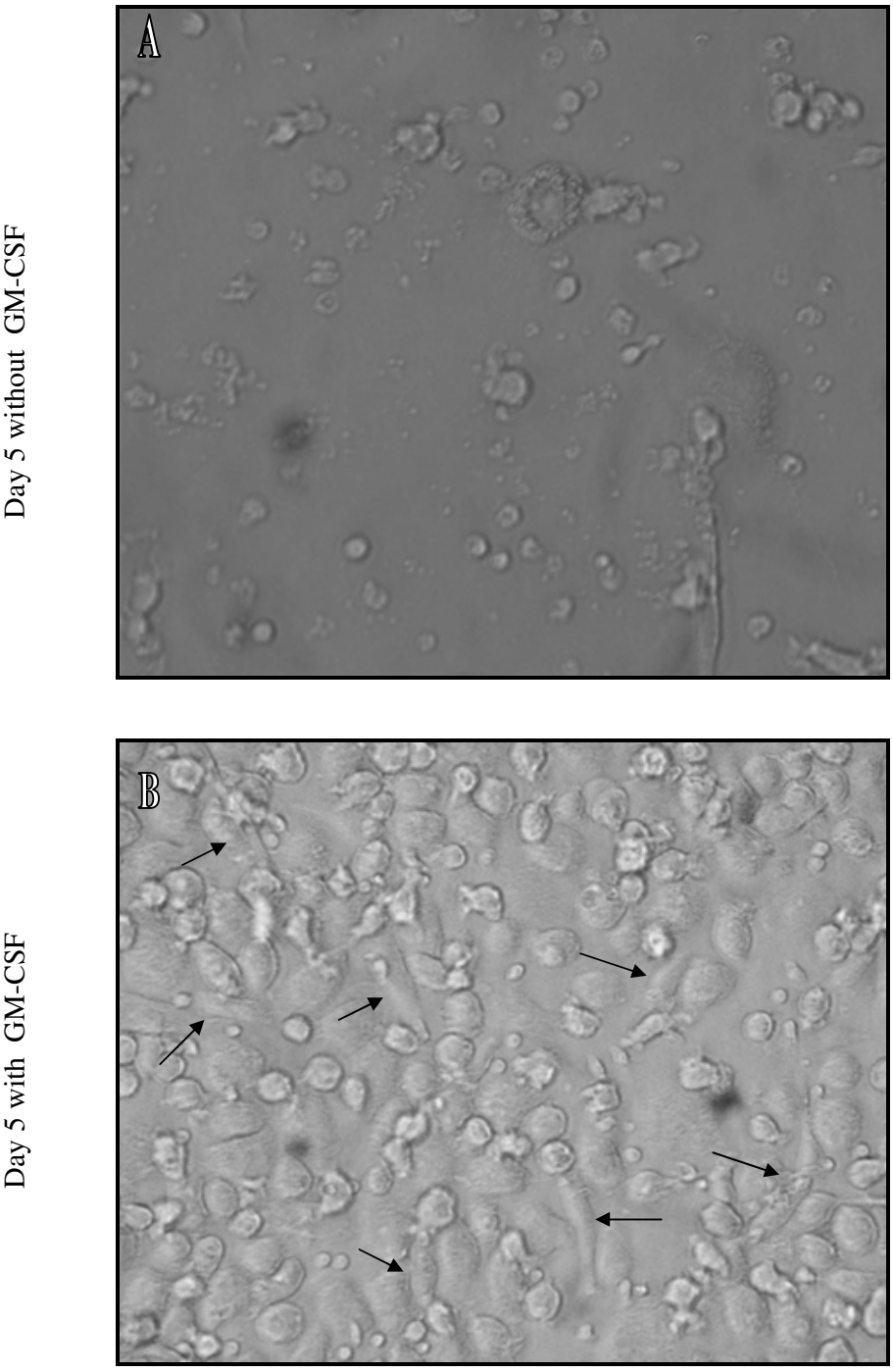

Figure 3.6 The effect of GM-CSF in the SFM on HMDMs growth on day 5 of culture.

HMDMs (5 x 10^6 cell/ml) were cultured in SFM without (a) and with GM-CSF (0.15 µg/ml) (b) in 12 well plates. Pictures were taken on day 5 of culture. Cells were viewed *in situ* in tissue culture wells using an inverted microscope. Arrows indicate elongated cellular processes. Original magnification of the microscope was 40x and the pictures were taken using a digital camera.

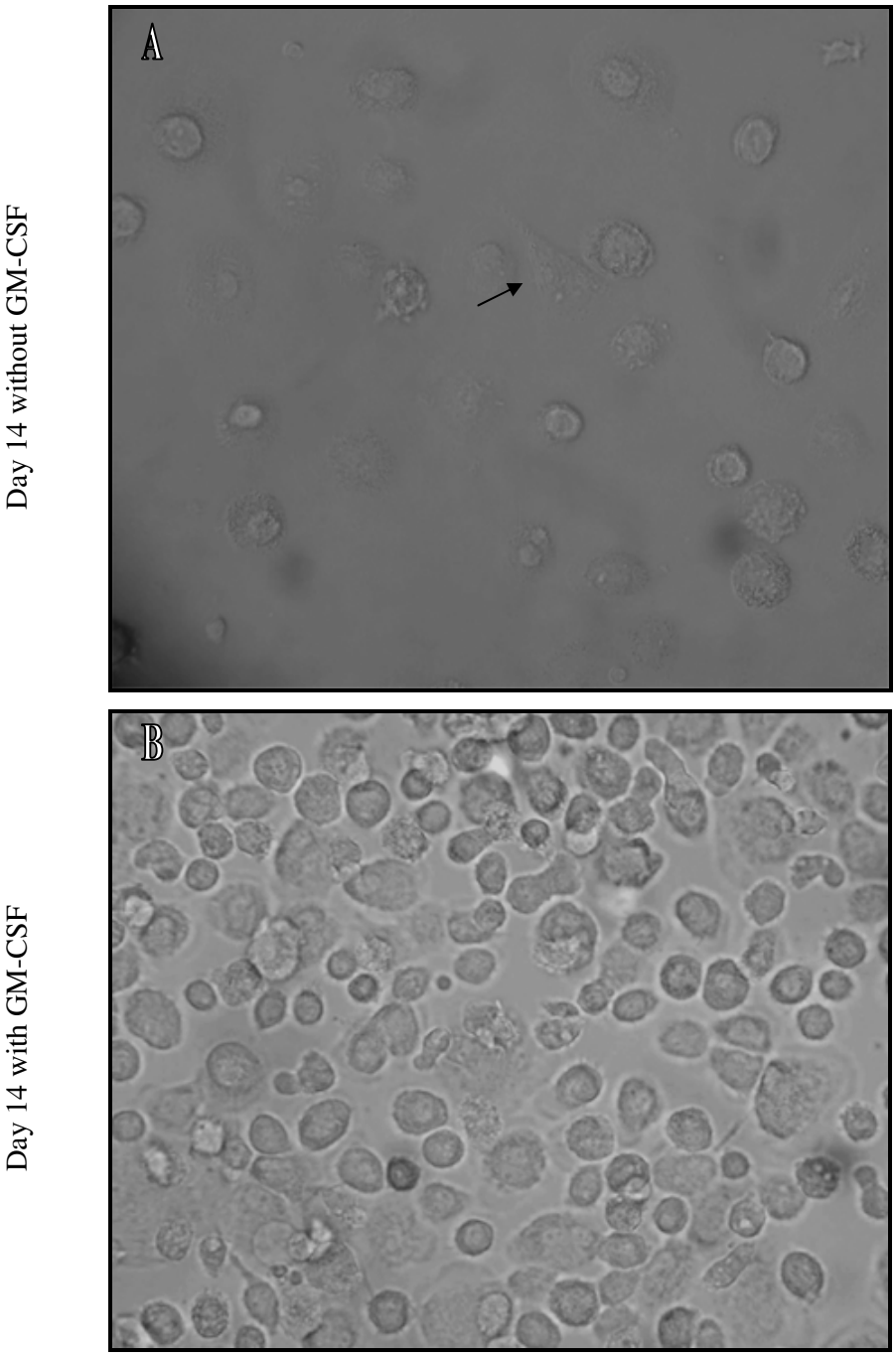

Figure 3.7 The effect of GM-CSF in the SFM on HMDMs growth on day 14 of culture.

HMDMs (5 x 10^6 cell/ml) were cultured in SFM without (a) and with GM-CSF (0.15 µg/ml) (b) in 12 well plates. Pictures were taken on day 14 of culture. Cells were viewed *in situ* in tissue culture wells using an inverted microscope. Arrows indicate elongated cellular processes. Original magnification of the microscope was 40x and the pictures were taken using a digital camera.

3.2.3 Culturing HMDMs in RPMI Containing 10% LPDS

HDL in the lipoprotein is an extracellular acceptor of cholesterol from cells, which could affect cholesterol accumulation within the macrophages. Thus serum containing lipoprotein would not be appropriate for cellular cholesterol loading experiments. Due to this the growth of cells in RPMI containing LPDS was explored. LPDS was prepared form HIHS according to the methods described in Chapter 2. HMDMs (5 x 10^6 cell/ml) were cultured in RPMI supplemented with 10% LPDS from day 1 of culture. The growth of cells in RPMI with 10% LPDS was compared to the growth of cells in RPMI with 10% HIHS isolated from the same blood donor and monitored daily by inverted light microscope.

Microscopic examination of the macrophages after 14 days in culture revealed that macrophages grown in RPMI with LPDS had less spread cytoplasm and were more rounded looking (Figure 3.8) compared to the fried-egg morphology of macrophages grown in RPMI containing HIHS. After 14 days in culture, oil red-O positive staining was more prevalent in cells grown in RPMI with HIHS than cells grown in RPMI with LPDS suggesting less lipid accumulation in the later culture system (Figure 3.9). In two other attempts to grow monocytes in RPMI with LPDS, there were less number of cells in RPMI with 10% LPDS compared to cells grown in RPMI with 10% HIHS throughout the culture period. This could suggest that the LPDS is less favourable for the growth of HMDMs possibly due to the lack of cholesterol, triacylgycerol or α-tocopherol in the LPDS.

3.2.4 Effect of OxLDL on HMDMs' Viability Incubated in RPMI Containing 10% LPDS or Without Serum

Effect of oxLDL on HMDMs viability when the serum in the RPMI was changed from HIHS to LPDS or without any serum was examined. In this experiment the cells were already in RPMI containing 10% HIHS for 14 days before the media was changed to RPMI containing 10% LPDS or no serum for 24 hours. Incubation of HMDMs with oxLDL media containing LPDS made them more sensitive to oxLDL (Figure 3.10). The cell viability was significantly lost at 0.1 mg/ml oxLDL while no viability loss was observed at this concentration when they were in media containing HIHS (Figure 5.3, Chapter 5). The 50% loss in cell viability at 1.0 mg/ml when the cells were in media containing LPDS was similar to cells in media containing HIHS (Figure 5.3, Chapter 5). Interestingly, oxLDL concentrations of above 1.0 mg/ml did not cause any further loss in the viability (Figure 3.10). This is rather surprising because when cells were in RPMI

containing HIHS the cell viability was less than 10% with oxLDL concentration greater than 1 mg/ml (Figure 5.3, Chapter 5).

The effects of removing HIHS from the media and replacing it with LPDS and no serum were examined. Cells that were initially cultured in media containing HIHS for 14 days were preincubated in media containing LPDS or no serum for 24 hours before further incubating them for another 24 hours in the presence of 1 mg/ml oxLDL. Changing the serum from HIHS to LPDS (Figure 3.11) did not significantly affect the cell viability which suggests that the lipoprotein portion of serum does not significantly contribute to the maintenance of the viability of the cells. The absence of serum in the media caused a massive 50% loss in the cell viability. The cell viability loss of the cells incubated in the HIHS or LPDS with 1 mg/ml oxLDL was not significantly different (approximately 50%). However, in the absence of serum, oxLDL caused 80% drop in the cell viability

The influence of serum deprivation on the viability of HMDMs was then further explored. The MTT assay shows that there was a drop in the cell viability when the media was deprived of serum (B as compared to A, Figure 3.12). The cell viability was greatly reduced even when subtoxic level of oxLDL (0.1 mg/ml) was added (C, Figure 3.12). Addition of oxLDL to the cells (E) slightly increased the cell viability compared to when the cells were just in the media containing serum (D) (Figure 3.12. The data suggests that there were some factors in the serum that can protect the cells from cell viability loss. This result was further supported by results shown in Figure 3.13. Removing the serum from the media decreased the cell viability in a time dependent manner. Similarly the addition of oxLDL to the media containing no serum greatly reduced the viability of the cells.

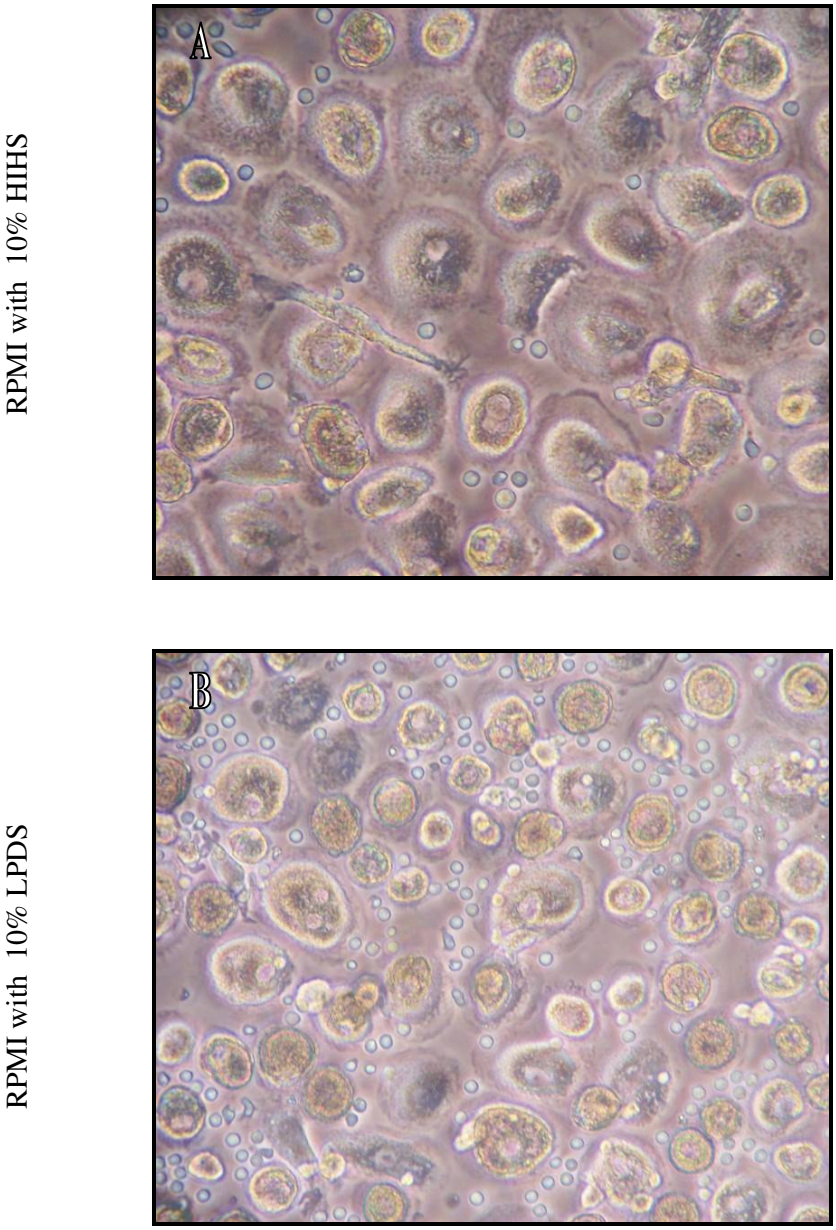

Figure 3.8 The effect of LPDS in RPMI on HMDMs growth.
HMDMs (5 x 10^6 cell/ml) were cultured in RPMI supplemented with 10% HIHS (a) or 10% LPDS (b) in 12 well plates. Pictures were taken on days 14 of culture. Cells were viewed *in situ* in tissue culture wells using an inverted microscope. Original magnification of the microscope was 40x and the pictures were taken using a digital camera. Data shown from one HMDMs preparation representative of three experiments.

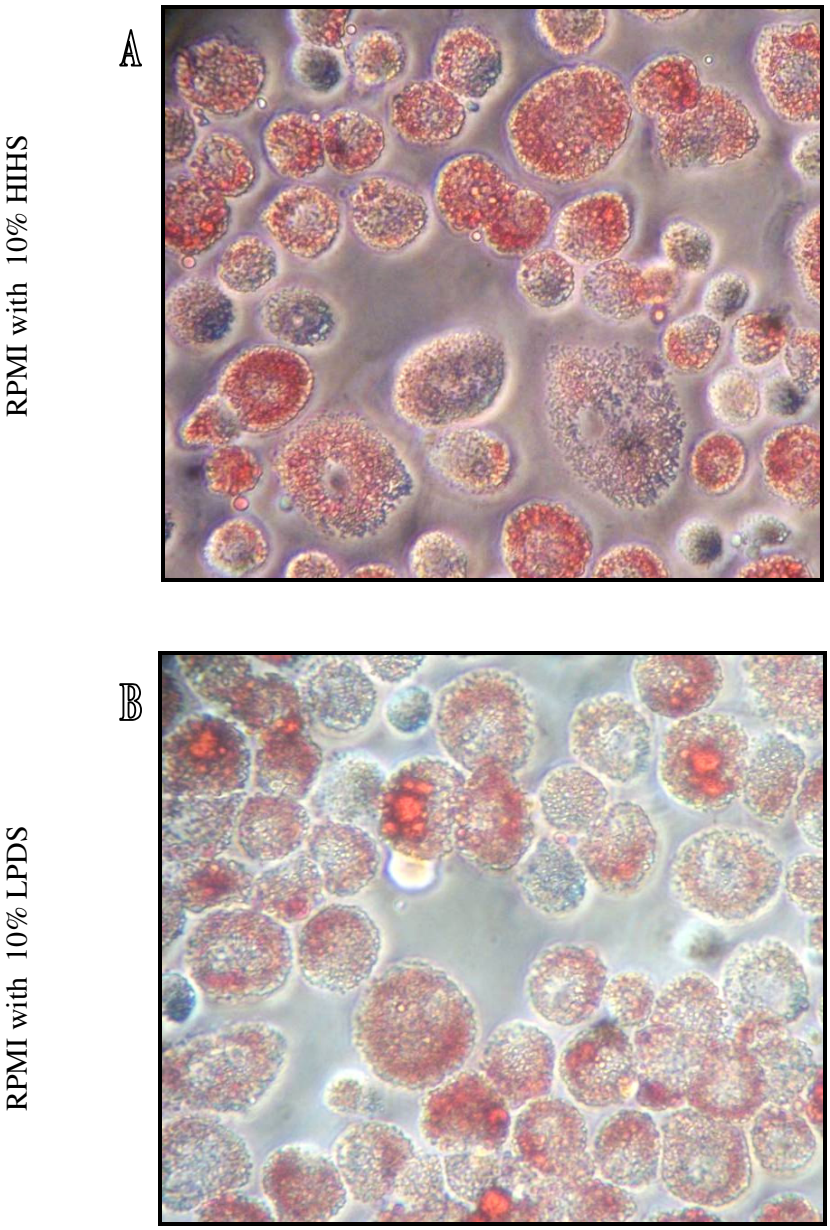

Figure 3.9 Culture of HMDMs in RPMI with 10% HIHS had more cells with oil red-O staining than cells in RPMI with 10% LPDS.
HMDMs (5 x 10^6 cell/ml) were cultured in RPMI containing 10% HIHS (a) or 10% LPDS (b) in 12 well plates for 14 days. Cells were stained with oil red-O staining as described in chapter 2 and viewed *in situ* in tissue culture wells using an inverted microscope. Original magnification was 40x and the pictures were taken using a digital camera.

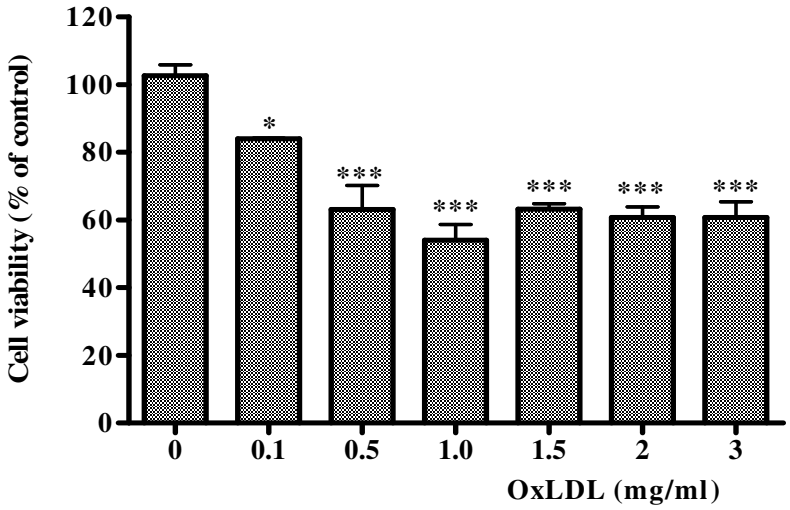

Figure 3.10 Effects of oxLDL on HMDMs viability after 24 h incubation in RPMI containing 10% LPDS.
HMDMs ($5x10^6$ cells/ml) were initially cultured in RPMI containing 10 % HIHS. The serum was changed to 10% LPDS for 24 h before incubation with increasing concentrations of oxLDL for another 24 h. The cell viability was analysed via MTT assay. Significance is indicated from 0 mg/ml oxLDL (control). Results are displayed as mean ± SD of triplicates from a single experiment, representative of three separate experiments.

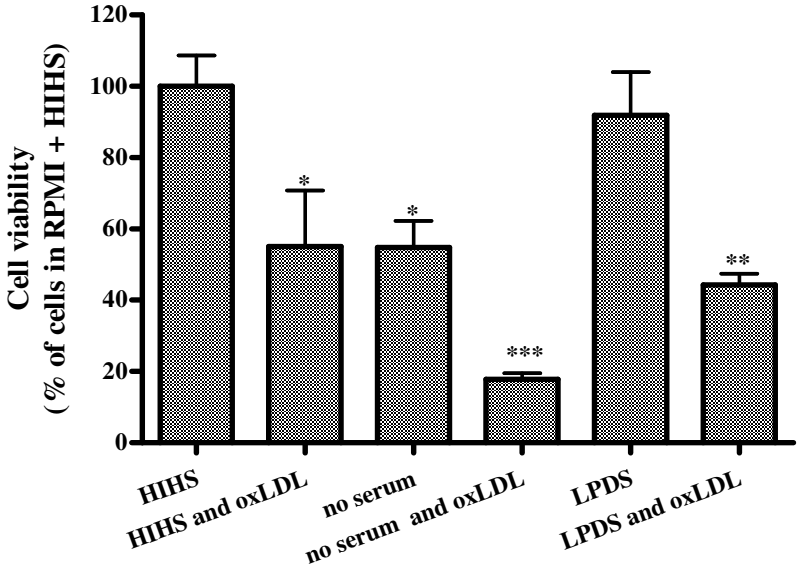

Figure 3.11 Effects of oxLDL and different serum on HMDMs viability.
HMDMs ($5x10^6$ cells/ml) were initially cultured at 37 °C in RPMI containing 10% HIHS. At the start of experiment the HIHS was changed to LPDS or no serum for 24 h. Then the cells were incubated with 1 mg/ml oxLDL in their respective media for another 24 hours. HMDMs were analysed for cell viability via MTT assay. Significance is indicated from cells in RPMI containing 10 % HIHS. Each value shown is the mean $\pm$ SD of triplicates from a single experiment representative of three separate experiments.

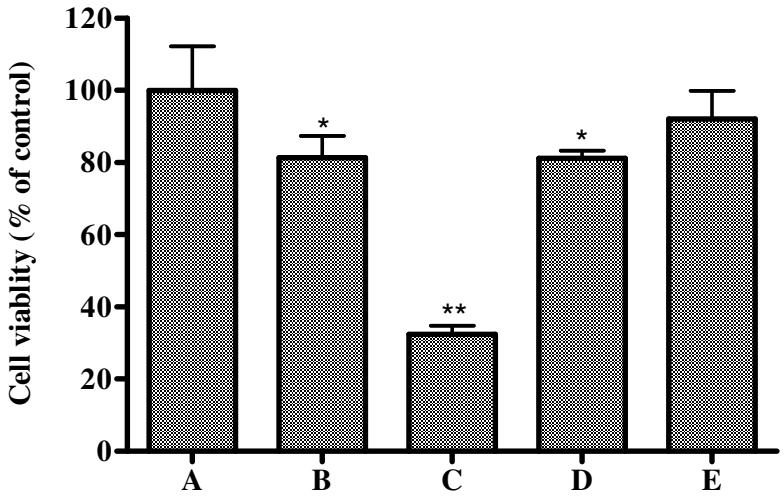

A: cells with serum whole time
B: cells with no serum for 48 hours
C: cells with no serum for 24 hours then add 0.1 mg/ml oxLDL in the absence of serum for another 24 hours.
D: cells with no serum for 24 hours then add 10 % HIHS for another 24 hours.
E: cells with no serum for 24 hours then add 10 % HIHS and 0.1 mg/ml oxLDL for another 24 hours.

Figure 3.12 Effect of serum in the presence of 0.1 mg/ml oxLDL on the viability of HMDMs.

HMDMs were initially cultured in RPMI containing 10 % HIHS. The conditions of experiments are as explained under the graph. After the incubation period, the cell viability was assessed via MTT assay. Significance is indicated from cells in RPMI containing 10 % HIHS. Results are displayed as mean ± SD of triplicates from a single experiment, representative of three separate experiments.

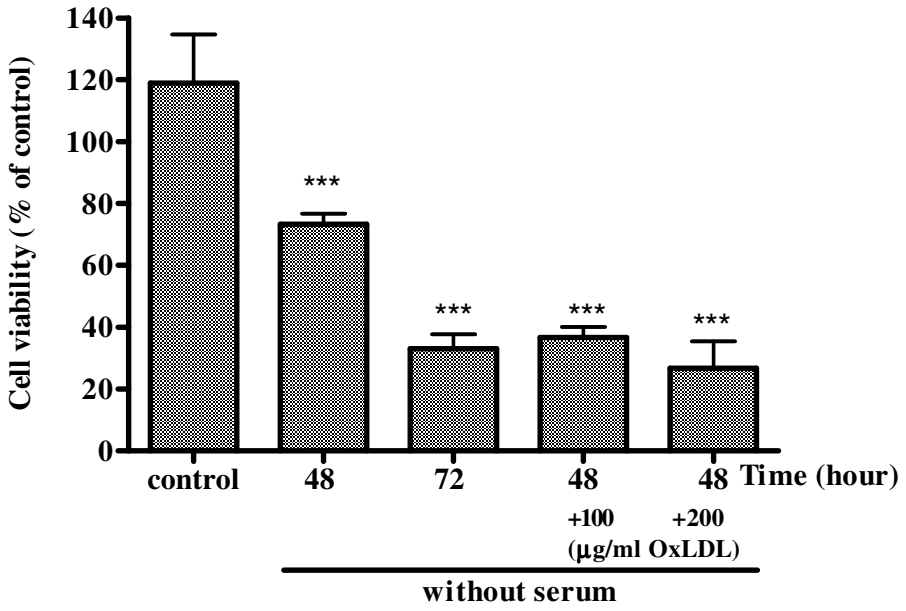

Figure 3.13 Effect of oxLDL on cell viability of HMDMs in the absence of serum. HMDMs (5 x 10^6 cell/ml) were in RPMI containing 10 % HIHS until before experiment the serum was taken out for duration indicated in the graph. Control was HMDMs in RPMI containing 10 % HIHS all the time. After the indicated incubation time with and without oxLDL the HMDMs were assessed for cell viability via MTT assay. Significance is indicated from control. Results are displayed as mean ± SD of triplicates from a single experiment.

3.2.5 Culturing HMDMs in Suspension Plates and then Seeded on to the Adherence Plates

This section investigates whether isolated blood human monocytes can survive and differentiate into macrophages when cultured in a non-adherent suspension plate. In addition, the possibility of growing these cells (cells that have been in a suspension culture for a period of time) can then adhere to an adherence plate and take on a macrophage-like appearance was also explored. Observation of the HMDMs plated in the suspension plate by the inverted light microscope was done on days 4, 8 and 14 of culture. In this experiment the isolated monocytes were initially cultured at 5 x 10^6 cell/ml in 12 well suspension plate (Greiner products, Greiner Bio-one, Frickenhausen, Germany). Since the cells were regarded as suspension cells, their number was counted every time the media was changed and the cells were put back into the same well after centrifugation at 500 g.

Isolated human blood monocytes were able to survive as suspension cells in the suspension plate over 14 days of experimenting period. These suspended cells did not differentiate into macrophages (Figure 3.14). Even though the manufacturer (Greiner Bio-one, Frickenhausen, Germany) claimed that no cell can attach to the bottom of the wells of

their suspension plates, interestingly this study had found the opposite. There was a subgroup of the suspended monocytes which adhere to the bottom of the wells and differentiated. The ability of the monocytes to adhere to the bottom of the suspension wells reflects the fact that these cells are adherent type of cells so; they will try to attach to the wells. The cells attached to the bottom of the wells as early as day 4. On day 8 of culture, the attached cells differentiated into elongated and spindle-like morphology and by day 14, a mixture of elongated and round cells were observed (Figure 3.15). These cells however, did not look like the normal macrophages as seen in Figure 3.1.

Then after 2 weeks in the suspension plate the cells were transferred to the adherence plate. Figure 3.16 shows that on day 2 in the adherence plate a mixture of large round, elongated and small round cells were observed. By day 5, the cells had already become much enlarged but their morphology did not look like the normal fried egg-like macrophages.

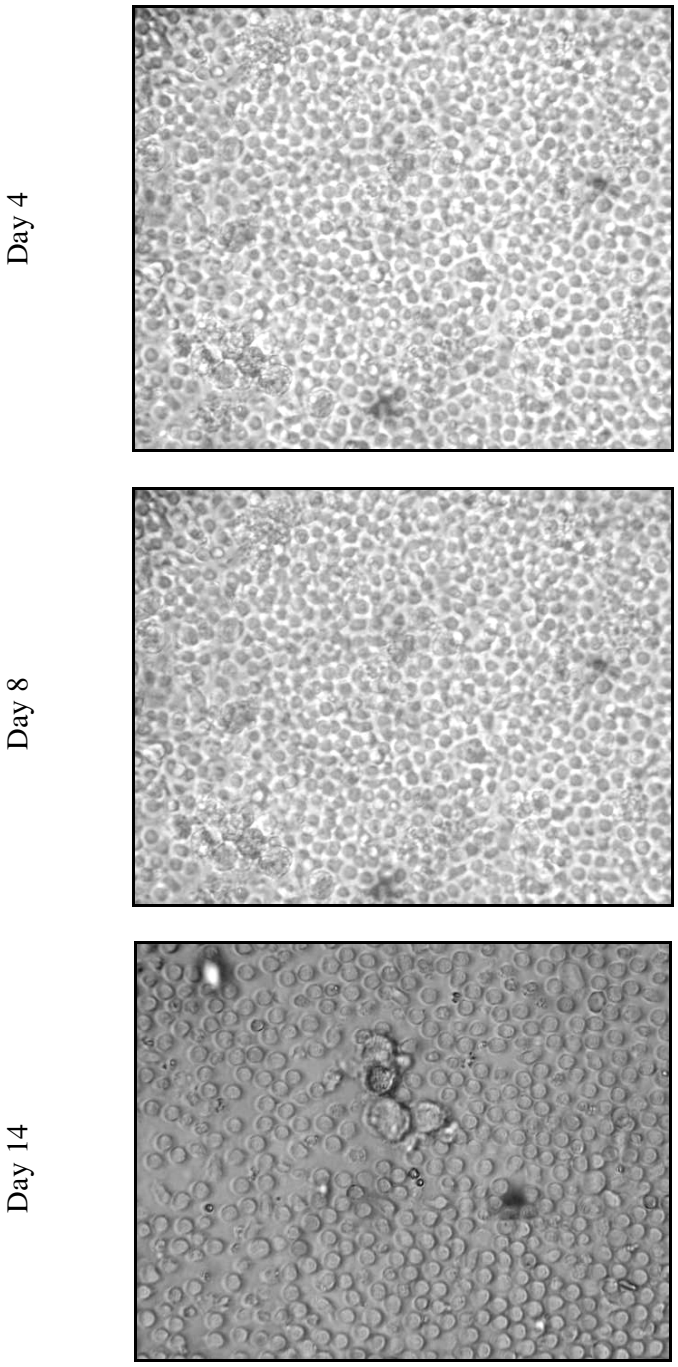

Figure 3.14 HMDMs in the suspension plate.
HMDMs (5 x 10^6 cell/ml) were cultured in RPMI supplemented with 10% HIHS in 12 well suspension plate. Pictures were taken on days 4, 8 and 14 of culture. Cells were viewed *in situ* in tissue culture wells using an inverted microscope. Original magnification of the microscope was 40x and the pictures were taken using a digital camera.

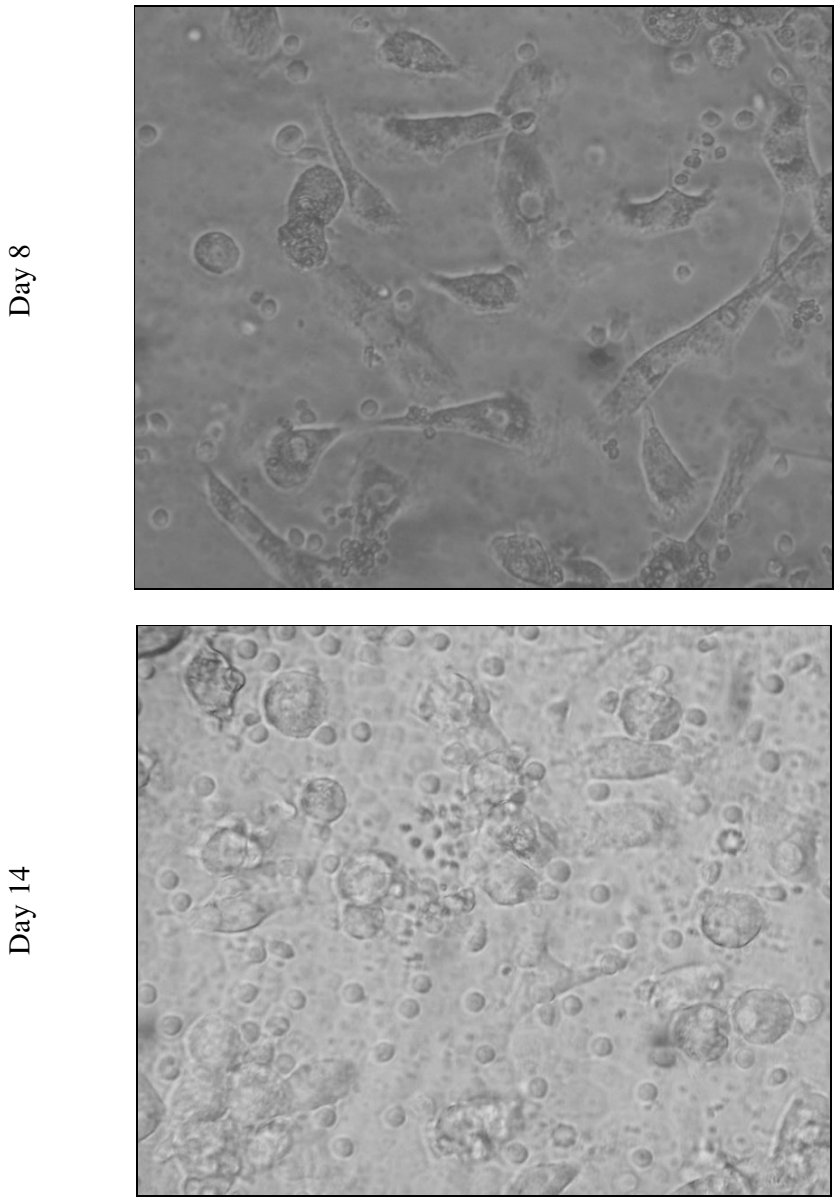

Figure 3.15 The appearance of HMDMs at the bottom of the suspension plate.
HMDMs (5 x 10^6 cell/ml) were cultured in RPMI supplemented with 10% HIHS in 12 well suspension plate. Pictures were taken on days 8 and 14 of culture. Cells were viewed *in situ* in tissue culture wells using an inverted microscope. Original magnification of the microscope was 40x and the pictures were taken using a digital camera.
day 8

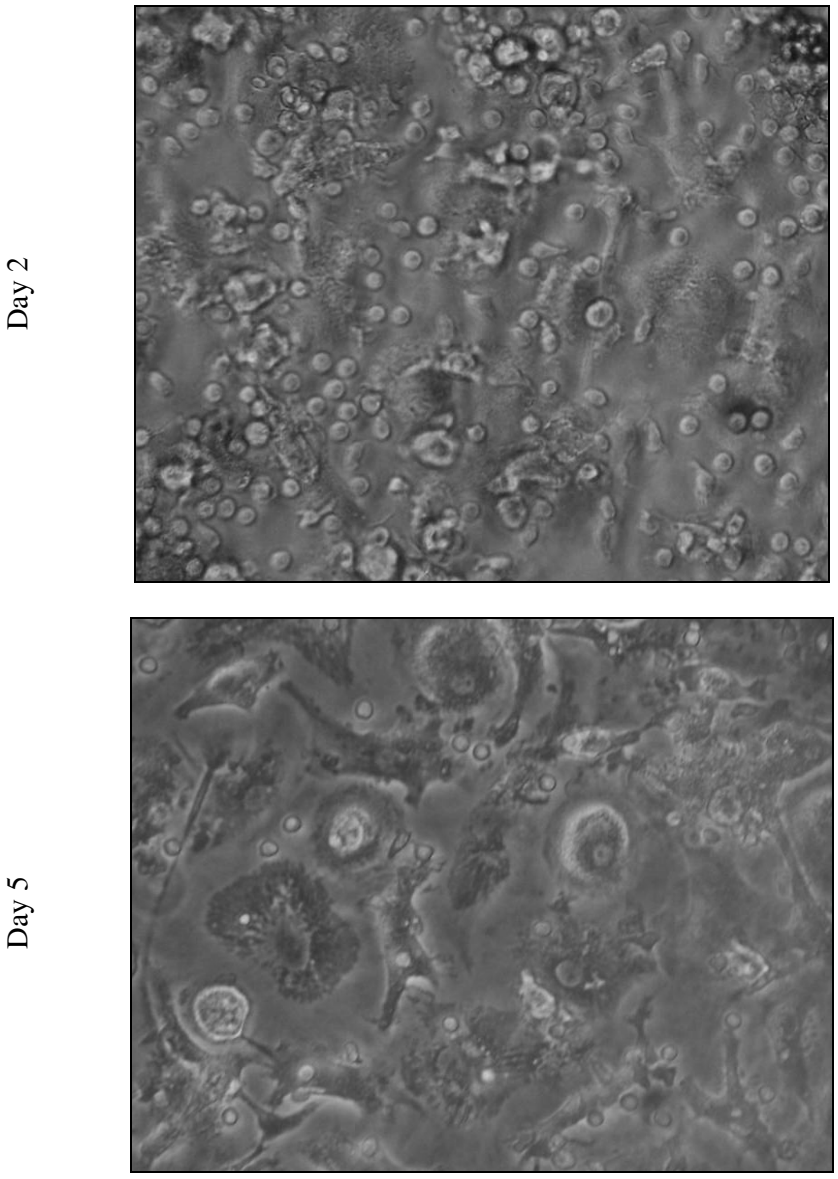

Figure 3.16 Growth of HMDMs on the adherent plate after being cultured in the suspension plate.

HMDMs (5 x 10^6 cell/ml) were initially cultured in RPMI supplemented with 10% HIHS in 12 well suspension plate. After 2 weeks in the suspension plate the cells were transferred to adherent plate and allowed to grow. Pictures were taken on days 2 and 5 in the adherent plate. Cells were viewed *in situ* in tissue culture wells using an inverted microscope. Original magnification of the microscope was 40x and the pictures were taken using a digital camera.

3.3 Discussion

It is known that the early event in lesion development is the recruitment of monocytes from the circulation to the intima by inflammatory processes (in part promoted by proinflammatory effects of oxLDL). Various adhesion and chemoattractant factors participate in this directed migration (see section 1.2.1 Chapter 1). Once resident in the intima, monocytes differentiate into macrophages and take up the modified lipoproteins via specific receptors. These processes give rise to the foam cell, a hallmark of the arterial lesion (Libby, 2002). While these events are clearly laid out, a specific condition of *in vitro* system for differentiating the monocytes into macrophages and hence developing foam cells are still not established and standardized from laboratory to laboratory. It had been shown that monocytes can differentiate into macrophage phenotype with different morphologies and functions depending on the culture conditions and differentiation factors included in the culture medium (Akagawa, 2002). This results in the difficulty in comparing the results from one laboratory to another laboratory.

Even though this laboratory routinely culture isolated blood monocytes in RPMI with 10% HIHS, this study is the first to document the characteristics of the monocytes differentiation into macrophages in this culture system. Almost 70% of the monocytes had differentiated into macrophages after 14 days in culture. They differentiated into macrophages with morphology that resembled a 'fried egg" (Figure 3.1). The macrophages looked foamy with wide spread cytoplasm and lipid accumulation probably induced by the presence of serum in the media could account for the foamy appearance of these cells. This was evidence by the presence of oil red-O droplets within the cells (Figure 3.2).

The present study shows that growing the cells in the SFM was not favorable for the cell growth (Figure 3.1). This is supported by lower cell viability and 'sick' looking appearance of the cells in the SFM (Figure 3.4). The large variation in the percentage of cell viability is probablydue to the unfavorable growth condition of SFM causing cell death and also probably because in SFM the monocytes or immature macrophages do not adhere firmly; therefore some cells could be dislodged during the renewal of media. Inclusion of granulocyte-macrophage colony-stimulating factor (GM-CSF) into the SFM was vital for healthy cell growth in the SFM (Figures 3.6 and 3.7). GM-CSF has been shown to be an important factor for the development, chemotaxis, proliferation, differentiation, and activation of monocytes and macrophages (Glass & Witztum, 2001). However, inclusion of GM-CSF in SFM induced morphological alterations to the cells. Observation using the

light microscope showed that macrophages had elongated processes although later on they converted to the fried egg-like macrophage morphology again.

Growing the cells in the RPMI with HIHS and also in SFM induces lipid accumulation as shown by the oil red-O staining (Figure 3.2). Cellular lipid accumulation observed in cells cultured in SFM was rather surprising. However, according to Dr. Keri Carpenter of Cambridge University (through personal communication) SFM contains cholesterol that probably explains how the cells accumulated lipids. Thus, the observation that HMDMs accumulate lipid in RPMI containing HIHS and SFM should be taken into account when using these culture system to study the characteristics of foam cells.

Previously, it had been shown that HMDMs cultured in RPMI with human serum were rapidly converted to lipid-loaded cells enriched in triglyceride, α-tocopherol and to a lesser degree, cholesterol (Asmis & Jelk, 2000b; Garner *et al*., 1997a). Human serum contains substantial amount of free cholesterol, triglyceride, cholesterol esters and phospholipid (Garner *et al*., 1997a). The ability of human serum to induce HMDM lipid accumulation was reduced after removal of lipid fraction from human serum. In addition, the lipid profile of HMDMs had been shown to be highly dependent on the types of serum used to culture the cells (Garner *et al*., 1997a). HMDMs cultured in media supplemented with human serum amass large quantities of lipid but HMDMs cultured in the presence of foetal calf serum do not (Garner *et al*., 1997a). By extension, it can be postulated that HMDMs cultured in human serum will accumulate lipid to a certain extent. The general *in vivo* significance of this serum-induced lipid accumulation in macrophages remains uncertain. It may however serve as a reasonable model for more specific situation particularly those involving macrophage foam cells in the atherosclerotic plaque.

Even though the cells can grow in RPMI supplemented with LPDS, the morphology of the cells were slightly different compared to cells in RPMI with HIHS. The cells looked rounder and less spreading. This may have been due to lower accumulation of lipids which is evidenced by less oil red-O staining in cells cultured in RPMI with LPDS compared to cells cultured in RPMI with HIHS (Figure 3.9). The lack of lipoprotein in LPDS could also explain for the reduction in the number of cells during the culture period which indicates cells death was occurring.

Although the monocytes can survive and differentiate in SFM supplemented with GM-CSF or in RPMI with LPDS, other issues have to be considered too. The media condition greatly influence not just the morphology but also cell surface antigen expression and functions of the macrophages. For example, when macrophages were differentiated from human monocytes in RPMI with human serum, the macrophages uptake of LDL can

occur by non-receptor mediated fluid-phase macropinocytosis (Kruth, *et al*., 2005). Meanwhile differentiation of macrophages from human monocytes in RPMI with foetal bovine serum and macrophage colony-stimulating factor (M-CSF) produced a macrophage phenotype demonstrating fluid-phase endocytosis of native LDL (Zhao *et al*., 2006).

Previous study (Akagawa, 2002) showed that GM-CSF and M-CSF stimulate the differentiation of human monocytes into two phenotypically distinct types of macrophages, fried egg-like morphology and elongated spindle-like morphology respectively. Moreover, $CD14^+$ adherent human monocytes can differentiate into $CD1^+relB^+$ dendritic cells (DC) by the combination of GM-CSF with interleukin-4 (IL-4). The $CD14^+$ adherent human monocytes can also differentiate into tartrate-resistant acid phosphatase (TRAP)-positive osteoclast-like multinucleated giant cells (MGC) by the cooperation of M-CSF with IL-4 (Akagawa *et al*., 1996). However, the monocyte-derived DC are not terminally differentiated cells; they could still convert to macrophages in response to M-CSF (Akagawa *et al*., 1996). Wintergerst *et al*., 1998 showed that even monocytes grown in same culture conditions can differentiate into three subpopulations with two of the three subsets decreased in size during further differentiation. Taken together, their studies provide evidence that human monocytes are flexible in their differentiation potential which partially depend on the culture conditions and how long they are kept in the culture system.

This study showed that serum starvation caused a drastic drop in the cell viability similar to the addition of toxic level of oxLDL (Figure 3.11). This was expected since serum contains cytokines (e.g. insulin-like growth factors and platelet-derived growth factor (PDGF)), chemokines and growth factors which are vital to maintain the growth and viability of the cells. Serum had been shown to have a protective effect on apoptosis (Bjorkerud & Bjorkerud, 1996b). It had been demonstrated that serum (Kulkarni & McCulloch, 1994) or growth factors in serum such as insulin-like factor-I (Sell *et al*., 1995) and PDGF (Harrington *et al*., 1994) inhibited the appearance of apoptosis. This study also shows that the removal of serum from the media made the cells more sensitive to oxLDL (Figure 3.11). This could be due to the fact that serum deprivation of cells increases ROS formation that places the cells under increased redox stress (Halliwell & Gutteridge, 2007). Serum contains an array of antioxidants which protect the cells. The main antioxidants include ascorbate, urate, α-tocopherol, coenzyme Q, carotenoids albumin-bound bilirubin and albumin (Asmis & Wintergerst, 1998; Frei *et al*., 1988; Stocker *et al*., 1987). Protein sulfhydryl groups have also been suggested to contribute significantly to the antioxidant capacity of serum (Wayner *et al*., 1987). Extracellular superoxide dismutase (Karlsson & Marklund, 1987) and a selenium-dependent glutathione

peroxidase (Maddipati & Marnett, 1987) have been proposed to be involved in antioxidant defenses in human serum. Therefore, removal of serum from the media will definitely caused the cells to be more susceptible to the toxic effect of oxLDL.

A study by Bjorkerud and Bjorkerud, (1996b) demonstrated that exposure of SMCs to oxLDL under serum-free conditions had a stronger apoptosis-inducing effects than in the presence of serum. It was observed that serum starvation leads to the loss of substrate attachment and cells could be seen floating to top of the liquid medium (Bjorkerud & Bjorkerud, 1996b). The addition of serum was shown to decrease the proportion of non-adherent cells and rescued the non-adherent cells from death (Bjorkerud & Bjorkerud, 1996b). In this study, the replacement of serum from HIHS to LPDS when the cells were initially cultured in RPMI supplemented with HIHS had no significant effect on the viability of HMDMs. Studies by Asmis and Wintergerst (1998) showed that addition of human serum as well as LPDS not only prevented apoptosis induced by serum deprivation but also protected HMDMs from the cytotoxicity of 100 µg/ml oxLDL. The ability of LPDS to inhibit apoptosis suggests that serum lipoproteins and their lipid-soluble antioxidants such as vitamin E, coenzyme Q, or carotenoids are at least not directly involved in protecting the cells from apoptosis (Asmis & Wintergerst, 1998).

It is interesting that the monocytes survived and did not differentiate when cultured in the suspension wells. The fact that some monocytes attached to the bottom of the suspension wells did not mean that they differentiate into macrophages as their morphology was different from that of the normal macrophages (macrophages cultured in RPMI with 10% HIHS). Although they can survive as monocytes in the suspension wells, the cells could not be stored for later use as they did not differentiate into normal macrophages when plated on to the adherence plate. This is probably due to these cells had undergone some sort of differentiation taking past the point of macrophage formation.

Atherosclerotic plaque is considered to be a site of chronic inflammation and high oxidative stress (Scott, 2004; Van Lente, 2000). Monocytes and macrophages must have special mechanisms to avoid cell death in order to survive this harsh environment. The presence of various factors provided by serum at the site where monocytes differentiate into macrophages or where macrophages developed into foam cells must have made it possible for the formation of the arterial lesions. Therefore, serum requirement for optimum growth of monocytes into macrophages parallel processes that take place *in vivo*. In the plaque, the ability of macrophages to synthesise CSF is important for the proliferation and differentiation of monocytes into macrophages (Glass & Witztum, 2001). In the tissue culture conditions, if enough macrophages were present, this CSF need not be

added exogenously as the cells can synthesise sufficient amounts to support their own growth. The ability of monocytes to differentiate into other morphological cell types raising the likelihood of their survival when the growth condition changes in response to the oxidative stress. However, a question arises whether all these different morphological type of cells will develop into foam cells and form the arterial lesions.

3.4 Summary

Monocytes cultured in RPMI with 10% HIHS differentiated into macrophages with fried egg-like, foamy morphology. The presence of GM-CSF was essential for growing the human monocytes in SFM. However, this caused the monocytes to differentiate into cells with elongated processes which then further differentiated into fried egg-like morphology by day 14 of culture period. When cultured in RPMI with 10% LPDS, the monocytes differentiated into macrophages with less spread cytoplasm. Monocytes were able to survive and did not differentiate into macrophages when cultured in the suspension plate; however, they failed to differentiate into macrophages when transferred to the adherence plate.

4 The Formation of Foam Cells from Human Monocyte-derived Macrophages

4.1 Introduction

The presence of lipid-laden cells, the so-called foam cells, is a hallmark of early atherosclerotic lesions. Initially, macrophages were not considered to be significant in foam cell formation, until later studies on cells isolated from rabbits and monkeys found 80-90 % of foam cells had characteristics of macrophages (Newman *et al*., 1971; Schaffner *et al*., 1980). It is now generally accepted that foam cells in atherosclerotic lesions are largely derived from macrophages (Ross, 1993).

Even though, there is no doubt about their important role in atherogenesis, their functional state and phenotype in the plaque are still not well characterized. This is partly due to difficulties in isolating macrophages from atherosclerotic plaques for detailed studies. Different methods are available to purify cells from tissue homogenates, such as density gradient centrifugation, cotton wool filtration, and antibody purification by panning or magnetic beads (Liu-Wu, *et al*., 1997). Macrophage-derived foam cells from atherosclerotic lesions are, however, fragile, and a large fraction of these cells break during isolation procedures, often resulting in low yields. The immunomagnetic beads for example did not result in a contamination-free cell preparation, as it is not possible to detach the beads from the macrophages after the separation procedure. The contaminations could affect analysis of other cell surface markers (Mattsson *et al*., 1993).

The exact mechanism for foam cell formation also has not been settled. This has been discussed in great detail in Chapter 1. It is widely accepted that intracytoplasmic accumulation of CE as membrane-free lipid droplet is the major characteristic and mechanism of foam cell formation. However, in rabbit atheromatous cells, lysosomes are the site of accumulation of intracellular cholesterol rather than the membrane-free cytoplasmic droplets (Shio *et al*., 1978). Macrophages do not become foam cells when incubated with native LDL but incubation with hypertriglyceridemic VLDL (Kosaka *et al*., 2001; Whitman *et al*., 1998) or modified LDL (oxidized, acetylated or aggregated) (Henriksen *et al*., 1981; Khoo *et al*., 1988; Steinbrecher *et al*., 1990) results in formation of lipid loaded cells. Contradictory to this, Tabas *et al*. (1985) claimed that incubation of J774 macrophages with unmodified LDL also causes CE accumulation in this cell line.

Macrophages are heterogeneous cells with a wide spectrum of morphologies as well as functional capacities (Akagawa, 2002; Dougherty & McBride, 1984). In humans, two major subsets of peripheral blood monocytes based on their distinctive migratory properties are defined as $CD14^{+}CD16^{-}$ and $CD14^{low}CD16^{+}$ (Draude *et al*., 1999). CD14-positive monocytes are of more inflammatory type of cells since they migrate easily to the inflammation sites. CD14 antigen is upregulated after incubation of HMDMs with oxLDL (Shashkin *et al*., 2005). In response to the monocyte chemotactic factors released from atherosclerotic lesions circulating monocytes move from the central axis of the bloodstream and are activated accompanied by expression of CD14 on the cell surface (Takahashi *et al*., 2002). Upregulation of CD14 by oxLDL was shown to be related to monocyte differentiation into macrophages.

The analysis of concentration of lipids from CD14-positive cells isolated from human atherosclerotic aorta (Table 4.1) (Mattsson *et al*., 1993) revealed that cholesterol ester accumulated the most followed by free cholesterol, and triglycerides in these cells. Foam cell from atherosclerotic plaques (Mattsson *et al*., 1993) contained on average four times more CE mass than triglyceride. Macrophage-derived foam cells isolated from rabbit atherosclerotic intima also contained large amounts of cholesterol that consisted mainly (more than 80%) of CE (Naito *et al*., 1997).

Table 4.1 Lipid distribution in isolated cells from human atherosclerotic intima media.

Lipid class	CD14-positive cells *μg/mg cell protein*
Cholesterol ester	408 ± 349
Triglycerides	133 ± 103
Free cholesterol	333 ± 200

Values are given as mean ± SD (n=11). Lipids were extracted from CD14-positive cells isolated from atherosclerotic tissue and analysed by a combination of TLC and FID. Adapted from Mattsson *et al*., (1993).

Mouse foam cells developed from mouse macrophages incubated with three types of LDL; acLDL, oxLDL and 7-KC acetylated LDL (7-KCacLDL) had variable lipid contents (Gellisen *et al*., 1999). Loading with acetylated LDL (acLDL) produced a 4- to 5-fold increase in cellular cholesterol over non-loaded cells, of which approximately half was esterified. 7-KCacLDL loading produced free and esterified cholesterol levels similar to acLDL but also to free and esterified 7-KC. In that study the total 7-KC content was approximately 25% of the total sterol and 85% was esterified. OxLDL-loaded cells

contained free and esterified cholesterol plus 7-KC and other oxysterol; (Brown *et al*., 1996). About 70% of the 7-KC in oxLDL-loaded cells was esterified.

Mouse peritoneal macrophages and human macrophages treated with aggLDL were rapidly converted to CE-rich foam cells. There was 15-fold and 37-fold increase in cellular CE compared to cells incubated with unmodified LDL in human foam cells (Asmis & Jelk, 2000b) and mouse foam cells respectively (Khoo *et al*., 1988). Therefore, different types of cells displayed different levels of CE contents.

This section of work initially concentrates on developing foam cells using HMDMs incubated with subtoxic level of copper oxidised LDL (oxLDL). GC will be used in conjunction with HPLC to investigate the quantitation of free and total cholesterol (total cholesterol = free cholesterol + CE) contents of the lipid loaded cells. Since 'foam cell' macrophages at atherosclerotic lesions contain massive cytoplasmic accumulation of CE droplets (Jessup *et al*., 2002), the accumulation of CEs in the HMDMs will be the indicator for foam cell formation. Oil red-O staining will also be used to characterise the accumulation of CE.

This section also aims to determine whether the level of de novo synthesis of 7,8-dihydroneoperin in foam cells when stimulated with γ-interferon is different from the HMDMs. The effect of oxLDL-induced damaged in foam cells will also be examined. If there was any different in the susceptibility between HMDMs and foam cells towards cytotoxic oxLDL, then the effects of 7,8-dihydroneoperin on oxLDL-induced damaged in foam cells will be explored. Collectively this section is designed to determine factors that affect the foam cell survival.

This study is important because even though oxLDL has been proposed to be responsible for foam cell formation, the exact mechanism by which foam cells are formed *in vivo* is still unknown and convincing evidence from *in vitro* studies is still lacking. In addition, the lack of *in vitro* studies using appropriate foam cell models has limited our information regarding foam cells' composition and hindered our understanding of the role of the macrophage foam cells in atherosclerosis.

Besides that, most previous studies generate foam cells *in vitro* by feeding oxLDL to either cultures of animal MDMs or immortal macrophage-like cell lines. Only a few studies used HMDMs. The exact nature of the foam cell formed in HMDMs will reflect *in vivo* processes more closely than cell lines and this would give a clue of the situation that might really occur at the atherosclerotic plaque. Moreover, while it is clear that oxLDL is readily endocytosed by macrophages, relatively little attention has been given to the nature and extent of lipid deposition that such uptake produces. Characterisation of lipid levels of

foam cells may provide a basis for exploring how sterols are metabolised by macrophages and how in turn the sterols influence cellular metabolism.

4.2 Results

4.2.1 GC Chromatograms of a Mixture of Standards (cholestane, cholesterol and 7-ketocholesterol)

Table 4.2 and Figure 4.1 show the retention time and GC peak areas of the standards; cholesterol, cholestane and 7-KC. The retention times of the standards were used as a reference to identify the cholesterol and 7-KC in the samples tested. Cholestane was added at the very beginning of the lipid extraction and therefore used as an internal standard to calculate the lipid contents in the sample. The GC analysis of each standard was done four times and there was a great consistency in the ratio of peak areas between cholesterol and cholestane, and 7-KC and cholestane. Figure 4.2 shows chromatograms of derivatised copper-oxLDL co-chromatographed with cholestane standard. 7-KC was detected in the oxLDL sample and it was 1.92 $\pm$ 0.07 % of the free cholesterol levels.

4.2.2 Analysis of Free and Total Cholesterol Contents of Macrophages Growth by Gas Chromatography

Data from several studies show different levels of lipids over the period of differentiation of monocytes into macrophages (Asmis & Jelk, 2000b; Garner *et al*., 1997a; Khoo *et al*., 1988). It was interesting to know whether in our culture conditions, were the cells' neutral lipid contents are different. To address this question, the lipid contents of HMDMs were extracted after 1, 4 and 10 days of seeding onto the adherence plates. The free cholesterol and total cholesterol were measured using GC analysis. In addition, the differentiation of monocytes to macrophages was monitored under the light microscope where the number of monocytes and macrophages were counted after 1, 4 and 10 days of seeding.

Within 24 hour of being plated, blood monocytes, adhered firmly to the culture plates and the cells started to accumulate free cholesterol and CE (Figure 4.3). After 4 days, the percentage number of macrophages (Figure 4.4) and lipid contents of monocytes/macrophages have already substantially increased (Figure 4.3). By day 10, 40% of the cells were macrophages though this varied depending on the blood donors (Figure 4.4). During the differentiation of monocytes to 10-day old HMDMs, these cells increase their free and total cholesterol contents by 11-folds and 5-folds respectively. The

free cholesterol and total cholesterol level have increased 2-folds by day 4 in comparison to day 1 monocytes (Figure 4.3). Since total cholesterol is the sum of free cholesterol and CE, it seems that the CE level increased 2-fold on day 4 in comparison to day 1. There was no further increment of CE level by day 10. Contrary to CE, the free cholesterol levels increased 4-fold by day 10 in comparison to day 4.

4.2.3 Analysis of Free Cholesterol and Total Cholesterol Contents of Monocytes and Macrophages Incubated with OxLDL by Gas Chromatography

It is unknown whether subtoxic level of oxLDL affects the growth of monocytes. Therefore, the effects of 0, 50, 100 and 200 μg/ml of oxLDL, on the percentage of differentiation of monocytes to macrophages per well were determined. Figure 4.4 shows that in comparison to the nontreated cells the differentiation of monocytes into macrophages did not seem to be affected by the presence of different concentrations of oxLDL.

Effects of oxLDL on the viability and lipid contents of monocytes were determined to address the issue of whether monocytes also accumulate lipid and change into foam cells. This is because it is uncertain whether *in vivo*, monocytes take up lipids while migrating across the endothelium. This was investigated by incubating 1 day old monocytes in RPMI containing 10% HIHS at 37 °C with various concentrations of oxLDL for 10 days before analysing the cells' viability by MTT assay and lipid levels by GC analysis.

Figure 4.5a shows that concentrations of oxLDL from 0-200 μg/ml did not affect the cell viability of monocytes which suggests that oxLDL up to 200 μg/ml was not toxic to the cells. It is noteworthy that by day 10 of the incubation period, 40-50% of the monocytes had transformed into macrophages. Figure 4.5b shows that the free and total cholesterol contents of the cells treated with oxLDL were not significantly different from the control cells and also not affected by increased oxLDL concentrations. The CE contents of the cells treated with increasing concentrations of oxLDL remained fairly similar.

The experiment was repeated using 14 day old culture of HMDMs where almost 70% of the HMDMs were macrophages. After 10 days incubation with increasing concentration of oxLDL, all the cells look morphologically similar under the microscope (Figure 4.6). The cells have foamy appearance and large cytoplasm. Concentrations of

oxLDL up to 200 μg/ml did not affect the viability of macrophages (Figure 4.7a). The result of lipid analysis using GC showed that there was no significant different in either the free cholesterol or total cholesterol contents between the oxLDL-treated and non-treated cells (Figure 4.7b). It was expected that the oxLDL did not affect the free cholesterol level. However, if the foam cells are formed by addition of oxLDL, the CE levels should be higher than that of the control cells.

Since concentrations of oxLDL up to 200 μg/ml did not affect the cell viability or lipid contents of HMDM, a concentration of oxLDL ranging from 0 to 500 μg/ml was examined. This exposed the cells to a more toxic concentration of oxLDL. The HMDMs were incubated with oxLDL for 48 hours before doing MTT and lipid analyses. Shorter incubation time i.e. 48 h was chosen to avoid cholesterol efflux and toxicity of oxLDL. The result (Figure 4.8a) shows that 0.5 mg/ml oxLDL reduced the cell viability by 10% suggesting that 0.5 mg/ml of oxLDL was partially toxic to the cells. Lipid accumulation was also examined microscopically following staining of cells with oil red-O stain. After 48 hours incubation of HMDMs with oxLDL, oil red-O positive droplets were clearly detected not just within the oxLDL treated cells but also within the control cells (Figure 4.9). The results of lipid analysis by GC showed that there was no significant different in either the free or total cholesterol contents between the oxLDL-treated and nontreated cells (Figure 4.8b). However, the foamy appearance of the cells and positive oil red-O staining suggests that the cells might have developed into foam cells whether in the presence or absence of oxLDL (Figure 4.9).

Since the media contained serum that have lipoproteins in it there was a possibility that the macrophages had oxidised the lipoprotein and take up the oxidised lipoprotein in the serum before oxLDL was added to the cells. This probably account for the lack of differences between the lipid contents of the controls and the oxLDL-treated cells. This process might also lead to the formation of foam cells before the addition of oxLDL to the media as suggested by the lack of difference in the oil red-O staining between the oxLDL-treated and control cells (Figure 4.9). To test this possibility, the level of lipid oxidation (formation of MDA) in the fresh media of the cells and the media that the cells had sat in for 3 days were measured by using TBARS/HPLC analysis (Table 4.3). The unpaired two tailed t-test showed that there was no significant different in the MDA contents of the fresh and old media which suggest that there was no oxidation of lipoprotein in the serum.

At this point there are probably two other explanations for this result. The first likely explanation is that treatment with oxLDL did not cause foam cell formation. Secondly, to form foam cells, the macrophages might need to be treated with aggregated

lipoproteins and not oxLDL as claimed by Asmis and Jelk, (2000b). To investigate the later, the cells were incubated with 200 μg /ml of nLDL, oxLDL, aggLDL and aggoxLDL for 48 hours. LDL and oxLDL were aggregated by vortexing for 60 seconds. MTT assay (Figure 4.10a) shows that treatment with these modified LDL did not affect the viability of HMDMs. The free cholesterol and CE compositions were then analysed by GC. One way ANOVA analysis revealed that there was no significant different in CE composition between the controls and LDL-modified treated cells (Figure 4.10b). Moreover, the oil red-O staining (Figure 4.11) shows that all the cells (regardless of the treatment) have lipid droplets characteristics of foam cells.

Another point that has to be noted here is that in comparison with Figures 4.5 and 4.7, the total cholesterol contents in Figures 4.8 and 4.10 are not 100% more than the free cholesterol contents. Similar results like Figures 4.8 and 4.10 were produced when these experiments were repeated twice. The GC chromatograms (Figure 4.12) where results for Figure 4.7 were extracted, clearly shows that the peaks areas of the hydrolysed samples (Figure 4.12b) were larger (with reference to cholesterol peak) compared to peak areas of the free cholesterol chromatograms (Figure 4.12a). Hence, higher values for the total cholesterol content was obtained compared to the free cholesterol contents. In contrast, the GC chromatograms (Figure 4.13) of HMDMs where results for Figure 4.8 were extracted clearly shows that chromatograms of total sterols (Figure 4.13b) had less and smaller peaks than the free cholesterol chromatograms (Figure 4.13a). This obviously accounts for the less total sterol contents in Figure 4.8. Figure 4.10b also demonstrated that the total cholesterol contents varied a lot and the values are similar to the free cholesterol levels. A lack of consistency in the trend of the free and total cholesterol contents is probably due to the unavoidable loss of samples during sample processing or during GC analysis. This will be discussed further in the discussion section.

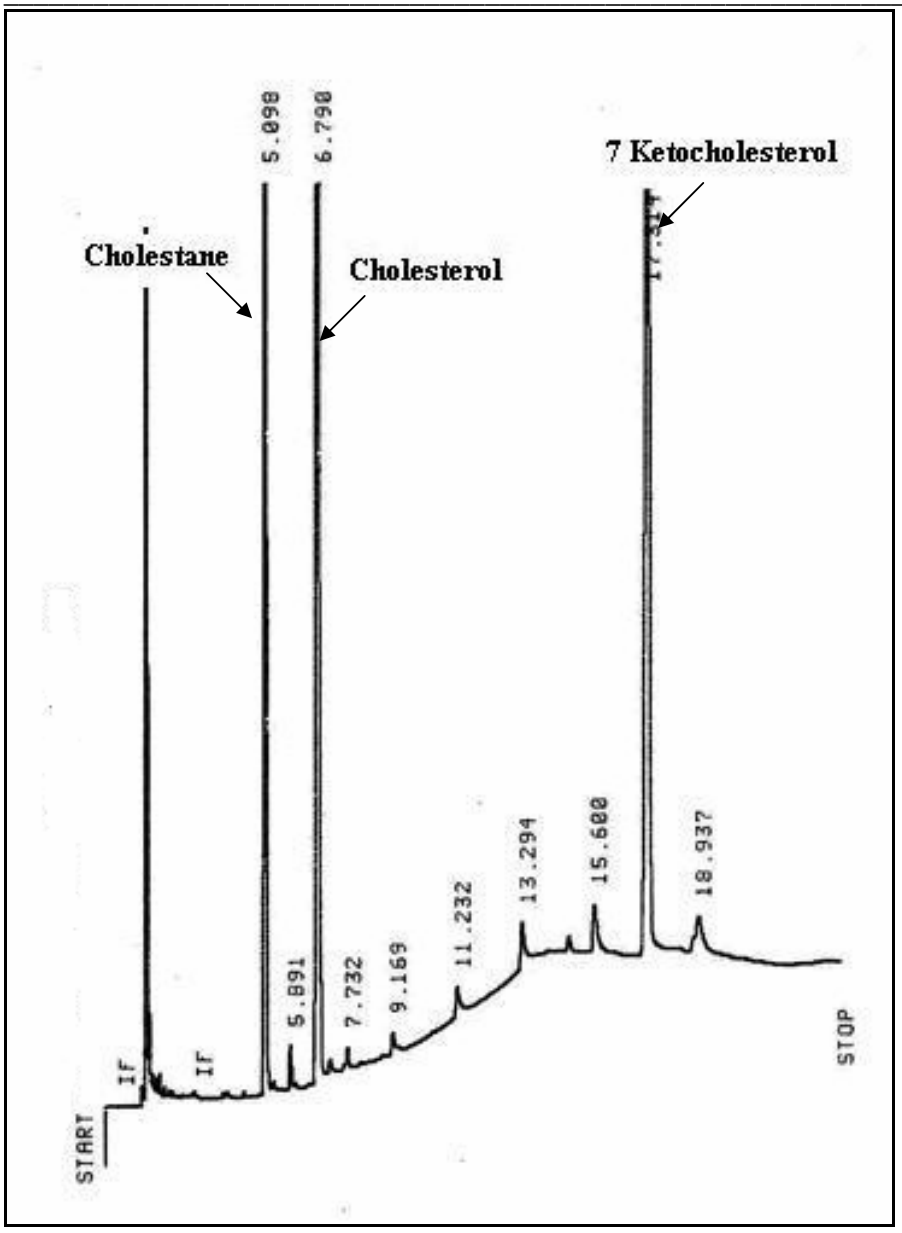

Figure 4.1 The GC chromatograms of mixture of standards of cholestane, cholesterol and 7 ketocholesterol.

50 µg of each cholesterol, cholestane and 7-KC were dissolved in hexane and mixed together. The mixture was dried down under nitrogen before going through alkaline hydrolysis (described in the methods). The residue was redissolved in 20 µl heptane and 2 µl was injected into GC.

Table 4.2a The GC's retention times and ratio of peak areas of cholestane, cholesterol and 7-KC standards.

Material	Run	Retention Time	Peak area
Cholestane	1	5.098	149955
	2	5.119	340619
	3	5.1	284523
	4	5.073	360808
Cholesterol	1	6.79	151091
	2	6.846	380898
	3	6.813	303564
	4	6.791	403146
7-KC	1	17.314	101785
	2	17.37	257721
	3	17.32	198582
	4	17.252	277085

Table 4.2b Ratios of peak areas

Run	Cholesterol/Cholestane	7-KC/cholestane
1	1.008	0.679
2	1.118	0.757
3	1.067	0.698
4	1.117	0.768
Mean $\pm$ Std dev	1.078 $\pm$ 0.725	0.725 $\pm$ 0.044

50 µg of each cholesterol, cholestane and 7-KC (dissolved in hexane) were dried down under nitrogen before going through alkaline hydrolysis. The residue was dissolved in 20 µl heptane and 2 µl was injected into GC for four runs.

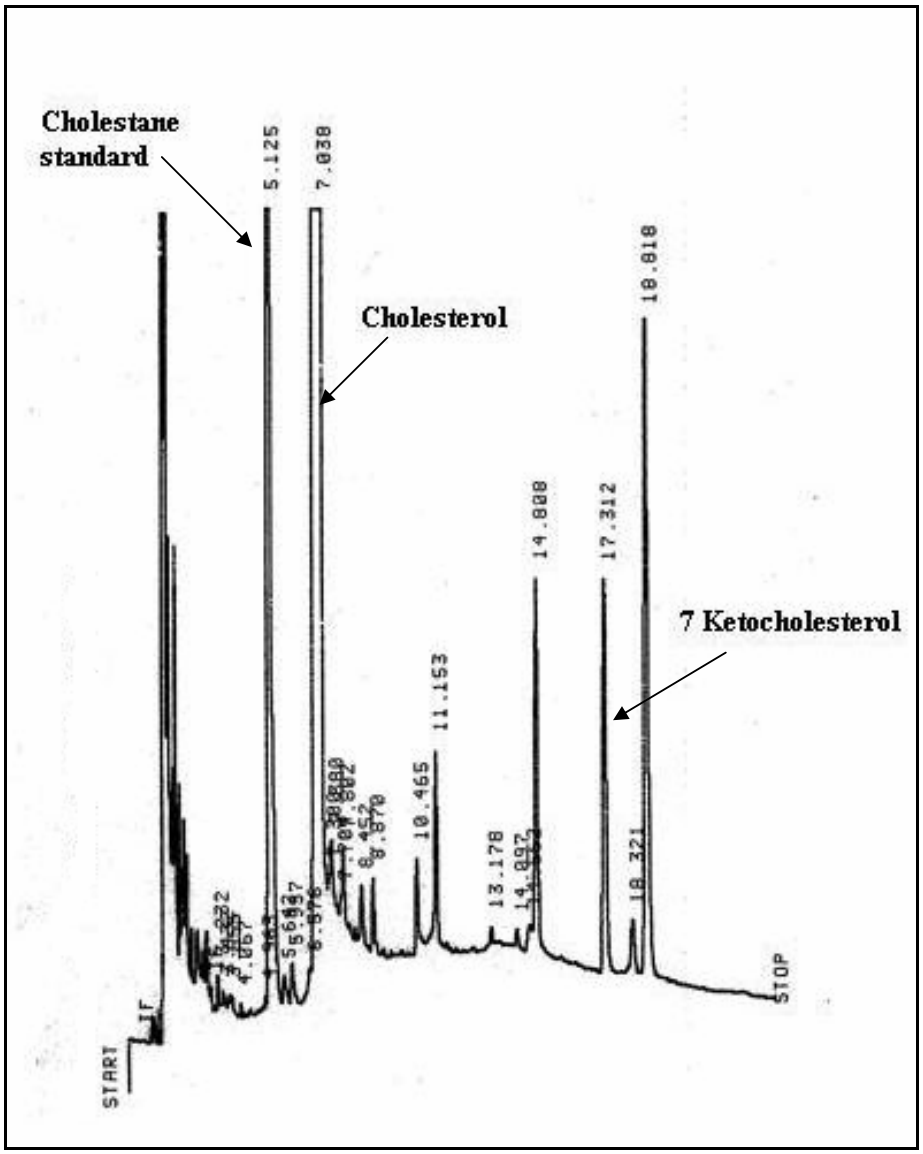

Figure 4.2 The GC chromatograms of oxLDL.
Analysis of oxLDL prepared by 24 hour Cu^{2+} oxidation extracted into chloroform and dried down under nitrogen before going through alkaline hydrolysis. The residue was redissolved in 20 µl heptane and 2 µl was injected into GC.

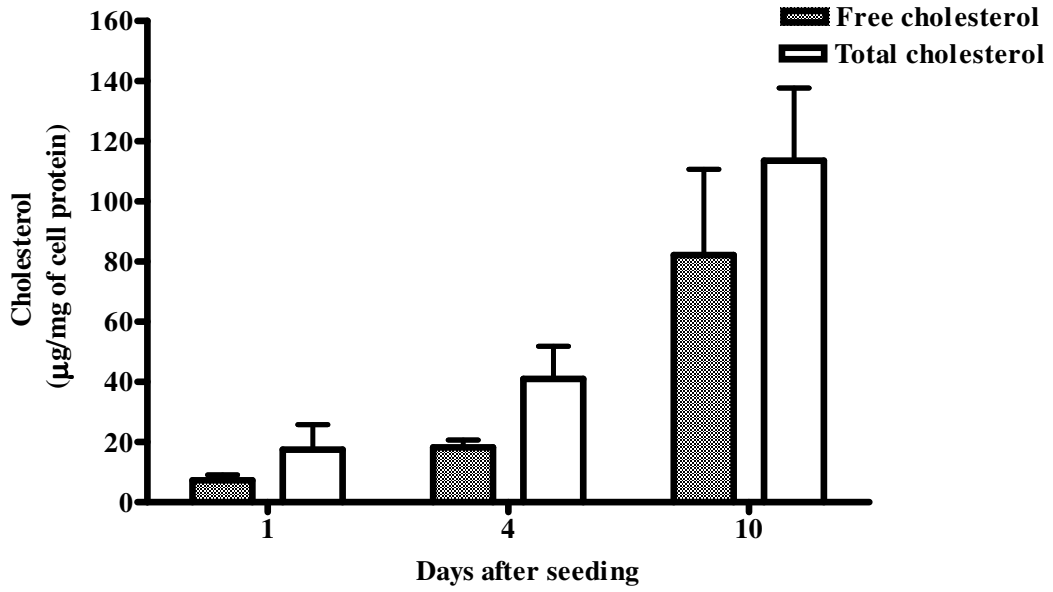

Figure 4.3 The free and total cholesterol contents of HMDMs on days 1, 4 and 10 after seeding.

Lipids analysis of HMDMs (10 x 10^6 cell/ml) in RPMI containing 10% HIHS in 6 well plates were performed after 1, 4 and 10 days after cell seeding/plating as described in chapter 2. Lipid analysis was performed using GC method. Results are displayed as mean ± SD of triplicates from a single experiment, representative of three separate experiments.

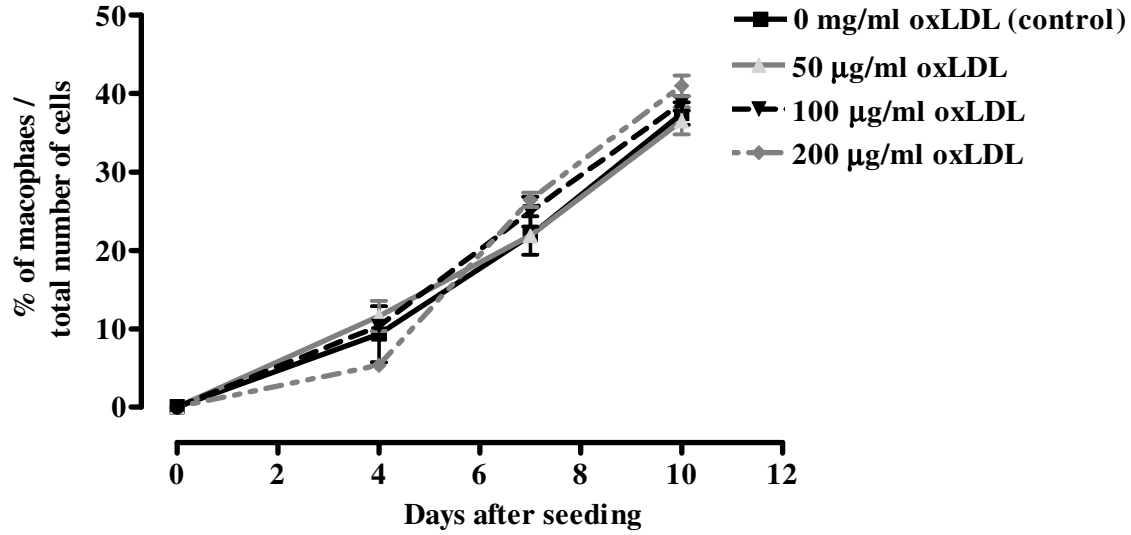

Figure 4.4 Effect of increasing oxLDL concentrations on the growth of HMDMs.

HMDMs (5 x 10^6 cell/ml) were cultured in RPMI containing 10 % HIHS and increasing concentration of oxLDL. The number of monocytes and macrophages were counted on the day of seeding (day 0) and days 4, 7 and 10 after seeding. The number of cells was counted in three wells from at least 5 views. Results are displayed as mean ± SD of triplicates.

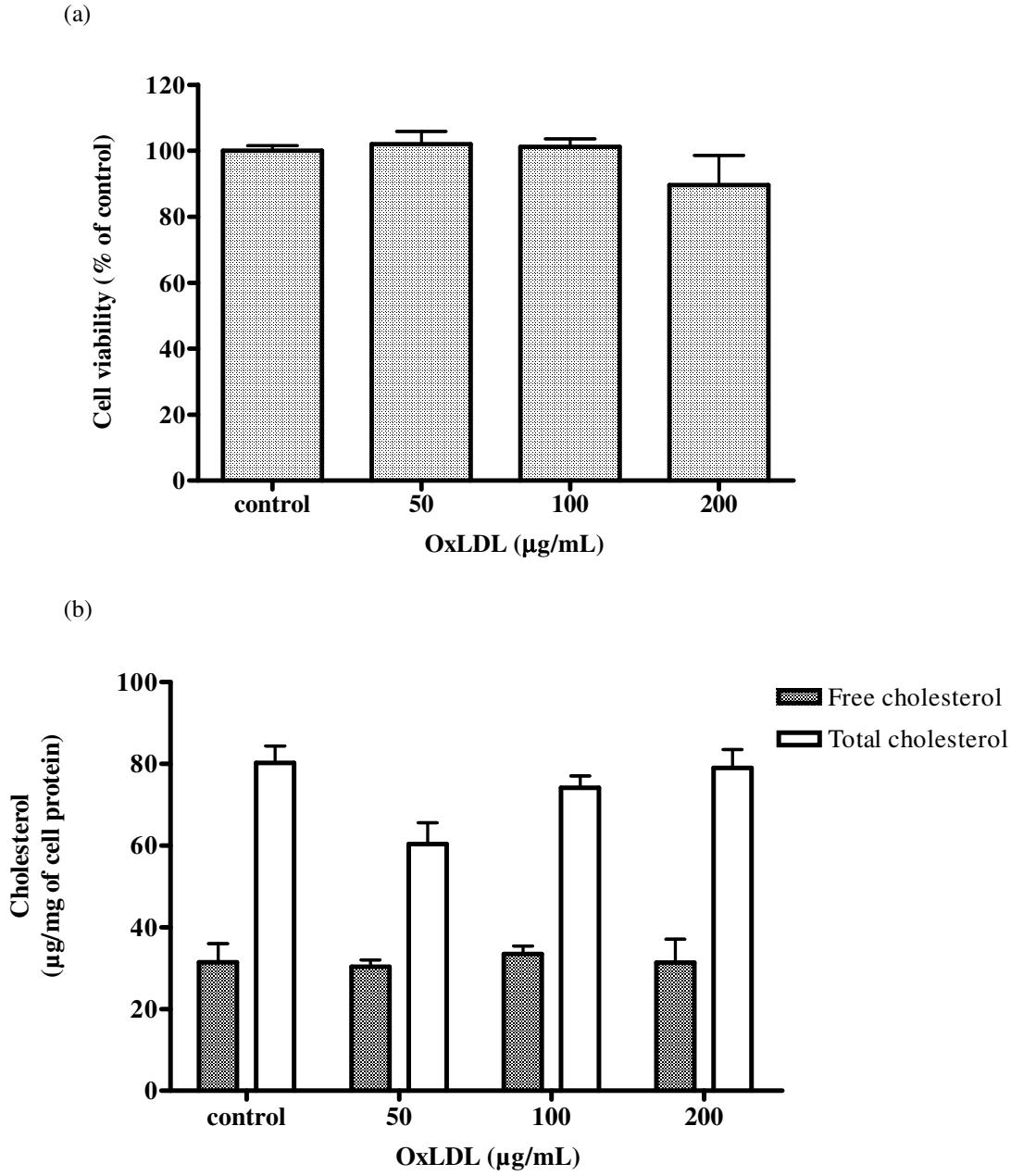

Figure 4.5 GC analysis of lipid composition and cell viability of monocytes (with 50% differentiation into macrophages) after treatment with increasing concentrations of oxLDL.

One day old monocytes ($10x10^6$ cell/ml) in RPMI containing 10% HIHS in 6 well plates were incubated in the absence (control) or in the presence of oxLDL. After 10 days incubation, the (a) cell viability was assessed via MTT assay and (b) cholesterol contents were analysed by GC analysis. ANOVA analysis revealed no statistical significance from control for free and total cholesterol contents. Results are displayed as mean ± SD of triplicates from a single experiment, representative of three separate experiments.

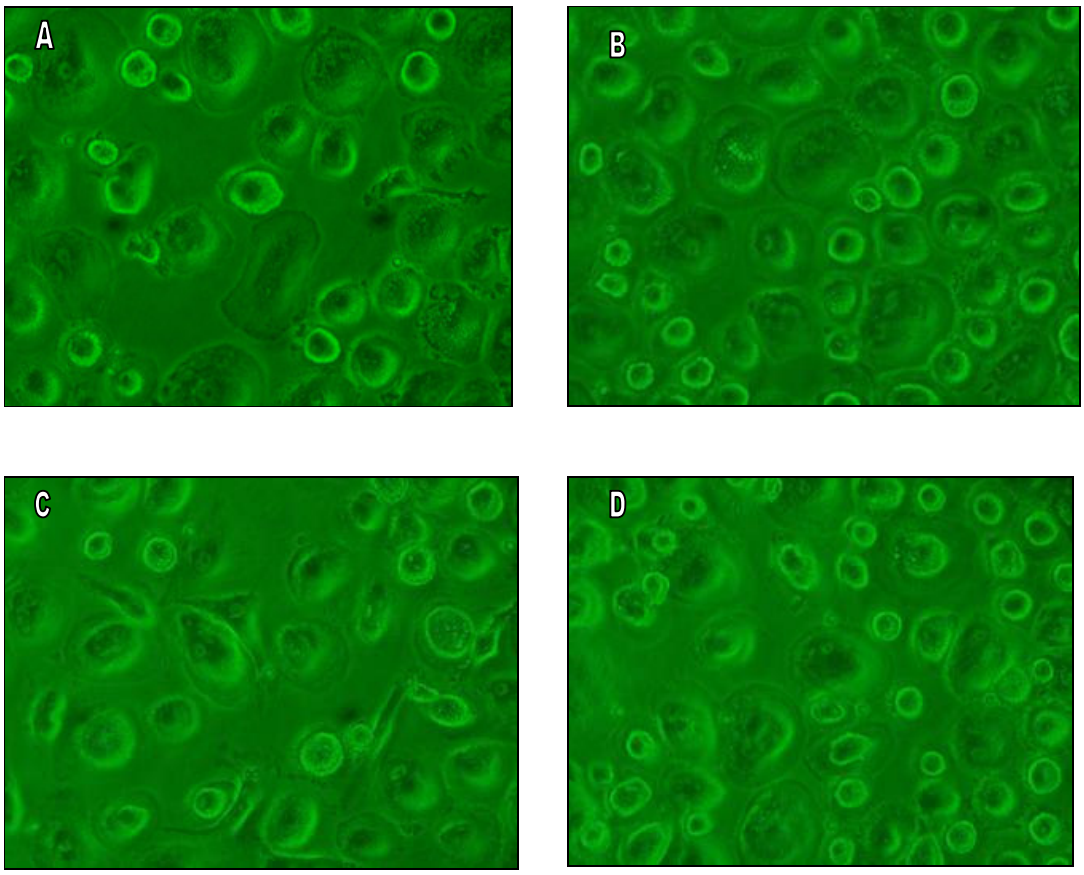

Figure 4.6 Effect of increasing concentration of oxLDL on HMDMs morphology. HMDMs (5 x 10^6 cell/ml) in RPMI containing 10 % HIHS in 12 well plates were incubated with increasing concentrations of oxLDL, (A) control; (B) 50 µg/ml, (C) 100 µg/ml; and (D) 200 µg/ml for 10 days. The media and oxLDL were renewed on the fourth and seventh day of incubation period. Cells were viewed *in situ* in tissue culture wells using an inverted microscope with green filter. Original magnification was 40x and the pictures were taken using a digital camera.

(a)

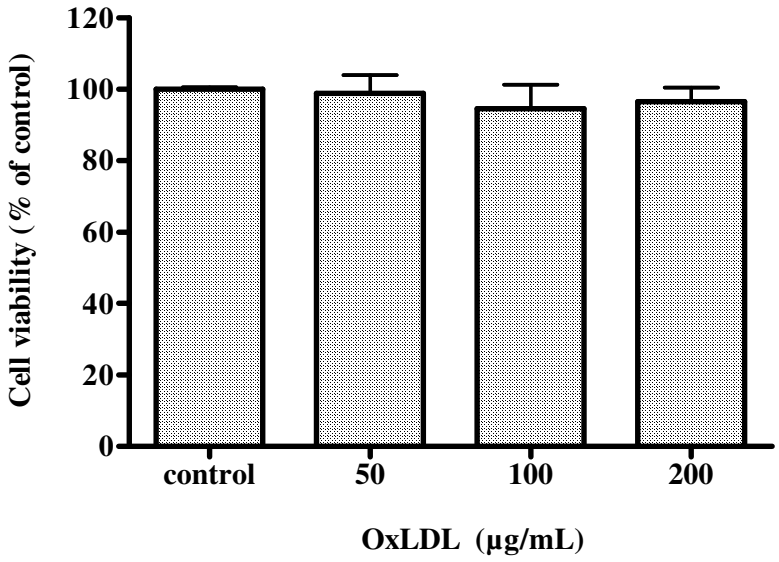

(b)

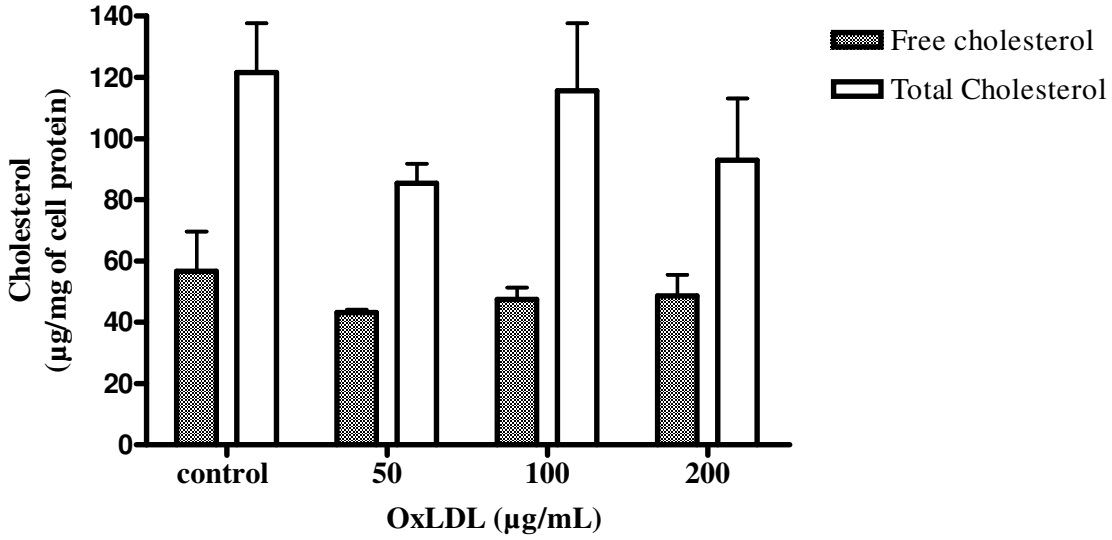

Figure 4.7 GC analysis of lipid composition and cell viability of HMDMs (with 70% differentiation into macrophages) after treatment with increasing concentrations of oxLDL.

HMDMs ($10x10^6$ cell/ml) in RPMI containing 10% HIHS in 6 well plates were incubated in the absence (control) or in the presence of oxLDL. After 10 days incubation, the (a) cell viability was assessed via MTT assay and (b) cholesterol contents were analysed using GC analysis. ANOVA analysis revealed no statistical significance from control for free or total cholesterol contents. Results are displayed as mean ± SD of triplicates from a single experiment, representative of three separate experiments.

(a)

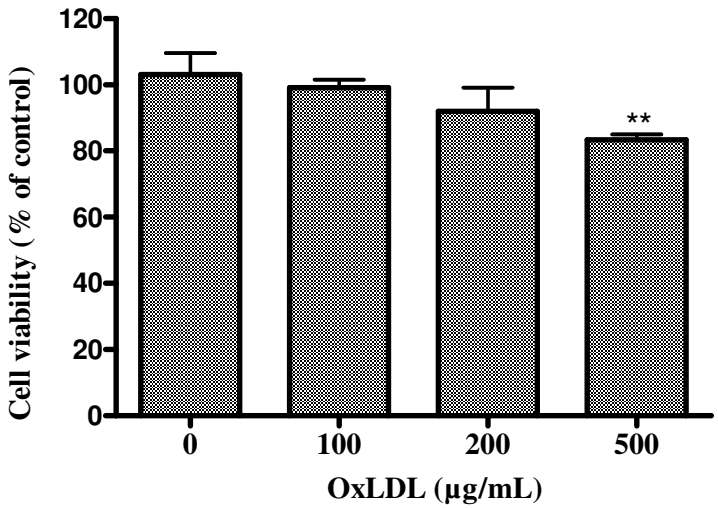

(b)

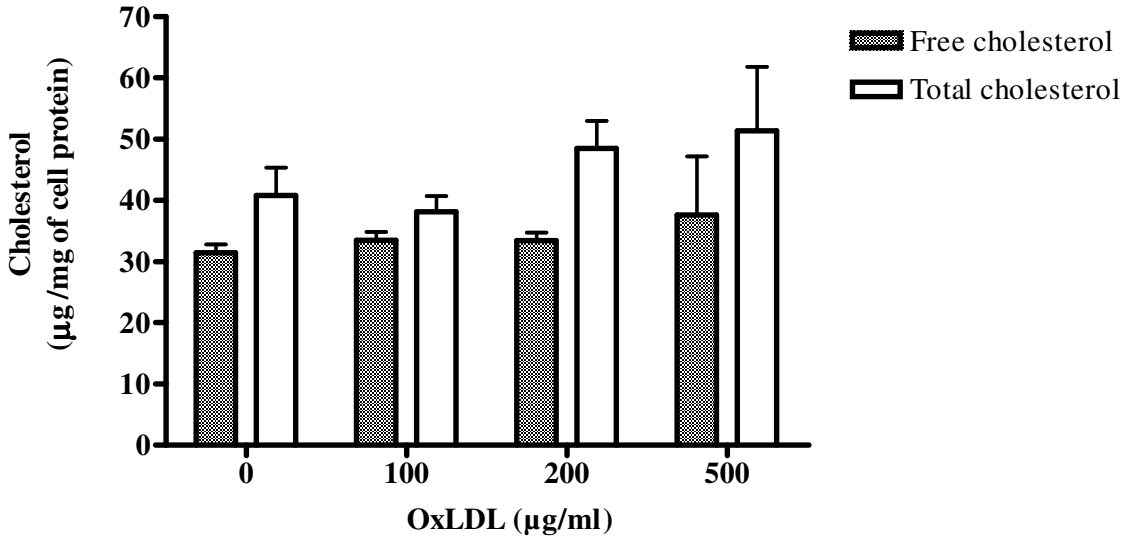

Figure 4.8 Effect of increasing concentration of oxLDL on HMDMs viability and lipid contents after 48 h incubation.

HMDMs (10 x 10^6 cell/ml) in RPMI containing 10% HIHS in 6 well plate were incubated with or without (control) oxLDL. After 48 hours incubation, HMDMs were analysed for (a) cell viability by MTT assay and (b) lipids were extracted and analysed for cholesterol contents by GC. ANOVA analysis revealed no statistical significance from control. Results are displayed as mean ± SD of triplicates from a single experiment, representative of three separate experiments.

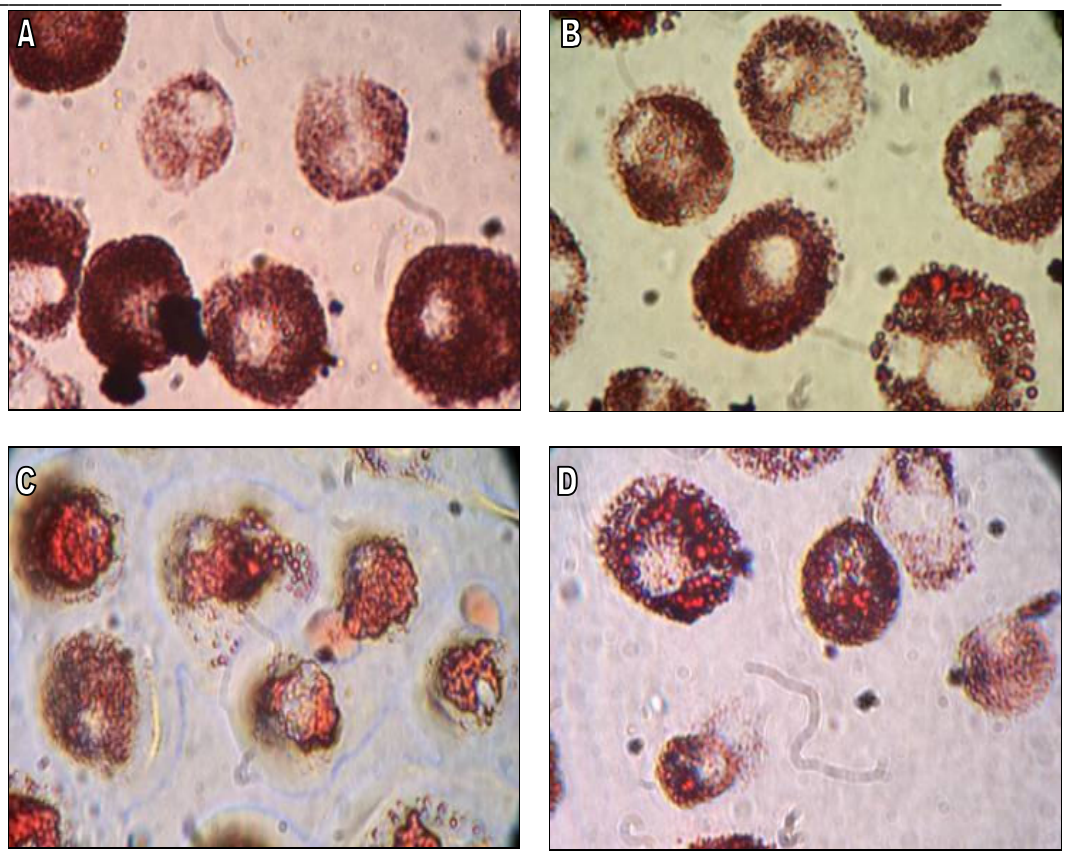

Figure 4.9 Culture of HMDMs in 10 % HIHS in the presence or absence of oxLDL produces oil red-O positive, lipid loaded cells.
HMDMs (5 x 10^6 cell/ml) in RPMI containing 10 % HIHS in 12 well plates were incubated with increasing concentrations of oxLDL (A) control, (B) 100 µg/ml, (C) 200 µg/ml, and (D) 500 µg/ml for 48 hours. Controls were conducted in the absence of oxLDL. Cells were viewed in situ in tissue culture wells using an inverted microscope. Original magnification was 100x and the pictures were taken using a digital camera.

Table 4.3 The TBARS measurement of fresh and old media.

Sample	[MDA] uM	Average ±SD
fresh 1	0.383	
fresh 2	0.347	0.353± 0.027
fresh 3	0.33	
old 1	0.371	
old 2	0.354	0.374 ± 0.022
old 3	0.398	

HMDMs ($5x10^6$ cells/ml) were incubated at 37 °C in RPMI containing 10% HIHS. Media was taken immediately (fresh) and 3 days after added to cells. Significance is indicated between the MDA values of the fresh and old media. Unpaired two tailed t-test revealed no statistical significance between the fresh and old media.

(a)

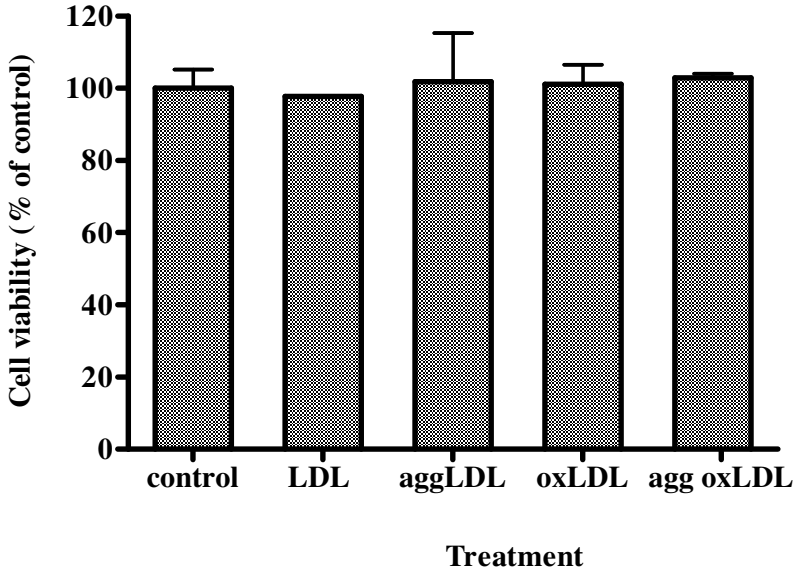

(b)

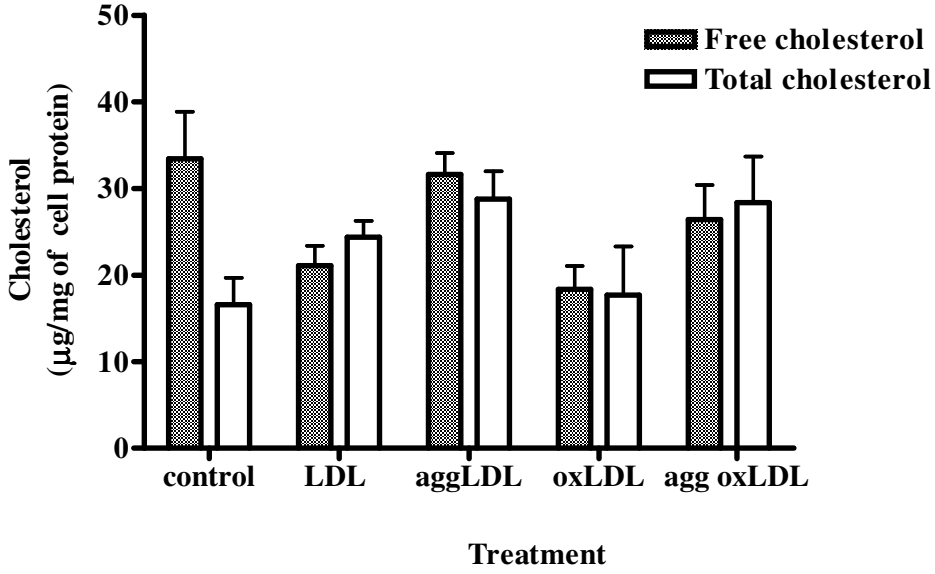

Figure 4.10 GC analysis of lipid composition and cell viability of HMDMs after treatment with various LDL modifications.

HMDMs ($10x10^6$ cell/ml) in RPMI containing 10% HIHS in 6 well plates were incubated in the absence of lipoprotein (control) or in the presence of either LDL, agg-LDL, oxLDL or agg-oxLDL at 0.2 mg/ml respectively. After 48 h incubation, the (a) cell viability was assessed via MTT assay and (b) cholesterol contents were analysed using GC analysis. ANOVA analysis revealed no statistical significance from control. Results are displayed as mean ± SD of triplicates from a single experiment, representative of three separate experiments.

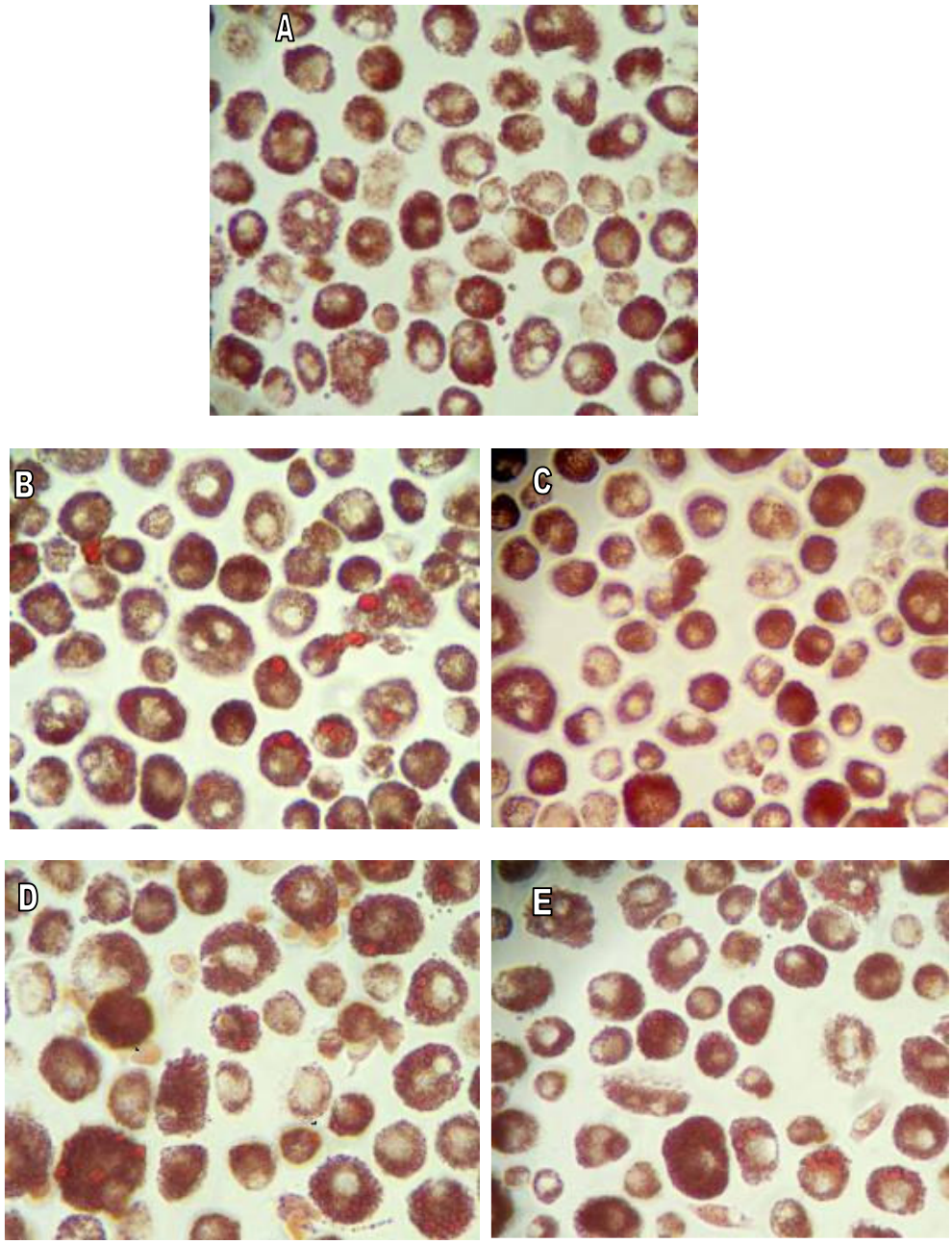

Figure 4.11 Culture of HMDMs in 10 % HIHS with various LDL modifications produces oil red-O positive, lipid loaded cells.
HMDMs (5 x 10^6 cell/ml) in RPMI containing 10 % HIHS in 12 well plates were incubated with (B) 200 μg/ml of LDL, (C) 200 μg/ml of aggLDL, (D) 200 μg/ml of oxLDL and (E) 200 μg/ml of aggoxLDL for 48 hours. (A) was control without lipoprotein. Cells were viewed in situ in tissue culture wells using an inverted microscope. Original magnification was 40x and the pictures were taken using a digital camera.

(a)

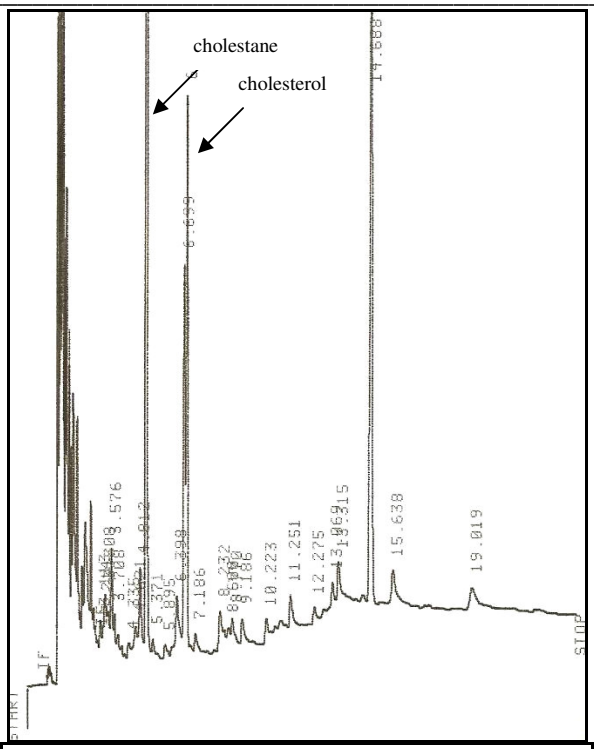

(b)

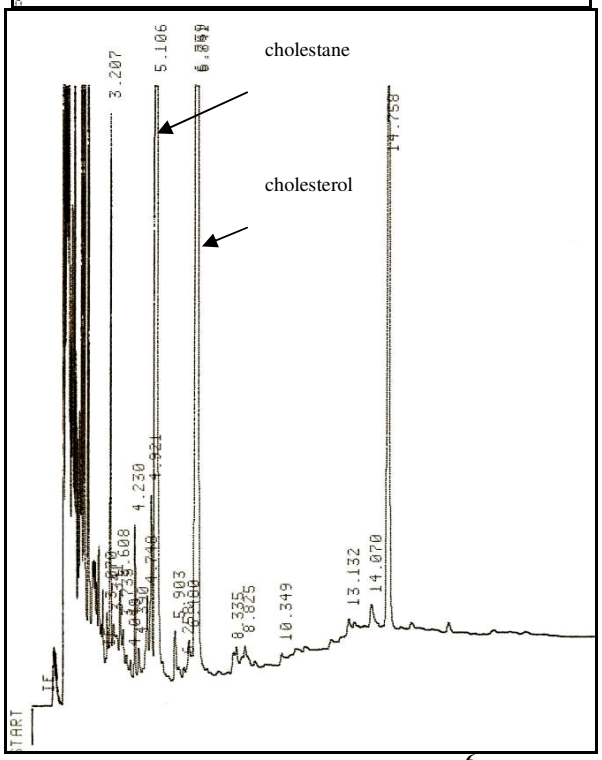

Figure 4.12 GC chromatograms of HMDMs (10 x 10^6 cell/ml) in RPMI containing 10% HIHS in 6 well plate incubated with 200 µg/ml oxLDL for 10 days.

Lipids were extracted and analysed for free cholesterol contents (a) or underwent alkaline hydrolysis to give total cholesterol (b).

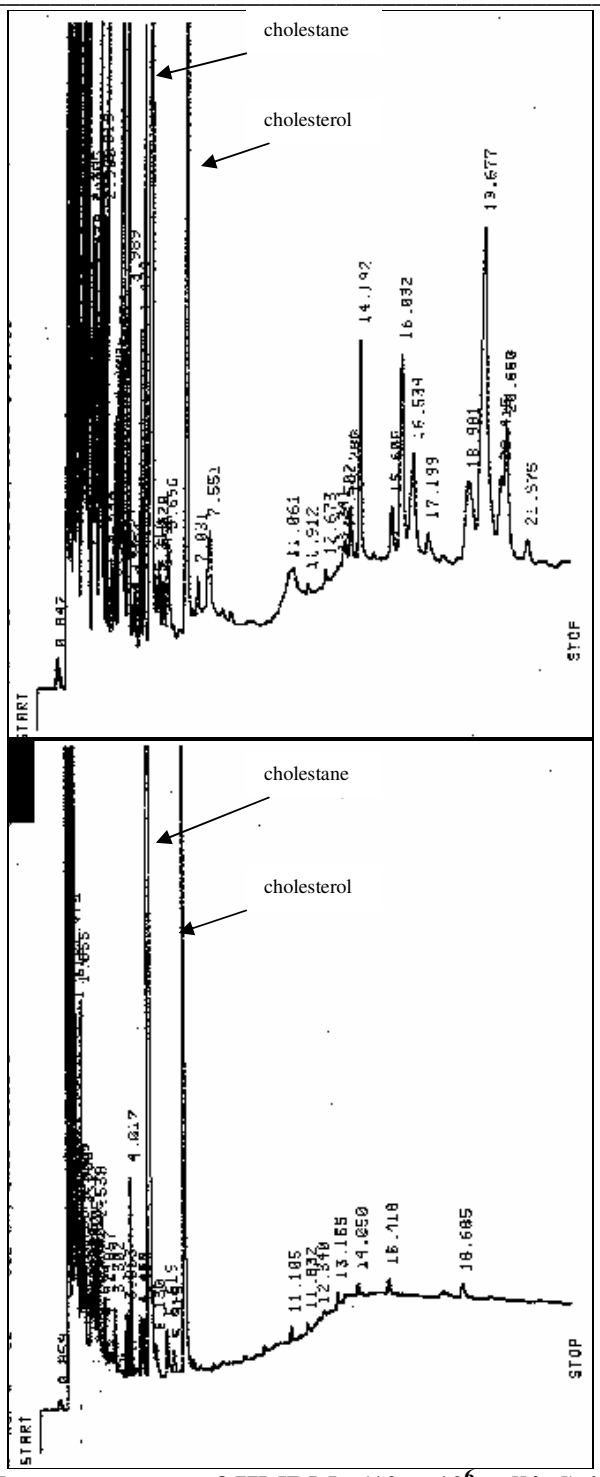

Figure 4.13 GC chromatograms of HMDMs (10 x 10^6 cell/ml) in RPMI containing 10% HIHS in 6 well plate incubated with 200 μg/ml oxLDL for 48 hours.
Lipids were extracted and analysed for free cholesterol contents (a) or underwent alkaline hydrolysis to give total cholesterol (b).

4.2.4 Analysis of Free Cholesterol and Cholesteryl Ester Contents of HMDMs Incubated with modified LDL by High Performance Liquid Chromatography (HPLC)

The inconsistency in the total cholesterol content results has raised the suspicion that GC is not a reliable method to analyse HMDMs' lipid content. Therefore, the lipid contents of HMDMs were reanalysed by HPLC according to the method established by Kritharides *et al*. (1993). There were fewer steps (refer to Chapter 2) in the sample preparation for HPLC analysis that can possibly reduce the probability of losing the samples or getting the samples oxidised. The HPLC analysis also identified individual cholesterol esters as well as free cholesterol. The examples of the HPLC chromatograms are shown in Figure 4.14.

Within 48 h addition of aggLDL, oxLDL and aggoxLDL to HMDMs, there was approximately 4-fold increase in the CE levels compared to cells incubated with LDL or control cells (Figure 4.15b). The CE accumulation was the sum of the concentrations of cholesteryl arachidonate; cholesteryl linoleate; cholesteryl oleate; and cholesteryl palmitate. Incubation of HMDMs with nLDL did not cause accumulation of CE. Even though incubation with aggLDL caused accumulation of CE the most, ANOVA analysis revealed that there was no significant difference between the CE levels between aggLDL, oxLDL and aggoxLDL. Incubation of HMDMs with the modified LDL did not change their free cholesterol levels as compared to control cells (Figure 4.15a).

There is a possibility that the presence of lipoprotein in the serum might promote CE efflux thus reducing cholesterol esterification. This was investigated by supplementing the RPMI media with 10% LPDS instead of 10% HIHS. There was (Figure 4.16b) a very significant difference in CE composition of the cells treated with oxLDL, aggLDL and aggoxLDL as compared to control cells and nLDL treated cells. As expected incubation with nLDL did not accumulation of CE. Incubation with agoxLDL, increased the CE levels of HMDMs by approximately 4-fold. In addition, incubation with aggLDL and oxLDL increased the CE levels of HMDMs by approximately 20 and 16 folds respectively. More increment in CE level when the cells were in media containing LPDS compared to cells in media containing HIHS suggesting that there was a possibility that CE efflux occurred when cells were grown in media containing 10% HIHS. In addition, the results (Figures 4.15 and 4.16) also suggest that there was transformation of macrophages into foam cells as characterised by a sharp increase in CE levels, whereas cholesterol levels essentially remain unchanged (Figure 4.16b).

4.2.5 Cholesteryl Ester Efflux from HMDMs in the Presence of HDL

Cholesterol removal from lipid-loaded macrophages is an important, potentially antiatherogenic process as this prevents the accumulation of CE, hence, preventing the formation of foam cells. Since HMDMs were cultured in RPMI containing HIHS, there is a possibility that they were overwhelmed with the high concentration of cholesterol in the media. Therefore, further incubation of HMDMs with oxLDL or aggregated lipoprotein did not cause any accumulation of CE. Besides that, even if there was a formation of cellular CE, the presence of HDL in the serum might promote the CE efflux since HDL is an extracellular acceptor for cholesterol. This hypothesis was tested by growing the HMDMs in RPMI containing LPDS starting from the time of seeding (refer to legends under Figure 4.17 for the set up of experiment). The growth of the HMDMs in this media was monitored daily and photos of the cells were also taken. Morphologically, the HMDMs grown in RPMI containing LPDS looked much rounder and had less spread cytoplasm compared to the HMDMs grown in RPMI containing HIHS (see Chapter 3, Figure 3.8). The membrane of the HMDMs grown in RPMI containing LPDS was more transparent then the HMDMs grown in RPMI containing HIHS. The HMDMs cultured in RPMI with 10% LPDS also had less cell materials staining with oil red-O (see Chapter 3, Figure 3.9).

Interestingly, the CE contents of HMDMs grown in media containing HIHS were similar to the HMDMs grown in media containing LPDS (Figure 4.17, plates 1 and 2). This could suggest that lipoprotein in the serum is not accountable for the accumulation of CE. Furthermore, incubation of HMDMs with aggoxLDL increased the CE levels of HMDMs to approximately 4-folds as compared to control (Figure 4.17 plate 2). This was consistent with the results in Figures 4.15 and 4.16 (section 4.2.2), where the cells incubated with aggoxLDL in media containing, HIHS, and LPDS respectively had 4-folds more CE than the control cells. The presence of extracellular acceptor HDL in the media promoted CE efflux as the CE level dropped almost 15% after incubation of the HMDMs in media containing HDL for 24 hours and another 70% after 72 hours.

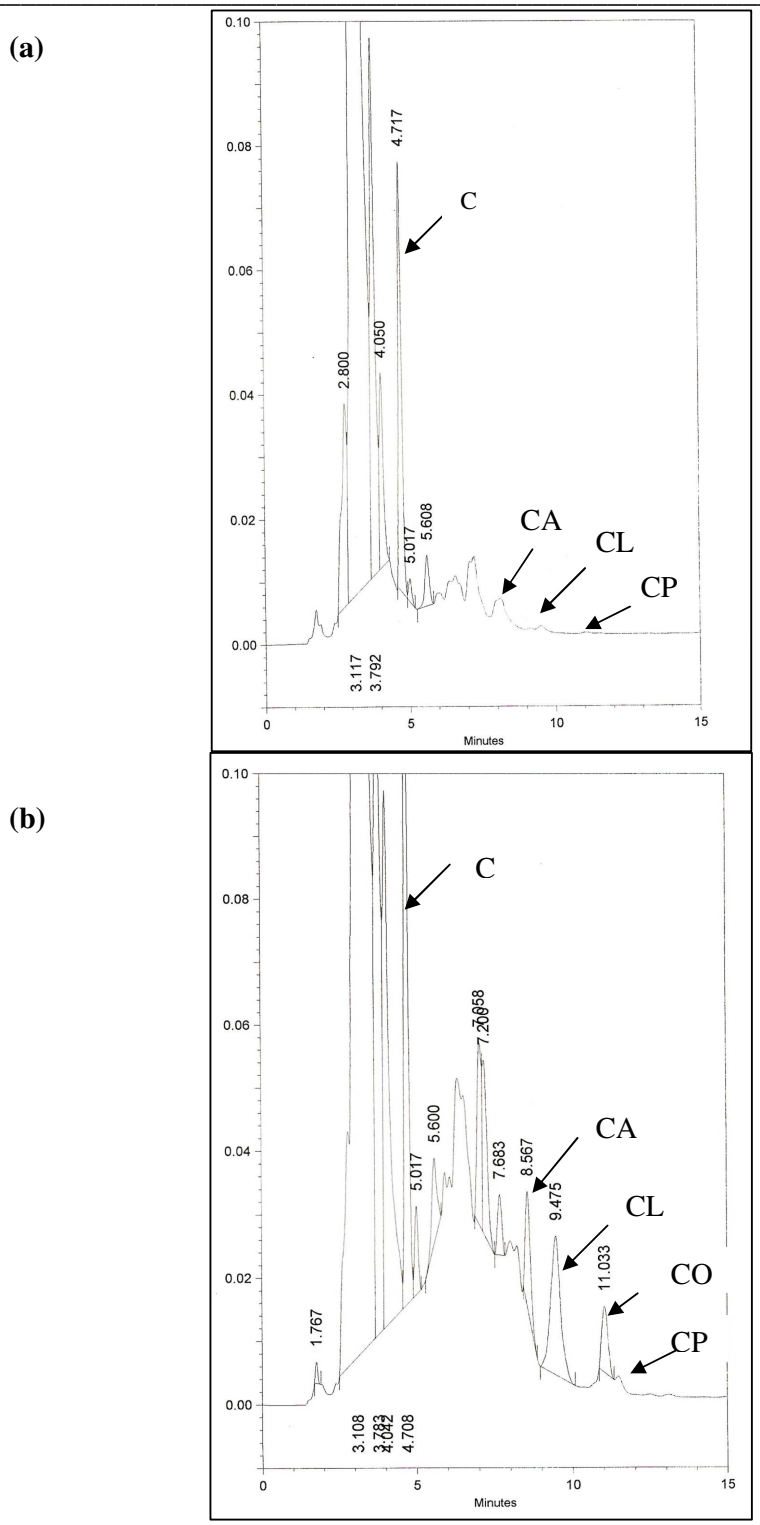

Figure 4.14 Identification of free cholesterol and cholesteryl esters by HPLC.
HMDMs (5 x 10^6 cells/ml) in RPMI containing 10% HIHS in 12 well plate were incubated with 200 µg/ml aggLDL for 48 hours (b). (a) is control HMDMs in the media only. Peaks were identified using standards. C, cholesterol; CA, cholesteryl arachidonate; CL, cholesteryl linoleate; CO, cholesteryl oleate; and CP, cholesteryl palmitate.

(a)

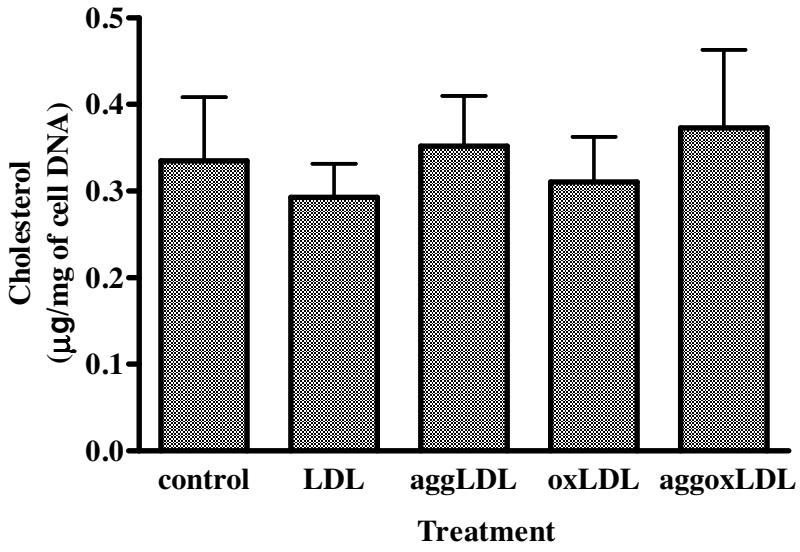

(b)

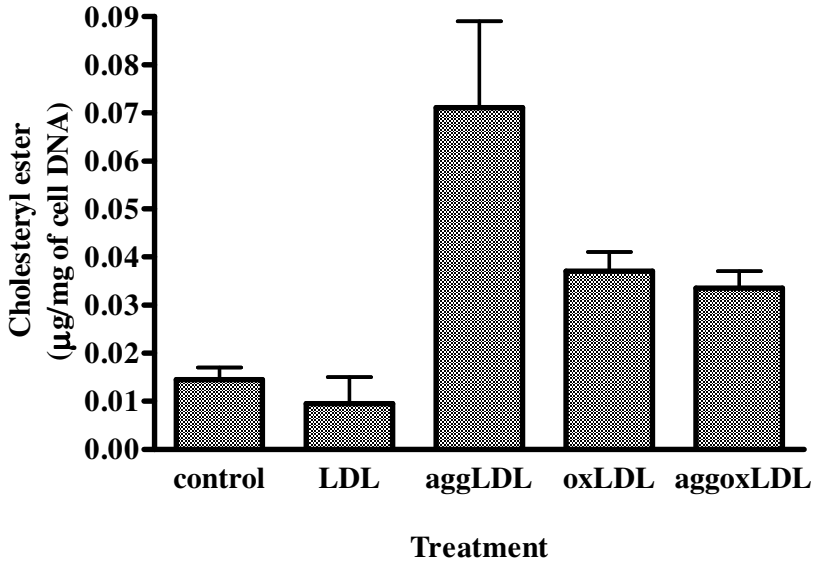

Figure 4.15 HPLC analysis of cholesteryl ester and cholesterol compositions of HMDMs in media containing 10 % HIHS.

HMDMs ($5x10^6$ cell/ml) in RPMI containing 10 % HIHS in 12 well plates were incubated in the absence of lipoprotein (control) or in the presence of 0.2 mg/ml LDL, aggLDL, oxLDL or aggoxLDL. After 48 h incubation, the CE and cholesterol contents were analysed by HPLC. ANOVA analysis revealed statistical significance from control for the CE contents and no statistical significance from control for the free cholesterol contents. Results are displayed as mean ± SD of duplicates from a single experiment, representative of three separate experiments.

(a)

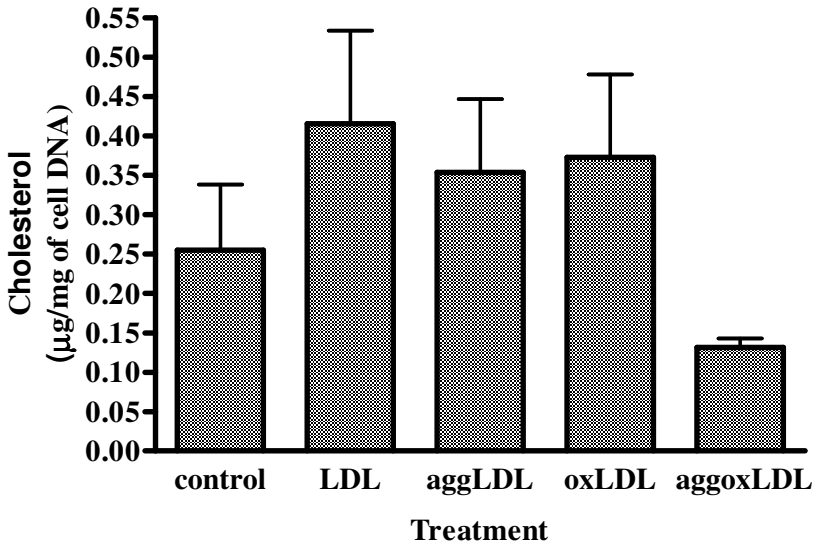

(b)

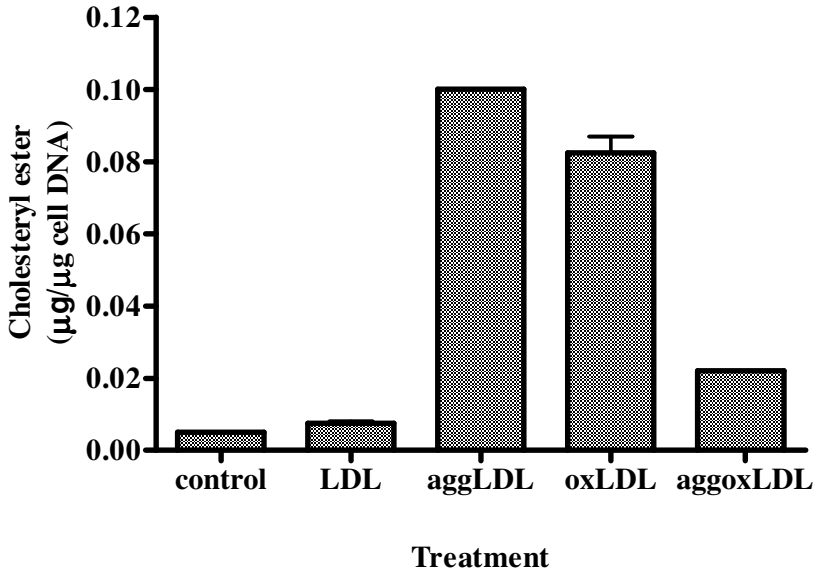

Figure 4.16 HPLC analysis of cholesteryl ester and cholesterol compositions of HMDMs in media containing LPDS

HMDMs ($5x10^6$ cell/ml) were initially cultured in RPMI containing 10% HIHS in 12 well plates. The media was changed to RPMI containing 10% LPDS for 24 hours before incubating further in the absence of lipoprotein (control) or in the presence of either LDL, aggLDL, oxLDL or aggoxLDL at 0.2 mg/ml respectively. After 48 h incubation the CE and cholesterol contents were analysed by HPLC. ANOVA analysis revealed statistical significance from control for the CE contents and no statistical significance from control for the free cholesterol contents. Results are displayed as mean ± SD of duplicates from a single experiment, representative of three separate experiments.

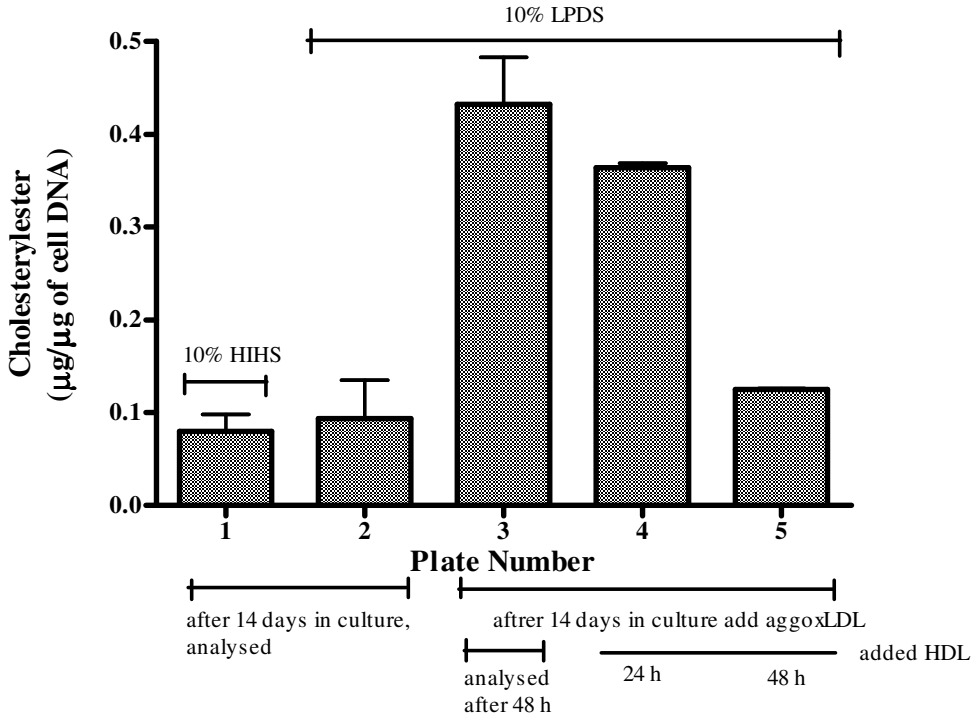

Figure 4.17 Effect of supplementing RPMI media with HDL on cholesteryl ester compositions of HMDMs.
HMDMS (5 x 10^6 cell/ml) were cultured in RPMI containing 10% HIHS for plate 1 and RPMI containing 10% LPDS for plates 2-5. After 14 days in culture, lipids were extracted and analysed from plates 1 and 2. 200 µg/mL of aggoxLDL were then added to plates 3-5 and incubated further in RPMI with 10% LPDS. After 48 h lipids were extracted and analysed from plate 3. Then the media in plates 4 and 5 was changed to RPMI containing 10% HDL. HDL was prepared according to the method described in section 2.2.1.4. Lipids were extracted and analysed from plate 4, 24 hours later and from plates 5, 72 hours later. CE contents were analysed by HPLC.

4.2.6 Determination of Susceptibility of Cholesteryl Ester Loaded HMDMs (Foam Cells) to Cytotoxic OxLDL

The susceptibility of CE loaded HMDMs or foam cells to a lethal dose of oxLDL has not been explored before. Therefore, it is interesting to find out whether CE loaded HMDMs are more resistant to a lethal dose of oxLDL or not.

HMDMs were induced to accumulate CE by incubation with a non lethal dose of oxLDL 0.1 mg/ml for 48 hours. At first, the foam cells were exposed to a highly toxic 2 mg/ml oxLDL for 48 h. Figure 4.18 (treatment A) shows that 2 mg/ml oxLDL caused 90% loss in HMDMs viability. Making the HMDMs to be CE loaded did not increase the HMDMs' viability (Figure 4.18, treatment B) or protect the HMDMs from the lethal dose 2.0 mg/ml of oxLDL (Figure 4.18 treatment C). There was a possibility that 2.0 mg/ml of oxLDL was too toxic to the HMDMs that all their protective mechanisms were affected

and shut down. Therefore, this experiment was repeated by using 1.0 mg/ml oxLDL. However a similar result was obtained (Figure 4.19).

Since there was no protection of CE loaded HMDMs against 1 and 2 mg/ml of oxLDL, there was a possibility that 2 days exposure to these doses of oxLDL was too long. This probably gave the HMDMs no chance to recover. Therefore, this experiment was repeated by exposing HMDMs to 1.0 mg/ml for just 24 h. Incubation of HMDMs with 1 mg/ml oxLDL for 24 h caused 50% loss in HMDMs's viability (Figure 4.20, treatment A). Similar results were also obtained where making HMDMs as CE loaded cells did not increase their viability (Figure 4.20, treatment B) or protect them from toxicity of 1 mg/ml oxLDL. These results suggest that CE loaded macrophages or foam cells are still susceptible to toxic oxLDL and died as a consequence.

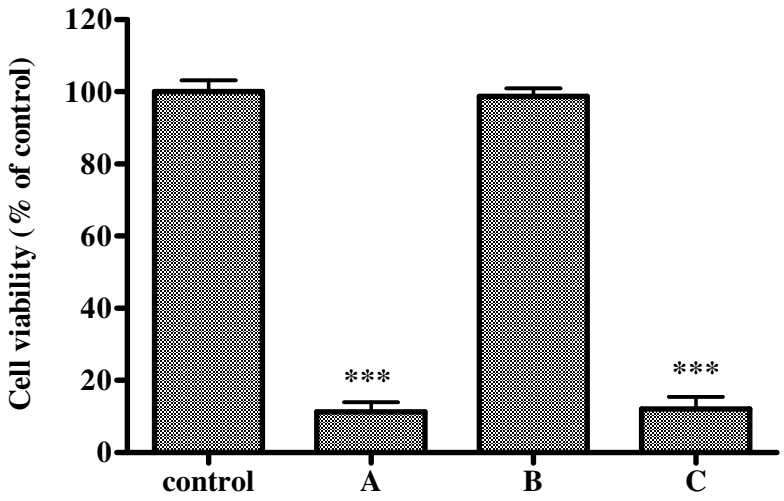

Figure 4.18 Loss of CE loaded HMDMs viability after 48 h incubation with 2 mg/ml oxLDL.

HMDMS (5 x 10^6 cell/ml) were preincubated with 0.1 mg/ml oxLDL in RPMI containing 10% HIHS for 48 hours and designated as B and C. Control and A were cells in RPMI containing 10% HIHS. Then 2 mg/ml oxLDL was added to (A) and (C). After 48 hours, HMDMs were analysed for cell viability via MTT assay. Significance is indicated from control cells. Results are displayed as mean ± SD of triplicates from a single experiment, representative of three separate experiments.

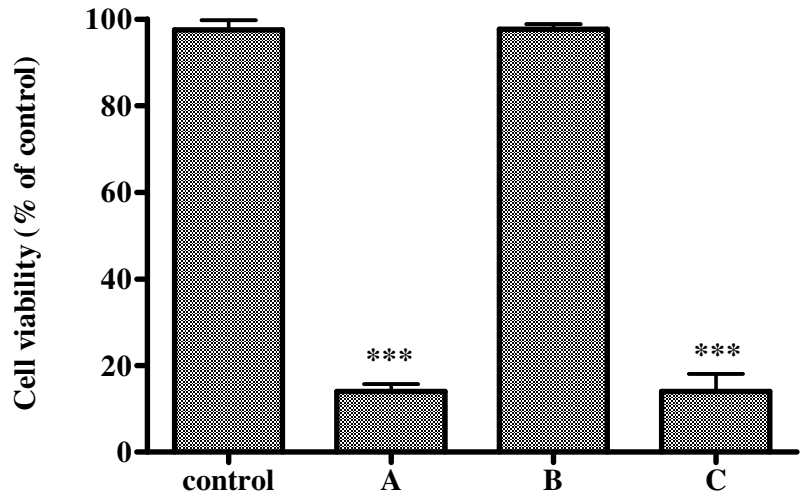

Figure 4.19 Loss of CE loaded HMDMs viability after 48 h incubation with 1 mg/ml oxLDL.

HMDMS (5 x 10^6 cell/ml) were preincubated with 0.1 mg/ml oxLDL in RPMI containing 10% HIHS for 48 hours and designated as B and C. Control and A were cells in RPMI containing 10% HIHS. Then 2 mg/ml oxLDL was added to (A) and (C). After 48 hours, HMDMs were analysed for cell viability via MTT assay. Significance is indicated from control cells. Results are displayed as mean ± SD of triplicates from a single experiment, representative of three separate experiments.

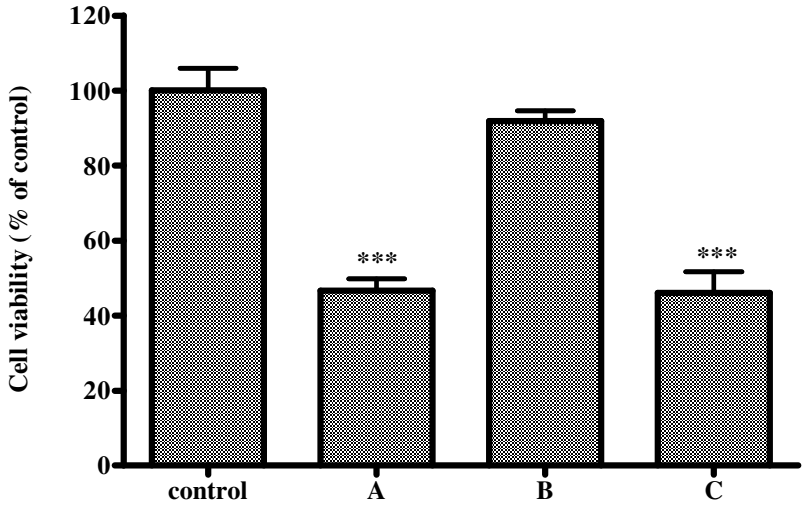

Figure 4.20 Loss of CE loaded HMDMs viability after 24 h incubation with 1 mg/ml oxLDL.

HMDMs (5x10^6 cells/ml) were incubated for 24 hours at 37 °C in RPMI containing 10 % HIHS (control and (A)) or with 0.1 mg/ml oxLDL ((B) and (C)). Then 1 mg/ml oxLDL was added to (A) and (C). After 24 hours, HMDMs were analysed for cell viability via MTT. Significance is indicated from 0 mg/ml oxLDL (control). Results are displayed as mean ± SD of triplicates from a single experiment, representative of three separate experiments.

4.2.7 Determination of 7,8-Dihjydroneopterin Production by CE Loaded HMDMs when Stimulated with IFN-γ

While being CE loaded HMDMs did not protect them from cytotoxicity of oxLDL, it is interesting to know whether HMDMs ability to synthesise 7,8-NP is different than the CE loaded cells. This was investigated by inducing HMDMs to synthesise *de novo* 7,8-NP with IFN-γ. In this experiment, 250 U/ml IFN-γ was used since earlier works in this laboratory (Firth, 2006) had shown that pterin detected in both the supernatant and in the HMDMs cellular extracts did not vary significantly between 250 and 1000 U/ml of IFN-γ. Furthermore 48 hours incubation of HMDMs with IFN-γ had been found to be optimal for 7,8-NP production (Firth, 2006).

Figure 4.21a shows that incubation of HMDMs with 200 μg/ml aggoxLDL, did not affect their cell viability. Furthermore, incubating the cells with 250 U/ml IFN-γ in the presence or absence of 200 μg/ml aggoxLDL also did not affect the viability of the HMDMs. Figure 4.21b shows that control cells and HMDMs incubated with aggoxLDL had similar contents of neopterin and total pterin. As expected incubation of HMDMs with 250 U/ml IFN-γ increased the neopterin production drastically by 6.6-fold as compared to control cells. The addition of aggoxLDL did not affect the level of neopterin produced. Interestingly, the cells produced 14% more total pterin when incubated with IFN-γ alone compared to when the cells had both IFN-γ and aggoxLDL. This small difference is statistically significant ($p < 0.05$). This could suggest that being CE loaded HMDMs made them less efficient in synthesising 7,8-NP to protect themselves.

(a)

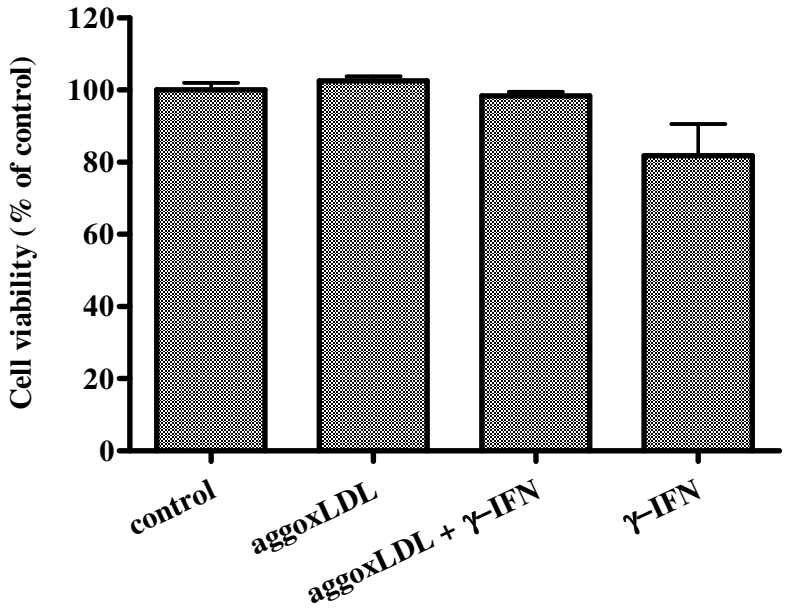

(b)

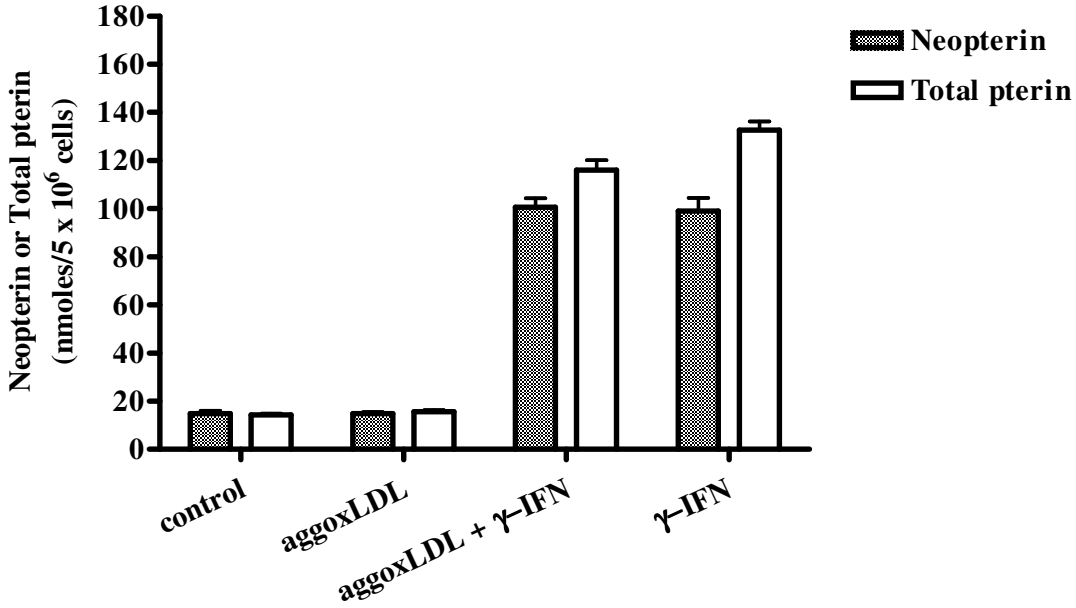

Figure 4.21 Neopterin and total pterin production by HMDMs exposed to γ-IFN. HMDMs were incubated at 37°C in RPMI containing 10% HIHS with 0.2 mg/ml agg-oxLDL for 24 hours. Then 250 U/ml γ-IFN was added and incubated for a further 48 hours. Controls were conducted in the absence of aggoxLDL and γ-IFN. HMDMs were analysed for cell viability by (a) MTT and (b) neopterin and total pterin (neopterin and 7,8-NP) production by HPLC analysis. Results are displayed as mean ± SEM of triplicates from a single experiment, representative of three separate experiments.

4.3 Discussion

4.3.1 Differentiation of Monocytes into Macrophage: Analysis of Lipid Content

GC analysis shows that during differentiation of monocytes into macrophages in media containing 10% HIHS, the cells continuously accumulated free cholesterol (Figure 4.3). In contrast the CE levels increased only up to day 4 in culture. Despite the constant level of CE, from day 4, the macrophages still developed into foamy cells appearance (Chapter 3, Figure 3.1) and stained with oil red-O (Chapter 3, Figure 3.2).

These results are in agreement with previous studies (Asmis & Jelk, 2000b; Garner *et al*., 1997a) that demonstrated large increase in free cholesterol and triglyceride levels but very little or no increase in CE contents during differentiation of monocytes into macrophages. Asmis & Jelk, (2000b) revealed a 3.4-fold increase in free cholesterol, 136-fold increase in triglyceride level and 78% decrease in CE level during differentiation of human monocytes into macrophages in media containing 5% human serum. Garner *et al*., (1997a) showed that the lipid composition of freshly elutriated monocytes comprised predominantly unesterified cholesterol (UC) with only traces of TG and no detectable CE. After 7 days cultured in RPMI with 10% HIHS, human monocytes accumulated 4 times more TG mass than UC and only a trace amount of CE (Table 4.4). The cells also stained positive with oil red-O. Both studies (Asmis & Jelk, 2000b; Garner *et al*., 1997a) show accumulation of lipid during the culture of HMDMs produces cells with a foam-like appearance. As the HMDMs in this study were also cultured in the presence of 10% HIHS, they too were expected to become foam-like.

Table 4.4 Lipid composition of HMDMs cultured for 7 days in RPMI with 10% HIHS. Adapted from Garner *et al*., (1997a).

Lipid Class	nmol/mg cell protein
Unesterified cholesterol	66 ± 7
Triglycerides	251 ± 78
CEs	0.7 ± 0.2

After 7 days of culture in RPMI 1640 containing 10% HIHS, HMDMs were washed 3 times in warm PBS and lipids were extracted and analysed by HPLC. Values are mean ± S.E.M. (n = 4).

These results raised a doubt whether foam cells can be formed by culture of monocytes in human serum without the presence of modified lipoproteins. However, foam

cells isolated from human atherosclerotic plaque, contain on average 4 times more CE mass than triglycerides (Mattsson *et al*., 1993) and foam cells isolated from rabbit atherosclerotic intima also had large amount of CE (Naito *et al*., 1997). Therefore, it is not appreciated that HMDMs grown in human serum are foam cells since their lipid content is almost exclusively triglyceride and not CE (Garner *et al*., 1997a). The foamy appearance and cellular lipid droplets which stained positive with oil red-O seen in this study can be attributed to the triglyceride (Garner *et al*., 1997a) and not the accumulation of CE which rule out the use of oil red-O stain to identify foam cells. Thus there are differences between the lipid composition of macrophage foam cells isolated from human plaque and the lipid loaded HMDMs here, despite their similar microscopic appearance and positive staining with oil red-O.

4.3.2 Analysis of Lipid Contents of Monocytes and Macrophages Incubated with OxLDL

OxLDL has been reported to induce enhanced expression of MHC II molecules on human monocytes and U937 and surface antigen LeuM3 in U937 cells (Frostegard *et al*., 1990). The expression of these surface molecules is a pattern compatible with expression of a more differentiated macrophage-like phenotype. In contrast, the GC analyses of monocytes incubated with oxLDL showed that the differentiation of monocytes to macrophages was not affected by the presence of oxLDL (Figure 4.4). In addition, the rates of monocytes differentiation into macrophages were similar across the oxLDL concentrations used. While this study supplemented the media with human serum, Frostegard *et al*., (1990) used fecal calf serum. In addition, U937 is a cell line that can divide and differentiate while human monocytes only undergo differentiation.

Likewise after 10 days incubation with oxLDL, there were no difference in the cell viability, free and total cholesterol contents (Figure 4.5) as well as the microscopic appearance in the oxLDL-treated HMDMS in comparison with the control HMDMs (Figure 4.6). A similar trend was also observed when mature HMDMs were incubated for 10 days with 0-200 μg/ml oxLDL (Figure 4.7) or 48 h with 0-500 μg/ml oxLDL (Figure 4.8). Most surprisingly, microscopic examination of oil red-O stained cells showed accumulation of lipid droplets in all of the treatments. This is in contrast with mouse macrophages incubated with oxLDL (Jessup, personal communication) and aggLDL (Khoo *et al*., 1988) where the cells demonstrated distinct changes in oil red-O stain only when treated with the modified LDL. Oil red-O stain is considered a hallmark of foam cell

identification yet all our treatments with and without oxLDL generated "foam cells" according to the stain.

These results led to a few speculations. Firstly, the cells may have been foam cells before incubation with oxLDL as there was a possibility that the cells might take up oxidised lipoprotein from the serum. However, results from Table 4.3 ruled out the possibility that oxidation of lipoprotein in serum occurred. So no oxLDL should have been present. Secondly, since GC analysis revealed that feeding the cells with oxLDL did not cause accumulation of CE there was a possibility that to form foam cells other forms of modified LDL was needed. The possibility was deduced since Asmis *et al*., (2000b) claimed that in their study oxLDL did not cause foam cell formation in human macrophages unless when it was in aggregated forms. In contrast to Asmis *et al*. (2000b) findings, GC analysis in this study shows that incubation of HMDMs with the modified lipoprotein whether or not it is aggregated did not induce accumulation of CE or free cholesterol in HMDMs (Figure 4.10). This was rather surprising since others (Heinecke *et al*., 1991; Khoo *et al*., 1988; Maor *et al*., 1997) also had shown that aggregated lipoprotein induced accumulation of CE in the macrophages. The results (Figures 4.8 and 4.10) also show that the total cholesterol contents were 50% less than the free cholesterol, which raise doubts about the reliability and suitability of using GC to analyse the lipid content of the HMDMs. A few studies had reported the nonreliability of GC to analyse the oxysterols contents leading to false values of the oxysterols measured (Heinecke *et al*., 1991; Maerker *et al*., 1988; Malavasi *et al*., 1992; Sevanian *et al*., 1994).

The lipid contents of HMDMs incubated with the modified lipoproteins were then reanalysed using HPLC by adopting methods established by Kritharides *et al*., (1993). When this experiment was repeated using HPLC, interestingly, there was 4-fold increase in CE levels of HMDMs incubated for 48 hours with the aggLDL, oxLDL and aggoxLDL in comparison to the control cells (Figure 4.14). As expected, incubation of HMDMs with nLDL did not cause accumulation of CE (Figure 4.15). The same 4-fold increment in CE levels of HMDMs treated with aggoxLDL was also observed when the cells were in RPMI containing 10% LPDS (Figure 4.16). It is noteworthy that cells in RPMI containing 10% LPDS had more increment in CE levels. There were 20-fold and 16-fold increment in CE level compared to control when HMDMs were incubated with aggLDL and oxLDL respectively. The absence of HDL in LPDS prevented cholesterol efflux, thus higher levels of CE in the cells incubated in RPMI with LPDS. This was proven by results shown in section 4.2.5. These results disagree with the finding of Asmis and Jelk (2000b) that claimed oxLDL only caused CE accumulation when it was in aggregated form.

Previous study (Brown *et al*., 1996) had shown that mouse macrophages that were incubated with 24 h copper-oxLDL for 24 hours displayed a profile of oxysterols remarkably similar to that of 24 h copper-oxLDL. The later comprised approximately 50% of total sterols, 30% 7-KC with other sterols comprising the remainder (7α- and 7β-OH, α- and β- epoxides, and 6β-hydroxycholesterol). The majority of CE and 7-KC in 24 h copper-oxLDL and copper-oxLDL macrophages contained fatty acyl chains which are presumed oxidised. The same study (Brown *et al*., 1996) showed that the cholesterol content of copper-oxLDL loaded cells was 5-fold greater in comparison to the non-loaded cells and similar increment was also observed with the total cholesterol levels. Another study (Asmis & Jelk, 2000b) showed that within 40 h after aggLDL and aggoxLDL were added to human macrophages, there were 15-fold and 10-fold increase in cellular CE levels respectively compared to cells incubated with unmodified LDL. Different level of increment in the amount of cellular CE from different laboratories reflects its dependency on the culture conditions for example types of media, types and percentage of serum used and most importantly the type of cells used to form the foam cells. Whatever the culture condition is, the accumulation of cellular CE is directly related to the uptake of the modified lipoprotein and it is the hallmark of formation of foam cells. Importantly, the HPLC results clearly shows that in our culture conditions, incubation of HMDMs with aggLDL, oxLDL and aggLDL caused accumulation of CE in HMDMs thus formation of foam cells.

4.3.3 High Performance Liquid Chromatography versus Gas Chromatography in Measuring the Lipid Contents of HMDMs

The HPLC results (Figure 4.14 and 4.15), confirm the suspicion that GC technique might be the reason why there was no difference in CE levels between the control and modified LDL -treated HMDMs. In this study the formation of foam cells cannot be shown by using GC technique but by using HPLC technique, the formation of CE loaded foam cells was clearly shown. The relatively poor reproducibility and lack of consistency in the trends for the total cholesterol contents with GC analyses made it difficult to determine whether in our culture conditions the foam cells were formed or not. There are several likely explanations for this inconsistency. GC analysis while sensitive and specific is restricted by several factors discussed below. Artifactual oxidation ex vivo during sample processing, storage and/or analysis are always a potential concern when dealing with oxidation products and this has been reported by many groups for oxysterols. Several

studies have found that the lengthy manipulations involved in extracting the samples and the high temperature conditions during GC analyses can decompose or oxidised (even though BHT was added) the samples. The HPLC approach may have spared the oxysterols high temperature during GC analyses. When using HPLC to analyse the samples, hot alkaline saponification and TMS derivatisation were avoided, and samples were immediately extracted into organic solvent where they are more stable (Sevanian *et al*., 1994). This could explain the ability to detect the differences in the CE levels of the treated and non treated HMDMs.

Analysis of samples by GC utilised a very high oven temperature for the detection of the desired peaks. Oxysterols for example cholesterol 7α-hydroperoxide is known to be thermally labile (Malavasi *et al*., 1992) and prone to degradation in the alkaline conditions used for alkali saponification (Maerker *et al*., 1988) and even unstable in aqueous solution (Sevanian *et al*., 1994). Although HPLC analysis of cholesterol oxides provided less resolution and lower sensitivity as compared to GC, a distinct advantage using HPLC was evident for direct measurements of cholesterol-7-hydroperoxides and 7-KC. These two cholesterol oxides are particularly sensitive to storage in solvents, derivatisation procedures, and analytical conditions used for GC analysis, which are minimized or avoided when using HPLC (Sevanian *et al*., 1994). Indeed when 7-OOH was analysed by GC, two peaks resulted with the retention times and mass spectra of 7-KC and 7α-hydroxycholesterol were observed (Malavasi *et al*., 1992). Hence it is likely that any 7-OOH present was thermally decomposed during GC analysis.

Besides that in this study the samples for GC analysis were subjected to heat treatment during alkaline hydrolysis. The heat treatment probably can lead to lost or reduced of sample yields during sample processing besides the possibility of conversion of oxysterols to other oxysterols. For instance, 7-KC is dehydrated to form 7-KCdiene during hot alkaline saponification and 7-hydroxyperoxycholesterol (7-OOH) decomposes at elevated temperatures to form 7-KC and 7-hydroxycholesterol (7-OH) (Brown *et al*., 1997). This gives false values of compounds being measured. In addition, cholesterol epoxides can be hydrolysed to the cholestane-triol (TRIOL) under acidic conditions (Maerker *et al*., 1988). Alkaline hydrolysis of sterol esters present in oxLDL should be avoided since 7-OOH and 7-OH showed their conversion to 7-KCdiene in these conditions (Malavasi *et al*., 1992)

The detection of sterols by HPLC and GC was compared in samples of LDL oxidised for various times by Brown *et al*., (1996). In their hands, HPLC and GC had given comparable estimates of free cholesterol content of LDL at all stages of oxidation.

This was possible because Brown and colleagues (1996) subjected LDL to room temperature or cold alkali saponification for the GC analysis. The saponification method was conducted on ice to minimize thermal decomposition of certain oxysterols. The TMS derivatives of the oxysterols were also done at room temperature (Brown *et al*., 1996). Thus, GC analysis with room temperature TMS derivitisation and cold alkali saponification enable measurement of esterified and free forms of both cholesterol and oxysterols, which complemented HPLC methods. Brown, *et al*., (1996) also showed that standard 7-KC produced a single peak on GC. However when standard 7-KC was injected onto GC after being subjected to the hot alkaline saponification procedure a consistent peak of 7-KCdiene was detected, and this compound is assumed as artefact in saponification process.

4.3.4 Susceptibility of Foam Cells to Cytotoxic OxLDL

CE loaded or foam cells and HMDMs displayed similar susceptibility towards the cytotoxic effect of oxLDL (Figures 4.18-4.20). There was no difference in the level of neopterin synthesised by the foam cells and HMDMs whether the cells were stimulated with γ-IFN or not (Figure 4.21). Earlier studies in this laboratory (Hicks *et al*., 2007 (unpublished data)[1]) showed that HMDMs stimulated with γ-IFN had both neopterin release and cell viability dropped hand in hand when exposed to increasing concentrations of oxLDL. Contrary to HMDMs, the giant cells (multinucleated macrophages) were able to sustain neopterin release at higher concentrations of oxLDL. This partially account for increased resistance of giant cells to oxLDL cytotoxicity as demonstrated by giant cells viability remaining at or above levels in the absence of oxLDL. It can be postulated from Hicks *et al*, (2007) (unpublished data) that the similar susceptibility of foam cells and HMDMs towards lethal dose of oxLDL was due to the similar levels of 7,8-NP synthesised by both cell types when being exposed to oxLDL. The fact that foam cells is less efficient than HMDMs in synthesising 7,8-NP (Figure 4.21b) increase the likelihood of their death due to the presence of various oxidants at the inflammatory site especially at the atherosclerotic plaques. Since foam cells are lipid loaded cells storing cytotoxic products of oxLDL, their death contribute further damage and more detrimental to their surroundings due the release of the cytotoxic lipids.

Another study showed that foam cell formation resulted in a 36% and 44% reduction in the cellular α-tocopherol/total cholesterol ratio in unsupplemented and

[1] Professor Barry Hicks was a visiting professor from U.S. Air Force Academy, CO.

vitamin E-supplemented foam cells, respectively (Asmis & Jelk, 2000a). The loss of vitamin E was accompanied by an increase in the susceptibility of these foam cells to succumb to the cell lytic effects of oxLDL. However, vitamin E supplementation did not protect macrophages or foam cells from oxLDL-mediated cell lysis suggesting that vitamin E loss is not the cause of their increased susceptibility to cell lysis. It would be interesting to know what is the 7,8-NP level during foam cell formation. The effect of supplementing the HMDMs with 7,8-NP on the toxic effect of oxLDL will be explored in the next chapter. Apart from the studies above, there was no data found in literature research on the subjects of foam cells and toxic effect of oxLDL whether or not supplemented with antioxidant.

4.4 Summary

The presence of oxLDL up to 200 μg/ml apparently did not affect the rate of monocyte differentiation into macrophages. Continuous increment in free cholesterol levels was observed during differentiation of monocytes into macrophages. In contrast, the CE contents only increased up to day 4 during the culture period. Therefore, even though the differentiated HMDMs appeared foamy and had oil red-O positive droplets, these are not due to the CE deposits but most probably attributed by triglycerides.

This study shows that HPLC is superior to GC when analysing the lipid contents of the foam cells is concerned. HPLC results show that foam cells were formed using the culture condition in this study. Foam cells are cells that accumulate CE. The HPLC demonstrated clearly that there were significant different in the CE levels between the control macrophages and macrophages treated with various modified LDL. It can be concluded that foam cells were successfully developed in the present study by incubation of HMDMs with 200 μg/ml of aggLDL, or oxLDL or aggoxLDL. The HPLC approach spares the samples of lengthy manipulations that may cause ex vivo oxidation. Analysing the samples by GC, exposed the samples to high temperature during alkaline saponification, TMS derivitisation and GC analyses which alter the lipid composition and therefore affect their quantification.

The oil red-O staining did not differentiate the foam cells from HMDMs since whether or not the cells accumulated CE, they still produced oil red-O positive droplets. Therefore, this study proves that foamy appearance and positive staining with oil red-O staining are not the criteria of foam cells.

Stimulation with γ-IFN caused similar level of neopterin production in the foam cells and HMDMs. The effects of 7,8-dihydroneoperin on oxLDL-induced damaged in foam cells was not explored since there was no different in the susceptibility to cytotoxic oxLDL between HMDMs and foam cells. Instead the effect of 7,8-dighydronepterin on oxLDL-induced damage in HMDMs was investigated as discussed further in Chapter 5.

5 OxLDL-induced Death in HMDM Cells and 7,8-Dihydroneopterin Protection

5.1 Introduction

One of the major oxidants present within the atherosclerotic plaque is oxLDL for which considerable evidence point to its involvement in the progression and development of atherosclerosis (Niu *et al*., 1999; Salvayre *et al*., 2002). In contrast to LDL, oxLDL is taken up by macrophages in a rapid and uncontrolled manner leading to the formation of cholesterol filled foam cells. High concentration of oxLDL is cytotoxic and can cause both necrosis and apoptosis in a variety of cell types including macrophages. Therefore, the change from fatty streak to complex plaque may be driven in part by the oxLDL-induced death of macrophages within the plaque (Hegyi *et al*., 1996).

The exact mechanism of oxLDL cytotoxicity is difficult to ascertain since oxLDL is not a single, well-defined entity, but has structural and physical properties, which vary according to its means and degree of oxidation. The nature of oxLDL prepared by laboratory to laboratory is different due to variations in the conditions for oxidation and the source of LDL. Slight variations in the conditions of oxidation might result in a different degree of toxicity of oxLDL. Also most authors do not characterise their oxLDL further than stating that it is oxidised. This may in the past have given rise to discrepancies in the reported biological effects or mechanisms implicated in oxLDL-induced death. The effect of oxLDL on various types of cells has been discussed in great detail in Chapter 1.

There have been a large number of studies examining the beneficial effects of various antioxidants in preventing the development of atherosclerosis in both animal models and humans. The majority of these studies have centred on the inhibition of oxLDL formation. A number of studies had explored the effects of antioxidants on oxLDL-induced damaged in the cells. α-Tocopherol has been shown to be a potent inhibitor of oxLDL cell toxicity even though it is uncertain whether this is due to its antioxidant effect. α-Tocopherol was found to inhibit apoptosis in smooth muscle cells (de Nigris *et al*., 2000) and prevented apoptosis in U937 cells incubated with 7-KC (Lizard *et al*., 2000). α-Tocopherol also inhibited oxLDL-induced apoptosis in mouse mesangial cells (Tashiro *et al*., 1999) and VSMCs (Guyton *et al*., 1995). 7*β*-hydroperoxycholesterol-induced death in human dermal fibroblasts was significantly inhibited by α-tocopherol (Coffey *et al*., 1995). Treatment of human aortic smooth muscle cells (HASMC) with

water soluble γ-tocopherol derivative Trolox suppressed oxLDL-specific increase in ROS and prevented down regulation of GAPDH (Sukhanov *et al*., 2006). In human coronary artery endothelial cells (HCAECs) γ-tocopherol significantly decreased ox-LDL-induced apoptosis by inhibiting the activation of NF-kappaB (Li *et al*., 1999). The down regulation effects of α-tocopherol on the scavenger receptors will be discussed in section 5.3.2.5.

Interestingly, α-tocopherol supplementation of HMDMs did not prevent foam cell formation or alter the susceptibility of foam cells to lysis by oxidized LDL (Asmis & Jelk, 2000a) suggesting that plasma membrane oxidation is not a significant factor in oxLDL toxicity. NADPH oxidase release of superoxide has been implicated as the possible source of oxLDL-induced radical production (Nguyen-Khoa *et al*., 1999). Yet, α-tocopherol supplementation of human monocytes was found to inhibit phorbol 12-myristate 13-acetate (PMA) respiratory burst decreasing the level of superoxide and superoxide derived oxidants within the plaque (Cachia *et al*., 1998). The mechanism appears to be impairment to the NADPH-oxidase assembly through attenuation of the action of protein kinase C which phosphorylates the cytosolic factor $p47^{phox}$ during translocation to the plasma membrane.

Results with ascorbic acid inhibition of oxLDL were rather inconsistent. Ascorbate gave almost complete inhibition of apoptosis in human endothelial cells (Dimmeler *et al*., 1997). Ascorbic acid also protected human vascular smooth muscle cells against apoptosis induced by "moderately oxLDL" which contained high levels of lipid hydroperoxides (Siow *et al*., 1999). However, later the same laboratory reported that ascorbic acid did not protect murine macrophage cell line J774 from moderately oxLDL, but produced a modest increase in apoptosis (Harris *et al*., 2006). Increase in apoptosis was not mediated by a pro-oxidant mechanism since pretreatment of macrophages with ascorbate attenuated the increase in the expression of the antioxidant stress protein heme oxygenase-1. The small increase in apoptosis observed may instead have been due to the ability of ascorbic acid to protect components of the apoptotic machinery against oxidative insult (Vissers *et al*., 2001).

In addition, Asmis *et al*., (1998) demonstrated that detoxification of oxLDL by dehydroascorbic acid (DHAA) but not ascorbic acid and isoascorbic acid completely inhibited apoptosis induced by oxLDL. In contrast to oxLDL treated with ascorbic or isoascorbic acid, TBARS levels and lipid peroxide levels of oxLDL treated with DHAA were not substantially reduced. This suggests that reduction of oxidized lipids is an unlikely mechanism for the inhibition of oxLDL-induced apoptosis by DHAA. There is a

possibility that the inhibitory effect of DHAA is due to it reacting with reactive groups in the ApoB100 (Asmis & Wintergerst, 1998).

Results with BHT also varied. It had no protective effect against oxLDL with rabbit aortic smooth muscle cells (Liu *et al*., 1998), gave partial protection in VSMCs (Guyton *et al*., 1995) and but gave complete protection to human umbilical vein endothelial cells (Harada-Shiba *et al*., 1998). BHT also blocked oxLDL-induced apoptosis of mouse peritoneal macrophages (Niu *et al*., 1996). Antioxidants thiol can also prevent oxLDL-induced apoptosis. NAC as well as GSH were successful in vascular smooth muscle cells mouse with oxLDL (Hsieh *et al*., 2001), mesanglia cells with oxLDL (Tashiro *et al*., 1999) and U937 cells with 7-KC as was GSH (Lizard *et al*., 2000). Increase in CPP32-like protease activity triggered by oxLDL was drastically reduced by the NAC, vitamin C and α-tocopherol. The decreased CPP32-like protease activity correlated with a reduction in proteolytic cleavage of the CPP32 into the active p17 subunit and therefore, probably inhibits apoptosis through inhibition of caspase-3 activation (Dimmeler *et al*., 1997). Probucol was partially protective with vascular smooth muscles (Guyton *et al*., 1995) and mouse mesangial cells (Tashiro *et al*., 1999). Probucol also inhibited loss of membrane integrity by *β*-hydroperoxycholesterol (Coffey *et al*., 1995).

7,8-NP is a redox active compound capable of acting as either a pro-oxidant or antioxidant depending on the chemical environment. This laboratory has previously shown that at low μM concentrations, 7,8-NP is a very potent antioxidant. It protects erythrocytes from lysis induced by peroxyl radicals, hydrogen peroxide and HOCL (Duggan *et al*., 2001; Gebicki *et al*., 2000). In separate studies, 7,8-NP has been demonstrated to protect free proteins, cellular proteins and protein thiols from oxidant damage (Duggan *et al*., 2001; Duggan *et al*., 2002). 7,8-NP has also been shown to dramatically increases, in a dose dependent manner, the lag time of LDL oxidation mediated by copper and peroxyl radical (Gieseg *et al*., 1995). 7,8-NP has also been observed to prevent cell mediated LDL oxidation (Firth, 2006; Gieseg & Cato, 2003). 7,8-NP also effectively protect U937 cells from oxLDL-induced death at μM concentrations (Baird *et al*., 2005). Altogether these findings led to the hypothesis that 7,8-NP is synthesised by γ-interferon-stimulated macrophages to protect themselves against the oxidants encounter within an inflammatory site (Gieseg *et al*., 2008a).

Previous work in this laboratory concentrated on investigating the effect of oxLDL on THP-1 and U937 cell lines. OxLDL caused necrotic death in U937 cells with a dramatic loss of cellular glutathione and caspase independent cell death which was associated with phosphatidylserine exposure on the plasma membrane (Baird *et al*., 2004). In contrast,

oxLDL initiated THP-1 cell apoptosis with small reduction in cellular thiols, caspase-3 activation and plasma membrane phosphatidylserine exposure (Baird *et al*., 2004). The difference in response to oxLDL could be related to the varying mechanisms of uptake of oxLDL. U937 cells express fourfold higher levels of CD36 scavenger receptor than do THP-1 cells (Nguyen-Khoa *et al*., 1999) which may result in an initial burst of oxLDL uptake and more intensive oxidative stress. In addition, U937 cells do not express the transcriptional regulator peroxisome proliferator-activated receptor-γ (PPAR- γ) in response to oxLDL, but THP-1cells do (Inoue *et al*., 2001).

Another striking difference between the two cell lines is on the effect of 7,8-NP on oxLDL-induced damage (Baird *et al*., 2005). The addition of 7,8-NP to THP-1 cells failed to inhibit oxLDL dependent loss of cell viability or restore the THP-1 cellular thiol content. Surprisingly, 7,8-NP was very effective at protecting U937 cells from oxLDL-induce viability and intracellular glutathione loss. Peroxyl radical scavengers, Trolox and α-tocopherol had been shown to inhibit oxLDL- and 7β-hydroperoxycholesterol- induced apoptosis in blood derived macrophages and U937 cells respectively (Asmis & Begley, 2003; Coffey *et al*., 1995). It is possible that a similar mechanism is established in the U937 cells since 7,8-NP is a potent peroxyl radical scavenger . NAC and GSH had been reported to inhibit oxLDL and 7-KC induced apoptosis by increasing the intracellular thiol pool in macrophages and U937 cells (Kinscherf *et al*., 1998; Lizard *et al*., 2000). Since 7,8-NP was unable to reduce the oxidized protein thiols it is unlikely that 7,8-NP can regenerate or increase the intracellular glutathione levels (Duggan *et al*., 2002). Therefore, it is very likely that with U937, 7,8-NP is protecting the intracellular thiol pool by scavenging ROS generated in the presence of oxLDL. It is unknown why with THP-1 cells this does not occur (Baird *et al*., 2005).

Since the literature on mechanisms implicated in oxLDL-induced death are controversial, the first aim of this section is to investigate whether the heavily oxidised oxLDL prepared in this laboratory exhibits a similar mechanism in inducing the death of HMDMs as reported in the literature (Asmis & Begley, 2003; Baird *et al*., 2004; Hsieh *et al*., 2001; Lee & Chau, 2001; Porn-Ares *et al*., 2003). In addition, by not using the immortal cell lines, HMDMs represent more closely of the physiological cells involved in the progression of atherosclerosis. This work will extend our knowledge on the effect of oxLDL on cell lines to HMDMs. Specifically, 7,8-NP mediated inhibition of oxLDL-induced death has also never been studied in HMDMs. The second aim of this section will be to determine whether 7,8-NP can protect oxLDL-mediated HMDMs' death and whether

the protection given is similar to U937 cells. From these two aims, the related mechanisms of 7,8-NP protection on oxLDL-induced damage will be further elucidated.

As outlined in Chapter 1, different degrees of LDL oxidation exert different effect in the phases of atherosclerotic development. Highly oxLDL appears to greatly increase the oxidative stress on cells leading to cell death in cells and other surrounding cells. Since this study encompasses oxLDL's effect on cell viability this type of oxLDL will be used. Besides that, highly oxLDL was used as it is very difficult to determine what mLDL is and also difficult to stop the oxidation process at this early stage.

The cytotoxic effects of oxLDL on HMDMs were determined by the loss in cell viability and changed in the morphology of HMDMs as monitored under the light microscope. The mode of HMDMs' death induced by oxLDL was investigated by exploring whether oxLDL cause glutathione loss, ROS production, cytochrome *c* release, caspase-3 activation and phosphatidylserine exposure. The effect of oxLDL at one oxLDL concentration that caused approximately 50% loss in cell viability was used to study the mechanism of 7,8-NP's inhibition on the oxLDL-induced damage. The mechanism of 7,8-NP protection on HMDMs from oxLDL cytotoxicity was explored, by looking at the possibility whether 7,8-NP can inhibit the glutathione loss, scavenge the generated superoxide, prevent cytochrome *c* release and PS exposure. Finally, the effect of 7,8-NP on the uptake of oxLDL was studied with the special interests on the ability of 7,8-NP to influence the scavenger receptors, SR-A and CD36 protein expression.

5.2 Results

5.2.1 Effects of OxLDL on HMDMs

5.2.1.1 Characterisation of Native LDL and OxLDL

The oxLDL prepared in this study was characterised relative to the native LDL (nLDL) to provide means of comparison with oxLDL used by other groups. Measurement of TBARs, relative electrophoretic mobility (REM) and degree of aggregation measured spectrophotometrically at wavelength 680 nm were used since these were the three most common properties mentioned in the literatures (Darley-Usmar *et al*., 1991; Ehrenwald *et al*., 1994; Fujiwara *et al*., 1998; Khoo *et al*., 1988; Maor *et al*., 1997).

OxLDL was prepared at a concentration of 0.5 mg/ml and was compared to nLDL at the same concentration (0.5 mg/ml). Native LDL contained very low levels of TBARs, which was significantly increased after oxidation, by approximately 52 –fold in the oxLDL. The REMs of oxLDL and native LDL were compared using lipoprotein gel electrophoresis. OxLDL's mobility was 2.7 -fold greater than that of native LDL (Table 5.1 and Figure 5.1).

OxLDL usually becomes aggregated which can be quantified by a spectrophotometric measurement at 680 nm. Both LDL and oxLDL were filtered through a 0.22 μm membrane filter before analysis. At 0.5 mg/ml, the oxLDL was approximately 7 -fold more aggregated than the native LDL.

Table 5.1 Characteristics of native LDL and oxLDL.

Analysis	(n)	Native LDL	Oxidised LDL
TBARs	4	56 $\pm$ 10 nmol/mg	2925 $\pm$ 361 nmol/mg
Absolute mobility	3	9 mm	24 mm
Aggregation (680 nm)	4	0.003 $\pm$ 0.001	0.026 $\pm$ 0.009

Data for TBARs, absolute mobility and degree of aggregation of 0.5 mg/ml native LDL and oxLDL. OxLDL was prepared by incubation of LDL with 300-350 μM $CuCl_2$ for 24 hours. All results are shown as the means $\pm$ SD where. n represents the number of preparation of LDL. The same preparation of LDL was used to prepare oxidised LDL.

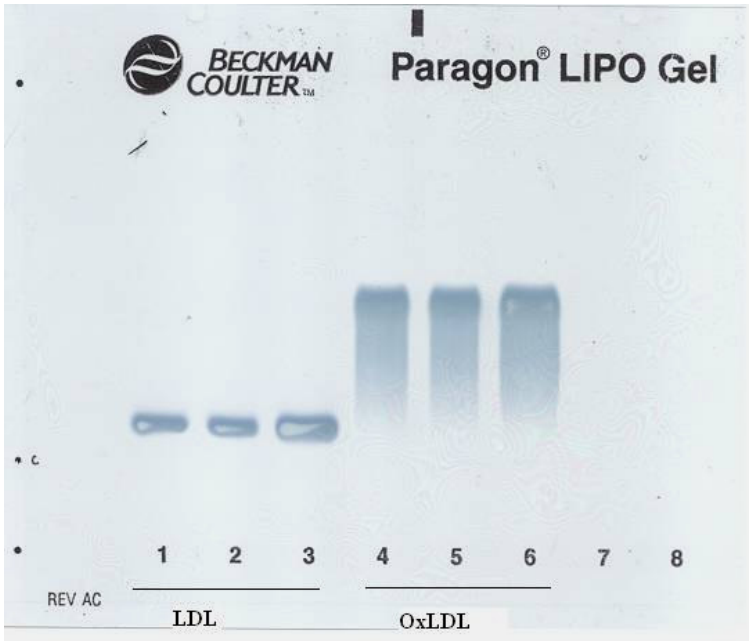

Figure 5.1 Lipoprotein gel of LDL and oxLDL.

Lanes 1 to 3 are native LDL and lanes 4-6 are LDL after incubation with 300-350 μM $CuCl_2$ for 24 hours.

5.2.1.2 Effect of OxLDL on HMDMs Viability Incubated in RPMI Containing 10% HIHS

All the experiments were conducted using HMDMs, which had been cultured for 14 days or longer since this was the period where more than 70% of the monocytes had differentiated into macrophages (Figure 3.3). Initial studies determined a suitable concentration of oxLDL that caused approximately 50% loss in the cell viability. HMDMs (5×10^6 cells/ml) in RPMI containing 10% HIHS were incubated for 48 hours with a range of oxLDL concentrations. Loss of HMDM viability was determined by MTT assay and the results were displayed as percentages of the control cells (no treatment). Figure 5.2 shows that oxLDL caused a concentration dependent loss in HMDMs viability. Incubation of HMDMs with 0.1 mg/ml of oxLDL did not cause a loss in their viability (Figure 5.2). A drastic 65% loss in cell viability was observed with 0.5 mg/ml oxLDL.

As 48 hours appeared to be a relatively long time to expose the cells to a toxic agent, the above experiment was repeated by incubating HMDMs with a range of oxLDL concentrations for 24 hours (Figure 5.3). In contrast to Figure 5.2, cell death reached approximately 50% with 1 mg/ml oxLDL (Figure 5.3a). Since 1 mg/ml oxLDL represented an approximately 50% viability loss, this was the concentration chosen in experiments examining the effect of 7,8-NP. This MTT assay result was reproducible

though there were a few exceptions when viability loss was as high as 60% or as low as 40% (data not shown). Figure 5.3 shows that the percentage of loss of HMDMs viability were not consistent between the MTT and the trypan blue assay. While the MTT assay showed 50% loss in HMDMs viability (Figure 5.3a), the trypan blue assay revealed only 30% loss in viability with 1 mg/ml oxLDL (Figure 5.3b). The explanation for this observation will be discussed further in section 5.3.1.2.

The effect of oxLDL on HMDMs was also monitored by observing HMDMs' morphology under the light microscope. The control cells showed classic macrophage morphology of large, poached egg-like cells (Figure 5.4a). After 24 hours incubation with 1 mg/ml oxLDL, some of the HMDMs (Figure 5.3b) became enlarge and had a dendritic-like appearance. Some other cells appeared shrunk and formed blebs. With 2 mg/ml oxLDL, damage to HMDMs was apparent with the loss of cellular contents, appearance of shrunken cells, disruption of cellular membranes and presence of cellular debris (Figure 5.2c). A significant number of detached cellular clumps floating in the media was also observed. These cellular morphologies appeared to be characteristic of both apoptotic and necrotic cell death.

A time course of oxLDL-mediated damage was conducted by incubating HMDMs in RPMI containing 10% HIHS with 1 mg/ml oxLDL for 24 hours. Cell death appeared to be initiated slowly in HMDMs with a small insignificant drop in cell viability after 3 hours (Figure 5.5). The HMDMs viability continued to decline by a slow 15% over the first 12 hours but then dropped by further 35% over the following 12 hours.

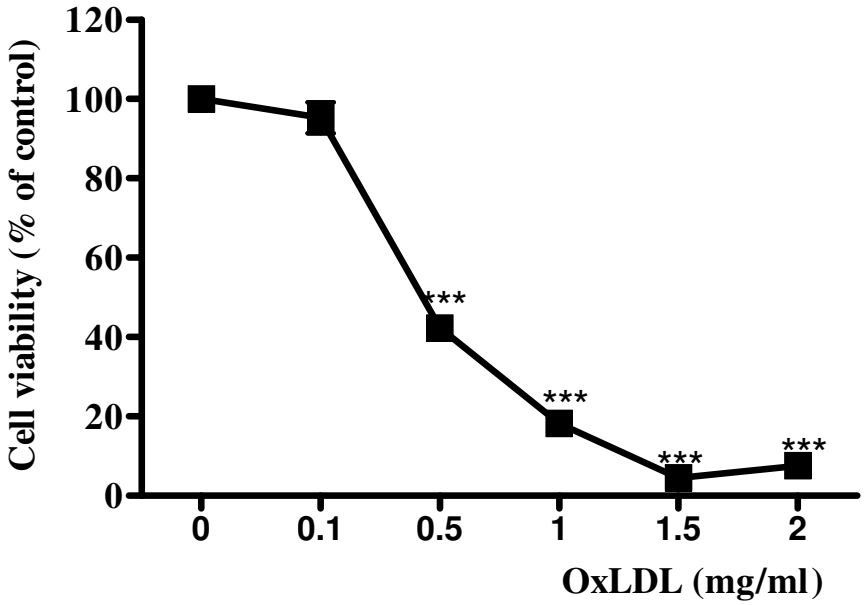

Figure 5.2 Loss of HMDM viability after 48 h incubation with increasing concentrations of oxLDL.

HMDMs ($5x10^6$ cells/ml) were incubated at 37 °C in RPMI containing 10% HIHS with increasing concentrations of oxLDL. After 48 hours, HMDMs were analysed for cell viability via MTT assay. Significance is indicated from 0 mg/ml oxLDL (control). Results are displayed as mean ± SD of triplicates from a single experiment, representative of three separate experiments.

(a)

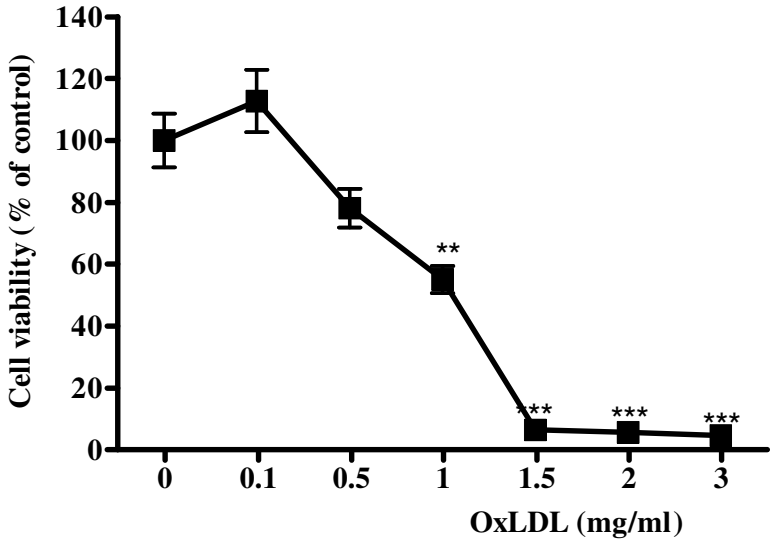

(b)

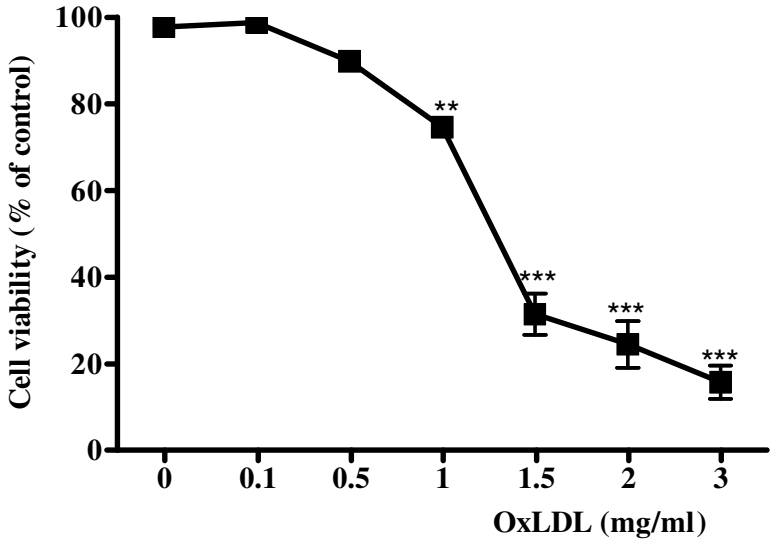

Figure 5.3 Loss of HMDM viability after 24 h incubation with increasing concentrations of oxLDL.

HMDMs ($5x10^6$ cells/ml) were incubated at 37 °C in RPMI containing 10% HIHS with increasing concentrations of oxLDL. After 24 hours, HMDMs were analysed for cell viability via (a) MTT and (b) trypan blue exclusion staining. Significance is indicated from 0 mg/ml oxLDL (control). Results are displayed as mean ± SD of triplicates from a single experiment, representative of three separate experiments.

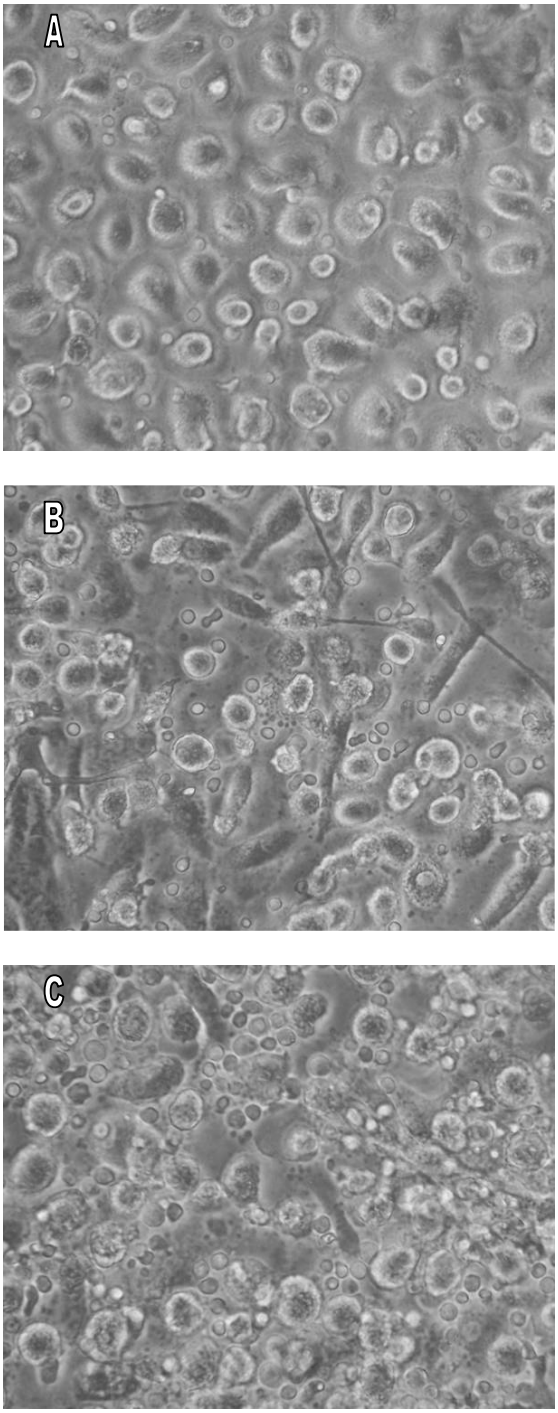

Figure 5.4 Morphological changes in cell appearance after 24 h incubation with varying concentrations of oxLDL.
HMDMs ($5x10^6$ cells/ml) were incubated at 37 °C in RPMI containing 10% HIHS with increasing concentrations of oxLDL. After 24 h, cells were viewed in situ in tissue culture wells using an inverted microscope, (A) control no oxLDL, (B) 1 mg/ml oxLDL, and (C) 2 mg/ml oxLDL. Original magnification was 40x and the picture was taken using a digital camera.

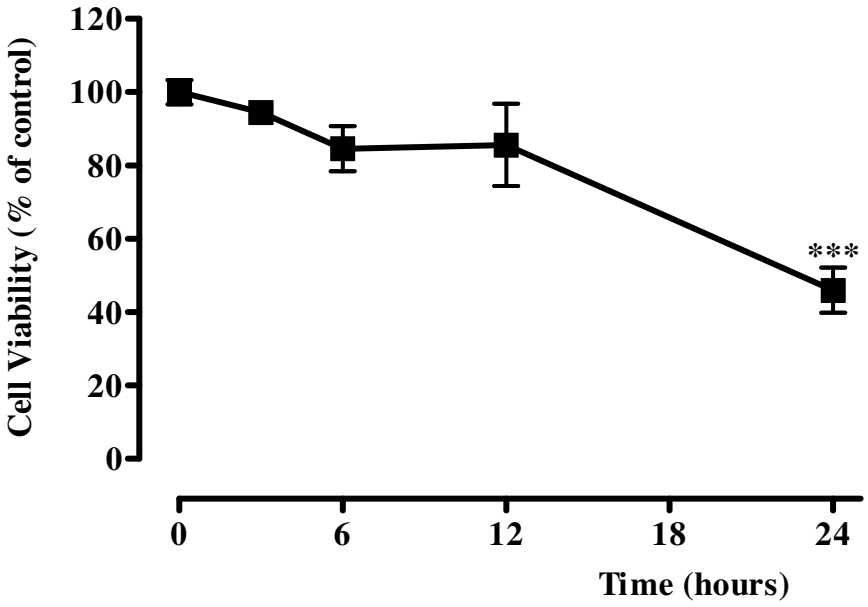

Figure 5.5 Time course of oxLDL-induced cell viability loss in HMDMs.
HMDMs ($5x10^6$ cells/ml) were incubated at 37 °C in RPMI containing 10% HIHS with 1 mg/ml of oxLDL. At various times, HMDMs were analysed for cell viability by MTT assay with data expressed as a percentage of zero hour levels (control). Significance is indicated from time zero. Results are displayed as mean ± SD of triplicates from a single experiment, representative of three separate experiments.

5.2.1.3 Effect of OxLDL on the Intracellular Glutathione Levels of HMDMs

Cellular glutathione is a very potent antioxidant and can efficiently neutralise reactive oxygen species. Analysis of the effect of oxLDL on the intracellular glutathione level of HMDMs was studied by incubating HMDMs with increasing oxLDL concentrations for 24 hours. Control HMDMs contained approximately 217 μmol/mg of cell protein glutathione and this level was reduced by 30% after exposure to 0.1 mg/ml oxLDL (Figure 5.6). As observed for the cell viability studies, 0.1 mg/ml of oxLDL concentration did not affect the cell viability, but it was potent enough to disrupt the intracellular glutathione level. Incubation with 0.5 mg/ml oxLDL caused approximately 50% loss in the glutathione level of HMDMs. Above 2 mg/ml of oxLDL, the intracellular glutathione was totally lost since no peak was detected on the HPLC chromatogram. Similar to MTT assay, the glutathione results were reproducible although sometimes inter-experimental variation did account for a few exceptions when glutathione loss was as great as 65% or as low as 40% (data not shown) with 1 mg/ml oxLDL treatment.

The intracellular glutathione loss in HMDMs over time was examined by incubating HMDMs with 1 mg/ml oxLDL for 24 hours. In contrast with the cell viability

studies, the glutathione loss was very rapid with 20% reduction after 3 hours (Figure 5.7). After 24 hours, the glutathione level was reduced by 60%.

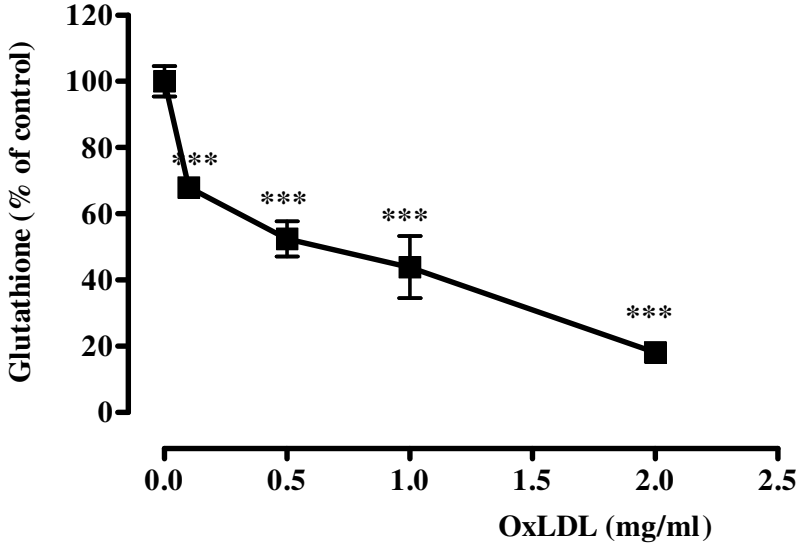

Figure 5.6 Loss of HMDM glutathione after 24 h incubation with increasing concentrations of oxLDL.
HMDMs ($5x10^6$ cells/ml) were incubated at 37 °C in RPMI containing 10% HIHS with increasing concentrations of oxLDL. After 24 hours, the glutathione levels of HMDMs were analysed using HPLC analysis. Data were expressed as a percentage of zero hour levels (control). Significance is indicated from 0 mg/ml oxLDL (control). Results are displayed as mean ± SD of triplicates from a single experiment.

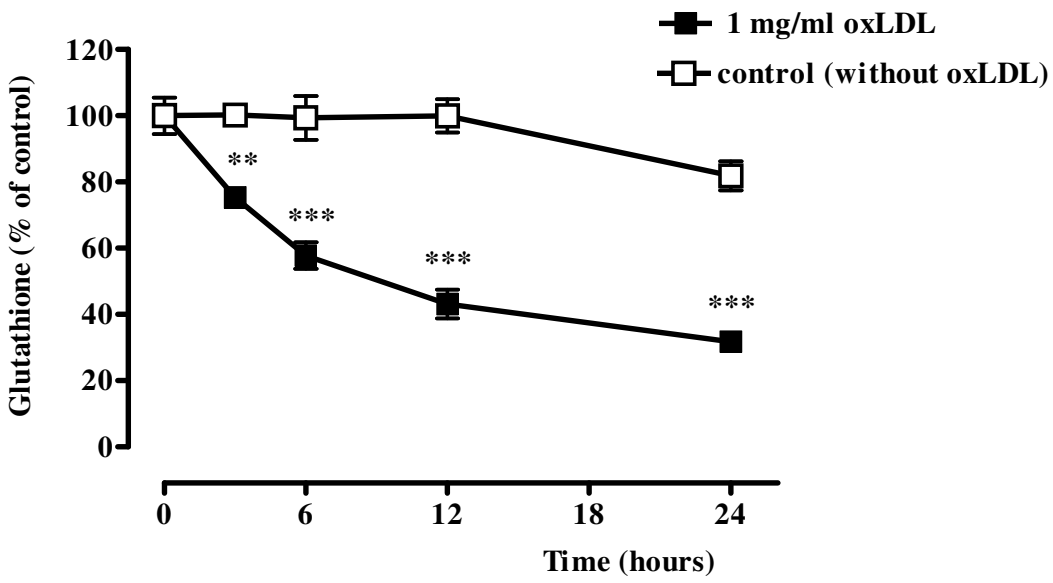

Figure 5.7 Time course of oxLDL-induced glutathione loss in HMDMs.
HMDMs ($5x10^6$ cells/ml) were incubated at 37 °C in RPMI containing 10% HIHS with 1 mg/ml of oxLDL. At various times, the glutathione levels of HMDMs were analysed by HPLC analysis. Data were expressed as a percentage of zero hour levels (control). Significance is indicated from time zero. Results are displayed as mean ± SD of triplicates from a single experiment, representative of three separate experiments.

5.2.1.4 Uptake of DiI-LDL and DiI-oxLDL by HMDMs

The uptake of LDL and oxLDL to HMDMs was measured by incubating HMDMs with 1 mg/ml LDL or oxLDL which had been labelled with fluorescent DiI at 37 °C in RPMI containing 10% HIHS over 24 hours. Figure 5.8 shows a very sharp increase in the uptake of DiI-LDL with HMDMs in the first 3 hours followed by a gradual increase until 12 hours. Then the association increased sharply again up to 24 hours.

In contrast, the uptake of DiI-oxLDL (Figure 5.9) increased sharply between 6 and 12 hours. After 12 hours the rate of uptake levelled off and there was no significant increase in uptake after 12 hours. This result agreed with HMDMs' viability over 24 hours incubation with 1 mg/ml oxLDL (Figure 5.5) where the viability declined sharply after 12 hours. Twelve hours was also the time at which the oxLDL had caused almost maximum amount of glutathione loss (Figure 5.7). Commitment to cell death might have occurred by this point.

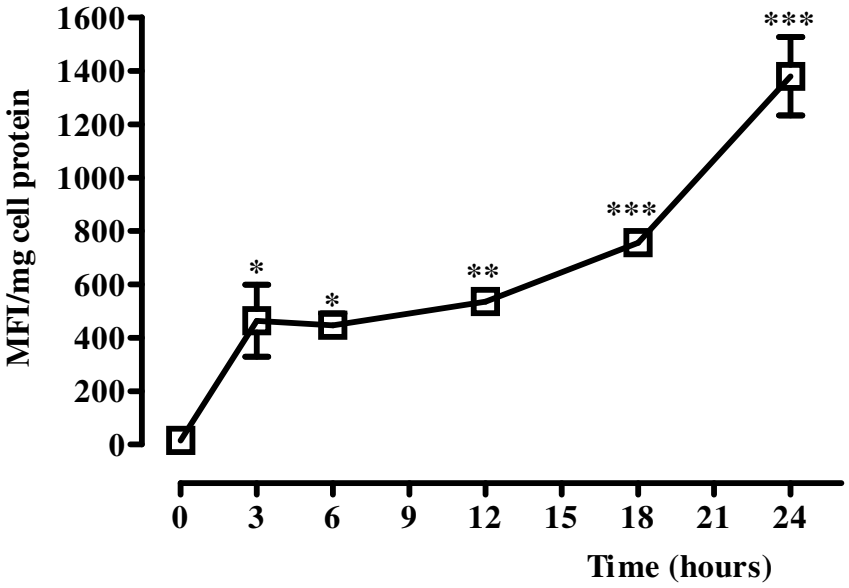

Figure 5.8 Time course of DiI-LDL uptake with HMDMs.
HMDMs ($5x10^6$ cells/ml) were incubated at 37 °C (to measure cell association) in RPMI containing 10% HIHS with 1 mg/ml DiI-LDL. At various times, the cells were harvested and the fluorescence intensity of DiI was measured as mentioned in the materials and methods. Significance is indicated from time zero. Each value shown is the mean $\pm$ SD of triplicates.

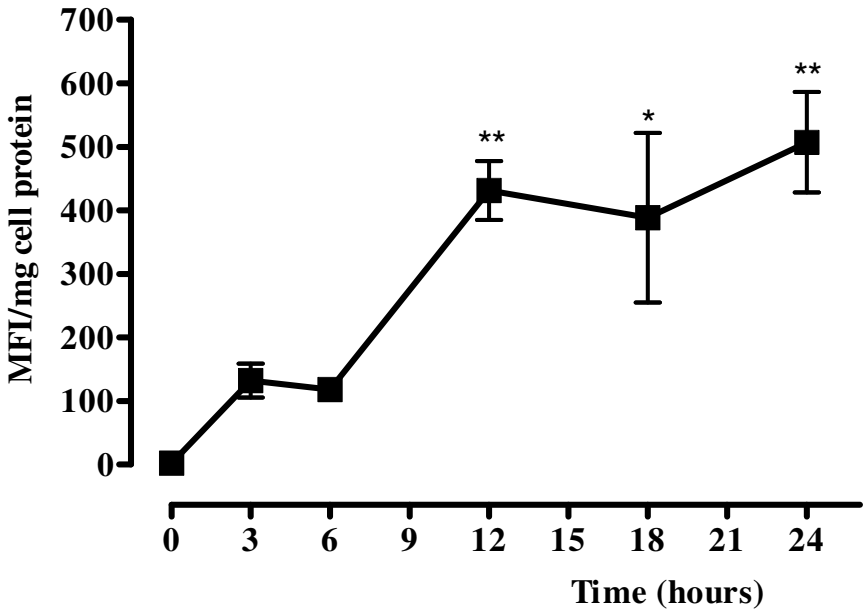

Figure 5.9 Time course of DiI-oxLDL uptake with HMDMs.
HMDMs ($5x10^6$ cells/ml) were incubated at 37 °C (to measure cell association) in RPMI containing 10% HIHS with 1 mg/ml DiI-oxLDL. At various times, the cells were harvested and the fluorescence intensity of DiI was measured as mentioned in the materials and methods. Significance is indicated from time zero. Each value shown is the mean ± SD of triplicates.

5.2.1.5 Effect of OxLDL on Generation of Reactive Oxygen Species by HMDMs

Reactive oxygen species (ROS) are important regulators of apoptosis. OxLDL has been reported to induce cellular apoptosis in a mechanism dependent upon ROS generation in vascular smooth muscle cells (Hsieh *et al*., 2001) and endothelial cells (Zmijewski *et al*., 2005a). The mitochondria has been suggested to be the main site of ROS production (Fleury *et al*., 2002). In this study the effect of oxLDL on the generation of ROS in the mitochondria was investigated by using dihydroethidium (DHE) staining. DHE is oxidised to ethidium fluorescent product by superoxide but to a much lower extent by hydrogen peroxide. The change of DHE fluorescence of living cells allows quantitation of intracellular ROS mainly superoxide ($O_2^{\bullet -}$).

A time-dependent increase in ROS generation was revealed when HMDMs were exposed to 1 mg/ml oxLDL (Figure 5.10) as reflected by increase in fluorescence intensity. The appearance of the DHE fluorescence after only 3 hours incubation with oxLDL implies that ROS generation induced by oxLDL is an early event in HMDMs. The ROS generation seems to reach maximum after 6 hours incubation.

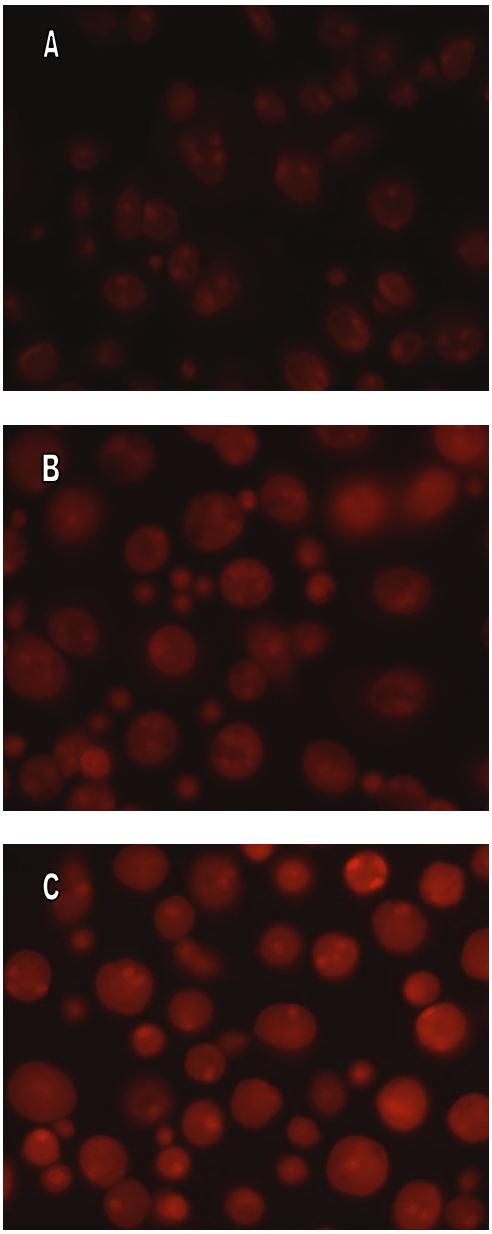

Figure 5.10 The effect of oxLDL on the generation of superoxide anion ($O_2^{\bullet-}$) in HMDM.

HMDM ($5x10^6$ cells/ml) were grown on coverslips in 6-well plate in RPMI containing 10% HIHS. Cells were incubated with 1 mg/ml oxLDL for 3 and 6 hours (B-C). Control (A) was cells without addition of oxLDL. The intracellular distribution of $O_2^{\bullet-}$ in the cells was detected by staining the cells with DHE staining.

5.2.1.6 Effect of OxLDL on Cytochrome *c* Release in HMDMs

Intracellular accumulation of ROS may perturb the cell's intracellular redox state and can cause the release of cytochrome *c* from the mitochondria into the cytoplasm (Chandra & Orennius, 2002). It may occur at the very early stage and therefore, an important trigger of apoptotic programme (Berridge *et al*., 1996)). Cytochrome *c* is required for the assembly of the apoptosome and hence, for the activation of the caspase cascade. It has also been shown that there was a time-dependent migration of cytochrome *c* from mitochondria to the cytoplasm then to the nucleus (Heinloth, *et al*., 2002).

In this study, immunofluorescence staining of HMDMs incubated with 1 mg/ml oxLDL for 12 hours showed a small increase in fluorescence intensity in both nuclei and the cytoplasm (Figure 5.11) when compared to control cells, suggesting the release of cytochrome *c* into the cytoplasm and translocation into the nuclei. The release of cytochrome *c* was much lower than expected.

Western Blot analysis of subcellular fractionation verified cytochrome *c* release induced by oxLDL as depicted in Figure 5.12. The cytochrome *c* band of 14 kDa was determined from the standard molecular weight marker and purified cytochrome *c* from bovine heart (gel not shown). The result showed that there was already a low rate of cytochrome *c* release under basal conditions (Figure 5.12, Lane 2). The presence of cytochrome *c* in the control cytosolic fractions were also detected by Heinloth *et al.,* (2002) and Walter *et al.,* (1998) indicating a variable amount of background apoptosis that led to cytochrome *c* release under cell culture conditions. This may also be an artefact of the subcellular fractionation procedure. The release of cytochrome *c* observed after 3 hours incubation with oxLDL was not different from that of control indicating that cytochrome *c* released at that time was not induced by oxLDL. Only after 6 hours incubation, anincrease in cytochrome *c* was clearly seen. Figure 5.13 shows a similar experiment with 12 hours incubation time of HMDMs with oxLDL. In this experiment, no cytochrome *c* was detected in the cytosol of control cells but very clear distinct band of cytosolic cytochrome *c* band from HMDMs treated with oxLDL was observed. The effect of 7,8-NP on cytochrome *c* release induced by oxLDL will be discussed in section 5.2.2.3.

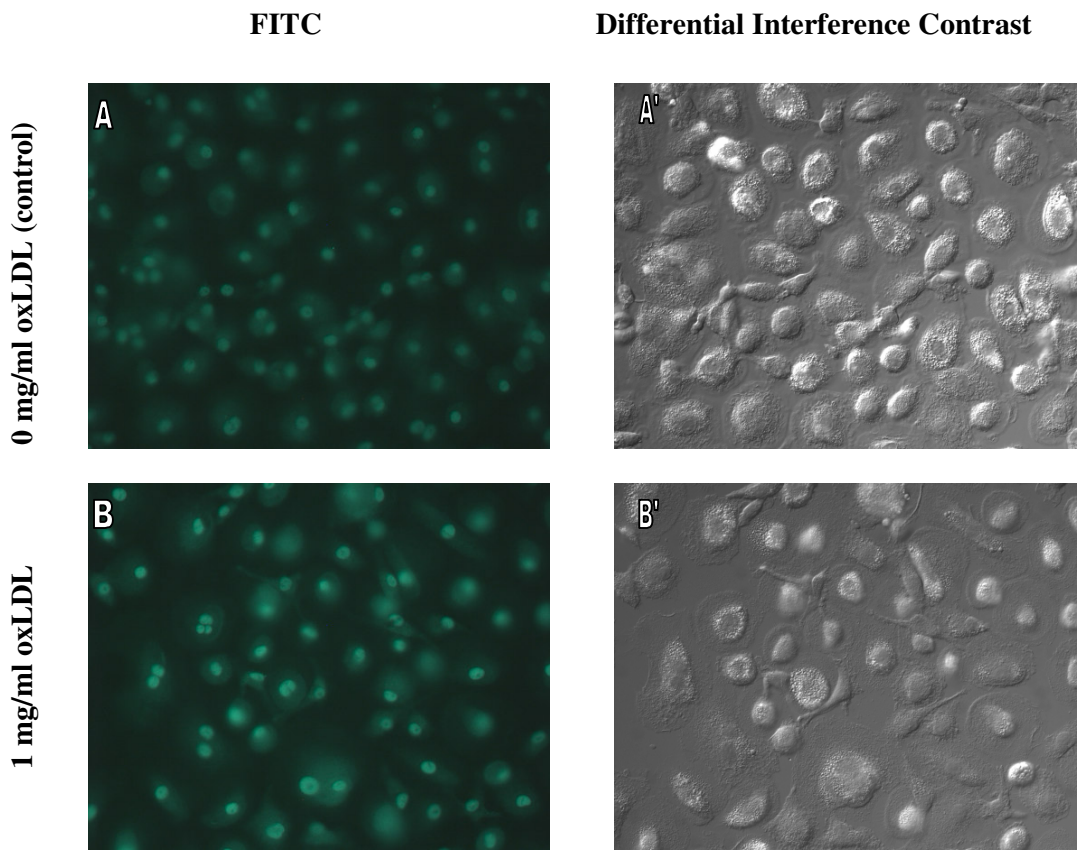

Figure 5.11 The effect of oxLDL on the cytochrome *c* release in HMDMs.
HMDM ($5x10^6$ cells/ml) were grown on coverslips in 6-well plate in RPMI containing 10% HIHS. Cells were incubated with 1 mg/ml oxLDL for 12 hours (B). The cytochrome *c* release in the cells was detected with anti-cytochrome *c* antibodies using fluorescence microscope. A' and B' represent differential interference contrast of A and B respectively.

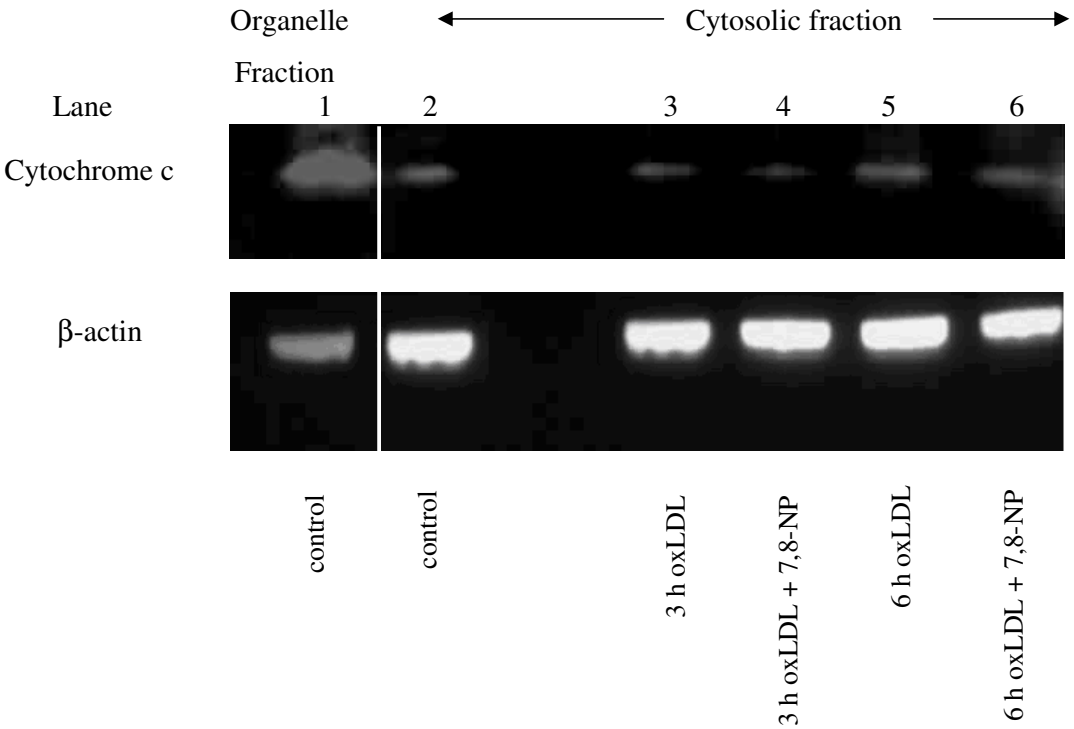

Figure 5.12 Effect of 7,8-NP on cytochrome *c* release induced by oxLDL, 0-6 hours.
HMDMs ($5x10^6$ cells/ml) were incubated at 37 °C in RPMI containing 10% HIHS and 1 mg/ml of oxLDL with and without 200 μM 7,8-NP for 3 and 6 hours. 30 μg proteins of the organelle fraction and 40 μg of the cytosolic fraction were loaded onto an SDS-PAGE. The presence of cytochrome *c* release was detected by Western Blot . β-actin was used as a control loading. Data are representative of three separate experiments.

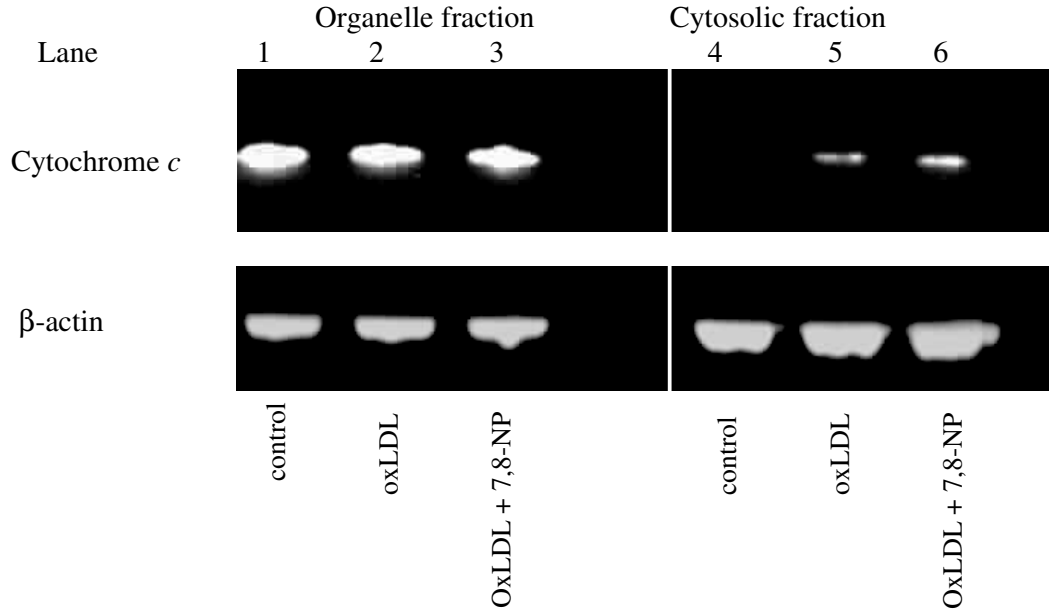

Figure 5.13 Effect of 7,8-NP on cytochrome *c* release induced by OxLDL after 12 hrs.
HMDMs ($5x10^6$ cells/ml) were incubated at 37 °C in RPMI containing 10% HIHS and 1 mg/ml of oxLDL with and without 200 μM 7,8-NP for 12 hours. 30 μg proteins of the organelle fraction and 40 μg of the cytosolic fraction were loaded onto an SDS-PAGE. The presence of cytochrome *c* release was detected by Western Blot. β-actin was used as a control loading. Data are representative of three separate experiments.

5.2.1.7 Effect of OxLDL on Caspase-3 Activation

Treatment of HMDMs with oxLDL caused the cells to have apoptotic and necrotic appearances (Figure 5.4). Caspase activation is believed to have a pivotal role in the regulation of apoptosis and it had been shown to play a critical role in apoptosis of vascular cells in atherosclerotic plaque and in cultured vascular cells (Geng *et al*., 1995; Grutter, 2000; Kroemer & Martin, 2005). Since caspase-3 is an effector caspase involved in activation of a large number of apoptotic processes within the cells (Geng *et al*., 1995), its activation induced by oxLDL was therefore determined using Western Blot analysis. On activation, proteolytic cleavage of procaspase-3 (32 kDa) releases two subunits as the active form (17 kDa or 20 kDa).

The incubation times of 12 and 24 hours; and oxLDL concentrations 1 and 2 mg/ml were chosen because these were the conditions that were found earlier to cause the appearance of apoptosis and or necrosis in the cells. Figure 5.14 shows that incubation of HMDMs with 1 and 2 mg/ml oxLDL for 12 and 24 hours did not show a cleavage of 32 kDa procaspase-3 into the p20 or p17 fragment of caspase–3. The result suggests that under the conditions in this study, caspase-3 was not activated. There seemed to be a small time dependent decrease in the 32 kDa band size of procaspase-3 of the treated samples (Lane 2-5, Figure 5.14) in comparison to control (Lane 1, Figure 5.14). It is unlikely that this is due to unequal loading of samples since the protein concentration were predetermined. The similar size of β-actin bands confirm equal loading of samples onto the gel. This raises the possibility that the procaspase-3 had been cleaved to some smaller products and this occurred in a time and concentration dependent manner.

5.2.1.8 Effect of OxLDL on HMDMs Phosphatidylserine Exposure

Cells lose their phospholipid membrane asymmetry and expose PS at the cell surface while maintaining their plasma membrane integrity intact, early during the process of apoptosis (van Engeland, *et al*., 1996). PS externalisation functions as part of the recognition process for phagocytes, which clear away apoptotic cells before they reach the pro-inflammatory stage of secondary necrosis (Carpenter *et al*., 1994). PS exposure as a result of incubation with oxLDL has been found in Jurkat T cells (Alcouffe *et al*., 1999), THP-1 monocytes (Baird *et al*., 2004; Vicca *et al*., 2000), U937 cells (Baird *et al*., 2004) and human vascular muscle cells (Siow *et al*., 1999). Annexin-V was shown to interact strongly and specifically with PS and can be used to detect apoptosis by targeting for the loss of plasma membrane asymmetry (van Engeland, *et al*., 1996).

The time course of the effect of oxLDL on the exposure of PS by HMDMs was explored by incubating HMDMs with 1 mg/ml oxLDL. The immunofluorescence staining demonstrated that oxLDL increased the exposure of PS in a time dependent manner (Figure 5.15). The exposure of PS was detected as early as 3 hours incubation but only after 6 hours that a significant number of cells having PS became very obvious. The number of cells having PS exposure was maximal after 12 hours incubation with oxLDL. This suggests that most of the cells were committed to apoptotic death at this stage. The differential interference contrast image also shows that after 12 hours incubation the cells appear smaller (possibly due to cells' shrinkage) than control cells. This data is in agreement with the viability time course study where a sudden drop in viability was observed after 12 hours incubation with oxLDL.

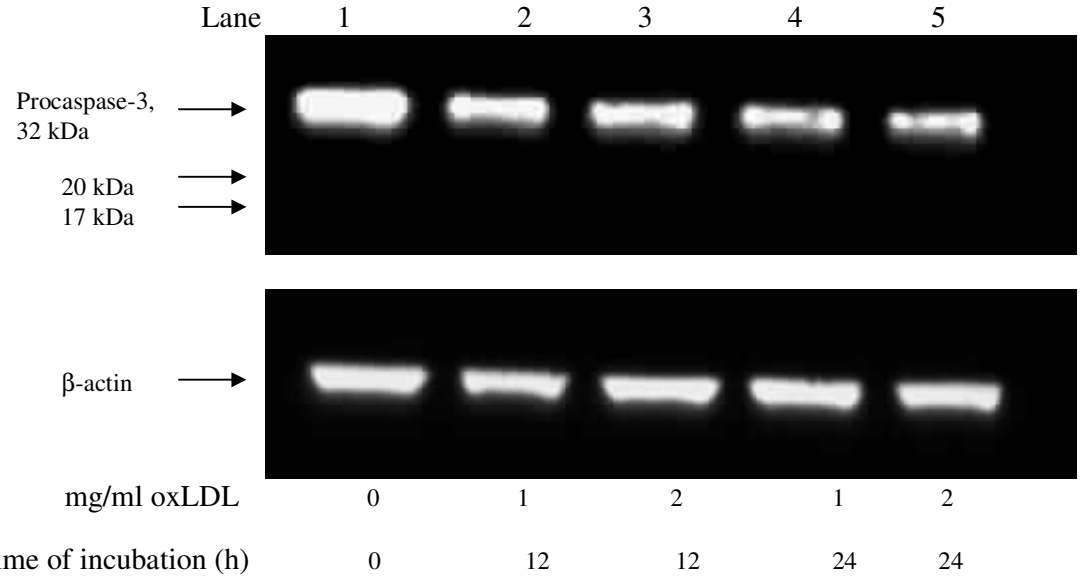

Figure 5.14 OxLDL does not induce caspase-3 activation.
HMDMs ($5x10^6$ cells/ml) were incubated at 37 °C in RPMI containing 10% HIHS and 1 or 2 mg/ml of oxLDL for 12 and 24 hours. 40 μg proteins of the total cell lysate were loaded onto an SDS-PAGE. The presence of caspase-3 (17 kDa) and procaspase-3 (32 kDa) was detected by Western Blot. β-actin was used as a control loading. Data are representatives of three independent experiments.

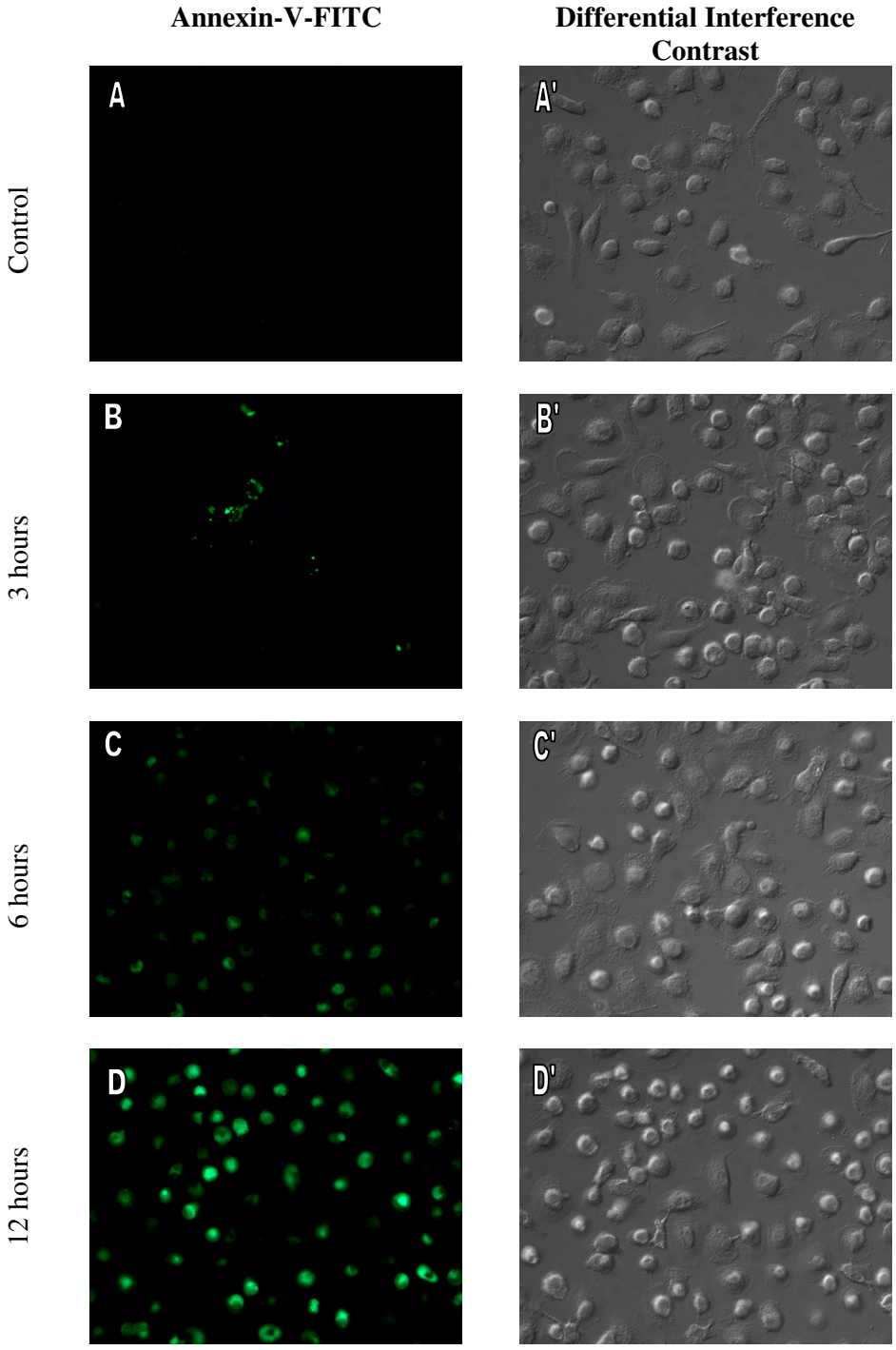

Figure 5.15 OxLDL induces phosphatidylserine exposure in HMDM in a time-dependent manner.

HMDM ($5x10^6$ cells/ml) were grown on coverslip in 6-well plate in RPMI containing 10% HIHS. After 14 days, cells were incubated with 1 mg/ml oxLDL for 3, 6 and 12 hours (B-D). Apoptotic cells were identified by immunofluorescence staining of phosphatidylserine with Annexin-FITC and viewed with 40x magnification under fluorescence microscope. A', B', C' and D' represent differential interference contrast correlates of A, B, C and D respectively. Data are representatives of three independent experiments.

5.2.2 7,8-Dihydroneopterin Effects on OxLDL-induced Damage on HMDMs

5.2.2.1 7,8-Dihydroneopterin Inhibits OxLDL-induced Loss of Cell Viability and Intracellular Glutathione in HMDMs

Gieseg and Cato (2003) noted that protection against cell-mediated LDL oxidation was maximum only when 7,8-NP was preincubated with the THP-1 adherent cells for 5 minutes. This was in agreement with Duggan, *et al.* (2002) that 10 minute pre-incubation of cells with 7,8-NP was necessary for 7,8-NP to give maximum protective effect on U937 cells against 2,2'-azobis (2-amidino propane) dihydrochloride (AAPH) peroxyl radicals. Consequently, a ten minute pre-incubation of HMDMs with 7,8-NP in RPMI containing 10% HIHS was performed in this study, before addition of oxLDL.

The potential antioxidant effect of 7,8-NP was studied by pre-incubating the HMDMs for ten minutes in RPMI containing 10% HIHS with various concentrations of 7,8-NP. OxLDL (1 mg/ml) was subsequently added and HMDMs were incubated for 24 hours before analysing the effect of 7,8-NP on the viability and intracellular levels of glutathione. The addition of 7,8-NP gave a concentration dependent protection on the HMDMs viability loss (Figure 5.16). A maximum protection was established with 100 of μM 7,8-NP, reducing the cell viability loss from 60% to 20% as compared to control. The presence of 7,8-NP alone, up to a concentration of 400 μM did not affect the HMDMs viability (Figure 5.17).

Incubation of 1 mg/ml oxLDL caused a 60% loss in the intracellular level of glutathione (Figure 5.18). 7,8-NP gave a concentration dependent protection against the intracellular glutathione loss, following the pattern of 7,8-NP protection against the cell viability loss. The maximum protection was given by 200 μM of 7,8-NP, reducing the glutathione loss to 30%. Surprisingly, 400 μM 7,8-NP did not further increase its protective effect (data not shown). Moreover, in agreement with the cell viability studies, the presence of 7,8-NP alone up to 400 μM did not significantly affect the HMDMs glutathione level (Figure 5.19). The difference in intracellular glutathione level when 100 or 200 μM of 7,8-NP were present seemed to be sufficient to diminish oxLDL-induced cytotoxicity by 40% (Figure 5.16) suggesting that GSH depletion is involved in oxLDL induced macrophage death.

Since 7,8-NP concentrations ranging from 100 to 400 μM exhibited a similar protection against cell death and 200 μM of 7,8-NP gave a maximum protection on

intracellular glutathione loss, therefore, 200 μM of 7,8-NP was used for subsequent experiments in testing the protective effect of 7,8-NP on HMDMs against oxLDL-induced damage.

The protective effect of the oxidised form of 7,8-NP, neopterin, on oxLDL-induced glutathione loss was also explored since some literatures had reported that neopterin could be a pro- or antioxidants. Co-incubation of HMDM with 1 mg/ml oxLDL and neopterin up to 200 μM did not provide any protective effect against the intracellular glutathione loss (Figure 5.20). Moreover, the concentrations of neopterin used in this study did not further enhance the toxicity of oxLDL.

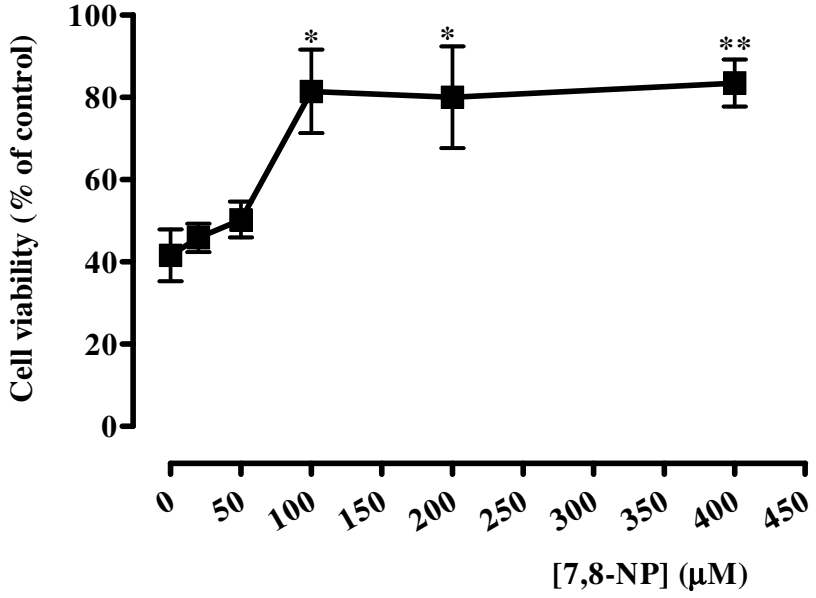

Figure 5.16 Effect of 7,8-NP on HMDM viability loss in the presence of 1 mg/ml oxLDL.

HMDMs ($5x10^6$ cells/ml) were incubated at 37 °C in RPMI containing 10% HIHS with 1 mg/ml oxLDL and increasing concentrations of 7,8-NP. Controls were conducted in the absence of oxLDL and 7,8-NP. After 24 hours, HMDMs were analysed for cell viability via MTT assay. Significance is indicated from 0 μM 7,8-NP (control). Results are displayed as mean ± SD of triplicates from a single experiment, representative of three separate experiments.

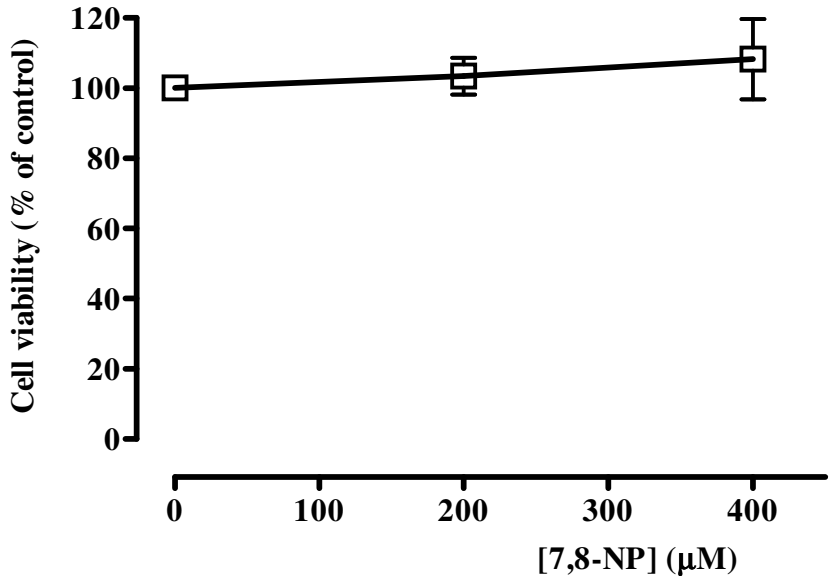

Figure 5.17 Effect of 7,8-NP on HMDM viability loss.
HMDMs ($5x10^6$ cells/ml) were incubated at 37 °C in RPMI containing 10% HIHS with increasing concentrations of 7,8-NP. Controls were conducted in the absence of 7,8-NP. After 24 hours, HMDMs were analysed for cell viability via MTT assay. Significance is indicated from 0 μM 7,8-NP. Each value shown is the mean ± SD of triplicates.

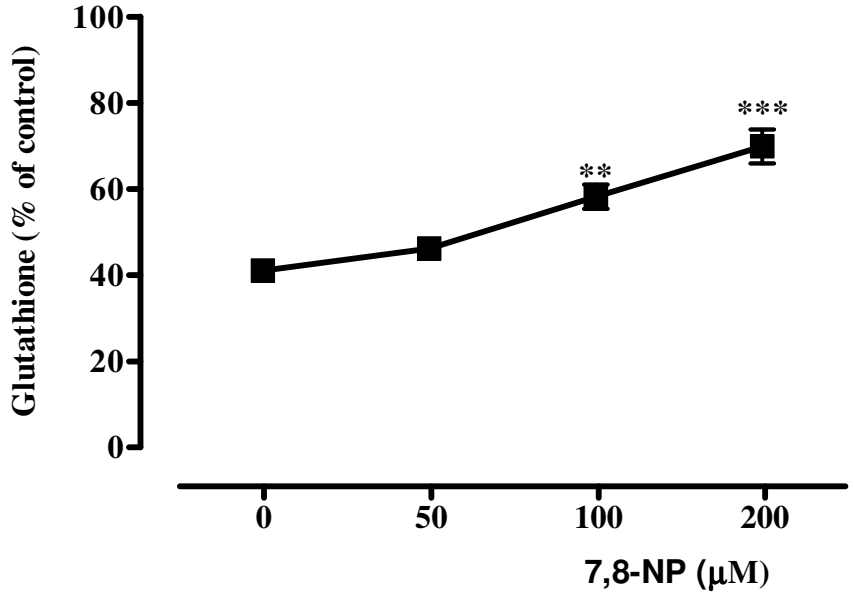

Figure 5.18 Effect of 7,8-NP on glutathione loss in the presence of 1 mg/ml oxLDL.
HMDMs ($5x10^6$ cells/ml) were incubated at 37 °C in RPMI containing 10% HIHS with 1 mg/ml oxLDL and increasing concentrations of 7,8-NP. Controls were conducted in the absence of oxLDL and 7,8-NP. After 24 hours the glutathione levels of HMDMs were analysed by HPLC analysis. Data were expressed as a percentage of control. Significance is indicated from 0 μM 7,8-NP. Results are displayed as mean ± SD of triplicates from a single experiment, representative of three separate experiments.

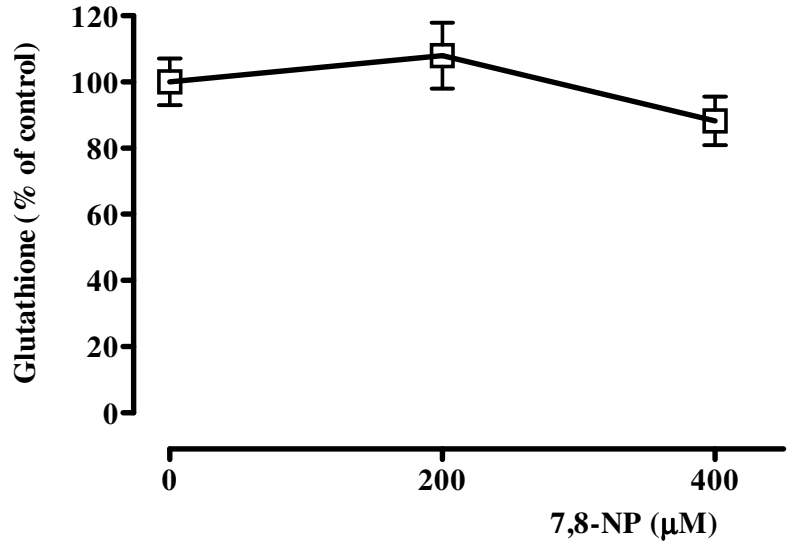

Figure 5.19 Effect of 7,8-NP on HMDM glutathione loss.
HMDMs ($5x10^6$ cells/ml) were incubated at 37 °C in RPMI containing 10% HIHS with increasing concentrations of 7,8-NP. Controls were conducted in the absence of 7,8-NP. After 24 hours the glutathione levels of HMDMs were analysed by HPLC analysis. Significance is indicated from 0 μM 7,8-NP. Each value shown is the mean ± SD of triplicates.

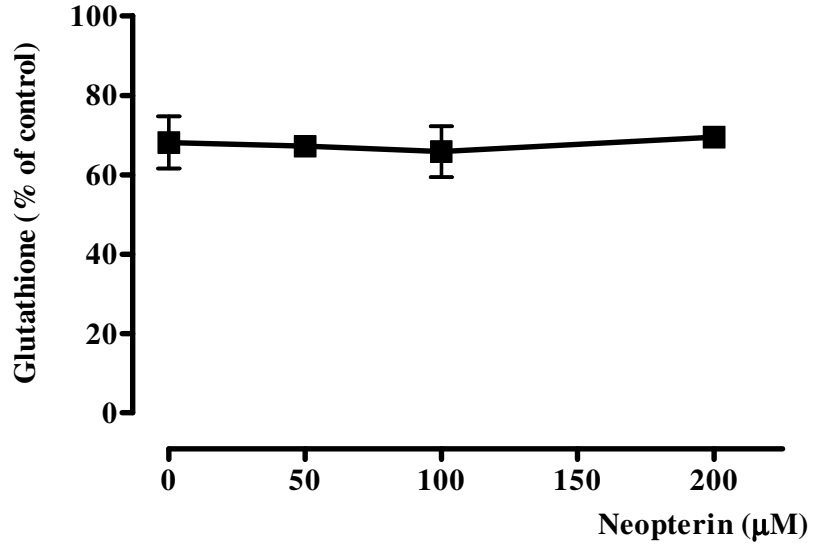

Figure 5.20 Effect of neopterin on glutathione loss in the presence of 1 mg/ml oxLDL.
HMDMs ($5x10^6$ cells/ml) were incubated at 37 °C in RPMI containing 10% HIHS with 1 mg/ml oxLDL and increasing concentrations of neopterin. Controls were conducted in the absence of oxLDL and neopterin. After 24 hours, the glutathione levels of HMDMs were analysed by HPLC analysis. Data were expressed as a percentage of control. ANOVA analysis revealed no statistical significance from 0 μM neopterin. Each value shown is the mean ± SD of triplicates.

5.2.2.2 Decreased in OxLDL-stimulated Reactive Oxygen Species Production of HMDMs with the Presence of 7,8-dihydroneopterin

There is a possibility that the protective effect of 7,8-NP on glutathione loss induced by oxLDL is due to 7,8-NP's ability to scavenge the ROS generated in the presence of oxLDL (Kappler *et al*., 2007). The inhibitive effect of 7,8-NP on the ROS generation induced by oxLDL was studied by incubating HMDMs with 1 mg/ml of oxLDL and 200 μM of 7,8-NP for 3 to 12 hours.

Figure 5.21 clearly shows that at 3 hours, the presence of 7,8-NP reduced the DHE fluorescence intensity. This suppressive effect of 7,8-NP could be seen up to 6 hours of incubation time. In a separate experiment, 7,8-NP was still able to suppress the DHE fluorescence intensity after 12 hours incubation with oxLDL (Figure 5.22). This result clearly indicates the role of 7,8-NP as radical scavenger. The data also suggests that 7,8-NP may be entering the cell to provide this apparent scavenging activity.

5.2.2.3 The Presence of 7,8-Dihydroneopterin Does Not Inhibit OxLDL-stimulated Cytochrome *c* Release from the Mitochondria of HMDMs

Mitochondrial-mediated ROS generation may promote or mediate the release of cytochrome *c* from mitochondria into the cytosol (Madesh & Hajnoczky, 2001; Petrosillo *et al*., 2003). Since 7,8-NP was able to scavenge the ROS, therefore, the effect of 7,8-NP on oxLDL-induced cytochrome *c* release in HMDMs was investigated. HMDMs were incubated with 1 mg/ml of oxLDL and 200 μM of 7,8-NP for 3 to 12 hours. Figure 5.12 (incubation up to 6 hours) shows that 7,8-NP clearly did not inhibit the release of cytochrome *c*. The 12 hours incubation (Figure 5.13) result also showed that 7,8-NP failed to inhibit the cytochrome *c* release from the mitochondria.

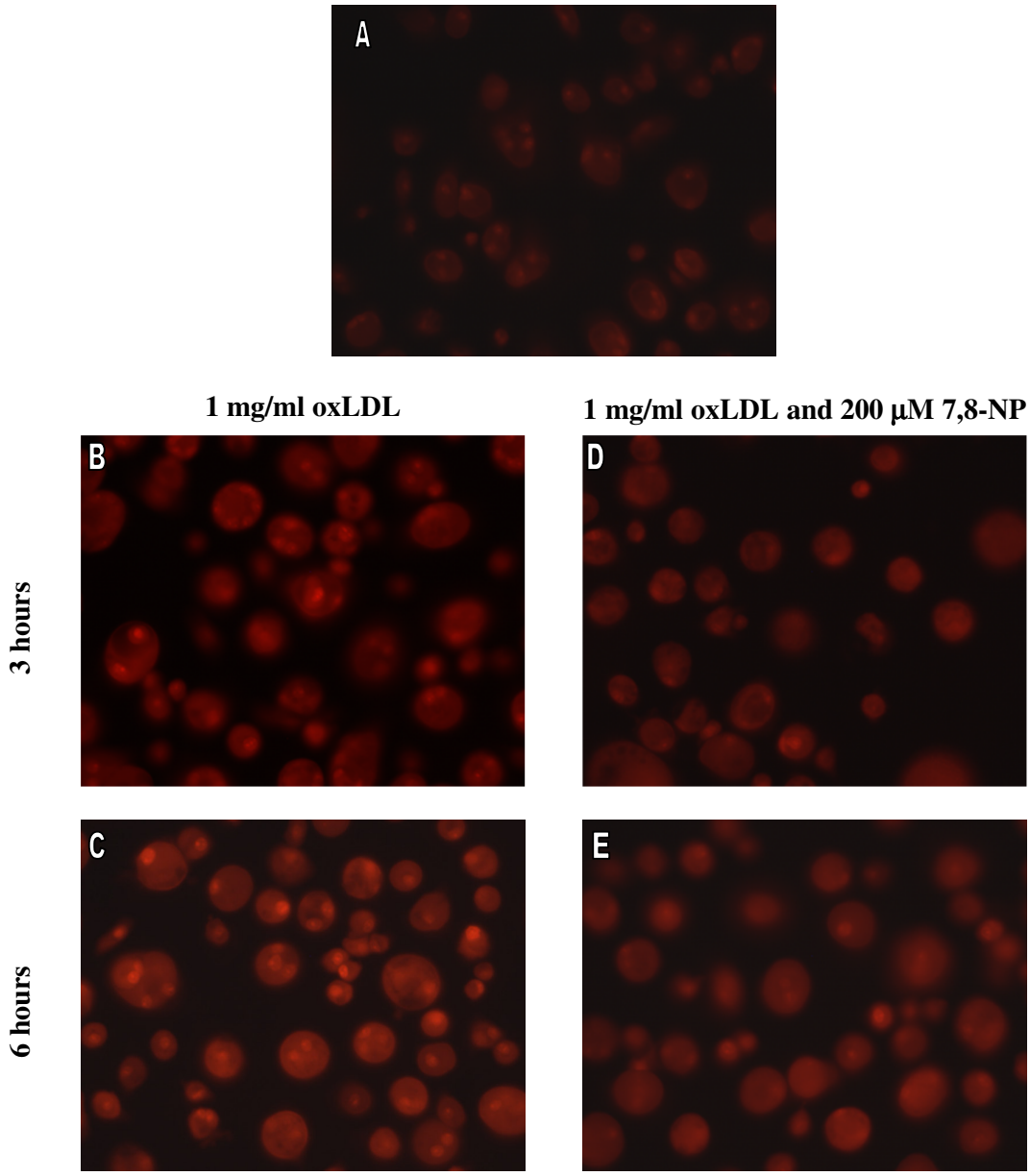

Figure 5.21 The effect of 7,8-NP and oxLDL on the ROS levels in HMDM.
HMDM ($5x10^6$ cells/ml) were grown on coverslips in 6-well plate in RPMI containing 10% HIHS. Cells were incubated with 1 mg/ml oxLDL (B-C) and 1 mg/ml oxLDL and 200 µM 7,8-NP (D-E) for 3 and 6 hours. The intracellular distribution of ROS in the cells was detected by staining the cells with DHE.

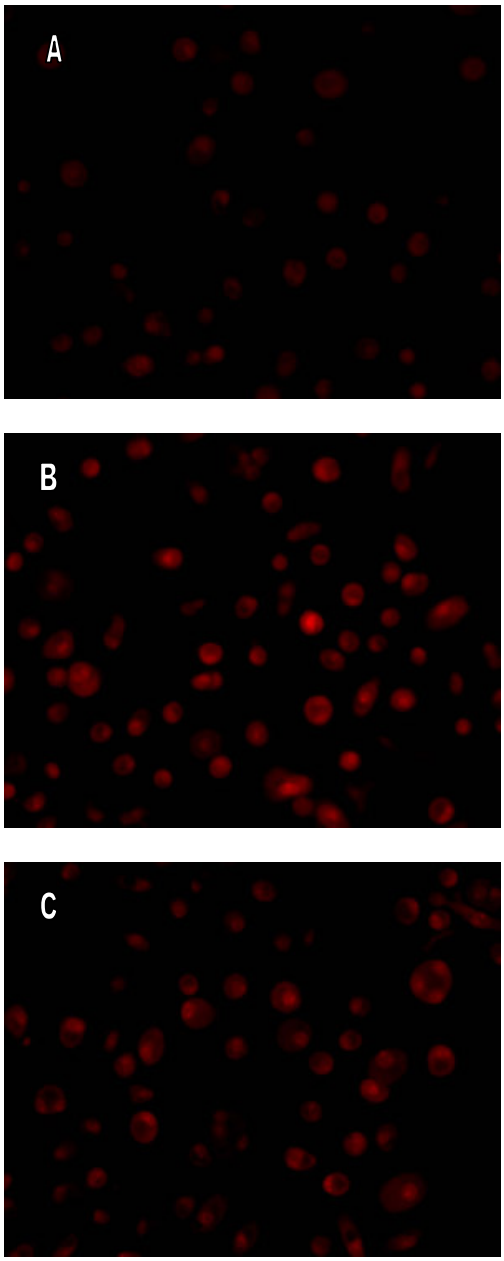

Figure 5.22 The effect of 7,8-NP and oxLDL on the superoxide anion ($O_2^{\bullet-}$) generation in HMDMs after 12 hours incubation.
HMDM ($5x10^6$ cells/ml) were grown on coverslips in 6-well plate in RPMI containing 10% HIHS. Cells were incubated with 1 mg/ml oxLDL (B) and 1 mg/ml oxLDL and 200 μM 7,8-NP (C) for 12 hours. Control (A) was cells without addition of oxLDL. The intracellular distribution of ROS in the cells was detected by staining the cells with DHE.

5.2.2.4 Decreased in OxLDL-stimulated Phosphatidylserine Exposure of HMDMs with the Presence of 7,8-dihydroneopterin

The 7,8-NP protective effect on the exposure of PS was first explored by incubating HMDMs with 1 mg/ml oxLDL up to 24 hours with 7,8-NP. Figure 5.23 shows that co-incubation with 7,8-NP at 100 and 200 μM (Figure 5.23c and d) did not reduce the number of HMDMs having PS exposure as compared to exposure to oxLDL alone (Figure 5.23b).

This experiment was repeated by incubating HMDMs with oxLDL and 7,8-NP for up to 12 hours. Figure 5.24 shows that 200 μM of 7,8-NP could delay the effect of 1 mg/ml of oxLDL. This result could suggest that the protective effect of 7,8-NP on oxLDL-induced damage can only be observed within certain time which agreed with Baird *et al* ., (2005). The greatest protective effect of 7,8-NP on HMDMs on PS exposure was seen by 6 hours incubation time even though the protective effect can still be seen up to 12 hours incubation with oxLDL. This clearly suggests that 7,8-NP can only slowing down the PS exposure over a 12 hour period.

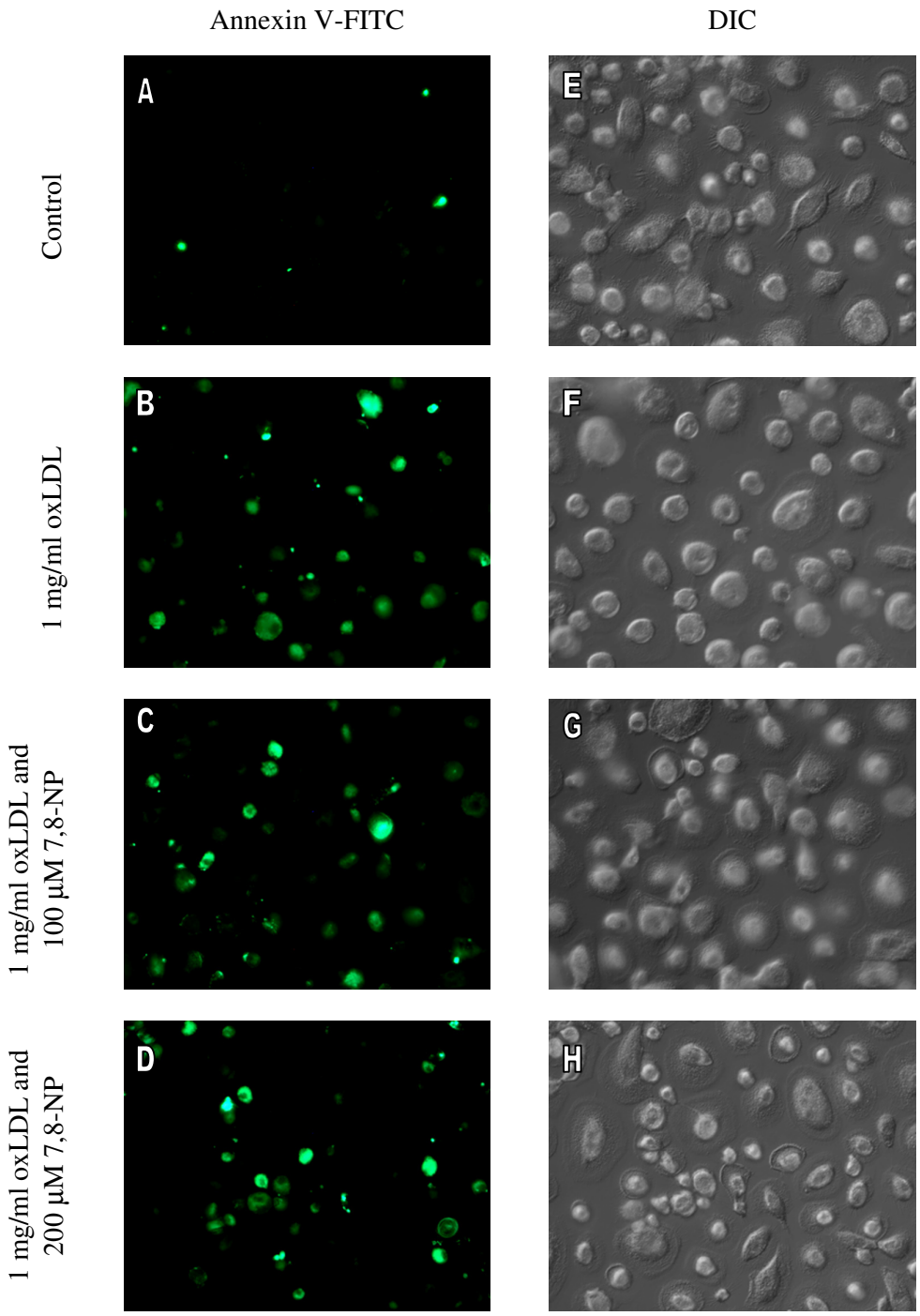

Figure 5.23 7,8-NP does not protect HMDM from oxLDL induced phosphatidylserine exposure after 24 h incubation.
HMDM ($5x10^6$ cells/ml) were grown on coverslips in 6-well plate in RPMI containing 10% HIHS. Cells were incubated with 1 mg/ml oxLDL in B, with 1 mg/ml oxLDL and 100µM 7,8-NP in C and 1 mg/ml oxLDL and 200µM 7,8-NP in D for 24 hours. Apoptotic cells were identified by immunofluorescence staining of phosphatidylserine with Annexin-FITC and viewed with 40x magnification under fluorescence microscope. Differential interference contrast (DIC) photos are shown in (E-H).

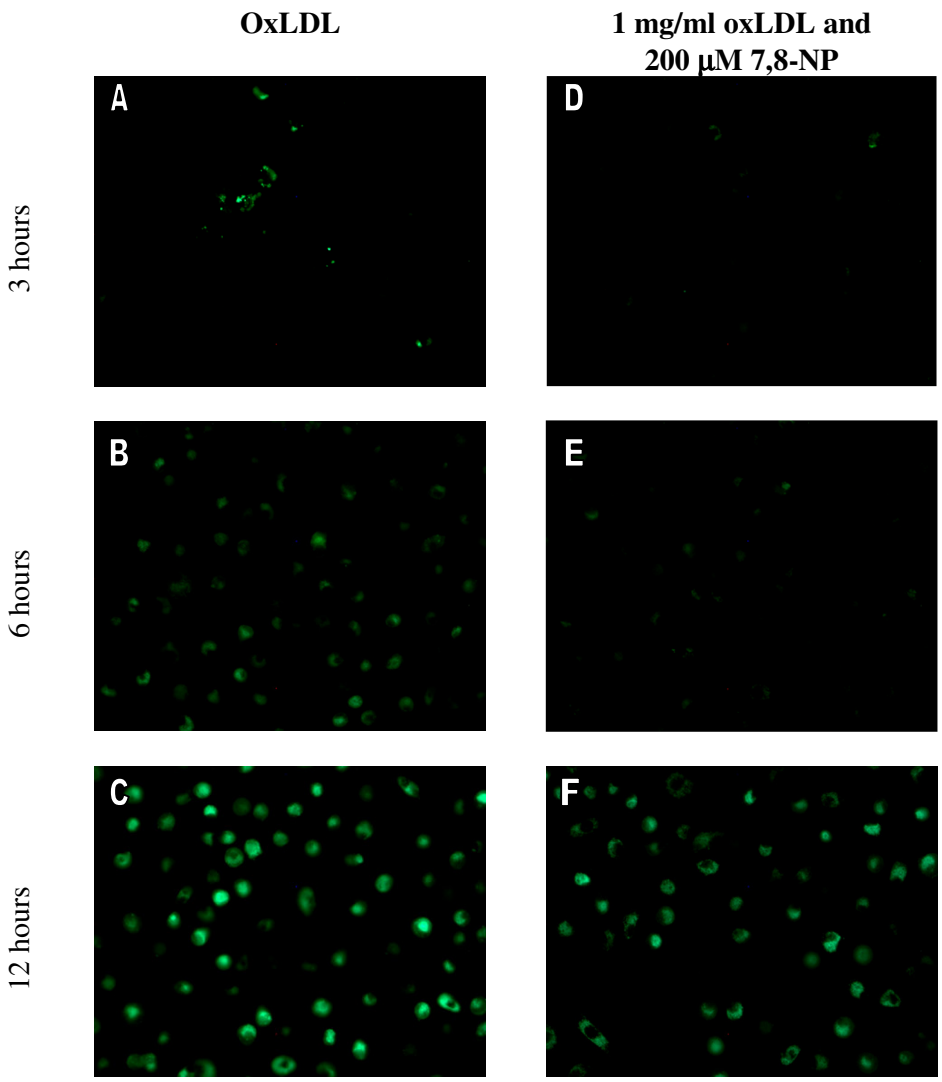

Figure 5.24 Phosphatidylserine exposure was reduced up to 12 hours incubation of HMDMs with oxLDL.

HMDM ($5x10^6$ cells/ml) were grown on coverslips in 6-well plate in RPMI containing 10% HIHS. Cells were incubated with 1 mg/ml oxLDL in (A-C) and with 1 mg/ml oxLDL and 200μM 7,8-NP in (D-F) for 3, 6 and 12 hours. Apoptotic cells were identified by immunofluorescence staining of phosphatidylserine with Annexin-FITC and viewed with 40x magnification under fluorescence microscope.

5.2.2.5 Role of 7,8-Dihydroneopterin in Protecting the Glutathione Loss Induced by OxLDL

There is a possibility that 7,8- NP inhibits the toxic effects of OxLDL, by protecting the intracellular glutathione pool. This was explored by first depleting the intracellular glutathione synthesis using L-buthionine-S-sulfoxomine (BSO), a specific inhibitor of γ-glutamylcysteine synthethase (GCS). GCS is the rate-limiting enzyme in glutathione *de novo* synthesis. In this experiment, the aim was to deplete the intracellular glutathione level as low as possible and see if in the presence of oxLDL, 7,8-NP has any effect on its repletion. Therefore, the HMDMs were first treated with varying concentrations of BSO and time of incubations to see the maximum glutathione level depletion with minimum time of incubation.

Incubation of HMDMs with 100 to 500 μM of BSO for 12 hours did not affect the cell viability (Figures 5.25a and 5.25b). Surprisingly, incubating the HMDMs with the same BSO concentrations (Figure 5.25c) for 12 hours depleted the GSH synthesis to the same level, that is 60% of that control untreated HMDMs. There is a possibility that these range of concentrations were too high and saturated the cells. Therefore, the experiment was repeated with longer incubation time, 24 hours and lower BSO concentrations, ranging from 50 to 200 μM. However, as Figure 5.26b shows, a similar 60% drop in GSH level was demonstrated. The cell viability remained 100% with 50 to 200 μM of BSO (Figure 5.26a). The effect of a higher BSO concentration was explored. Figure 5.27 shows that 1 mM of BSO depleted the GSH level of HMDMs to approximately 60% after 20 and 26 hours incubation. This suggests that the HMDMs intracellular glutathione pool was quite resistant to glutathione depletion as compared to other cells (Esteban-Pretel & López-García, 2006). The viability assays show that the BSO concentrations used (Figure 5.27a) had no effect on the viability of HMDMs. Therefore, in subsequent experiments a low concentration of BSO and shorter exposure time i.e. 200 μM and 12 hours respectively, were used. Lower concentration of BSO and shorter exposure time are favoured to avoid cell adaptation to oxidative stress and the difference in metabolic capabilities and competence of BSO-treated cells from that of controls.

Macrophages treated with BSO (Figure 5.28) were able to restore their glutathione content almost to the same level as control cells after 24 hours (treatment D, Figure 5.28). As previously shown, there was a protective effect of 7,8-NP on glutathione loss induced by oxLDL (comparing treatments B and C, Figure 5.28). Interestingly, adding 7,8-NP together with BSO was able to restore the glutathione level to the same level as treatment

of HMDMs with oxLDL and 7,8-NP (treatments C and E, Figure 5.28). This suggests that there is a possibility that oxLDL acts by inhibiting the synthesis of glutathione, and 7,8-NP to a certain extent is able to protect γ-glutamylcysteine synthethase.

(a)

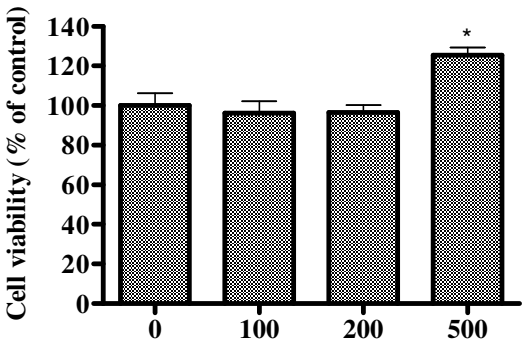

(b)

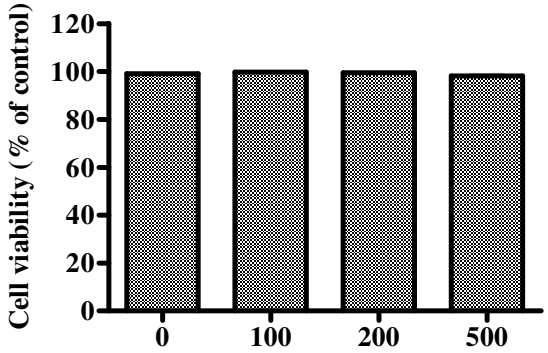

(c)

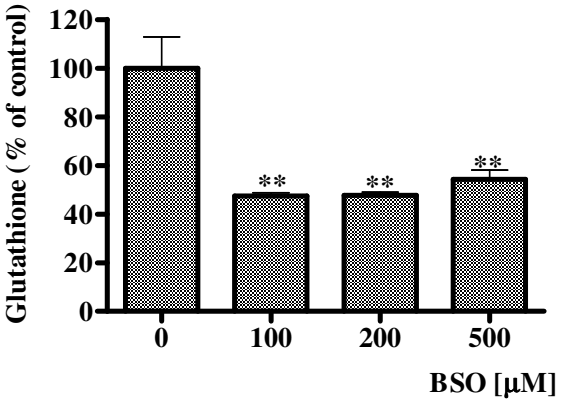

Figure 5.25 Loss of HMDMs viability and glutathione after 12 h incubation with increasing concentration of BSO.

HMDMs ($5x10^6$ cells/ml) were incubated at 37 °C in RPMI containing 10% HIHS with increasing concentrations of BSO. After 12 hours, HMDMs were analysed for cell viability via (a) MTT assay and (b) trypan blue exclusion staining and (c) glutathione levels with HPLC analysis. Significance is indicated from 0 μM BSO. Each value shown is the mean ± SD of triplicates.

(a)

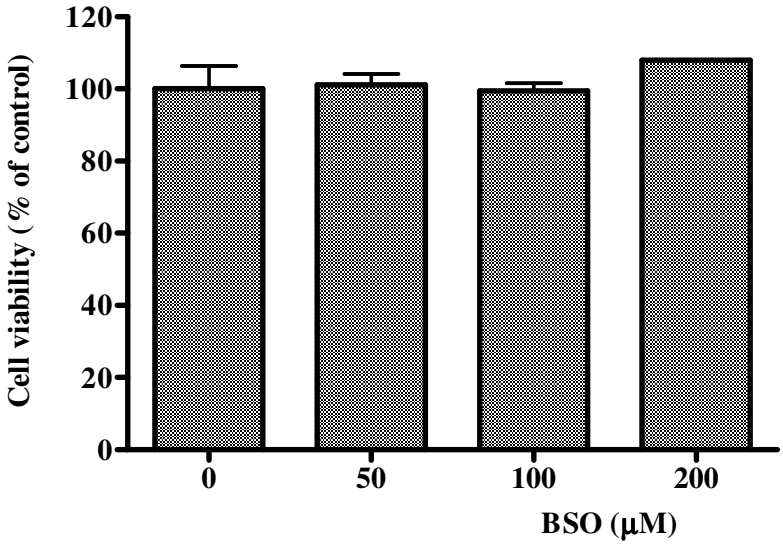

(b)

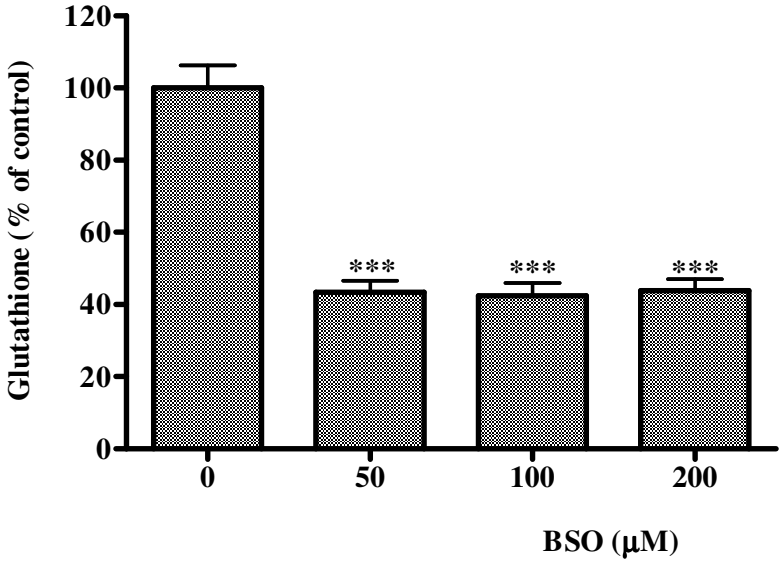

Figure 5.26 Loss of HMDMs viability and glutathione after 24 h incubation with increasing concentration of BSO.

HMDMs ($5x10^6$ cells/ml) were incubated at 37 °C in RPMI containing 10% HIHS with increasing concentrations of BSO. After 12 hours, HMDMs were analysed for cell viability via (a) MTT assay and (b) glutathione levels with HPLC analysis. Significance is indicated from 0 μM BSO. Each value shown is the mean ± SD of triplicates.

(a)

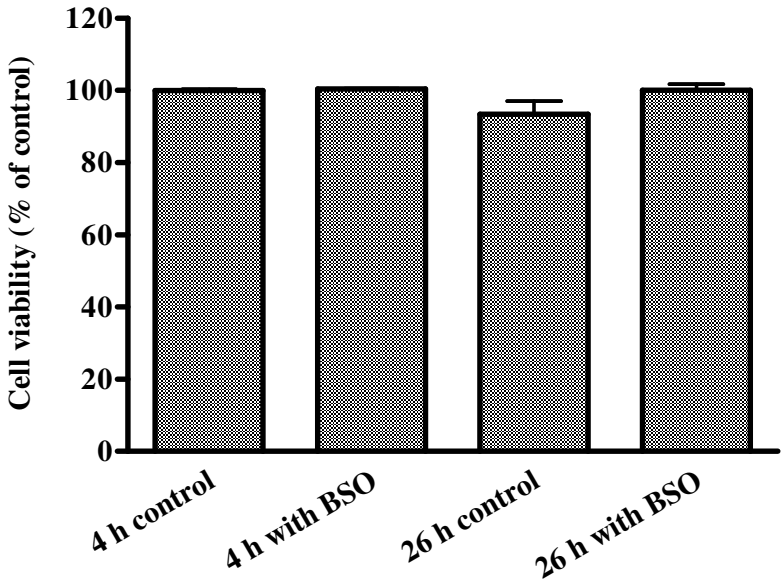

(b)

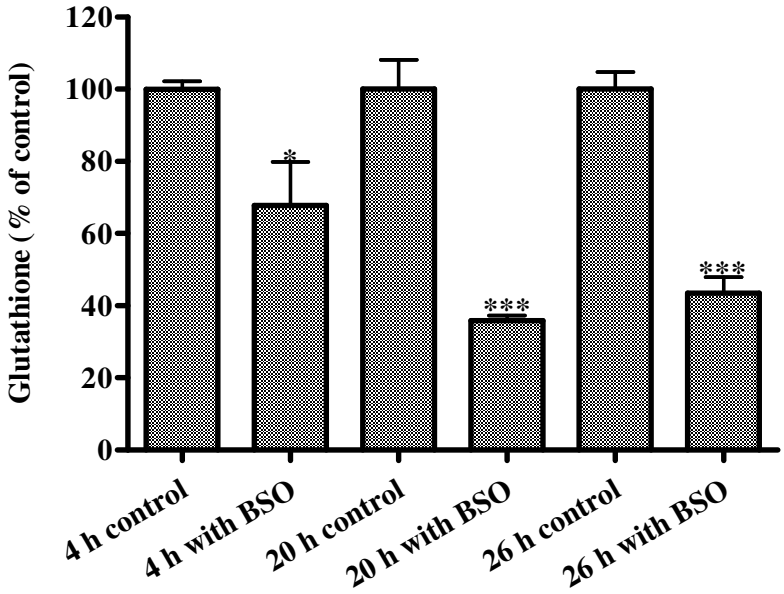

Figure 5.27 Time course for the loss of HMDMs viability and glutathione after incubation with 1 mM of BSO.

HMDMs ($5x10^6$ cells/ml) were incubated at 37 °C in RPMI containing 10% HIHS 1 mM of BSO. After 4, 20 and 26 hours, HMDMs were analysed for cell viability via (a) trypan blue exclusion staining and (b) glutathione levels with HPLC analysis. Significance is indicated from control of each time of incubation. Each value shown is the mean $\pm$ SD of triplicates.

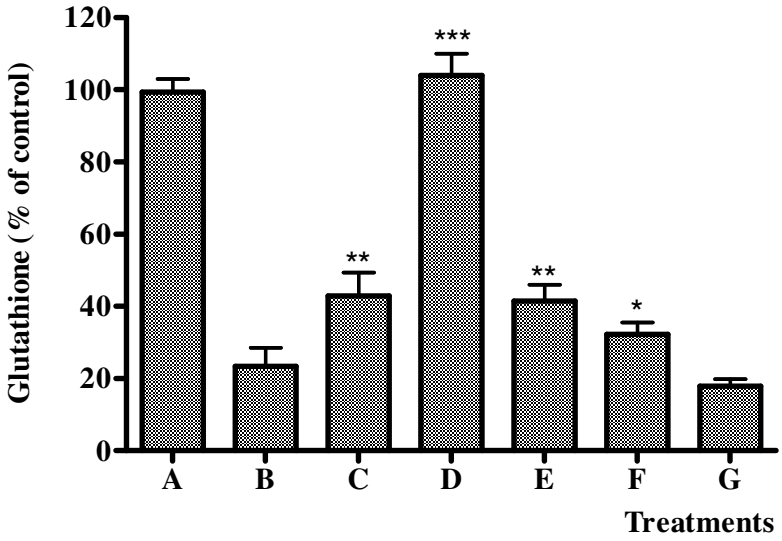

A. control
B. incubate with 1 mg/ml oxLDL for 24 h
C. incubate with 1 mg/ml oxLDL and 200 μM 7,8-NP for 24 h
D. pretreat with 200 μM BSO for 12 h then add full media back for another 24 h
E. pretreat with 200 μM BSO for 12 h then add 200 μM 7,8-NP and 200 μM BSO for 24 h
F. pretreat with 200 μM BSO for 12 h then add 1 mg/ml oxLDL and 200 μM 7,8-NP for 24 h
G. pretreat with 200 μM BSO for 12 h then add 1 mg/ml oxLDL for 24 h

Figure 5.28 Effect of glutathione depletion on the protective effect of 7,8-NP.
HMDMs ($5x10^6$ cells/ml) were incubated for 12 hours with 200 μM BSO in RPMI containing 10% HIHS at 37 °C. Then the cells were washed twice in PBS and incubated further with 7,8-NP or oxLDL or BSO as indicated under the Figure above. The glutathione levels were measured using HPLC analysis. Results are displayed as mean ± SD of triplicates from a single experiment, representative of three separate experiments. Significance is indicated from treatment B.

5.2.2.6 7,8-Dihydroneopterin Inhibits Uptake of Non-toxic Concentrations of DiI-oxLDL by HMDMs

There is a possibility that 7,8-NP's protective effect against oxLDL-induced damage is established by influencing the uptake of oxLDL. This was studied by incubating HMDMs with 200 μM of 7,8-NP and 1 mg/ml of DiI-oxLDL. The amount of association and binding of DiI-oxLDL to HMDMs were measured as described in chapter 2. The amount of DiI-oxLDL uptake was calculated by subtracting the value of binding from the value of association.

There was a time dependent uptake of DiI-oxLDL by HMDMs (Figure 5.29c). A decrease in DiI-oxLDL uptake in the presence of 7,8-NP after 1 and 24 hours incubation was observed (Figure 5.29c), however it was not statistically significant. It is possible that the toxic effect of 1 mg/ml oxLDL overwhelmed any ability of 7,8-NP to inhibit the oxLDL uptake. This theory was investigated by incubating the HMDMs with lower oxLDL concentrations, 0.2 and 0.12 mg/ml. These concentrations had been shown before not to affect the cell viability. With these oxLDL concentrations, a very significant inhibitory effect of 7,8-NP on the uptake of oxLDL (Figure 5.30 and Figure 5.31) was clearly shown. The oxLDL uptake was reduced by 50% (Figure 5.30) and 80% after exposure to 0.2 and 0.12 mg/ml oxLDL respectively. 7,8-NP had no effect on DiI-oxLDL uptake within one hour incubation (Figure 5.30) possibly because there was not enough time for it to establish its effect on the cells. However, after 2 hours incubation there was an inhibitory effect even though it was not significant (Figure 5.31). Therefore, 7,8-NP was able to inhibit the oxLDL uptake when non-toxic oxLDL concentrations were used.

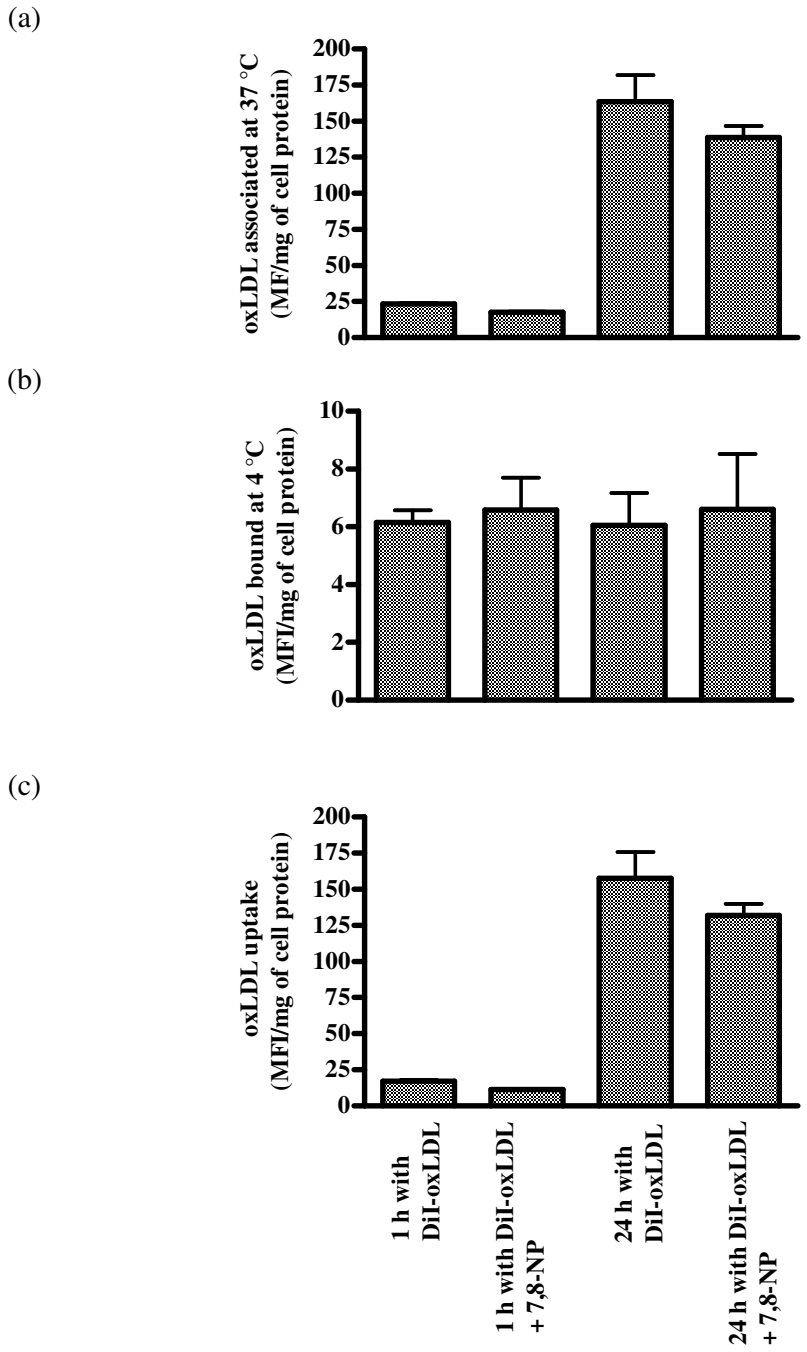

Figure 5.29 Effect of 7,8-NP on DiI-oxLDL uptake by human macrophages.
HMDMs ($5x10^6$ cells/ml) were incubated at (a) 37 °C to measure cell-association and (b) 4 °C to measure binding in RPMI containing 10% HIHS with 1 mg/ml DiI-oxLDL and with or without 200 µM 7,8-NP. After 1 and 24 hours, the cells were harvested and fluorescence intensities were measured. The uptake of oxLDL (c) was calculated as the difference between (a) and (b). Each value shown is the mean $\pm$ SD of triplicates. Significance is indicated from treatment with DiI-oxLDL for the same hour of incubation.

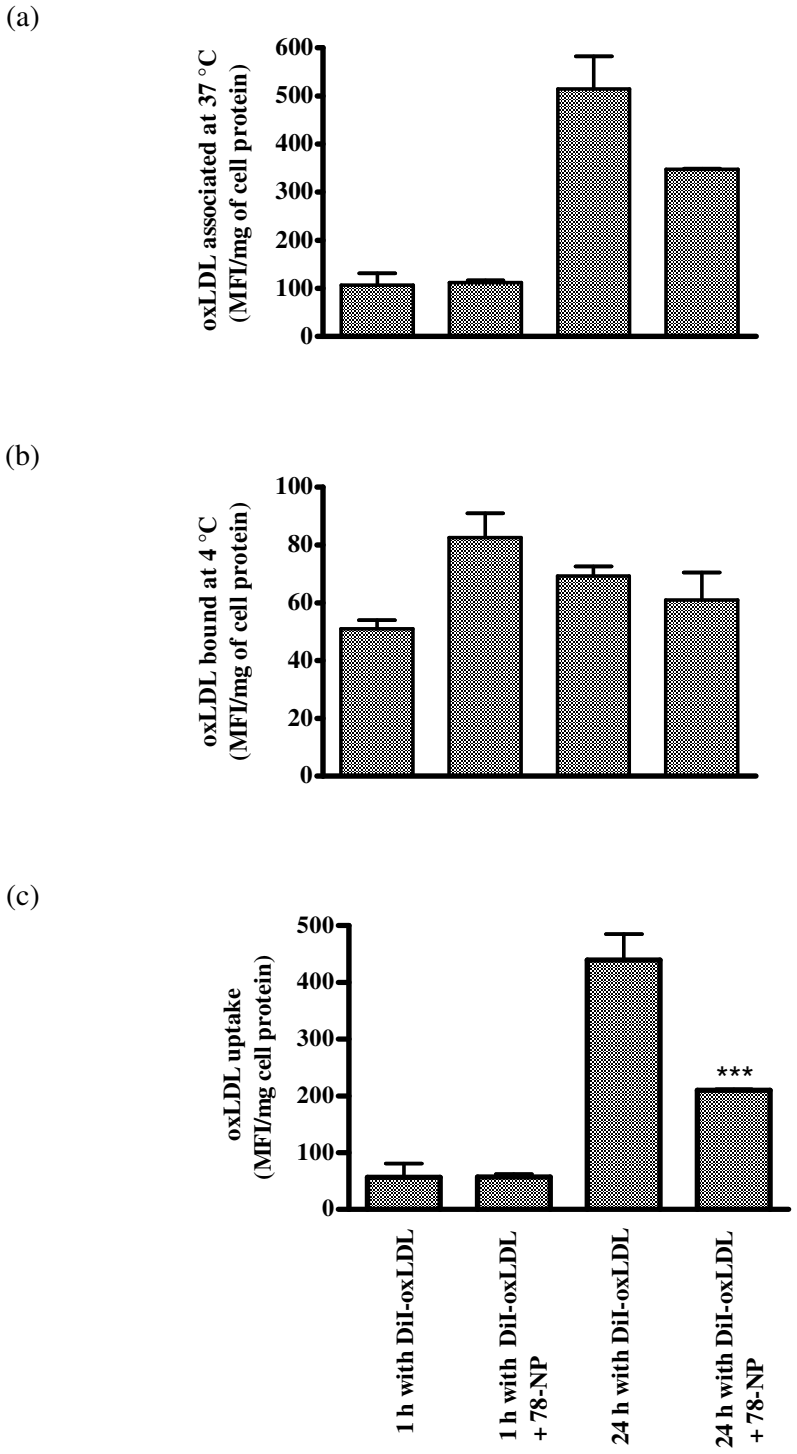

Figure 5.30 Effect of 7,8-NP on DiI-oxLDL uptake by human macrophages.
HMDMs ($5x10^6$ cells/ml) were incubated at (a) 37 °C to measure cell-association and (b) 4 °C to measure binding in RPMI containing 10% HIHS with 40 μg protein/ml (200 μg/ml) DiI-oxLDL and with or without 200 μM 7,8-NP. After 1 and 24 hours, the cells were harvested and fluorescence intensities were measured. The uptake of oxLDL (c) was calculated as the difference between (a) and (b). Each value shown is the mean ± SD of triplicates from a single experiment. Significance is indicated from treatment with DiI-oxLDL for the same hour of incubation.

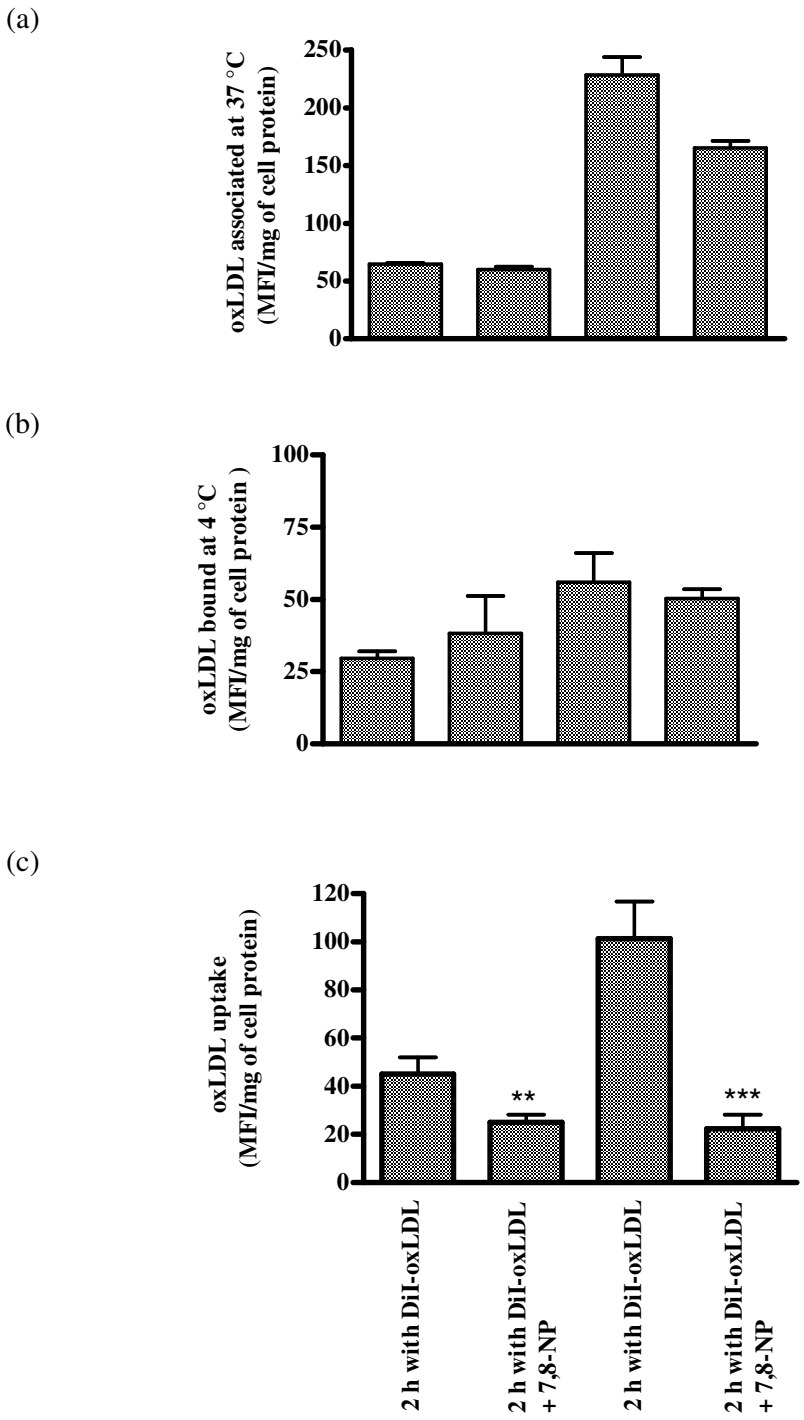

Figure 5.31 Effect of 7,8-NP on DiI-oxLDL uptake by human macrophages.
HMDMs ($5x10^6$ cells/ml) were incubated at (a) 37 °C to measure cell-association and (b) 4 °C to measure binding in RPMI containing 10% HIHS with 25 μg protein/ml (125 μg/ml) DiI-oxLDL and with or without 200 μM 7,8-NP. After 2 and 24 hours, the cells were harvested and fluorescence intensities were measured. The uptake of oxLDL (c) was calculated as the difference between (a) and (b). Each value shown is the mean $\pm$ SD of triplicates from a single experiment. Significance is indicated from treatment with DiI-oxLDL for the same hour of incubation.

5.2.2.7 Enrichment of HMDMs with 7,8-Dihydroneopterin Does Not Influence SR-A Protein Expression But Has Ambiguous Effect on CD36 Protein Expression

There are at least six classes of scavenger receptors (SRA, SR-B, SR-D, SR-E, SR-PSOX and SR-G) so far reported to be involved in the uptake of oxLDL. SR-A and CD36 of SRA and SR-B classes respectively have been repeatedly shown to play an important role in the early uptake of oxLDL and deletion of these receptors can limit atherosclerotic progression in mouse model (Febbraio *et al*., 2000; Kunjathoor *et al*., 2002). In addition it appears that the majority of modified LDL processed by macrophages is via CD36 and SR-A (40-90%) (Febbraio *et al*., 2000; Huh *et al*., 1996; Nakagawa *et al*., 1998). Therefore, the discovery of reduced uptake of oxLDL in the presence of 7,8-NP in the present study might suggest that 7,8-NP might modulate at least these two receptors in exerting its protective effect against oxLDL-induced damage.

This theory was investigated by incubating the HMDMs with various concentrations of 7,8-NP for 24 hours. The levels of protein expression of SR-A and CD36 were investigated by using Western Blot analysis. According to Gough, *et al* . (1999) under the nonreducing SDS-PAGE conditions, SR-A should migrate predominantly as a mixture of monomers (M_r ≈90 to 70 kDa) and disulphide-linked dimers (M_r ≈170 to 150 kDa) with a small amount of trimers (M_r ≈240 to 220 kDa). As a result of varying degrees of CD36 glycosylation more than one of CD36 bands can be observed (Alessio *et al*., 1996; Munteanu *et al*., 2005). These bands are of different molecular masses and they correspond to different glycoforms. The molecular massed displayed also depend on the type of cell (Alessio *et al*., 1996; Greenwalt *et al*., 1990). Alessio *et al* ., (1996) showed that phorbol 12-myristate 13-acetate induced the expression of CD36 in U937 and THP-1 cells. A 74-kDa intracellular precursor was first synthesised that later processed into mature form of 90-105 kDa (Alessio *et al*., 1996).

In this study, the Western Blot analysis of SR-A of HMDMs did not reveal the presence of dimers and trimers (Figure 5.32a). However, four distinct bands of monomers were detected and they migrated predominantly between 70 and 102 kDa. If anything, the presence of 50 to 200 μM of 7,8-NP caused a very small increase in the intensity of 81 and 91 kDa bands as compared to control (Figure 5.32a). However, the analysis of the band signals (Figure 5.32b) showed that the increase is so small and not significant since 2 repeats of this experiment showed that the presence of 7,8-NP did not have any effect on the protein expression of any of the bands.

(a)

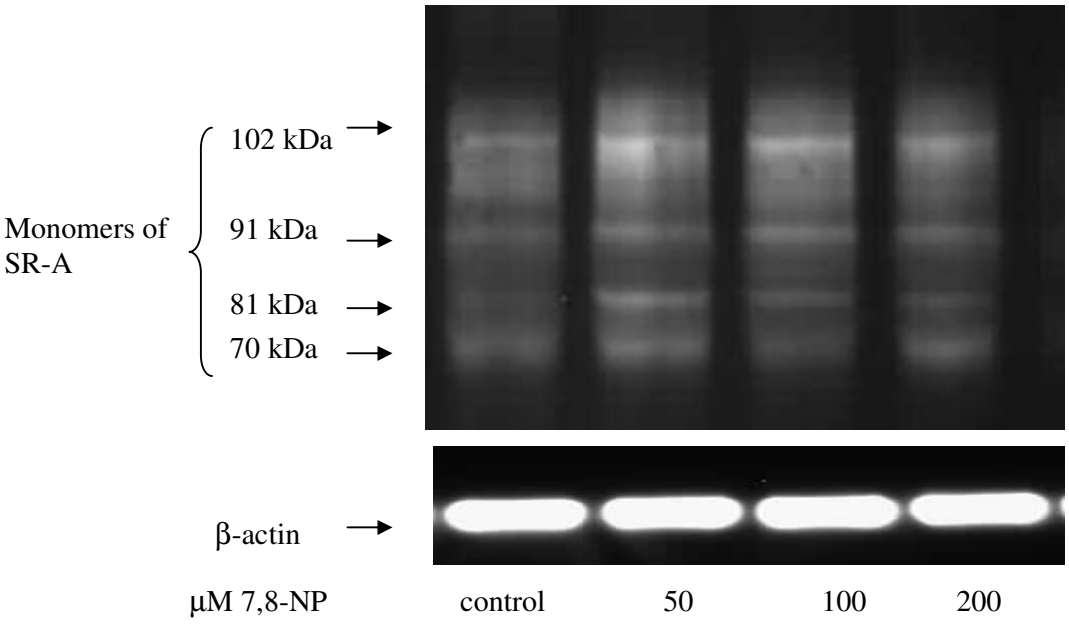

(b)

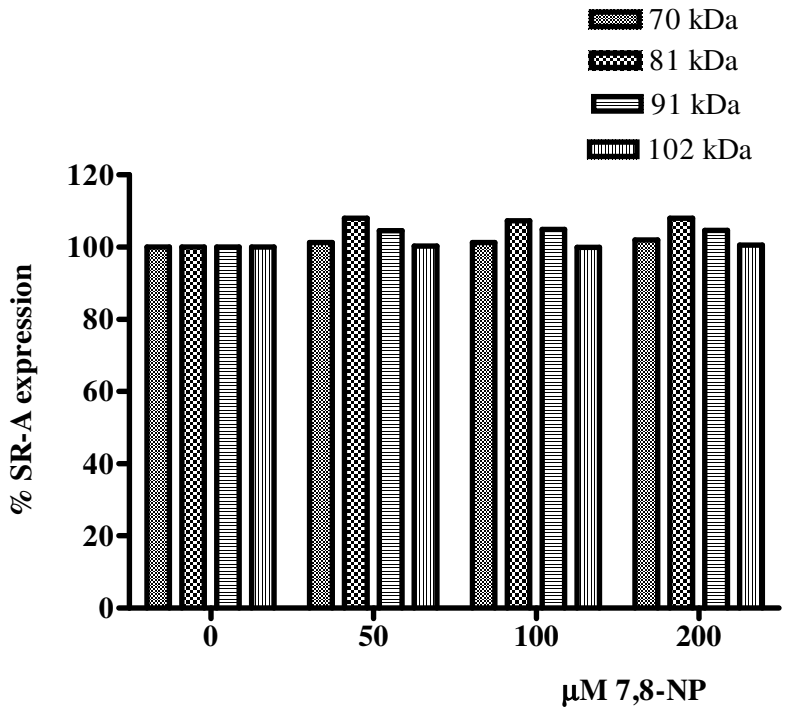

Figure 5.32 Effect of 7,8-NP enrichment of HMDMs on expression of SR-A protein. HMDMs ($5x10^6$ cells/ml) were incubated at 37 °C in RPMI containing 10% HIHS and 7,8-NP for 24 hours. 40 μg proteins of the total cell lysate were loaded onto an SDS-PAGE. (a) The presence of SR-A was detected by Western Blot. Data for (a) and (b) is from single experiment, and representatives of three independent experiments. β-actin was used as a control loading. (b)The % of SR-A expression was determined from signals of the monomer bands on the membranes analysed using Syngene Tool.

The results below are the preliminary data on the of enrichment of HMDMs with increasing concentrations of 7,8-NP on the CD36 protein expression. Interestingly the results varied from one experiment to another. As shown in Figure 5.33, two well separated bands of CD36 of molecular weights 80 and 100 kDa were seen after incubation of HMDMs with 7,8-NP for 24 hours. The presence of more than one CD36 band is probably due to the product of CD36 glycosylation. The intensity of the 80-kDa band decreased with increasing concentrations of 7,8-NP (Figure 5.33a) and this was complemented by Figure 5.33b that shows that 7,8-NP down regulated the percentage of the 80-kDa's expression in a concentration dependent manner. At 200 μM, 7,8NP decreased the 80-kDa's expression by 55%. However, 7,8-NP had different effect on the 100-kDa's expression. The treatment with increasing concentrations of 7,8-NP increased the intensity of the 100 kDa's band (Figure 5.33a) and this was confirmed by increased in the percentage of its expression. The down regulation effect of 7,8-NP on the 80-kDa's expression was achieved twice but further repetitions of the experiment gave different results as discussed below.

Figure 5.34 shows that treatment of HMDMs with increasing concentrations of 7,8-NP for 24 hours results in the presence of two distinct bands. However, in contrast to Figure 5.33, the bands were quite close together and the bands had molecular weights of 75 and 86 kDa (Figure 5.34a). Moreover, the percentage CD36 expression of both bands increased with increasing concentrations of 7,8-NP (Figure 5.34b) peaking with 100 μM concentration of 7,8-NP for 86 kDa and 200 μM for 75 kDa. This result suggests that 7,8-NP did not down regulate CD36 expression.

The above two results were further complicated with another Western Blot results. Even though the protein concentration used for gel loading (Figure 5.35a vs. Figures 5.33a and 5.34b) was doubled (from 40 to 80 μg/well), the bands still looked weaker in intensity. Besides that, Figure 5.35a shows that treatment of HMDMs with increasing concentrations of 7,8-NP for 24 hours results in the presence of only single CD36 band of 86 kDa. The percentage of CD36 expression also increased with increasing concentrations of 7,8-NP (Figure 5.35a). Taken together, the CD36 Western Blot results suggest that CD36 protein expression is decreased by 7,8-NP when two bands of far apart present together. In this situation, 7,8-NP could only down regulate the expression of the lower molecular weight proteins and increased the protein expression of the 100 kDa.

Perhaps the effect of 7,8-NP was not clearly seen because the incubation time was too long. As the previous data for inhibitory effect of 7,8-NP on PS exposure and ROS production shown, the protective effect of 7,8-NP was maximum up to 12 hours incubation

of HMDMs with 7,8-NP. Therefore, it is necessary to repeat these experiments with shorter incubation times. Figures 5.36 and 5.37 show the time course of effect of 7,8-NP enrichment on the expression of CD36 protein. It is to be noted that the experiments were carried out by Tina Yang, a PhD student in this laboratory and under the author's supervision. Interestingly the results of time course experiment were also inconsistent. Figure 5.36 shows the presence of 3 glycoforms of CD36 with molecular weights of 75, 86 and 115 kDa. Two hundred μM 7,8-NP had remarkably down regulated the CD36 protein expression of all the 3 glycoforms even though the 115-kDa's expression was up regulated during the first hour. After 24 hours incubation with 7,8-NP, all three glycoforms protein expression dropped to below 30%. 7,8-NP also seemed to down regulate the CD36 protein expression in a time dependent manner. Figure 5.37 shows that there was only two glycoforms present which were of 75 and 115 kDa. In contrast to Figure 5.36, the incubation of HMDMs with 7,8-NP up regulated the 115-kDa's expression, while the effect on the 75-kDa's expression seemed to be subtle.

(a)

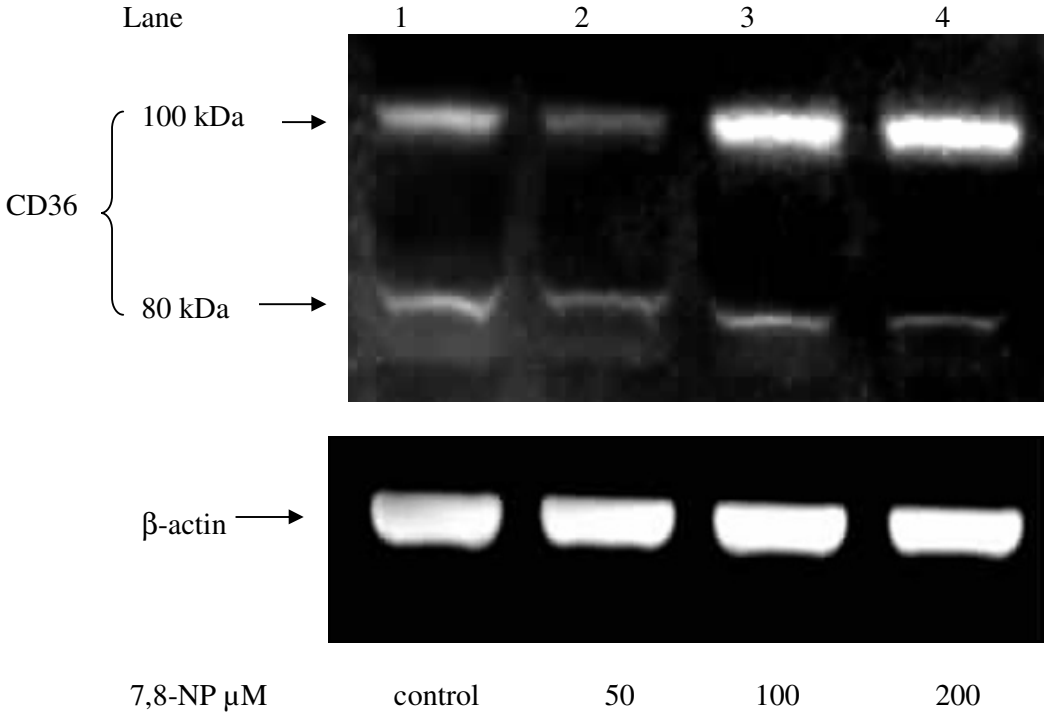

(b)

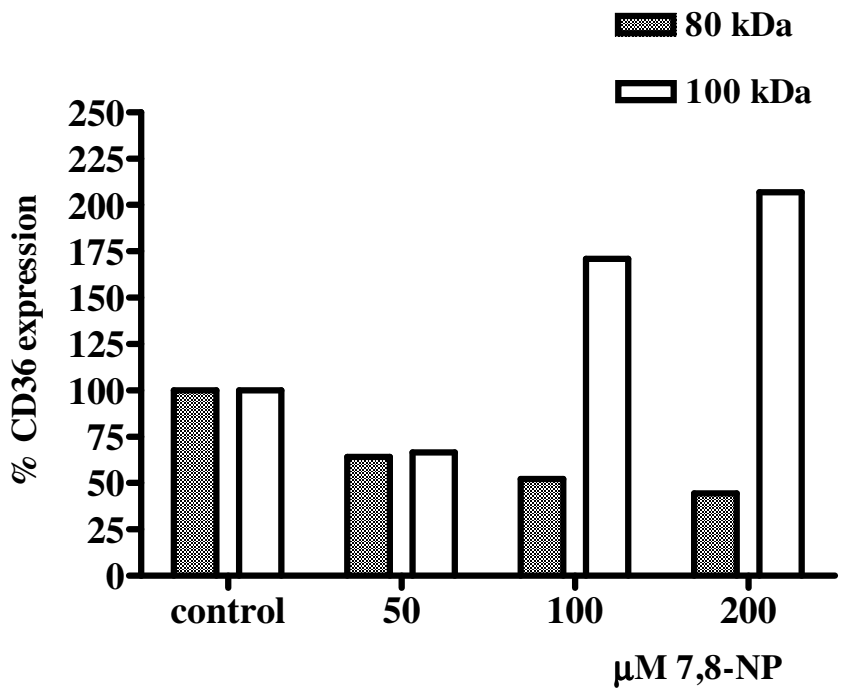

Figure 5.33 Effect of 7,8-NP enrichment of HMDMs on expression of CD36 protein. HMDMs ($5x10^6$ cells/ml) were incubated at 37 °C in RPMI containing 10% HIHS and 7,8-NP for 24 hours. 40 μg proteins of the total cell lysate were loaded onto an SDS-PAGE. (a) The presence of CD36 was detected by Western Blot. β-actin was used as a control loading. (b) The % of CD36 expression was determined from signals of the bands on the membrane and analysed using Syngene Tool. Data is representative of two separate experiments.

(a)

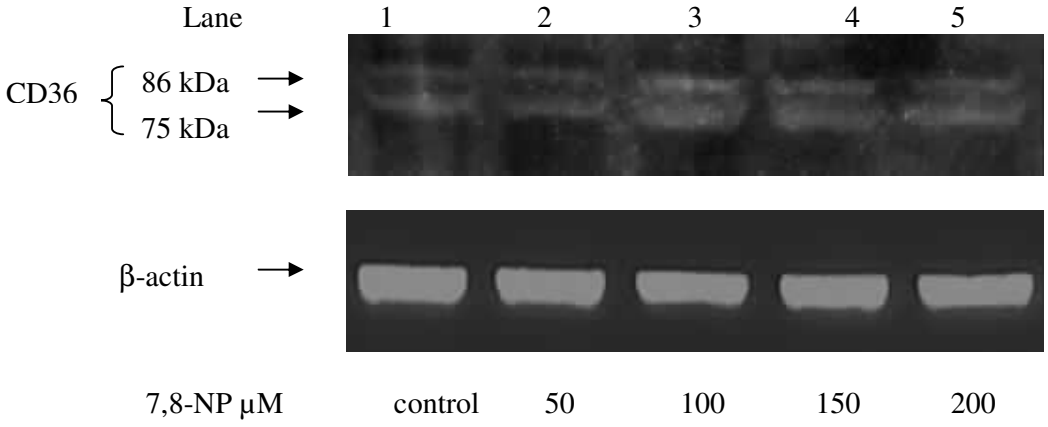

(b)

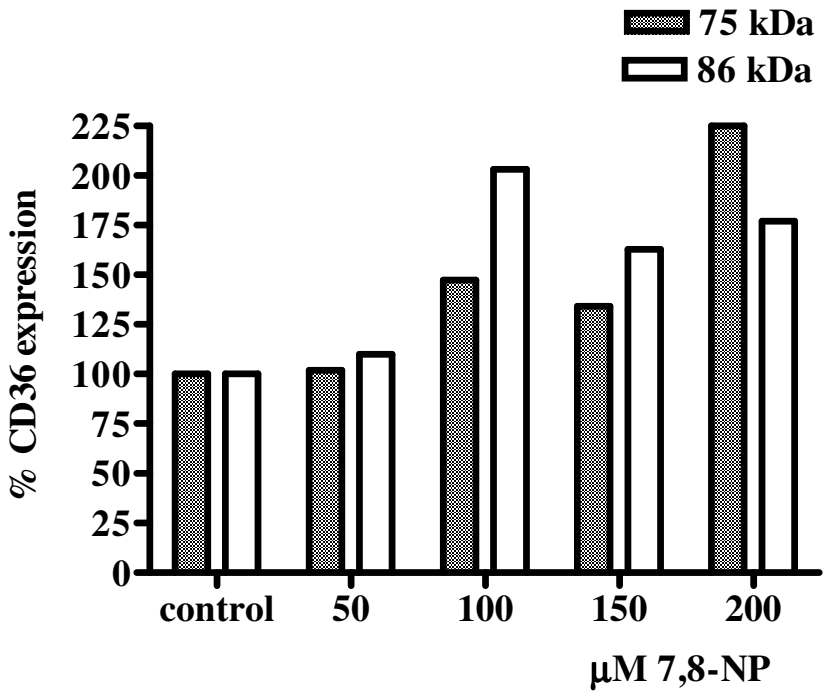

Figure 5.34 Effect of 7,8-NP enrichment of HMDMs on expression of CD36 protein. HMDMs ($5x10^6$ cells/ml) were incubated at 37 °C in RPMI containing 10% HIHS and 7,8-NP for 24 hours. 40 μg proteins of the total cell lysate were loaded onto an SDS-PAGE. (a) The presence of CD36 was detected by Western Blot. β-actin was used as a control loading. (b) The % of CD36 expression was determined from signals of the bands on the membrane and analysed using Syngene Tool. Data is from single experiment.

(a)

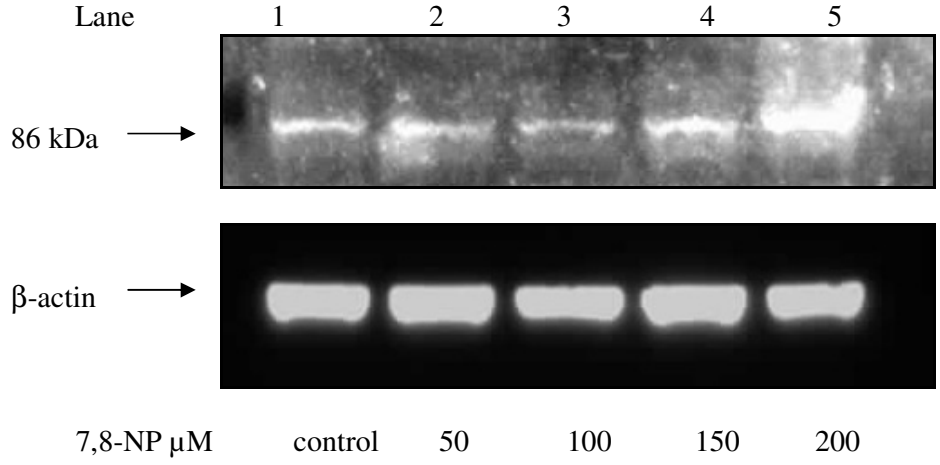

(b)

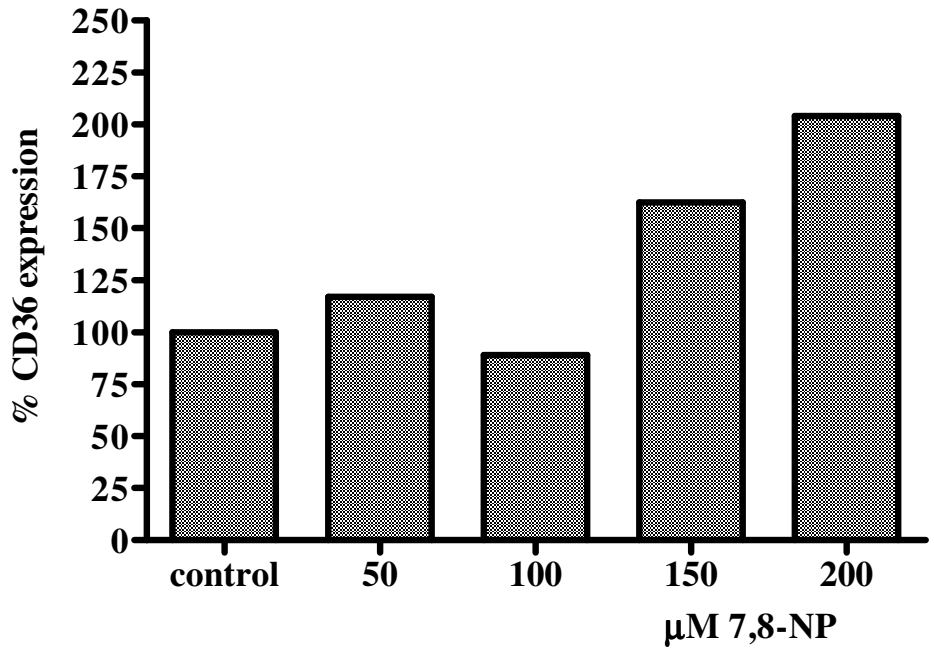

Figure 5.35 Effect of 7,8-NP enrichment of HMDMs on expression of CD36 protein. HMDMs ($5x10^6$ cells/ml) were incubated at 37 °C in RPMI containing 10% HIHS and 7,8-NP for 24 hours. 80 μg proteins of the total cell lysate were loaded onto an SDS-PAGE. (a) The presence of CD36 was detected by Western Blot. β-actin was used as a control loading. (b) The % of CD36 expression was determined from signals of the bands on the membrane and analysed using Syngene Tool . Data is representative of two separate experiments.

(a)

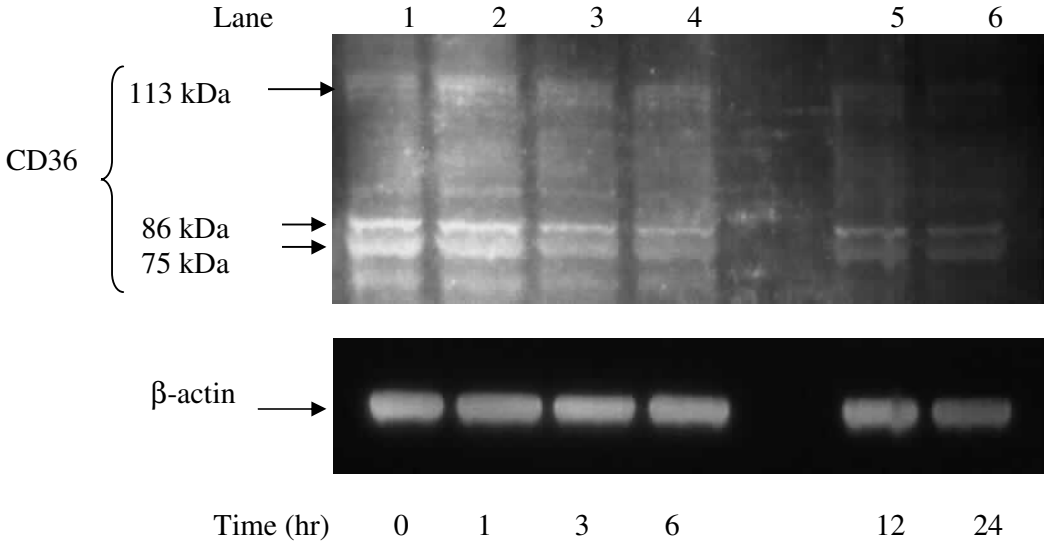

(b)

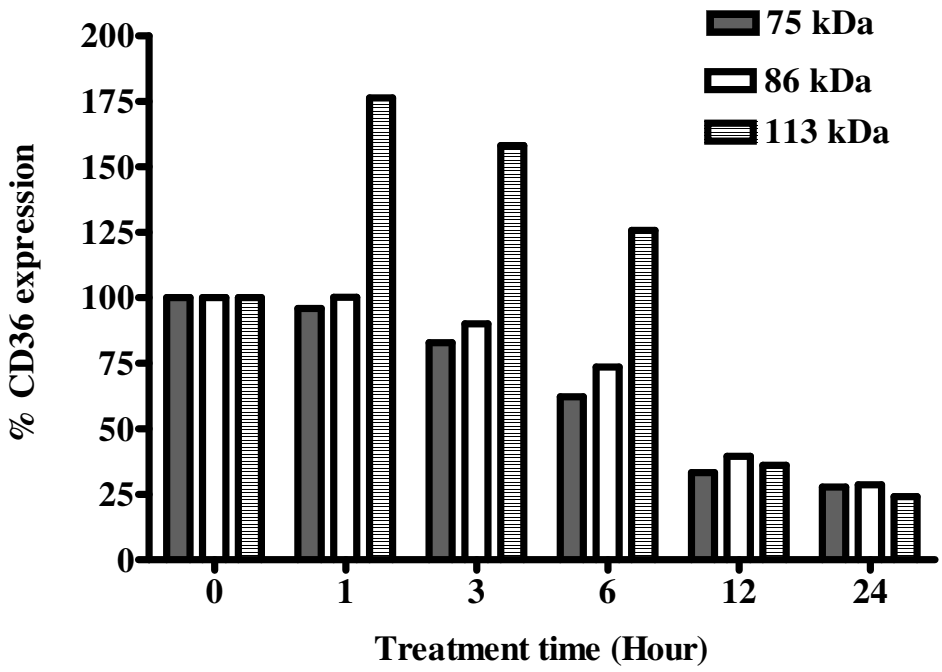

Figure 5.36 Time course of effect of 7,8-NP enrichment of HMDMs on expression of CD36 protein.

HMDMs ($5x10^6$ cells/ml) were incubated at 37 °C in RPMI containing 10% HIHS and 200 μM 7,8-NP for 0-24 hours. 40 μg proteins of the total cell lysate were loaded onto an SDS-PAGE. (a) The presence of CD36 was detected by Western Blot (a). β-actin was used as a control loading. Three different molecular masses of CD36 were detected (113, 86 and 75 kDa). (b) The % of CD36 expression was determined from signals of the bands on the membrane and analysed using Syngene Tool. Data is from a single experiment.

(a)

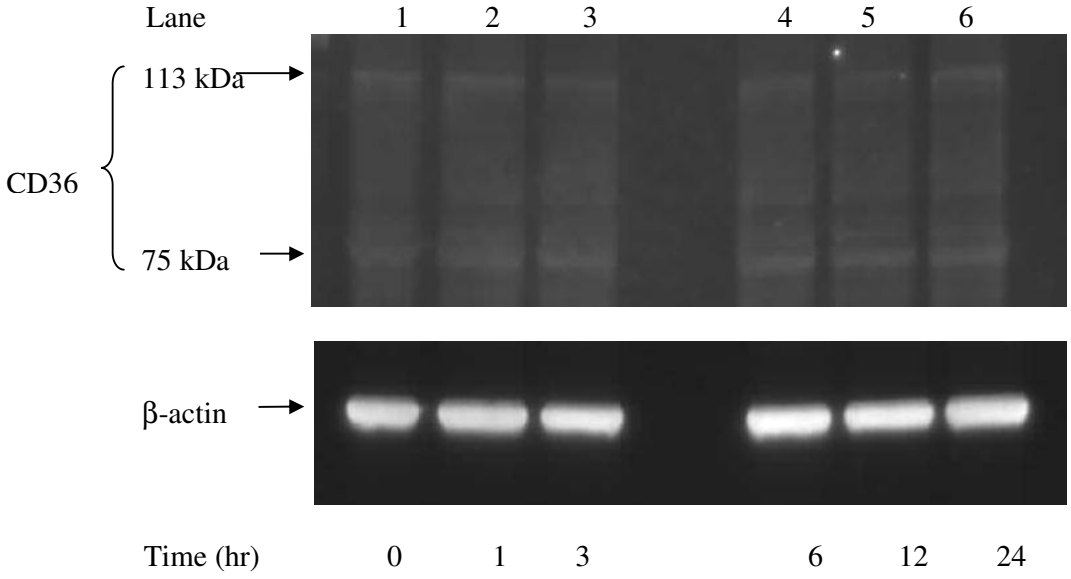

(b)

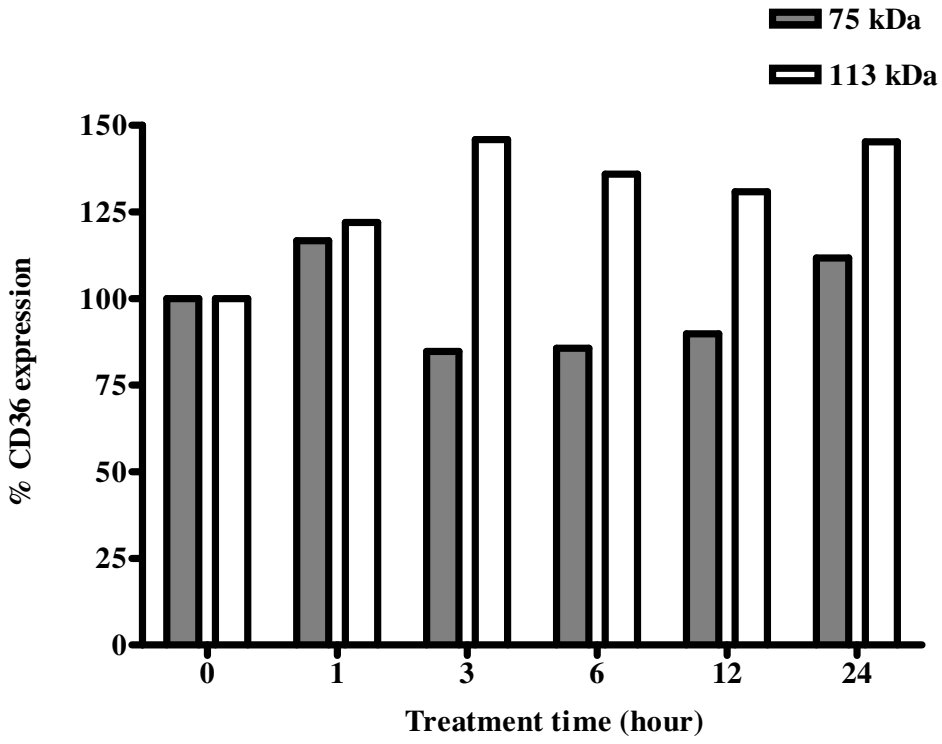

Figure 5.37 Time course of effect of 7,8-NP enrichment on the expression of CD36 protein.

HMDMs ($5x10^6$ cells/ml) were incubated at 37 °C in RPMI containing 10% HIHS and 200 μM 7,8-NP for 0-24 hours. 40 μg proteins of the total cell lysate were loaded onto an SDS-PAGE. (a) The presence of CD36 was detected by Western Blot. β-actin was used as a control loading. Two different molecular masses of CD36 were detected (115 and 75 kDa). (b) The % of CD36 expression was determined from signals of the bands on the membrane and analysed using Syngene Tool. Data is from a single experiment.

5.3 Discussion

5.3.1 Effect of OxLDL on HMDMs

5.3.1.1 Characterisation of Native LDL and OxLDL

There are significant differences in the characteristics of oxLDL prepared by different laboratories. A few factors can contribute to the differences which include the concentration of LDL when oxidised, types of oxidants and their concentrations, the length of the oxidation, temperature of oxidation and transition metal or metal chelator concentration (Lougheed & Steinbrecher, 1996; Ziouzenkova *et al*., 1998).

The REM value of oxLDL prepared in this study was similar to those published by Darley-Usmar, *et al.* (1991), Asmis and Jelk (2000b) and Baird, (2003), while the degree of oxLDL's aggregation prepared in this study was similar to that of Baird, (2003). OxLDL was more aggregated than the native LDL even though it was filtered before analysis that would have removed very large aggregates. However, LDL is known to aggregate during oxidation or even during handling (Maor *et al*., 1997).

OxLDL prepared in this study also had a very high TBAR value i.e 52 -fold more than the native LDL. In contrast, oxLDL prepared by (Baird, 2003) had only 9 –fold more TBARs than the native LDL even though comparatively same concentration of $CuCl_2$ was used to oxidise LDL. This study used 300-350 μM $CuCl_2$ to oxidise 3 mg/ml LDL whereas Baird, (2003) used 50 μM $CuCl_2$ to oxidise 0.5 mg/ml oxLDL. Therefore, same ratio of copper to LDL molecule which is 250 copper per LDL molecule was used, (refer to appendix I for calculation). Hence, the extent of oxidation of LDL may depend on the absolute concentration of LDL and copper, even if the ration of of copper to LDL is kept constant. Another most likely explanation for the disparity in the TBARs values is that nLDL is very heterogeneous. It has different ratios of components such as PUFAs and antioxidants from each group of donors, which will then affect the properties of the oxLDL (Esterbauer *et al*., 1990). The high value of TBARs gave indication that the oxLDL was highly toxic and all three characteristics mentioned above suggest that the oxLDL prepared in this study was heavily oxidised.

5.3.1.2 Loss of Cell Viability and Intracellular Glutathione Levels in the Presence of OxLDL

The loss of viability was dependent on oxLDL concentration and time of incubation (Figures 5.3 and 5.5). In this study, the oxLDL concentrations greater than 0.2 mg/ml were

toxic to the HMDMs in terms of loss in the cell viability. The presence of toxic concentrations of oxLDL caused the HMDMs to undergo death processes of both apoptotic and necrotic appearance. Analyses of plaque and time course investigations have indicated that 7-KC and 7-OH are later stage products (Brown *et al*., 1997; Jessup & Kritharides, 2000; Upston *et al*., 2002). In addition, analysis of highly oxLDL revealed that it contained almost exclusively of 7-KC (Harris *et al*., 2006). Therefore, there was a possibility that 7-KC accounted for the cytotoxicity of oxLDL. 7-KC had been shown to be potent inducers of apoptosis in various cell types (Berthier *et al*., 2004; Leonarduzzi *et al*., 2006; Lizard *et al*., 1998).

The trypan blue assay showed smaller decrease in cell viability compared to the MTT assay with all concentrations of oxLDL (Figure 5.3). This disparity may be due to the difficulty in determining the dead cell (blue in colour) from the live cells (transparent in colour) in trypan blue assay. The HMDMs were quite large and the blue dye that entered them appeared as little dots instead of the whole cells becoming blue in colour. This caused an uncertainty in assigning them as dead or live cells. In contrast, the MTT assay measures the cells ability to reduce MTT to the formazan may be by mitochondrial enzymes distinct from the plasma membrane/phagosome enzyme NADPH oxidase (Mosmann, 1983). This makes the assay very sensitive to changes in the cell's metabolic state. The trypan blue exclusion measures the failure of the cell membrane and therefore, tends to be less sensitive (Duggan *et al*., 2001).

By labelling oxLDL with DiI, it was demonstrated that oxLDL was taken up by the HMDMs in a time dependent manner that correlates with the time point where the HMDMs were committed to death (Figure 5.9). Interestingly, there was a lag phase in DiI-LDL and DiI-oxLDL uptake between 3 and 6 hours. It is not known why there was a lag phase in uptake between these times. There was a linear relationship between the association of DiI-oxLDL with HMDMs and incubation time up to 12 hours (Figure 5.9). After 12 hours, there was no more increase in the association of DiI-oxLDL with HMDMs. This result was complemented by the finding that HMDMs required 12 hours exposure to oxLDL before a drastic drop in cell viability happened (Figure 5.5). 12-hour incubation was possibly required to saturate all the scavenger receptors to oxLDL before the free oxLDL can exert its toxic effect maximally, and this led to a sudden drop in cell viability (Figure 5.5). However, the loss of intracellular glutathione has been shown to happen between 3 and 12 hours.

The 24 h-incubation with 1 mg/ml of oxLDL (Figures 5.6 and 5.7) depleted intracellular glutathione level to a similar extent as treatment with 50 μM to 1 mM BSO

(Figures 5.25 to 5.27). HMDMs treated with diethyl maleate (DEM) a reagent that alkylates glutathione also caused a similar loss in glutathione level (Tina Yang, personal communication[2]). However, glutathione depletion by BSO or DEM, even by as much as 60% by themselves, did not promote HMDMs death, indicating that oxLDL-induced decrease in intracellular glutathione is necessary. In addition, the time course of the cell viability and glutathione loss (Figures 5.5 and 5.7 respectively) show that the loss of glutathione occurred immediately and at all time points were at faster rates than the loss of the cell viability. This could indicate that the gradual collapse of the glutathione level induced by oxLDL preceded macrophage death. This could also suggest that glutathione depletion was required for oxLDL-induced macrophage toxicity. These observations are in good agreement with results obtained by Darley-Usmar *et al.* (1991), Gotoh *et al.* (1993) and Wang *et al.* (2006) demonstrating that depletion of reduced glutathione enhances oxLDL cytotoxicity in human macrophages. The most likely explanation for this is that the depletion of reduced glutathione by oxLDL (Wang *et al*., 2006) alters the glutathione thiol redox state (GSH/GSSG ratio). Since GSH/GSSG ratio is one of the principal determinants of the cellular redox environment, any alteration in the redox environment can lead to cellular dysfunction and cell death (Schafer & Buettner, 2001). Depletion of cellular glutathione by BSO or DEM alone was not sufficient to promote macrophage death and a likely explanation for this observation is that in contrast to oxLDL, BSO treatment did not significantly alter thiol redox environment.

Glutathione has been observed to be expelled from cells as a mechanism of apoptosis (Ghibelli *et al*., 1998; van den Dobbelsteen *et al*., 1996). Cells induced to apoptosis extrude glutathione in the reduced form concomitantly with (U937 cells) or before (HepG2 cells) the development of apoptosis, much earlier than plasma membrane leakage and the presence of inhibitors of carrier mediated GSH extrusion, methionine or cystathionine, are capable of decreasing the GSH efflux and the extent of apoptosis.

Interestingly, both undifferentiated and PMA-differentiated THP-1 cells respond to lower concentration of oxLDL (concentrations that did not affect the cell viability) by increased GSH synthesis (Darley-Usmar *et al*., 1991; Gotoh *et al*., 1993). Increased in reduced thiol levels was also observed in U937 cells treated with lower oxLDL concentration by Baird (2003) but in contrast to Darley-Usmar *et al.* (1991) and Gotoh *et al.* (1993), Baird (2003) did not detect any increase in the reduced thiols in THP-1 cells. Increased expression of enzymes involved in GSH synthesis in response to oxLDL was observed in murine macrophage-like cell lines RAW 264.7 and J774 A.1 as well as mouse

[2] Tina Yang is a PhD student in Dr. Steven Gieseg's laboratory.

peritoneal macrophages (Bea *et al*., 2003; Shen & Sevanian, 2001). In contrast to these cell lines, this study and the study of Wang *et al.* (2006) did not detect an increase in total glutathione levels in primary HMDMs in response to any oxLDL concentration tested, even at the concentrations that did not affect the cell viability (Figures 5.3 and 5.6). The possibility that oxLDL stimulated GSH synthesis in HMDMs cannot be ruled out. However, any increase in GSH synthesis induced by oxLDL clearly was insufficient to compensate for the GSH-depleting effect of oxLDL. Probably, the apparent inability of HMDMs to respond to thiol oxidative stress with increased GSH synthesis distinguishes primary human macrophages for widely used immortalised and highly proliferative cell lines.

Study by Wang *et al.* (2006), suggested that oxLDL promotes intracellular GSH depletion by alkylation of GSH and not through accumulation of GSSG or GSH efflux. They further confirmed this finding by showing that the peroxyl radical scavenger Trolox (a potent inhibitor of oxLDL-induced macrophage death) did not prevent GSH depletion and restore the GSH/GSSG, ratio confirming that nonoxidative mechanisms, e.g. alkylation, are likely to contribute to the depletion of GSH by oxLDL. Treatment with Trolox prevents oxLDL-induced protein-S-glutathionylation suggesting that peroxides and/ or peroxyl radicals may be directly involved in the enhanced S-glutathionylation of proteins induced by oxLDL. Wang *et al*., (2006) using knockdown experiments with siRNA directed against glutathione reductase and glutaredoxin showed that both enzymes are essential for the protection of macrophages against oxLDL.

5.3.1.3 OxLDL Induces the Generation of Mitochondrial ROS in HMDMs

This study also revealed a correlation between the loss of intracellular glutathione and inductions of oxidative stress in HMDMs upon exposure to oxLDL. Glutathione is a key component of the cellular defence mechanisms against oxidative and nitrosative stresses and play important roles in the detoxification of free radicals. Loss of glutathione would then certainly exacerbate the oxidative effect of the oxLDL.

ROS generation occurred as early as 3 hours and the possibility that it happened earlier than 3 hours (Figure 5.10) cannot be ruled out. The time of ROS (Figure 5.10) generation observed in this study is paralleled with the sudden drop in glutathione level (Figure 5.6) as well as sharp association of DiI-oxLDL with HMDMs (Figure 5.9). It is difficult to determine whether the loss of glutathione level precedes ROS generation or

vice versa as the fluorescent intensity observed under the fluorescent microscope was just a qualitative measurement.

OxLDL has been reported to be able to induce the generation of ROS (Hsieh *et al*., 2001; Zmijewski *et al*., 2005a; Zmijewski *et al*., 2005b) in the vascular cells and mitochondria are the major site of ROS production (Fleury *et al*., 2002). When ROS is released it will react with cellular macromolecules, either damaging them directly or setting in motion a chain reaction wherein the free radical is passed form one macromolecule to another, resulting in extensive damage to cellular structures such as membranes. ROS production may induce some modifications at various cellular levels.

ROS could react with the thiol groups of glutathione localised at the mitochondrial membrane level (Zamzami *et al*., 1997) and contribute to lower glutathione level. A low level of glutathione could favour the decrease in mitochondrial membrane potential which would subsequently affect the mitochondrial permeability transition (MPT) to finally induce the release of AIF and/ or cytochrome *c* (Stridth *et al*., 1998).

Studies of Lizard, Monier *et al.* (1999) have extensively examined major oxysterols such as 7β-OH as active components of human oxLDL and inducers for cell death. Another study (Lizard *et al*., 1998) demonstrated that glutathione is implicated in the control of 7-KC-induced apoptosis of U937 cells associated with the production of ROS. NAC, a scavenger of free radicals or a precursor of glutathione contributes to the observed protection against VSMC death induced by oxLDL-treatment (Hsieh *et al*., 2001).

5.3.1.4 Effect of OxLDL on Cytochrome *c* Release, Phosphatidylserine Exposure and Caspase-3 Activation

Incubation of cells with toxic concentrations of oxLDL induces progressive alterations of cell morphology and finally induces either apoptosis or necrosis of cultured cells depending on the balance between pro- and anti-apoptotic proteins. Cells undergoing apoptosis show an early reduction of the mitochondrial transmembrane potential with concomitant release of the mitochondrial protein cytochrome *c*. In the cytosol, cytochrome *c* in combination with Apaf-1 activates caspase-9, which finally leads to activation of caspase-3 (Stridth *et al*., 1998). Caspase-8 via plasma membrane receptors can also activate caspase-3. Caspase-3 is an executioner caspase, carrying out the protein cleavage processes of apoptosis, rather than merely forming part of the signalling cascade (Ashkenazi, *et al*., 1998). Its presence would therefore be a reliable indicator of the occurrence of caspase-mediated apoptosis in the cells. Apoptosis is further characterised

by labelling of the cell for clearance by phagocytes through exposure of phosphatidylserine on the cell's surface. In the absence of other cells to engulf the apoptotic cells secondary necrosis may follow apoptosis.

This study shows that the generation of ROS precede the release of cytochrome *c* and phosphatidylserine exposure when HMDMs were exposed to oxLDL. Cytochrome *c* release occurred after 6 hours incubation with oxLDL. OxLDL significantly triggered the cells to exhibit PS exposure after 6 hours incubation and maximum number of cells had PS exposure after 12 hours incubation indicating that apoptosis death start occurring after 6 hours exposure to oxLDL.

Caspase-3 is believed to be a key enzyme in the apoptosis program yet, in this study, Western Blot analysis of procaspase-3 revealed no proteolytic activation in oxLDL-treated cells regardless of the oxLDL concentrations (1 and 2 mg/ml oxLDL) and time of incubations (12 and 24 hours) used (Figure 5.14). This is in agreement with an earlier work in this laboratory (Gieseg *et al*., 2008b) showing no caspase-3 activity through the absence of DEVD-AMC (acetyl-asp-glu-val-asp-7-amido-4-methyl-coumarin) cleavage in HMDMs treated with 0 to 3 mg/ml oxLDL for 24 hours. Even though Gieseg *et al*., (2008b) (Figure 2 in Gieseg *et al*., 2008b) used 3 mg/ml of oxLDL to achieve 50% death of HMDMs, and in the present study 1 mg/ml oxLDL was used, the data is comparable since both concentrations caused approximately 50 % loss in cell viability.

Previous studies with HMDMs showed that oxLDL induced caspase-3 activation (Wintergerst *et al*., 2000; Muralidhar *et al*., 2004), though activation of caspase-3 does not promote macrophage lysis or death (Wintergerst *et al*., 2000). However, oxLDL induced-apoptosis were carried out in serum free RPMI (Asmis & Jelk, 2000) or in RPMI containing foetal calf serum (Muralidhar *et al*., 2004). By indirect immunofluorescent staining of the 7A6 antigen, an apoptosis-related mitochondrial membrane protein, Wintergerst *et al.,* (2000) clearly showed that apoptosis induced by oxLDL was completely suppressed when human serum was present in the media.

Incubation of macrophages with oxLDL resulted in a prominent cytochrome *c* translocation has been demonstrated earlier (Heinloth, *et al*., 2002). Cytochrome *c* translocation has been found to parallel the accumulation of p53 and enhanced nuclear condensation (Heinloth, *et al*., 2002). The relevance of cytochrome *c* released with no caspase-activation in the present study was not clear, since it is presumed that release of cytochrome *c* from mitochondria into the cytosol is a central event in intrinsic apoptosis signalling: the Apaf-1-driven formation of apoptosomes and downstream caspase activation designating a point-of-no-return in apoptosis. Formation of apoptosome

requires ATP or dATP (Aoshima *et al*., 1997; Hampton *et al*., 1998; Zou *et al*., 1999). OxLDL has been shown to down regulate intracellular glyceraldehydes-3-phosphate dehydrogenase (GAPDH) level in U937 cells (Katouah[3], unpublished data). Moreover, in endothelial cells, oxLDL downregulated GAPDH via a H_2O_2-dependent decrease in protein stability as shown by pulse-chase labelling experiments (Sukhanov *et al*., 2006). Down regulation of GAPDH resulted in reduction in glycolysis rate and consequently marked depletion of cellular ATP levels (Sukhanov *et al*., 2006). Since ATP was needed for the assembly of apoptosome to execute caspase-3 (Fadeel *et al*., 1998), its depletion could also correlate to the inhibition of caspase-3 activation.

In addition, only a small fraction of cytochrome *c* is commonly utilised in the formation of apoptosome and redox characteristics of cytochrome *c* are not essential for this process (Fadeel *et al*., 1998). Recent finding suggest that cytochrome *c* has two other important functions (Kagan, *et al*., 2004). Both functions are directed towards oxidation of two phospholipids: cardiolipin in the mitochondria and PS in the plasma membrane. Binding of cardiolipin with cytochrome *c* yields the cytochrome *c*/CL complex (Kagan, *et al*., 2006) that leads to the generation of cardiolipin hydroperoxides. This happens after the production of reactive oxygen species (Fernandez *et al*., 2002) in the mitochondria. The oxidised cardiolipin binds to cytochrome *c* poorly (Shidoji, *et al*., 1999) and, therefore, can participate in the formation of the mitochondrial permeability transition pore that facilitates the release of cytochrome *c* from the mitochondria into the cytosol. Cytochrome *c* released into the cytosol also binds to PS located at the cytoplasmic surface of the plasma and induces its oxidation (Tyurina, *et al*., 2000; Bayir, *et al*., 2006). This leads to redistribution of PS to the outer membrane and recognition of PS on the cell surface by specialised receptors of phagocytes.

The present study also revealed that PS exposure occurred in the presence of oxLDL in the absence of caspase-3 activation. Similar observation was seen in U937 cells (Baird *et al*., 2004). PS exposure was initially described as strictly caspase-dependent but now it is known that it can be regulated by caspase dependent or independent pathways (Yu *et al*., 2000). Experiments with stimulated neutrophils have suggested that the flipping of PS might instead depend on oxidative stress (Fadeel *et al*., 1998; Hampton *et al*., 2002).

The mitochondrial permeability transition pore (mPTP) is a multi-ion thiol sensitive channel (Crompton, 1999). The oxLDL-induced loss of cellular glutathione could result in the oxidation of the mPTP and therefore the loss of the mitochondrial transmembrane potential. The changes in mPTP have the effect of regulating the release of mitochondrial

[3] Katouah is currently a PhD student in Dr Steven Gieseg's laboratory

molecules such as AIF and cytochrome *c*, though this may not account for all activating agents and cells types (Stridh, *et al*.,1998). The idea of a thiol sensitive channel on mitochondria is also supported by a study where incubation of U937 cells with 7-KC caused a loss of endogenous glutathione that favoured apoptotic features such as decreased mitochondrial membrane potential and cytochrome *c* release (Lizard, *et al*., 1998). OxLDL-induced release of AIF from mitochondria and thereby promote caspase-independent apoptosis was recently reported in endothelial cells (Chen *et al*., 2004; Vindis, *et al*., 2005). The immunofluorescence staining reported by Vindis *et al.* (2005) revealed that oxLDL treated cells exhibited a partial relocation of AIF in the cytoplasm and the nucleus. Their data showed that AIF release is calcium dependent but independent of mPTP opening and calpain activation which is in contrast to cytochrome *c* release.

In the present study (Figure 5.11), the immnunofluorescent staining of cytochrome *c* showed increase in fluorescence intensity of the nuclei and cytosol in oxLDL-treated cells in comparison to the control cells. Studies by Nur-E-Kamal *et al.* (2004) using HeLa cells also showed that cytochrome *c* released from mitochondria gradually accumulates in the nucleus upon apoptosis induction with ultraviolet and campthothecin. Parallel to nuclear accumulation of cytochrome *c* was the released of acetylated histone H2A which preceded chromatin condensation and independent of caspase-3 activity. Changes in nuclear morphology in U937 and THP-1 cells treated with oxLDL (Baird, 2003) had been demonstrated in this lab using Hoechst 33342 staining. Therefore, there is a possibility that oxLDL-induced nuclear accumulation of cytochrome *c* in HMDMs may be directly involved in the remodelling of chromatin in inducing caspase-independent nuclear apoptosis.

Caspase activities require the presence of a free thiol residue within the active site of the enzymes. The active thiol groups which include a reduced cysteine thiol residue, are prone to oxidation in the presence of oxidants such as hydrogen peroxide, resulting in caspase inactivation (Hampton, *et al*., 2002; Fadeel, *et al*., 1998). The rapid loss of HMDMs intracellular glutathione, which precedes the viability loss, would make caspase thiols prone to oxidation and activity loss. The importance of the glutathione in caspase activity is highlighted by comparison between monocyte like, U937 and THP-1 cells. U937 cells treated with oxLDL rapidly lose cellular glutathione and fail to activate caspase-3 while THP-1 cells glutathione levels are only reduced by 25% with caspase-3 being activated along with the appearance of an apoptotic annexin-V staining population (Baird *et al*., 2005). Similarly, in THP-1 cells rapid loss of glutathione caused by the AAPH peroxyl radicals also resulted in the loss of caspase activity (Kappler *et al*., 2007).

Macrophage like RAW264.7 cells treated with BSO has also been reported to lose caspase activity during nitric oxide donor initiated apoptosis (Boggs, *et al*., 1998).

While some studies (Chen *et al*., 2004; Vindis *et al*., 2005; Walter *et al*., 1998) showed that oxLDL induced caspase-3 activation, other (Porn-Ares *et al*., 2003)) reported that apoptosis in the endothelial cells is independent of caspase-3. Porn-Ares *et al* . (2003) demonstrated that oxLDL induced polyubiquitination of caspase-3 which cause degradation and hence loss of caspase-3 activity. Ubiquitination (covalent conjugation of 8.5 kDa ubiquitin molecules, in the form of multi-ubiquitin chains) of caspases has been reported previously to inactivate the caspases (Huang, *et al*., 2000; Suzuki, *et al*., 2001). The discrepancy in their results is probably due to differences in the level of LDL oxidation. The oxLDL of Vindis *et al.* (2005) and Chen *et al.* (2004) are mildly oxidised (6 to 9 nmol TBARS per mg apoB), whereas those used by Porn-Ares *et al.* (2003) were extensively oxidised (25 to 45 nmol BARS per mg apoB). The higher level of oxidised lipids may explain both ubiquitination and enzyme inactivation, because highly oxidised LDL may induce cell protein modification and enzyme inactivation. This is consistent with the finding that moderately oxidised oxLDL (8 to 8.4 nmol/mg TBARS) promoted caspase-3 activation in human macrophages (Asmis & Begley, 2003; Wintergerst *et al*., 2000).

5.3.2 7,8-Dihydroneopterin and Protection Against OxLDL-induced Damaged on HMDMs

5.3.2.1 7,8-Dihydroneopterin Inhibits Cell Viability Loss

The present study found that 7,8-NP provided significant protection for HMDMs against oxLDL's toxic effect (Figure 5.16). The loss of viability induced by oxLDL on HMDMs was reduced in the presence of 7,8-NP. Previous study in this laboratory had shown that incubation of the oxLDL with 7,8-NP during 2 hours prior to addition to U937 did not decrease the toxicity of oxLDL (Baird, 2003). This suggests that 7,8-NP did not influence the oxLDL directly and the inhibition of oxLDL-induced damage was mediated via cellular processes. Trolox, a peroxyl radical scavenger, had also been shown to completely prevent human macrophage death from oxLDL-induced death (Wang *et al*., 2006). Since this study utilised heavily oxLDL whose characteristics include high lipid peroxyl radical contents, it is therefore possible that 7,8-NP's protective effect is also partly due to its ability to scavenge peroxyl radical. This idea is supported by previous studies in which

7,8-NP had been shown to protect erythrocytes from lysis induced by peroxyl radical (Duggan *et al*., 2001; Gebicki *et al*., 2000). Moreover, spin trapping study had clearly demonstrated that 7,8-NP effectively scavenged peroxyl radical (Oettl *et al*., 1997). This laboratory had shown that 7,8-NP inhibited cellular damage to red blood cells and the monocyte like human-derived U937 cells from a range of oxidants including hydrogen peroxide, HOCL, aqueous peroxyl and direct plasma membrane oxidation by ferrous ions (Duggan *et al*., 2002; Gieseg *et al*., 2000a; Gieseg *et al*., 2000b)

The effective protective concentrations of 7,8-NP was significantly higher than those in serum during immune activation. However, taking into account that activated T-lymphocytes, macrophages and neutrophils accumulate at the site of inflammation and release cytokines, oxygen-free radicals and pteridines, the concentration of 7,8-NP may be much higher than that in serum. It should be noted that in this study, 7,8-NP concentrations utilised was not toxic to cells.

The protective effect of 7,8-NP depends on the type of oxidants and cell types. For example, it protected U937 cells but not THP-1 cells from oxLDL-induced death and it offered no protective effect on ethanol-induced death on U937 cells (Baird, 2003). 7,8-NP also delays the development of the cytopathic effect of influenza A virus in canine kidney epithelial cells (MDCK) but not the cytopathic effect by Coxsackie B5 virus in human larynx carcinoma epithelial (Hep-2) cells (Bratslavska *et al*., 2007). Treatment of virus with 7,8-NP prior to addition to cells did not decrease the virus titer, which further support that 7,8-NP's effect was mediated via cellular processes.

5.3.2.2 7,8-Dihydroneopterin Inhibits Intracellular Glutathione Loss and Scavenges ROS Generated in the Presence of OxLDL

Loss of glutathione may exacerbate the oxidative stress effect of the oxLDL on HMDMs. Co-incubation of oxLDL with 200 μM 7,8-NP restored 40% of the glutathione loss caused by 1 mg/ml oxLDL (Figure 5.18). Similar experimental condition also restored 40% of the cell viability (Figure 5.16). It is usually assumed that GSH depletion reflects an intracellular oxidation, although direct evidence for it causing ROS production is difficult to obtain. In the present study, increased in ROS generation in a time-dependent manner was observed when HMDMs were challenged with oxLDL (Figure 5.10). The protection given by 7,8-NP up to 6 hours incubation (Figure 5.21) points to the ability of 7,8-NP to potently quench the ROS thus helping to create a more reducing environment and revive the cells.

Prevention of glutathione loss is important as it is required to maintain a reducing environment within the cells and hence maintaining their viability. For example in U937 cells, a rapid decrease in intracellular glutathione content was observed during 7-KC-induced apoptosis. The addition of glutathione and NAC was able to prevent the cell death implying the role of glutathione in the 7-KC-induced apoptosis (Lizard, *et al*., 1998). By using a laser confocal microscopy, an early involvement of ROS overproduction was proven to occur during 7-KC induced apoptosis in J774A.1 macrophages (Leonarduzzi *et al*., 2006). The almost complete inhibition of 7-KC-dependent ROS increase by two selective inhibitors of NADPH-oxidase (diphenylene iodonium and aminoethyl-benzenesulfonylfluoride) points to the ability of 7-KC to potently and rapidly induce oxidative burst in J774A.1 cells by activating NADPH-oxidase. In addition antioxidant epicatechin was also able to quench the ROS production induced by 7-KC (Leonarduzzi *et al*., 2006).

Thiol loss caused by 2-oxoaldehydes methylglyoxal and 3-deoxyglucosone was suppressed by NAC and enhanced by BSO in U937 cells and this was reflected in the viability (Okado *et al*., 1996). U937 cells lost 50% of their reduced glutathione with t-BuOOH (agent that caused rapid oxidation of mitochondrial pyridine nucleotides) followed by mitochondrial production of ROS by 2 hours (Nieminen *et al*., 1997) and the addition of antioxidant caffeic acid halved this loss (Nardini *et al*., 1998). GSH and NAC could also impair apoptosis caused by etoposide (inhibitor of topoisomerase II) but not cycloheximide (inhibitor of protein synthesis) (Lizard *et al*., 1998). NAC, deferoxamine and catalase all of which are radical scavenging agents were found to contribute to the observed protection against vascular smooth muscle cells induced by oxLDL (Hsieh *et al*., 2001). Altogether these studies support the idea that protecting the cellular glutathione loss and eliminating the ROS will protect the cells from death.

5.3.2.3 7,8-Dihydroneopterin Does Not Inhibit Cytochrome *c* Release From Mitochondria into the Cytosol Induced by OxLDL

The presence of 7,8-NP in HMDMs culture that had been exposed to oxLDL did not prevent the release of cytochrome *c* from the mitochondria (Figures 5.12-13). This is not surprising since oxLDL generated high level of ROS species in the mitochondria. Even though 7,8-NP can scavenge the ROS to a certain extent, the damage done by oxLDL on the mitochondrial membrane does not appear to be prevented. One of the proposed mechanisms for ROS induction of apoptosis is that, ROS act upon mitochondria, causing a

disruption of mitochondrial membrane potential and the release of cytochrome *c* (Chandra & Orennius, 2002; Stridth *et al*., 1998). The ROS could also possibly assist in the formation of the mitochondrial permeability transition pore that facilitates in the release of cytochrome *c* from the mitochondria into the cytosol (Shidoji, *et al*., 1999). OxLDL-induced apoptosis has been shown to be caused by a decrease in mitochondrial membrane potential and increased cytochrome *c* release in human aortic vascular smooth muscle cells (Li *et al*., 2003), endothelial cells (Walter *et al*., 1998) and human macrophages (Asmis & Begley, 2003). Treatment of endothelial cells with cyclosporin A completely inhibited the oxLDL-induced release of cytochrome *c* (Walter *et al*., 1998). This implies the importance of restoring the mitochondrial membrane potential in preventing the cytochrome *c* release. The inability of 7,8-NP to prevent the cytochrome *c* release in the present study, suggests that 7,8-NP has very little effect on restoring the mitochondrial membrane potential.

5.3.2.4 7,8-Dihydroneopterin Inhibits Phosphatidylserine Exposure in the HMDMs Exposed to OxLDL

7,8-NP failed to inhibit PS exposure in HMDMs when HMDMs were exposed to oxLDL for 24 hours (Figure 5.23). Interestingly, when HMDMs were exposed to oxLDL for a shorter time, a significant decrease in PS externalisation was observed (Figure 5.24). Similar to the ROS quenching ability, the 7,8-NP inhibitory effect on PS exposure was best achieved up to 6 hours incubation of the HMDMs with oxLDL. These results suggest that there is a correlation between the time of HMDMs exposure to oxLDL and the effective protective effect of 7,8-NP. The ability of 7,8-NP to quench ROS and inhibit the PS exposure clearly showed that the best protective effect of 7,8-NP was up to 6 hours' incubation of HMDMs with oxLDL. These results complemented the finding of previous studies in this lab (Baird *et al*., 2005) where 7,8-NP could be added toU937 cells up to 6 hours after oxLDL exposure and still provided a significant increase in U937 cells viability.

PS is being externalised to the outer plasma membrane when it is being oxidised. Therefore, once again it is the ability of 7,8-NP to scavenge the ROS, thus, providing a more reducing environment that prevents the PS from being oxidised and externalised.

5.3.2.5 7,8-Dihydroneopterin Inhibits OxLDL Uptake – The Role of CD36 and SR-A

ANOVA analysis revealed that 1 and 24 hour incubation of 7,8-NP with 1 mg/ml of DiI-oxLDL did not significantly reduce the DiI-oxLDL uptake by HMDMs (Figure 5.29). However, when lower concentrations of DiI-oxLDL (not toxic to HMDMs) were used, a significant decrease in the DiI-oxLDL uptake was observed (Figures 5.30-31). This is intriguing because earlier, the present study has shown that 7,8-NP was able to restore the viability, inhibit the glutathione loss, quench the ROS and inhibit the PS exposure caused by oxLDL at 1 mg/ml concentration. There is a possibility that the protective effect of 7,8-NP is a time-effect. For instance, as shown in Figure 5.23, incubation of 7,8-NP with 1 mg/ml oxLDL for 24 hours did not show inhibition in PS exposure. However, time course study demonstrated that 7,8-NP gave maximum protection against 1 mg/ml oxLDL-induced PS exposure up to 12 hours incubation (Figure 5.24). Similarly ROS generation were efficiently inhibited when HMDMs were incubated with 7,8-NP and oxLDL up to 12 hours incubation (Figure 5.21 and 5.22). Therefore, future studies could investigate the existence of time correlation in 7,8-NP preventing the oxLDL uptake. Nevertheless, the reduction in oxLDL uptake by HMDMs might imply that 7,8-NP has the capacity to prevent oxLDL from being taken up by HMDMs. Another implication of this finding is that 7,8-NP might influence oxLDL uptake either through modulation of scavenger and/or non-scavenger receptor mechanisms.

The dominant paradigm in atherosclerosis, is that uptake of oxLDL by SR-A and CD36 constitutes the major pathways for cholesteryl ester accumulation and therefore foam cell formation and atherogenesis. This paradigm arises from the experiments in mice in which these macrophage SR pathways were inactivated by homologous recombination. Several studies, though not all, suggested that deletion of the gene locus that codes for SR-A or CD36 substantially decrease arterial lipid accumulation in hyperlipidemic mouse models (de Winther *et al*., 1999; Febbraio *et al*., 2000; Gough *et al*., 1999). This is supported by a study that demonstrated that macrophages lacking both SR-A and CD36 show an 80-90% reduction in the internalisation and degradation of oxLDL and acLDL (Kunjathoor *et al*., 2002). The same study also revealed that the predominant receptor involved was CD36 and the combined effect of absence of both SRs was not significantly greater than the absence of CD36 alone.

Treatment of vascular cells with antioxidant and anti-inflammatory agent seemed to be able to reduce the SRs expression. In THP-1 cell lines and PBMCs obtained from

healthy volunteers, IL-10 reduced baseline CD36 expression and stimulate the expression of the cellular cholesterol exporters, ABCA1 and ABCG1 (Rubic & Lorenz, 2006). Marleau, *et al.* (2005) reported that EP 80317, a CD36 ligand derived from the growth hormone (GH)-releasing peptide family but devoid of any GH releasing activity reduced oxidized low density lipoproteins internalisation and up-regulated genes involved in cholesterol efflux, including peroxisome proliferator-activated receptor γ (PPARγ), liver x receptor α (LXRα), and the ATP binding cassette (ABC) transporters ABCA1 and ABCG1. Long-term treatment of apoE/CD36 double-deficient mice with EP 80317 did not modulate the expression of genes of the PPARγ-LXRα-ABC transporters pathway suggesting that the effect of EP 80317 was CD36 dependent. These two studies (Marleau *et al*., 2005; Rubic & Lorenz, 2006) support a role of CD36 in regulating peripheral cholesterol trafficking.

Treatment of smooth muscle cells with α-tocopherol inhibits oxLDL uptake by a mechanism involving downregulation of CD36 protein and mRNA expression (Ricciarelli, *et al*., 2000). In J774 cells, vitamin E reduces the uptake of DiI-acLDL and suppresses ACAT activity, resulting in less cholesterol esterification in macrophages (Shige *et al*., 1998). Another study (Teupser *et al*., 1999) associates this effect with a reduced SR-A mRNA expression and activity of AP-1 binding transcription factors in the presence of α-tocopherol. Devaraj *et al.* (2001) has further characterised the effect of α-tocopherol on CD36 mRNA human macrophages where down regulation of CD36 mRNA was clearly demonstrated to reduce the DiI-AcLDL and DiI-oxLDL uptake with concomitant decrease in cholesteryl ester accumulation.

Therefore, in the present study interest has been focused on the effect of 7,8-NP on SR-A and CD36 protein expression in HMDMs. 7,8-NP up to 200 μM failed to exert any effect on the SR-A protein expression. None of the monomer bands seemed to be reduced in the presence of 100 and 200 μM of 7,8-NP.

Interestingly, the effect of 7,8-NP on the CD36 protein expression was quite ambiguous. Another interesting finding was that, while most authors showed their Western Blot of CD36 as only a single band of 88 kDa protein, the present study was in agreement with others (Alessio *et al*., 1996; Munteanu *et al*., 2005) where CD36 could undergo glysosylation and have more than one glycoforms. The present study showed that CD36 could display a single or up to three glycoforms while Alessio *et al.,* (1996) and Munteanu *et al.,* (2005) showed that the U937 and THP-1 cells had three glycoforms. The present study and that of Alessio *et al.,* (1996) and Munteanu *et al.,* (2005) also showed that the molecular weight of the glycoforms were between 75 to 115 kDa.

In the present study the down regulation of CD36 expression was seen when the two glycoforms present were of further apart (80 and 100 kDa) with only the lower molecular weight, 80 kDa, decreased in its intensity and protein expression (Figure5.33). However, when the bands were very close to each other (75 and 86 kDa) or presence as a single band (86 kDa), their intensity seemed to be increased with increasing concentrations of 7,8-NP (Figures 5.34 and 5.35). If time course of 7,8-NP effect on oxLDL-induce PS exposure and ROS generation revealed that 7,8-NP protective was indeed time-related, effect of 7,8-NP on CD36 protein expression was still uncertained. The time course studies gave inconsistent results in terms of down regulatory effect of 7,8-NP on CD36 protein expression. While one result showed a remarkable time-dependent down regulatory effect of 7,8-NP on all the glycoforms present (Figure 5.36) , the other result showed increase in the CD36 protein expression with increasing incubation time with 7,8-NP (Figure5.37).

It is not understood why the CD36 bands were different in molecular weight with each experiment and also why the number of bands (CD36 glycoforms) present was also different. It has been shown that when THP1 and U937 were stimulated with PMA the 74-kDa CD36 band was converted to 90-106 kDa glycoforms (Alessio *et al*., 1996). However, since the HMDMs that were utilised for all the experiments in the present study were of the same age and were predominantly macrophages, the maturation of CD36 could not be accounted for the presence of different pattern of bands. Also the human serum used for culturing these cells was of the same age, therefore the variation in the factors presence in the serum that could influence the CD36 expression could also be ruled out. Perhaps the variable effect of 7,8-NP on CD36 protein expression is because of many critical factors that might interact with 7,8-NP. However, which factor that influence the effect of 7,8-NP is difficult to ascertain here.

However, if there is a down regulation effect of 7,8-NP on CD36 specifically the 80-kDA band, this can be related to Kunjathoor, *et al.*, (2002) study where they showed that the predominant receptor involved in the processing of oxLDL and acLDL was CD36 since the combined effect of absence of both SRs was not significantly greater than the absence of CD36 alone. This result points to the ability of 7,8-NP to downregulate the CD36 surface receptor and therefore decrease the oxLDL uptake by HMDMs to a certain extent. However, since this was not a 100% inhibition in oxLDL uptake, other mechanisms of oxLDL uptake should also be accounted to.

There is considerable evidence pointing out that LDL-derived lipids can enter macrophage via other pathways. According to the response-to-retention hypothesis

(Carpenter *et al*., 1995a), serum lipoproteins accumulate in the arterial intima where a variety of modifications, including but not limited to oxidation, can alter their structure and enhance their uptake by recruited macrophages. LDL needs oxidation or acetylation to become a high-affinity ligand for the scavenger receptors. In contrast modifications induced by enzymes (e.g., sphingomyelinase, phospholipase C, or secretory phospholipase A2) can lead to increased retention of lipoproteins by matrix proteoglycans and aggregation into large macromolecular complexes that are internalised by non-scavenger receptor-mediated pathways, such as phagocytic, patocytic, or pinocytic uptake mechanisms (Kruth *et al*., 2005; Lougheed & Steinbrecher, 1996). Krieger and Herz (1994) reported that both SR-AI and SR-AII mediates endocytosis of acLDL and oxLDL. Furthermore, another study reported that (Kruth, *et al*., 2005) native LDL can also be internalised by macropinocytosis thus recognising foam cell formation via a non-receptor-mediated mechanisms. As the concentrations of native or aggregated LDL determined in human intimal samples typically exceed 100 mg/dl, these forms of LDL may provide substantially greater amounts of lipid than can be taken up by the SR pathways, which saturates at lipoprotein concentrations 25-50 μg/ml (Rohrer *et al*., 1990).

The involvement of SR-A or CD36 in the uptake of oxLDL in the present study was not really proven and therefore, should be considered for future studies. However, the fact that CD36 is more specific in taking up oxLDL (Boullier *et al*., 2000; Endemann *et al*., 1993) whereby SR-A is being related more to acLDL than oxLDL (Kunjathoor *et al*., 2002; Suzuki *et al*., 1997), and also 7,8-NP has an effect on CD36 and not SR-A probably relate to the involvement of CD36 in taking up the oxLDL in the present study.

Some literature reported that the heterogeneity in terms of the extent of oxidation of LDL and/or the degree of aggregation in oxLDL also affect the mechanisms of oxLDL uptake. Lougheed and Steinbrecher (1996) reported that the extent of copper oxidation of LDL affects its mechanism of uptake and that about half of the uptake of very extensively oxLDL appears to be via a pathway distinct from the SR-AI and SR-AII. The uptake of very extensively oxidised LDL was not affected by cytochalasin D, an inhibitor of phagocytosis and also by an antibody to CD36 in HMDM or in THP-1 cells, suggesting that this alternate pathway does not involve CD36. In addition, studies of SR-A or CD36 knockout mice showed that disruption of SR-A or CD36 only partially inhibits oxLDL uptake in macrophages and prevents atherosclerotic progression in hypercholesterolemic mice (Febbraio *et al*., 2000; Suzuki *et al*., 1997) implying that other SRs or other mechanisms of oxLDL were involved.

5.4 Summary

Macrophage derived foam cells have been identified as the most abundant cells found in the proximity of necrotic core. The involvement of macrophage injury and death in the lesion progression and the formation of necrotic core have been extensively studied for a few decades. A lot of oxidants can cause the injury and death. However, since oxLDL is a prominent component of atherosclerotic lesions it is therefore believed to be the major factor that caused the macrophage injury and death.

In the present study, the heavily oxLDL caused loss in HMDMs' viability and the death caused by 1 mg/ml of oxLDL was of apoptotic and necrotic appearances. Higher concentration of oxLDL caused the HMDMs to commit necrotic death. Therefore, the mechanism of death caused by 1 mg/ml of oxLDL was investigated in the present study. Even though oxLDL induced cytochrome *c* released into the cytosol, apoptotic death through caspase-3 activation was unlikely since oxLDL failed to activate caspase-3 activity. This was not surprising since the glutathione loss caused by oxLDL was very tremendous and this affect the thiol group of the caspases. ROS was generated by the HMDMs shortly after exposure to oxLDL causing oxidative stress to the cells and therefore creating a less reducing environment which favours the rapid loss of glutathione. The present study further demonstrated that glutathione depletion was required for oxLDL-induced toxicity to HMDMs. The oxidative stress also caused cytochrome *c* to be released into the cytosol and PS being externalised to the outer plasma membrane.

The protective effects of 7,8-NP on HMDMs seemed to be due to its ability to scavenge the ROS and inhibit oxLDL uptake. 7,8-NP at 200 μM effectively reduced the cell viability loss caused by oxLDL. 7,8-NP was shown to scavenge the mitochondrial ROS generated due to oxLDL, inhibit glutathione loss and PS from being externalised to the outer membrane. 7,8-NP also significantly inhibited the uptake of oxLDL but only at non-toxic concentration of oxLDL. This admittedly was only measured at 1 and 24 hours. 7,8-NP clearly did not affect SRA protein expression. However, in 50% of the experiments 7,8-NP significantly reduced the CD36 protein expression. This inconsistent effect of 7,8-NP on CD36 still needs to be defined. The ability of 7,8-NP to protect HMDMs from oxLDL-induced death provides evidence that this antioxidant is secreted by HMDMs to protect them against the oxidative damage in the highly oxidative environment of atherosclerotic plaque. The relevance of these data on the possible action of 7,8-NP to inhibit or slow cell death in the advance plaque formation will be discussed in Chapter 6.

6 General Discussion and Conclusions

6.1 Effect of OxLDL on HMDMs

Exposure to subtoxic concentration of oxLDL causes monocyte-macrophages to proliferate (Chisolm & Chai, 2000). Macrophages take up oxLDL, accumulate CE and transform into foam cells which is a hallmark of atherosclerosis. This thesis shows that the foamy appearance and presence of lipid droplets stained with oil red-O was not dependent on accumulation of CE. This raises a doubt on the suitability of using oil red-O stain to identify the foam cells. The fact that foam cells were as susceptible as HMDMs to toxic oxLDL contributes a greater detrimental effect to the atherosclerotic plaque.

HMDMs were found to undergo concentration-dependent viability loss in the presence of oxLDL. Concentrations of oxLDL above 0.2 mg/ml were toxic to HMDMs with 1 mg/ml causing approximately 50% loss in cell viability after 24 hour incubation. The time course study with 1 mg/ml oxLDL showed that the cell viability drop was quite gradual with a sudden drop in viability occurring after 12 hours incubation. Twelve hours incubation period was also the time point where the association of HMDMs with DiI-oxLDL plateau off suggesting that 12 hours exposure to 1 mg/ml was the time point where the cells committed to death. There is a high possibility that 7-KC contributes most to the toxicity of oxLDL in this study since time course investigations by other researchers (Brown *et al*., 1997; Harris *et al*., 2006; Jessup & Kritharides, 2000; Upston *et al*., 2002) demonstrated that highly oxLDL contain almost exclusively of 7-KC. This is of relevance to the *in vivo* situation where analysis of plaque revealed that 7-KC was the major sterol detected at late stage of lesion development (Brown *et al*., 1997).

The drop in cell viability caused by oxLDL was correlated to the loss of intracellular glutathione. At any time point, the percentage loss of glutathione was greater than the loss of cell viability. The sublethal dose of 0.1 mg/ml oxLDL caused 30% loss of HMDMs glutathione indicating that HMDMs' intracellular glutathione content was very sensitive to oxLDL. Moreover, the loss of glutathione was very rapid with 30% loss after 3 hours exposure to 1 mg/ml of oxLDL. Potential mechanism of glutathione loss reported previously in HMDMs was through alkylation of GSH and not through accumulation of GSSG or GSH efflux (Wang *et al*., 2006). Treatment of HMDMs with BSO and DEM for 24 hours also caused a similar drop in glutathione level. However, glutathione depletion by BSO or DEM, did not promote HMDMs death, indicating that oxLDL-induced decrease in intracellular glutathione was necessary. It is possible that depletion of reduced glutathione by oxLDL alters the glutathione thiol redox state (GSH/GSSG ratio) (Wang *et*

al., 2006) leading to cellular dysfunction and cell death (Schafer & Buettner, 2001). Depletion of cellular glutathione by BSO or DEM was not sufficient to promote HMDMs probably because they did not significantly alter the thiol redox environment.

OxLDL had been reported previously to be able to induce the generation of ROS in the SMCs and ECs (Hsieh *et al*., 2001; Zmijewski *et al*., 2005a; Zmijewski *et al*., 2005b). Similarly, HMDMs also generated ROS in the presence of oxLDL just after 3 hours of incubation. This thesis cannot ascertain whether ROS generation caused the drop in intracellular glutathione level or *vice versa*. However, these two events already contributed to a significant oxidative stress to macrophages.

This thesis demonstrated clearly that the generation of ROS and glutathione loss precede the release of cytochrome *c* and phosphatidylserine exposure since the last two events occur significantly after 6 hours exposure of HMDMs to oxLDL. The loss of glutathione contributed to decreased mitochondrial membrane potential with subsequent release of cytochrome *c* (Lizard *et al*., 1998; Stridth *et al*., 1998; Zmijewski *et al*., 2005a) In addition mitochondrial ROS generation can lead to the formation of cardiolipin hydroperoxides (Kagan *et al*., 2006) that binds to cytochrome *c* poorly (Shidoji, *et al*., 1999). The complex can participate in the formation of the mitochondrial permeability transition pore that facilitates the release of cytochrome *c* from the mitochondria into the cytosol. Cytochrome *c* can then bind to PS inducing its oxidation and redistribution to the outer membrane (Tyurina, *et al*., 2000; Bayir, *et al*., 2006).

The release of cytochrome c from mitochondria into the cytosol is known to be a central event in intrinsic apoptosis signalling. However, despite the occurrence of PS exposure, no caspase-3 activation was detected within 24 hours incubation of HMDMs with oxLDL. PS exposure was initially described as strictly caspase-dependent but experiments with stimulated neutrophils have suggested that the flipping of PS might instead depend on oxidative stress (Fadeel *et al*., 1998; Hampton *et al*., 2002) as mentioned above. Thus, future studies is needed to investigate the exact mechanism of how oxLDL-induced PS externalisation.

Others had reported that oxLDL induced caspase-3 activation (Chen *et al*., 2004; Vindis *et al*., 2005; Walter *et al*., 1998). The absence of caspase-3 activity in this thesis probably correlated with the rapid loss of glutathione. Caspases activities require the presence of free thiol residues within the active site of the caspase enzymes. These active thiol groups are prone to oxidation (Hampton, *et al*., 2002; Fadeel, *et al*., 1998). Therefore, the rapid loss of HMDMs intracellular glutathione causes oxidation of caspase thiols and therefore loss of their activities. Modulation of apoptotic pathways by oxidative

stress, through Bcl-2 or ceramide for example, can also replace caspase regulation of events. Another explanation for the absence of caspase-3 activity is the ability of oxLDL to induce polyubiquitination of caspase-3 which cause degradation and ultimately loss of caspase-3 activity (Huang, *et al.*, 2000). The differences in the level of LDL oxidation could also affect caspase-3 activity. The higher level of oxidised lipids may cause both ubiquitination and enzyme inactivation, since highly oxidised LDL may induce cell protein modification and enzymes inactivation. The execution of caspase-3 also requires dATP and or ATP. Therefore, it is of interest to investigate the effect oxLDL on HMDMs energy metabolism in order to clarify whether rapid loss of energy could contribute to caspase inactivation. The uptake of oxLDL against loss of metabolic function is also another area that needs to be explored.

6.2 The Protective Effect of 7,8-NP on OxLDL-induced Damage

This thesis shows that supplementation of HMDMs with 200μM 7,8-NP able to restore 40% of the HMDMs viability and glutathione losses caused by 1 mg/ml oxLDL. Previous study had shown that incubation of 7,8-NP with oxLDL (in the absence of cells) does not reduce oxLDL cytotoxicity (Baird, 2003) suggesting that inhibition of oxLDL-induced damage was mediated via cellular processes. The mechanism appears to involve the protection of the intracellular glutathione pool by scavenging the intracellular oxidants generated by the oxLDL thus maintaining the redox status of the cell. The same mechanism appears to occur with 7,8-NP protection of U937 cells on oxLDL-induced necrosis (Baird *et al.*, 2005).

Although 7,8-NP can quench the ROS, it provides no protection against oxLDL-induced cytochrome c release from mitochondria to the cytosol. This is rather intriguing. It is postulated that the absence of protection may be caused by the failure of the 7,8-NP to restore the mitochondrial membrane potential which lead to the release of cytochrome c. Perhaps, future research that measures the timing of loss of mitochondrial membrane potential and cytochrome c release will give a better understanding of 7,8-NP's role on the cytochrome c release.

Similar to the ROS quenching ability, the 7,8-NP inhibitory effect on PS exposure is best achieved up to 6 hours incubation of the HMDMs with oxLDL which suggest a correlation between the time of HMDMs exposure to oxLDL and the effective protective effect of 7,8-NP. Thus, the best protective effect of 7,8-NP was up to 6 hours' incubation

of HMDMs with oxLDL. These results complement the finding of Baird *et al*., (2005) where 7,8-NP could be added to U937 cells up to 6 hours after oxLDL exposure and still provided a significant increase in U937 cells viability. Since the externalisation of PS involves its oxidation, this further support 7,8-NP's protective mechanism which is scavenging the ROS thus, providing a more reducing environment that prevents the PS from being oxidised and externalised.

The most surprising finding was that 7,8-NP efficiently inhibits the uptake of oxLDL labelled with DiI after 24 hours incubation. However, it does so with only subtoxic concentration of oxLDL and not with 1 mg/ml oxLDL. Therefore, a future study investigating the existence of time correlation in 7,8-NP preventing the oxLDL uptake is needed since 7,8-NP inhibition of ROS generation and PS externalisation were correlated with time of incubation. The inhibition of oxLDL uptake by 7,8-NP implies that 7,8-NP might influence oxLDL uptake by interacting with the scavenger receptors or other mechanisms of oxLDL uptake. Since administration of 7,8-NP decreases the uptake of oxLDL it is beneficial to measure whether 7,8-NP affect the CE accumulation. If 7,8-NP inhibits CE accumulation, this could suggest a protective effect against the conversion of macrophages into foam cells.

7,8-NP up to 200 μM failed to exert any effect on the SR-A protein expression. It has been shown previously that SR-A is being related more to acLDL than oxLDL (Kunjathoor *et al*., 2002; Suzuki *et al*., 1997). 7,8-NP has no effect on SR-A probably because it does not involve in the uptake of oxLDL. Having said that a further study is therefore needed to clarify whether SR-A involve in the uptake of oxLDL by HMDMs in this thesis.

The down regulation of CD36 protein and mRNA expression by α-tocopherol which correlates to reduce uptake of oxLDL has been reported elsewhere (Devaraj, *et al*., 2001; Ricciarelli, *et al*., 2000). This thesis shows that in 50% of experiments, 7,8-NP effectively down regulated the levels of CD36 receptor protein in HMDM cells. It is important to note that the number of CD36 isoform varied from one sample to another and normally there was more than one CD36 isoform. The presence of isoforms is due to the glycosylation of CD36. Interestingly, 7,8-NP exerts different effects on the isoforms present in the same sample. It could lower the expression of one isoform but had no effect or increased the expression of the other isoform in the same sample. This pattern of results was displayed after 24 hours incubation or using time course examinations. Perhaps the variable effect of 7,8-NP on CD36 protein expression is because of many critical factors that might interact with 7,8-NP. However, which factor that influence the effect of 7,8-NP

is difficult to ascertain here. More experiments are needed to determine the exact role of 7,8-NP on CD36.

6.3 7,8-NP in the Atherosclerotic Plaque

Atherosclerotic plaque represents site of chronic inflammation and contain a range of reactive oxidants including oxLDL that can trigger cells death. This thesis contributes more evidence that high concentration of oxLDL is cytotoxic to macrophages and to the hypothesis that 7,8-NP is synthesised *in vivo* to protect macrophages from oxidative damage.

The finding that 7,8-NP can protect HMDMs from oxLDL-induced death is very important to the atherosclerotic plaque development since 7,8-NP is synthesised by the macrophages themselves. *In vivo*, the production of 7,8-NP is expected to occur predominantly at sites of inflammation since this is where macrophages are recruited. Even though the protective concentration of 7,8-NP used *in vitro* is far higher than the level found *in vivo*, this should not be trivialised since, over the course of years it could contribute significantly to minimising the oxidative damage. In addition, when the cells produce the antioxidant by themselves as oppose to having it exogenously added, it can therefore be a better antioxidant. The ability of 7,8-NP to inhibit LDL oxidation and macrophage death could then prevent the growth of plaques and their development to complex and unstable plaques.

References

Abdalla, D. S., Campa, A. & Monteiro, H. P. (1992). Low density lipoprotein oxidation by stimulated neutrophils and ferritin. *Atherosclerosis*, **97**(2-3), 149-59.

Acton, S. L., Scherer, P. E., Lodish, H. F. & Krieger, M. (1994). Expression cloning of SR-BI, a CD36-related class B scavenger receptor. *J Biol Chem*, **269**(33), 21003-9.

Adam, W., Kurz, A. & Saha-Moller, C. R. (2000). Peroxidase-catalyzed oxidative damage of DNA and 2'-deoxyguanosine by model compounds of lipid hydroperoxides: involvement of peroxyl radicals. *Chem Res Toxicol*, **13**(12), 1199-207.

Akagawa, K. S., Takasuka, N., Nozaki, Y., Komuro, I., Azuma, M., Ueda, M., Naito, M. & Takahashi, K. (1996). Generation of CD1+RelB+ dendritic cells and tartrate-resistant acid phosphatase-positive osteoclast-like multinucleated giant cells from human monocytes. *Blood*, **88**(10), 4029-39.

Akagawa, K. S. (2002). Functional heterogeneity of colony-stimulating factor-induced human monocyte-derived macrophages. *Int J Hematol*, **76**, 27-34.

Akeson, A. L., Schroeder, K., Woods, C., Schmidt, C. J. & Jones, W. D. (1991). Suppression of interleukin-1 beta and LDL scavenger receptor expression in macrophages by a selective protein kinase C inhibitor. *J Lipid Res*, **32**(10), 1699-707.

Alcouffe, J., Caspar-Bauguil, S., Garcia, V., Salvayre, R., Thomsen, M. & Benoist, H. (1999). Oxidized low density lipoproteins induce apoptosis in PHA-activated peripheral blood mononuclear cells and in the Jurkat T-cell line. *J Lipid Res*, **40**(7), 1200-10.

Alessio, M., De Monte, L., Scirea, A., Gruarin, P., Tandon, N. N. & Sitia, R. (1996). Synthesis, processing, and intracellular transport of CD36 during monocytic differentiation. *J Biol Chem* **271**(3), 1770-5.

Amento, E. P., Ehsani, N., Palmer, H. & Libby, P. (1991). Cytokines and growth factors positively and negatively regulate interstitial collagen gene expression in human vascular smooth muscle cells. *Arterioscler Thromb* **11**(5), 1223-30.

Anderson, F., Game, B. A., Atchley, D., Xu, M., Lopes-Virella, M. F. & Huang, Y. (2002). IFN-gamma pretreatment augments immune complex-induced matrix metalloproteinase-1 expression in U937 histiocytes. *Clin Immunol*, **102**(2), 200-7.

Aoshima, H., Satoh, T., Sakai, N., Yamada, M., Enokido, Y., Ikeuchi, T. & Hatanaka, H. (1997). Generation of free radicals during lipid hydroperoxide-triggered apoptosis in PC12h cells. *Biochim Biophys Acta*, **1345**(1), 35-42.

Ashkenazi, A. & Dixit, V. M. (1998). Death receptors: Signaling and modulation. *Science*, **281**(5381), 1305-8.

Ashkenazi, A. (2002). Targeting death and decoy receptors of the tumour-necrosis factor superfamily. *Nat Rev Cancer*, **2002**(2), 420-30.

Asmis, R. & Wintergerst, E. S. (1998). Dehydroascorbic acid prevents apoptosis induced by oxidized low-density lipoprotein in human monocyte-derived macrophages. *Eur J Biochem*, **255**, 147-55.

Asmis, R. & Jelk, J. (2000a). Vitamin E supplementation of human macrophages prevents neither foam cell formation nor increased susceptibility of foam cells to lysis by oxidized LDL. *Arterioscler Thromb Vasc Biol*, **20**(9), 2078-86.

Asmis, R. & Jelk, J. (2000b). Large variations in human foam cell formation in individuals: a fully autologous *in vitro* assay based on the quantitative analysis of cellular neutral lipids. *Atherosclerosis*, **148**(2), 243-53.

Asmis, R. & Begley, J. G. (2003). Oxidized LDL promotes peroxide-mediated mitochondrial dysfunction and cell death in human macrophages: a caspase-3-independent pathway. *Circ Res*, **92**(1), e20-9.

Auge, N., Garcia, V., Maupas-Schwalm, F., Levade, T., Salvayre, R. & Negre-Salvayre, A. (2002). Oxidized LDL-induced smooth muscle cell proliferation involves the EGF receptor/PI-3 kinase/Akt and the sphingolipid signaling pathways. *Arterioscler Thromb Vasc Biol*, **22**(12), 1990-5.

Aupiex, K., Weltin, D., Mejia, J. E., Christ, M., Marchal, J., Freyssinet, J. & Bischoff, P. (1995). Oxysterol-induced apoptosis in human monocytic cell lines. *Immunobiol*, **194**, 415-28.

Babaev, V. R., Gleaves, L. A., Carter, K. J., Suzuki, H., Kodama, T., Fazio, S. & Linton, M. F. (2000). Reduced atherosclerotic lesions in mice deficient for total or macrophage-specific expression of scavenger receptor-A. *Arterioscler Thromb Vasc Biol*, **20**(12), 2593-9.

Baier-Bitterlich, G., Fuchs, D., Murr, C., Reibnegger, G., Werner-Felmayer, G., Sgonc, R., Bock, G., Dierich, M. P. & Wachter, H. (1995). Effect of neopterin and 7,8-dihydroneopterin on tumor necrosis factor-alpha induced programmed cell death. *FEBS Lett*, **364**(2), 234-8.

Baier-Bitterlich, G., Baier, G., Fuchs, D., Bock, G., Hausen, A., Utermann, G., Pavelka, M. & Wachter, H. (1996a). Role of 7,8-dihydroneopterin in T-cell apoptosis and HTLV-1 transcription *in vitro*. In *Oncogene*, Vol. 13, pp. 2281-2285.

Baier-Bitterlich, G., Fuchs, D. & Wachter, H. (1996a). 7,8-Dihydroneopterin upregulates interferon-gamma promoter in T cells. *Immunobiology*, **196**(4), 350-5.

Baier-Bitterlich, G., Fuchs, D. & Wachter, H. (1997a). Chronic immune stimulation, oxidative stress, and apoptosis in HIV infection. *Biochem Pharmacol*, **53**(6), 755-63.

Baier-Bitterlich, G., Fuchs, D., Zangerle, R., Baeuerle, P. A., Werner, E. R., Fresser, F., Überall, F. & Wachter, H. (1997b). Trans-activation of the HIV type 1 promoter by 7,8-dihydroneopterin *in vitro*. *AIDS Res and Human Retrovir*, **13**(2), 173-8

Baird, S. (2003). 7,8-Dihydroneopterin inhibition of oxidised low density lipoprotein-induced cellular death. *PhD Thesis,* University of Canterbury, New Zealand.

Baird, S. K., Hampton, M. B. & Gieseg, S. P. (2004). Oxidized LDL triggers phosphatidylserine exposure in human monocyte cell lines by both caspase-dependent and -independent mechanisms. *FEBS Lett*, **578**(1-2), 169-74.

Baird, S. K., Reid, L., Hampton, M. B. & Gieseg, S. P. (2005). OxLDL induced cell death is inhibited by the macrophage synthesised pterin, 7,8-dihydroneopterin, in U937 cells but not THP-1 cells. *Biochim Biophys Acta*, **1745**(3), 361-9.

Balogh, A., Mittermayr, M., Schlager, A., Balogh, D., Schobersberger, W., Fuchs, D. & Margreiter, J. (2005). Mechanism of neopterin-induced myocardial dysfunction in the isolated perfused rat heart. *Biochim Biophys Acta*, **1724**(1-2), 17-22.

Barak, M. & Gruener, N. (1991). Neopterin augmentation of tumor necrosis factor production. *Immunol Lett*, **30**(1), 101-6.

Bayir, H., Fadeel, B., Palladino, M. J., Witasp, E., Kurnikov, I. V., Tyurina, Y. Y., Tyurin, V. A., Amoscato, A. A., Jiang, J. & Kochanek, P. M. e. a. (2006). Apoptotic interactions of cytochrome c: Redox flirting with anionic phospholipids within and outside of mitochondria. *14th European Bioenergetics Conference*, **1757**(5-6), 648-59.

Bea, F., Hudson, F. N., Chait, A., Kavanagh, T. J. & Rosenfeld, M. E. (2003). Induction of glutathione synthesis in macrophages by oxidized low-density lipoproteins is mediated by consensus antioxidant response elements. *Circ Res* **92**(4), 386-93.

Berliner, J. A., Navab, M., Fogelman, A. M., Frank, J. S., Demer, L. L., Edwards, P. A., Watson, A. D. & Lusis, A. J. (1995). Atherosclerosis: basic mechanisms. Oxidation, inflammation, and genetics. *Circulation*, **91**(9), 2488-96.

Berliner, J. A. & Heinecke, J. W. (1996). The role of oxidized lipoproteins in atherogenesis. *Free Radic Biol Med*, **20**(5), 707-27.

Berridge, M. V., Tan, A. S., McCoy, K. D. & Wang, R. (1996). The biochemical and cellular basis of cell proliferation assays that use tetrazolium salts. *Biochemica*, **4**, 15-20.

Berthier, A., Lemaire-Ewing, S., Prunet, C., Monier, S., Athias, A., Bessède, G., Pais de Barros, J. P., Laubriet, A., Gambert, P., Lizard, G. & Néel, D. (2004). Involvement of a calcium-dependent dephosphorylation of BAD associated with the localization of Trpc-1 within lipid rafts in 7-ketocholesterol-induced THP-1 cell apoptosis. *Cell Death Differ*, **11**(8), 897-905.

Bird, D. A., Gillotte, K. L., Horkko, S., Friedman, P., Dennis, E. A., Witztum, J. L. & Steinberg, D. (1999). Receptors for oxidized low-density lipoprotein on elicited mouse peritoneal macrophages can recognize both the modified lipid moieties and the modified protein moieties: Implications with respect to macrophage recognition of apoptotic cells. *Proc Natl Acad Sci USA*, **96**, 6347–52.

Bjorkerud, S. & Bjorkerud, B. (1996a). Apoptosis is abundant in human atherosclerotic lesions, especially in inflammatory cells (macrophages and T cells), and may contribute to the accumulation of gruel and plaque instability. *Am J Pathol*, **149**(2), 367-80.

Bjorkerud, B. & Bjorkerud, S. (1996b). Contrary effects of lightly and strongly oxidized LDL with potent promotion of growth versus apoptosis on arterial smooth muscle cells, macrophages, and fibroblasts. *Arterioscler Thromb Vasc Biol*, **16**(3), 416-24.

Boggs, S. E., McCormick, T. S. & Lapetina, E. G. (1998). Glutathione levels determine apoptosis in macrophages. *Biochem Biophys Res Commun*, **247**(2), 229-33.

Boring, L., Gosling, J., Cleary, M. & Charo, I. F. (1998). Decreased lesion formation in CCR2-/- mice reveals a role for chemokines in the initiation of atherosclerosis. *Nature*, **394**(6696), 894-7.

Boullier, A., Gillotte, K. L., Horkko, S., Green, S. R., Friedman, P., Dennis, E. A., Witztum, J. L., Steinberg, D. & Quehenberger, O. (2000). The binding of oxidized low density lipoprotein to mouse CD36 is mediated in part by oxidized phospholipids that are associated with both the lipid and protein moieties of the lipoprotein. *J Biol Chem*, **275**(13), 9163-9.

Boullier, A., Li, Y., Quehenberger, O., Palinski, W., Tabas, I., Witzum, J. L. & Miller, Y. I. (2006). Minimally oxidised LDL offsets theapoptotic effects of extensively oxidised LDL and free cholesterol in macrophages. *Arterioscler Thromb Vasc Biol*, **26,** 1169-76.

Bratslavska, O., Platace, D., Miklasevics, E., Fuchs, D. & Martinsons, A. (2007). Influence of neopterin and 7,8-dihydroneopterin on the replication of Coxsackie type B5 and influenza A viruses. *Med Microbiol Immunol*, **196**, 23-9.

Brown, M. S., Goldstein, J. L., Krieger, M., Ho, Y. K. & Anderson, R. G. (1979). Reversible accumulation of cholesteryl esters in macrophages incubated with acetylated lipoproteins. *J Cell Biol*, **82**(3), 597-613.

Brown, A. J., Dean, R. T. & Jessup, W. (1996). Free and esterified oxysterol: formation during copper-oxidation of low density lipoprotein and uptake by macrophages. *J Lipid Res*, **37**, 320-35.

Brown, A. J., Leong, S. L., Dean, R. T. & Jessup, W. (1997). 7-Hydroperoxycholesterol and its products in oxidized low density lipoprotein and human atherosclerotic plaque. *J Lipid Res*, **38**(9), 1730-45.

Brown, A. J., Mander, E. L., Gelissen, I. C., Kritharides, L.. Dean, R. T. & Jessup, W. (2000). Cholesterol and oxysterol metabolism and subcellular distribution in macrophage foam cells. Accumulation of oxidized esters in lysosomes. *J Lipid Res*, **41**(2), 226-37.

Brunk, C. F., Jones, K. C. & James, T. W. (1979). Assay for nanogram quantities of DNA in cellular homogenates. *Anal Biochem*, **92**(2), 497-500.

Burnaugh, L., Sabeur, K. & Ball, B. A. (2006). Generation of superoxide anion by equine spermatozoa as detected by dihydroethidium. *Theriogenology*, **67**(3), 580-9

Cachia, O., Benna, J. E., Pedruzzi, E., Descomps, B., Gougerot-Pocidalo, M.-A. & Leger, C.-L. (1998). alpha -Tocopherol inhibits the respiratory burst in human monocytes. Attenuation of p47phox membrane translocation and phosphorylation. *J Biol Chem*, **273**(49), 32801-5.

Cai, J. & Jones, D. P. (1998). Superoxide in apoptosis. Mitochondrial generation triggered by cytochrome c loss. *J Biol Chem*, **273**(19), 11401-4.

Camejo, G., Halberg, C., Manschik-Lundin, A., Hurt-Camejo, E., Rosengren, B., Olsson, H., Hansson, G. I., Forsberg, G. B. & Ylhen, B. (1998). Hemin binding and oxidation of lipoproteins in serum: mechanisms and effect on the interaction of LDL with human macrophages. *J Lipid Res*, **39**(4), 755-66.

Carmody, R. J. & Cotter, T. G. (2001). Signalling apoptosis: a radical approach. *Redox Rep*, **6**(2), 77-90.

Carpenter, K. L., Wilkins, G. M., Fussell, B., Ballantine, J. A., Taylor, S. E., Mitchinson, M. J. & Leake, D. S. (1994). Production of oxidized lipids during modification of low-density lipoprotein by macrophages or copper. *Biochem J*, **304 (Pt 2)**, 625-33.

Carpenter, K. L., Taylor, S. E., van der Veen, C., Williamson, B. K., Ballantine, J. A. & Mitchinson, M. J. (1995a). Lipids and oxidised lipids in human atherosclerotic lesions at different stages of development. *Biochim Biophys Acta*, **1256**(2), 141-50.

Carpenter, K. L., van der Veen, C., Taylor, S. E., Hardwick, S. J., Clare, K., Hegyi, L. & Mitchinson, M. J. (1995b). Macrophages, lipid oxidation, ceroid accumulation and alpha-tocopherol depletion in human atherosclerotic lesions. *Gerontology*, **41 Suppl 2**, 53-67.

Carpenter, K. L., Dennis, I. F., Challis, I. R., Osborn, D. P., Macphee, C. H., Leake, D. S., Arends, M. J. & Mitchinson, M. J. (2001). Inhibition of lipoprotein-associated phospholipase A2 diminishes the death-inducing effects of oxidised LDL on human monocyte-macrophages. *FEBS Lett*, **505**(3), 357-63.

Carpenter, K. L., Challis, I. R. & Arends, M. J. (2003). Mildly oxidised LDL induces more macrophage death than moderately oxidised LDL: roles of peroxidation, lipoprotein-associated phospholipase A2 and PPARgamma. *FEBS Lett*, **553**(1-2), 145-50.

Carr, A. C., McCall, M. R. & Frei, B. (2000). Oxidation of LDL by myeloperoxidase and reactive nitrogen species: reaction pathways and antioxidant protection. *Arterioscler Thromb Vasc Biol*, **20**(7), 1716-23.

Chandra, J. & Orennius, S. (2002). Mitochondria, oxygen metabolism and the regulation of cell death. *International Congress Series*, **1233**, 259-72.

Cheeseman, K. H. & Slater, T. F. (1993). An introduction to free radical biochemistry. *Br Med Bull*, **49**(3), 481-93.

Chen, J., Mehta, J. L., Haider, N., Zhang, X., Narula, J. & Li, D. (2004). Role of caspases in ox-LDL-induced apoptotic cascade in human coronary artery endothelial cells. *Circ Res,* **94**(3), 370-6.

Chisolm, G. M., Ma, G., Irwin, K. C., Martin, L. L., Gunderson, K. G., Linberg, L. F., Morel, D. W. & DiCorleto, P. E. (1994). 7 beta-hydroperoxycholest-5-en-3 beta-ol, a component of human atherosclerotic lesions, is the primary cytotoxin of oxidized human low density lipoprotein. *Proc Natl Acad Sci USA*, **91**(24), 11452-6.

Chisolm, G. M., 3rd, Hazen, S. L., Fox, P. L. & Cathcart, M. K. (1999). The oxidation of lipoproteins by monocytes-macrophages. Biochemical and biological mechanisms. *J Biol Chem*, **274**(37), 25959-62.

Chisolm, G. M., 3rd & Chai, Y. (2000). Regulation of cell growth by oxidized LDL. *Free Radic Biol Med*, **28**(12), 1697-707.

Coffey, M. D., Cole, R. A., Colles, S. M. & Chisolm, G. M. (1995). *In vitro* cell injury by oxidized low density lipoprotein involves lipid hydroperoxide-induced formation of alkoxyl, lipid, and peroxyl radicals. *J Clin Invest*, **96**(4), 1866-73.

Cole, K. E., Strick, C. A., Paradis, T. J., Ogborne, K. T., Loetscher, M., Gladue, R. P., Lin, W., Boyd, J. G., Moser, B., Wood, D. E., Sahagan, B. G. & Neote, K. (1998). Interferon-inducible T cell alpha chemoattractant (I-TAC): a novel non-ELR CXC chemokine with potent activity on activated T cells through selective high affinity binding to CXCR3. *J Exp Med*, **187**(12), 2009-21.

Cory, S. & Adams, J. M. (2005). Killing cancer cells by flipping the Bcl-2/Bax switch. *Cancer Cell*, **8**(1), 5-6.

Cotgreave, I. A. & Modleus, P. (1986). Methodologies for the application of monobromobimane to the simultaneous analysis of soluble and protein thiol components of biological systems. *J Biochem Biophys Methods*, **13**, 231-49.

Crompton, M. (1999). The mitochondrial permeability transition pore and its role in cell death. *Biochem J*, **341**, 233-49.

Darley-Usmar, V. M., Severn, A., O'Leary, V. J. & Rogers, M. (1991). Treatment of macrophages with oxidized low-density lipoprotein increases their intracellular glutathione content. *Biochem J*, **278 (Pt 2)**, 429-34.

de Beer, M. C., Zhao, Z., Webb, N. R., van der Westhuyzen, D. R. & de Villiers, W. J. S. (2003). Lack of a direct role for macrosialin in oxidized LDL metabolism. *J Lipid Res,* **44**(4), 674-85.

Devaraj, S., Hugou, I. & Jialal, I. (2001). Alpha-tocopherol decreases CD36 expression in human monocyte-derived macrophages. *J Lipid Res*, **42**(4), 521-7.

de Nigris, F., Franconi, F., Maida, I., Palumbo, G., Anania, V. & Napoli, C. (2000). Modulation by [alpha]- and [gamma]-tocopherol and oxidized low-density lipoprotein of apoptotic signaling in human coronary smooth muscle cells. *Biochem Pharmacol*, **59**(11), 1477-87.

de Winther, M. P. J., van Dijk , K. W., van Vlijmen B.J.M., Gijbels, M. J. J., Heus, J. J., Wijers, E. R., van den Bos, A. C., Breuer, M., Frants, R. R., Havekes, L. M. & Hofker, M. H. (1999). Macrophage specific overexpression of the human macrophage scavenger receptor in transgenic mice, using a 180-kb yeast artificial chromosome, leads to enhanced foam cell formation of isolated peritoneal macrophages. *Atherosclerosis*, **147**(2), 339-7.

Dickson, B. C. & Gotlieb, A. I. (2003). Towards understanding acute destabilization of vulnerable atherosclerotic plaques. *Cardiovasc Pathol*, **12**(5), 237-48.

Dimmeler, S., Haendeler, J., Galle, J. & Zeiher, A. M. (1997). Oxidized low-density lipoprotein induces apoptosis of human endothelial cells by activation of CPP32-like proteases. *Circulation*, **95**, 1760-3.

Dong, Z. M., Chapman, S. M., Brown, A. A., Frenette, P. S., Hynes, R. O. & Wagner, D. D. (1998). The combined role of P- and E-selectins in atherosclerosis. *J Clin Invest*, **102**(1), 145-52.

Dougherty, G. J. & McBride, W. H. (1984). Macrophage heterogeneity. *J Clin Lab Immunol*, **14**(1), 1-11.

Draper, H. H., Squires, E. J., Mahmoodi, H., Wu, J., Agarwal, S. & Hadley, M. (1993). A comparative evaluation of thiobarbituric acid methods for the determination of malondialdehyde in biological materials. *Free Radic Biol Med*, **15**(4), 353-63.

Draude, G., von Hundelshausen, P., Frankenberger, M., Ziegler-Heitbrock, H. W. L. & Weber, C. (1999). Distinct scavenger receptor expression and function in the human CD14+/CD16+ monocyte subset. *Am J Physiol Heart Circ Physiol*, **276**(4), H1144-9.

Duggan, S., Rait, C., Gebicki, J. M. & Gieseg, S. P. (2001). Inhibition of protein oxidation by the macrophage-synthesised antioxidant 7,8-dihydroneopterin. *Redox Rep*, **6**(3), 188-90.

Duggan, S., Rait, C., Platt, A. & Gieseg, S. (2002). Protein and thiol oxidation in cells exposed to peroxyl radicals is inhibited by the macrophage synthesised pterin 7,8-dihydroneopterin. *Biochim Biophys Acta*, **1591**(1-3), 139-45.

Duke, R. C., Ojcius, D. M. & Young, J. D. (1996). Cell suicide in health and disease. *Sci Am*, **275**(6), 80-7.

Ehrenwald, E., Chisolm, G. M. & Fox, P. L. (1994). Intact human ceruloplasmin oxidatively modifies low density lipoprotein. *J Clin Invest*, **93**(4), 1493-501.

Ehrenwald, E. & Fox, P. L. (1996). Role of endogenous ceruloplasmin in low density lipoprotein oxidation by human U937 monocytic cells. *J Clin Invest*, **97**(3), 884-90.

Endemann, G., Stanton, L. W., Madden, K. S., Bryant, C. M., White, R. T. & Protter, A. A. (1993). CD36 is a receptor for oxidized low density lipoprotein. *J Biol Chem*, **268**(16), 11811-6.

Enzinger, C., Wirleitner, B., Bock, G., Baier-Bitterlich, G. & Fuchs, D. (2001). Influence of cytokines tumor necrosis factor-alpha and interferon-gamma on signaling cascades associated with apoptosis in rat PC12 cells. *Neurosci Lett*, **316**(3), 157-60.

Enzinger, C., Wirleitner, B., Spottl, N., Bock, G., Fuchs, D. & Baier-Bitterlich, G. (2002). Reduced pteridine derivatives induce apoptosis in PC12 cells. *Neurochem Int*, **41**(1), 71-8.

Ermak, N., Lacour, B., Drueke, T. B. & Vicca, S. (2008). Role of reactive oxygen species and Bax in oxidized low density lipoprotein-induced apoptosis of human monocytes. *Atherosclerosis*, **In Press, Corrected Proof**.

Escargueil-Blanc, I., Salvayre, R. & Salvayre, A. (1994). Necrosis and apoptosis induced by oxidised low density lipoproteins occur through two calcium-dependent pathways in lymphoblastoids cells. *FASEB J.*, **8**, 1075-80.

Esteban-Pretel, G. & López-García, M. P. (2006). An experimental design for the controlled modulation of intracellular GSH levels in cultured hepatocytes. *Free Radicl Biol Med*, **41**(4), 610-9.

Esterbauer, H., Striegl, G., Puhl, H. & Rotheneder, M. (1989). Continuous monitoring of *in vitro* oxidation of human low density lipoprotein. *Free Radic Res Commun*, **6**(1), 67-75.

Esterbauer, H., Dieber-Rotheneder, M., Waeg, G., Striegl, G. & Juergens, G. (1990). Biochemical structural and functional properties of oxidized low-density lipoprotein. *Chem Res Toxicol*, **3**(2), 77-92.

Esterbauer, H., Puhl, H., Dieber-Rotheneder, M., Waeg, G. & Rabl, H. (1991). Effect of antioxidants on oxidative modification of LDL. *Ann Med*, **23**(5), 573-81.

Esterbauer, H., Gebicki, J., Puhl, H. & Jurgens, G. (1992). The role of lipid peroxidation and antioxidants in oxidative modification of LDL. *Free Radic Biol Med*, **13**(4), 341-90.

Esterbauer, H., Wag, G. & Puhl, H. (1993). Lipid peroxidation and its role in atherosclerosis. *Br Med Bull*, **49**(3), 566-76.

Esterbauer, H., Gieseg, S., Giessauf, A., Ziouzenkova, O. & Ramos, P. (1995). Free radicals and oxidative modification of LDL: role of natural antioxidants. In *Atherosclerosis X*, eds. F. P. Woodford, J. Davignon & A. Sniderman, Vol. 10, Elsevier. Netherlands.

Fadeel, B., Ahlin, A., Henter, J.-I., Orrenius, S. & Hampton, M. B. (1998). Involvement of caspases in neutrophil apoptosis: Regulation by reactive oxygen species. *Blood*, **92**(12), 4808-18.

Falk, E. (2006). Pathogenesis of atherosclerosis. *J American College Cardiol*, **47**(8), C7-C12.

Febbraio, M., Podrez, E. A., Smith, J. D., Hajjar, D. P., Hazen, S. L., Hoff, H. F., Sharma, K. & Silverstein, R. L. (2000). Targeted disruption of the class B scavenger receptor CD36 protects against atherosclerotic lesion development in mice. *J Clin Invest*, **105**(8), 1049-56.

Fernandez, M. G., Troiano, L., Moretti, L., Nasi, m., Marcello, P., Salvioli, S., Dobrucki, J. & Cossarizza, A. (2002). Early changes in intramitochondrial cardiolipin distribution during apoptosis. *Cell Growth Differentiation*, **13**, 449-55.

Firth, C. A. (2006). 7,8-dihydroneopterin-mediated protection of low density lipoprotein, but not human macrophages, from oxidative stress. *PhD Thesis,* University of Canterbury, New Zealand.

Firth, C. A., Yang, Y. & Gieseg S. P. (2007). Lipid oxidation predominates over protein hydroperoxide formation in human monocyte-derived macrophages exposed to aqueous peroxyl radicals *Free Radic Res*, **41**, 839-48.

Firth, C.A., Laing, A.D., Baird, S.K., Pearson, J. & Gieseg, S.P. (2008). Inflammatory sites as a source of plasma neopterin: measurement of high levels of neopterin and markers of oxidative stress in pus drained from human abscesses. *Clin Biochem*, **41**(13), 1078-83.

Fleury, C., Mignotte, B. & Vayssière, J.-L. (2002). Mitochondrial reactive oxygen species in cell death signaling. *Biochimie,* **84**(2-3), 131-41.

Folcik, V. A., Aamir, R. & Cathcart, M. K. (1997). Cytokine modulation of LDL oxidation by activated human monocytes. *Arterioscler Thromb Vasc Biol*, **17**(10), 1954-61.

Freeman, N. E., Rusinol, A. E., Linton, M., Hachey, D. L., Fazio, S., Sinensky, M. S. & Thewke, D. (2005). Acyl-coenzyme A:cholesterol acyltransferase promotes oxidized LDL/oxysterol-induced apoptosis in macrophages. *J Lipid Res*, **46**(9), 1933-43.

Frei, B., Stocker, R. & Ames, B. N. (1988). Antioxidant defenses and lipid peroxidation in human blood plasma. *Proc Natl Acad Sci USA*, **85**(24), 9748-52.

Frostegard, J., Nilsson, J., Haegersstrand, A., Hamsten, A., Wigzell, H. & Gidlund, M. (1990). Oxidised low density lipoprotein induces differentiation and adhesion of human monocytes and the monocytic cell line U937. *Proc Natl Acad Sci USA*, **87**, 904-8.

Frostegard, J., Ulfgren, A. K., Nyberg, P., Hedin, U., Swedenborg, J., Andersson, U. & Hansson, G. K. (1999). Cytokine expression in advanced human atherosclerotic plaques: dominance of pro-inflammatory (Th1) and macrophage-stimulating cytokines. *Atherosclerosis*, **145**(1), 33-43.

Fuchs, D., Stahl-Hennig, C., Gruber, A., Murr, C., Hunsmann, G. & Wachter, H. (1994). Neopterin--its clinical use in urinalysis. *Kidney Int Suppl*, **47**, S8-11.

Fujiwara, K., Sato, H. & Bannai, S. (1998). Involvement of endotoxins or tumor necrosis factor-alpha in macrophage-mediated oxidation of low density lipoprotein. *FEBS Lett*, **431**(1), 116-20.

Galis, Z. S., Sukhova, G. K., Lark, M. W. & Libby, P. (1994). Increased expression of matrix metalloproteinases and matrix degrading activity in vulnerable regions of human atherosclerotic plaques. *J Clin Invest*, **94**(6), 2493-503.

Garner, B., Baoutina, A., Dean, R. T. & Jessup, W. (1997a). Regulation of serum-induced lipid accumulation in human monocyte-derived macrophages by interferon-gamma. Correlations with apolipoprotein E production, lipoprotein lipase activity and LDL receptor-related protein expression. *Atherosclerosis*, **128**(1), 47-58.

Garner, B., van Reyk, D., Dean, R. T. & Jessup, W. (1997b). Direct copper reduction by macrophages. Its role in low density lipoprotein oxidation. *J Biol Chem*, **272**(11), 6927-35.

Gebicki, J. M., Collins, J., Gay, C., Duggan, S. & Gieseg, S. (2000). The dissection of oxidative changes in human blood serum and U937 cells exposed to free radicals. *Redox Rep*, **5**(1), 55-6.

Gelissen, I. C., Brown, A. J., Mander, E. L., Kritharides, L., Dean, R. T. & Jessup, W. (1996). Sterol efflux is impaired from macrophage foam cells selectively enriched with 7-ketocholesterol. *J Biol Chem*, **271**(30), 17852-60.

Gelissen, I. C., Rye, K., Brown, A. J., Dean, R. T. & Jessup, W. (1999). Oxysterol efflux from macrophage foam cells: the essential reole of acceptor phospholipid. *J Lipid Res*, **40**, 1636-46.

Geng, Y. J. & Hansson, G. K. (1992). Interferon-gamma inhibits scavenger receptor expression and foam cell formation in human monocyte-derived macrophages. *J Clin Invest*, **89**(4), 1322-30.

Geng, Y. J., Holm, J., Nygren, S., Bruzelius, M., Stemme, S. & Hansson, G. K. (1995). Expression of the macrophage scavenger receptor in atheroma. Relationship to immune activation and the T-cell cytokine interferon-gamma. *Arterioscler Thromb Vasc Biol*, **15**(11), 1995-2002.

Gerry, A. B. & Leake, D. S. (2008). A moderate reduction in extracellular pH protects macrophages against apoptosis induced by oxidized low density lipoprotein. *J Lipid Res*, **49**(4), 782-9.

Ghibelli, L., Fanelli, C., Rotilio, G., Lafavia, E., Coppola, S., Colussi, C., Civitareale, P. & Ciriolo, M. R. (1998). Rescue of cells from apoptosis by inhibition of active GSH extrusion. *Faseb J*, **12**(6), 479-86.

Gibco Product Information. Macrophage-SFM. http://tools.invitrogen.com/content/sfs/brochures/SpecialtySFMediaforCC.pdf

Gieseg, S. P. & Esterbauer, H. (1994). Low density lipoprotein is saturable by pro-oxidant copper. *FEBS Letters*, **343**, 188-94.

Gieseg, S. P., Reibnegger, G., Wachter, H. & Esterbauer, H. (1995). 7,8 Dihydroneopterin inhibits low density lipoprotein oxidation *in vitro*. Evidence that this macrophage secreted pteridine as an anti-oxidant. *Free Radic Res*, **23**(2), 123-36.

Gieseg, S., Duggan, S. & Gebicki, J. M. (2000a). Peroxidation of proteins before lipids in U937 cells exposed to peroxyl radicals. *Biochem J*, **350 (Pt 1)**, 215-8.

Gieseg, S. P., Maghzal, G. & Glubb, D. (2000b). Inhibition of haemolysis by the macrophage synthesized antioxidant, 7,8-dihydroneopterin. *Redox Rep*, **5**(2-3), 98-100.

Gieseg, S. P., Maghzal, G. & Glubb, D. (2001). Protection of erythrocytes by the macrophage synthesized antioxidant 7,8 dihydroneopterin. *Free Radic Res*, **34**(2), 123-36.

Gieseg, S. P., Pearson, J. & Firth, C. A. (2003). Protein hydroperoxides are a major product of low density lipoprotein oxidation during copper, peroxyl radical and macrophage-mediated oxidation. *Free Radic Res*, **37**(9), 983-91.

Gieseg, S. P. & Cato, S. (2003). Inhibition of THP-1 cell-mediated low-density lipoprotein oxidation by the macrophage-synthesised pterin, 7,8-dihydroneopterin. *Redox Rep*, **8**(2), 113-5.

Gieseg, S. P., Crone, E. M., Flavall, E. & Amit, Z. (2008a). Potential to inhibit growth of atherosclerotic plaque development through modulation of macrophage neopterin/7,8-dihydroneopterin synthesis. *Brit J Pharmacol*, **153**, 627-35.

Gieseg, S.P.; Leake, D.S.; Flavall, E.; Amit, Z. & Yang, Y.T. (2008b). Macrophage antioxidant protection within atherosclerotic plaques, *Frontiers in Biosciences*, **14**, 1230-46

Giessauf, A., Steiner, E. & Esterbauer, H. (1995). Early destruction of tryptophan residues of apolipoprotein B is a vitamin E-independent process during copper-mediated oxidation of LDL. *Biochim Biophys Acta*, **1256**(2), 221-32.

Gimbrone, M. A. (1999). Vascular endothelium, hemodynamic forces, and atherogenesis. *Am J Pathol*, **155**(1), 1-5.

Glass, C. K. & Witztum, J. L. (2001). Atherosclerosis. the road ahead. *Cell*, **104**(4), 503-16.

Gotoh, N., Graham, A., Nikl, E. & Darley-Usmar, V. M. (1993). Inhibition of glutathione synthesis increases the toxicity of oxidized low-density lipoprotein to human monocytes and macrophages. *Biochem J*, **296 (Pt 1)**, 151-4.

Gough, P. J., ., Greaves, D. R., ., Suzuki, H., Hakkinen, T., Hiltunen, M. O., Turunen, M., Herttuala, S. Y., Kodama, T. & Gordon, S. (1999). Analysis of macrophage scavenger receptor (SR-A) expression in human aortic atherosclerotic lesions. *Arterioscler Thromb Vasc Biol*, **19**(3), 461-71.

Greaves, D. R. & Gordon, S. (2005). Thematic review series: the immune system and atherogenesis. Recent insights into the biology of macrophage scavenger receptors. *J Lipid Res*, **46**(1), 11-20.

Greenwalt, D. E., Watt, K. W., Hasler, T., Howard, R. J. & Patel, S. (1990). Structural, functional, and antigenic differences between bovine heart endothelial CD36 and human platelet CD36. *J Biol Chem*, **265**(27), 16296-9.

Greilberger, J., Oettl, K., Cvirn, G., Reibnegger, G. & Jurgens, G. (2004). Modulation of LDL oxidation by 7,8-dihydroneopterin. *Free Radic Res*, **38**(1), 9-17.

Grewal, T., Priceputu, E., Davignon, J. & Bernier, L. (2001). Identification of a gamma-interferon-responsive element in the promoter of the human macrophage scavenger receptor A gene. *Arterioscler Thromb Vasc Biol*, **21**(5), 825-31.

Grutter, M. G. (2000). Caspases: key players in programmed cell death. *Curr Opin Struct Biol*, **10**(6), 649-55.

Gu, L., Okada, Y., Clinton, S. K., Gerard, C., Sukhova, G. K., Libby, P. & Rollins, B. J. (1998). Absence of monocyte chemoattractant protein-1 reduces atherosclerosis in low density lipoprotein receptor-deficient mice. *Mol Cell*, **2**(2), 275-81.

Guyton, J. R., Lenz, M. L., Mathews, B., Hughes, H., Karsan, D., Selinger, E. & Smith, C. V. (1995). Toxicity of oxidized low density lipoproteins for vascular smooth muscle cells and partial protection by antioxidants. *Atherosclerosis*, **118**(2), 237-49.

Haberland, M. E., Olch, C. L. & Folgelman, A. M. (1984). Role of lysines in mediating interaction of modified low density lipoproteins with the scavenger receptor of human monocyte macrophages. *J Biol Chem*, **259**(18), 11305-11.

Hajek, P., Villani, G. & Attardi, G. (2000). Rate-limiting step preceding cytochrome *c* release in cells primed for Fas-mediated apoptosis revealed by analysis of cellular mosaicism of respiratory changes. *J Biol Chem*, **276**, 606-15.

Halliwell, B. & Gutteridge, J. M. C. (2007). *Free Radicals in Biology and Medicine. Fourth ed*. Oxford Univeristy Press, Oxford.

Hamerlinck, F. F. (1999). Neopterin: a review. *Exp Dermatol*, **8**(3), 167-76.

Hampton, M. B. & Orennius, S. (1997). Dual regulation of caspase activity by hydrogen peroxide: implications for apoptosis. *FEBS Letters*, **414**, 552-6.

Hampton, M. B., Zhivotovsky, B., Slater, A. F. G., Burgess, S. H. & Orennius, S. (1998). Importance of the redox state of cytochrome c during caspase activation in cytosolic extracts. *Biochem J*, **329**, 95-9.

Hampton, M. B., Morgan, P. E. & Davies, M. J. (2002). Inactivation of cellular caspases by peptide-derived tryptophan and tyrosine peroxides. *FEBS Lett*, **527**(1-3), 289-92.

Hansson, G. K., Holm, J. & Jonasson, L. (1989a). Detection of activated T lymphocytes in the human atherosclerotic plaque. *Am J Pathol*, **135**(1), 169-75.

Hansson, G. K., Hellstrand, M., Rymo, L., Rubbia, L. & Gabbiani, G. (1989b). Interferon gamma inhibits both proliferation and expression of differentiation-specific alpha-smooth muscle actin in arterial smooth muscle cells. *J Exp Med*, **170**(5), 1595-608.

Hansson, G. K. (2001). Regulation of immune mechanisms in atherosclerosis. *Ann N Y Acad Sci*, **947**, 157-65; discussion 165-6.

Hansson, G. K., Robertson, A.-K. L. & Soderberg-Naucler, C. (2006). Inflammation and atherosclerosis. *Annual Review of Pathology: Mechanisms of Disease*, **1**, 297-329.

Harada-Shiba, M., Kinoshita, M., Kamido, H. & Shimokado, K. (1998). Oxidized low density lipoprotein induces apoptosis in cultured human umbilical vein endothelial cells by common and unique mechanisms. *J Biol Chem*, **273**(16), 9681-7.

Harada, K., Ishibashi, S., Miyashita, S., Osuga, J., Yagyu, H., Ohashi, K., Yazaki, Y. & Yamada, N. (1997). Bcl-2 protein inhibits oxysterol-induced apoptosis through suppressing CPP32-mediated pathway. *FEBS Lett*, **411**, 63-6.

Harrington, E. A., Bennett, M. R., A Fanidi, A. & Evan, G. I. (1994). c-Myc-induced apoptosis in fibroblasts is inhibited by specific cytokines. *EMBO J.* , **13**(14), 3286-95.

Harris, L. K., Mann, G. E., Ruiz, E., Mushtaq, S. & Leake, D. S. (2006). Ascorbate does not protect macrophages against apoptosis induced by oxidised low density lipoprotein. *Arch Biochem Biophys*, **455**(1), 68-76.

Haunstetter, A. & Izumo, S. (1998). Apoptosis: basic mechanisms and implications for cardiovascular disease. *Circ Res*, **82**(11), 1111-29.

Hazell, L. J. & Stocker, R. (1993). Oxidation of low-density lipoprotein with hypochlorite causes transformation of the lipoprotein into a high-uptake form for macrophages. *Biochem J*, **290 (Pt 1)**, 165-72.

Hazen, S. L. & Heinecke, J. W. (1997). 3-Chlorotyrosine, a specific marker of myeloperoxidase-catalyzed oxidation, is markedly elevated in low density lipoprotein isolated from human atherosclerotic intima. *J Clin Invest*, **99**(9), 2075-81.

Hazen, S. L., Zhang, R., Shen, Z., Wu, W., Podrez, E. A., MacPherson, J. C., Schmitt, D., Mitra, S. N., Mukhopadhyay, C., Chen, Y., Cohen, P. A., Hoff, H. F. & Abu-Soud, H. M. (1999). Formation of nitric oxide-derived oxidants by myeloperoxidase in monocytes: pathways for monocyte-mediated protein nitration and lipid peroxidation *In vivo*. *Circ Res*, **85**(10), 950-8.

Heales, S. J., Blair, J. A., Meinschad, C. & Ziegler, I. (1988). Inhibition of monocyte luminol-dependent chemiluminescence by tetrahydrobiopterin, and the free radical oxidation of tetrahydrobiopterin, dihydrobiopterin and dihydroneopterin. *Cell Biochem Funct*, **6**(3), 191-5.

Heermeier, K., Leicht, W., Palmetshofer, A., Ullrich, M., Wanner, C. & Galle, J. (2001). Oxidized LDL suppresses NF-kB and overcomes protection from apoptosis in activated endothelial cells. *J Am Soc Nephrol* **12**, 456–63.

Hegyi, L., Skepper, J. N., Cary, N. R. & Mitchinson, M. J. (1996). Foam cell apoptosis and the development of the lipid core of human atherosclerosis. *J Pathol*, **180**(4), 423-9.

Heinecke, J. W., Rosen, H. & Chait, A. (1984). Iron and copper promote modification of low density lipoprotein by human arterial smooth muscle cells in culture. *J Clin Invest*, **74**(5), 1890-4.

Heinecke, J. W., Suits, A. G., Aviram, M. & Chait, A. (1991). Phagocytosis of lipase-aggregated low density lipoprotein promotes macrophage foam cell formation. Sequential morphological and biochemical events. *Arterioscler Thromb Vasc Biol*, **11**(6), 1643-51.

Heinecke, J. W., Li, W., Daehnke, H. L., 3rd & Goldstein, J. A. (1993). Dityrosine, a specific marker of oxidation, is synthesized by the myeloperoxidase-hydrogen peroxide system of human neutrophils and macrophages. *J Biol Chem*, **268**(6), 4069-77.

Heinecke, J. W. (1999). Mass spectrometric quantification of amino acid oxidation products in proteins: insights into pathways that promote LDL oxidation in the human artery wall. *Faseb J*, **13**(10), 1113-20.

Heinecke, J. W. (2002). Oxidized amino acids: culprits in human atherosclerosis and indicators of oxidative stress(1,2). *Free Radic Biol Med*, **32**(11), 1090-101.

Heinloth, A., Brüne, B., Fischer, B. & Galle, J. (2002). Nitric oxide prevents oxidised LDL-induced p53 accumulation, cytochrome c translocation, and apoptosis in macrophages via guanylate cyclase stimulation. *Atherosclerosis*, **162**(1), 93-101.

Henriksen, T., Mahoney, E. M. & Steinberg, D. (1981). Enhanced macrophage degradation of low density lipoprotein previously incubated with cultured endothelial cells: recognition by receptors for acetylated low density lipoproteins. *Proc Natl Acad Sci USA*, **78**(10), 6499-503.

Henriksen, T., Mahoney, E. M. & Steinberg, D. (1983). Enhanced macrophage degradation of biologically modified low density lipoprotein. *Arteriosclerosis*, **3**(2), 149-59.

Herijgers, N., de Winther, M. P. J., Van Eck, M., Havekes, L. M., Hofker, M. H., Hoogerbrugge, P. M. & Van Berkel, T. J. C. (2000). Effect of human scavenger receptor class A overexpression in bone marrow-derived cells on lipoprotein metabolism and atherosclerosis in low density lipoprotein receptor knockout mice. *J Lipid Res*, **41**(9), 1402-9.

Herpfer, I., Greilberger, J., Ledinski, G., Widner, B., Fuchs, D. & Jurgens, G. (2002). Neopterin and 7,8-dihydroneopterin interfere with low density lipoprotein oxidation mediated by peroxynitrite and/or copper. *Free Radic Res*, **36**(5), 509-20.

Hockenbery, D. M., Oltvai, Z. N., Yin, X. M., Milliman, C. L. & Korsmeyer, S. J. (1993). Bcl-2 functions in an antioxidant pathway to prevent apoptosis. *Cell*, **75**(2), 241-51.

Hoffmann, G., Schobersberger, W., Frede, S., Pelzer, L., Fandrey, J., Wachter, H., Fuchs, D. & Grote, J. (1996). Neopterin activates transcription factor nuclear factor-kappa B in vascular smooth muscle cells. *FEBS Lett*, **391**(1-2), 181-4.

Hoffmann, G., Kenn, S., Wirleitner, B., Deetjen, C., Frede, S., Smolny, M., Rieder, J., Fuchs, D., Baier-Bitterlich, G. & Schobersberger, W. (1998). Neopterin induces nitric oxide-dependent apoptosis in rat vascular smooth muscle cells. *Immunobiology*, **199**(1), 63-73.

Hoffmann, G., Rieder, J., Smolny, M., Seibel, M., Wirleitner, B., Fuchs, D. & Schobersberger, W. (1999). Neopterin-induced expression of intercellular adhesion molecule-1 (ICAM-1) in type II-like alveolar epithelial cells. *Clin Exp Immunol*, **118**(3), 435-40.

Hoffmann, G., Wirleitner, B. & Fuchs, D. (2003). Potential role of immune system activation-associated production of neopterin derivatives in humans. *Inflamm Res*, **53**, 313-21.

Hsieh , C. C., Yen, M. H., Yen , C. H. & Lau, Y. T. (2001). Oxidized low density lipoprotein induces apoptosis via generation of reactive oxygen species in vascular smooth muscle cells. *Cardiovasc Res* **49**(1), 135-45.

Huang, H.-k., Joazeiro, C. A. P., Bonfoco, E., Kamada, S., Leverson, J. D. & Hunter, T. (2000). The inhibitor of apoptosis, cIAP2, functions as a ubiquitin-protein ligase and promotes *in vitro* monoubiquitination of caspases 3 and 7. *J Biol Chem*, **275**(35), 26661-4.

Huh, H. Y., Pearce, S. F., Yesner, L. M., Schindler, J. L. & Silverstein, R. L. (1996). Regulated expression of CD36 during monocyte-to-macrophage differentiation: potential role of CD36 in foam cell formation. *Blood*, **87**(5), 2020-8.

Innerarity, T. L., Pitas, R. E. & Mahley, R. W. (1986). Lipoprotein-receptor interactions. *Methods in Enzymol*, **129**, 542-65.

Inoue, M., Itoh, H., Tanaka, T., Chun, T. H., Doi, K., Fukunaga, Y., Sawada, N., Yamshita, J., Masatsugu, K., Saito, T., Sakaguchi, S., Sone, M., Yamahara, K., Yurugi, T. & Nakao, K. (2001). Oxidized LDL regulates vascular endothelial growth factor expression in human macrophages and endothelial cells through activation of peroxisome proliferator-activated receptor-gamma. *Arterioscler Thromb Vasc Biol*, **21**(4), 560-6.

Izadi, H., Motameni, A. T., Bates, T. C., Olivera, E. R., Villar-Suarez, V., Joshi, I., Garg, R., Osborne, B. A., Davis, R. J., Rincon, M. & Anguita, J. (2007). c-Jun N-Terminal Kinase 1 is required for Toll-Like Receptor 1 gene expression in macrophages. *Infect Immun*, **75**(10), 5027-34.

Jang, I. K., Lassila, R. & Fuster, V. (1993). Atherogenesis and inflammation. *Eur Heart J*, **14 Suppl K**, 2-6.

Jessup, W., Rankin, S. M., De Whalley, C. V., Hoult, J. R., Scott, J. & Leake, D. S. (1990). Alpha-tocopherol consumption during low-density-lipoprotein oxidation. *Biochem J*, **265**(2), 399-405.

Jessup, W. & Kritharides, L. (2000). Metabolism of oxidized LDL by macrophages. *Curr Opin Lipidol*, **11**(5), 473-81.

Jessup, W., Wilson, P., Gaus, K. & Kritharides, L. (2002). Oxidised lipoproteins and macrophages. *Vasculr Pharmacol*, **38**, 239-48.

Jessup, W., Kritharides, L. & Stocker, R. (2004). Lipid oxidation in atherogenesis: an overview. *Biochem Soc Trans*, **32**(1), 134-8.

Jonasson, L., Hansson, G. K., Bondjers, G., Noe, L. & Etienne, J. (1990). Interferon-gamma inhibits lipoprotein lipase in human monocyte-derived macrophages. *Biochim Biophys Acta*, **1053**(1), 43-8.

Johnston, D. T., Gagos, M., Raio, N., Ragolia, L., Shenouda, D., Davis-Lorton, M. A. & De Leon, J. R. (2006). Alterations in serum neopterin correlate with thrombolysis in myocardial infarction risk scores in acute coronary syndromes. *Coron Artery Dis*, **17**(6), 511-6.

Jovinge, S., Mikko P.S. Ares, M. P. S., Kallin, B. & Nilsson, J. (1996). Human monocytes/macrophages release TNF- in response to Ox-LDL. *Arterioscler Thromb and Vasc Biol.*, **16**, 1573-9.

Joza, N., Susin, S. A., Daugas, E., Stanford, W. L., Cho, S. K., Li, C. Y., Sasaki, T., Elia, A. J., Cheng, H. Y., Ravagnan, L., Ferri, K. F., Zamzami, N., Wakeham, A., Hakem, R., Yoshida, H., Kong, Y. Y., Mak, T. W., Zúñiga-Pflücker, J. C., Kroemer, G. & Penninger, J. M. (2001). Essential role of the mitochondrial apoptosis-inducing factor in programmed cell death. *Nature*, **410**(6828), 549-54.

Kagan, V. E., Borisenko, G., Tyurina, Y. Y., Tyurin, V. A., Jiang, J., Potapovich, A. I., Kini, V., Amoscato, A. A. & Fujii, M. (2004). Oxidative Lipidomics of apoptosis: Redox catalytic ineractions of cytochrome c with cardiolipin and phosphatidylserine. *Free Radic Biol Med*, **37**(12), 1963-85.

Kagan, V. E., Tyurina, Y. Y., Bayir, H., Chu, C. T., Kapralov, A. A., Vlasova, I. I., Belikova, N. A., Tyurin, V. A., Amoscato, A., Epperly, M., Greenberger, J., Dekosky, S., Shvedova, A. A. & Jiang, J. (2006). The "pro-apoptotic genies" get out of mitochondria: Oxidative lipidomics and redox activity cytochrome c/cardiolipin complexes. *Chemico-Biol Interactions*, **163**, 15-28.

Kalkan, A., Ozden, M. & Akbulut, H. (2005). Serum neopterin levels in patients with chronic hepatitis B. *Jpn J Infect Dis*, **58**(2), 107-9.

Kappler, M., Gerry, A. B., Brown, E., Reid, L., Leake, D. S. & Gieseg, S. P. (2007). Aqueous peroxyl radical exposure to THP-1 cells causes glutathione loss followed by protein oxidation and cell death without increased caspase-3 activity. *Biochim Biophys Acta*, **1773**(6), 945-53.

Karlsson, K. & Marklund, S. L. (1987). Heparin-induced release of extracellular superoxide dismutase to human blood plasma. *Biochem J*, **242**, 55-9.

Kataoka, H., Kume, N., Miyamoto, S., Minami, M., Morimoto, M., Hayashida, K., Hashimoto, N. & Kita, T. (2001). Oxidized LDL modulates Bax/Bcl-2 through the

Lectinlike Ox-LDL Receptor-1 in vascular smooth muscle cells. *Arterioscler Thromb Vasc Biol*, **21**(6), 955-60.

Khoo, J. C., Miller, E., McLoughlin, P. & Steinberg, D. (1988). Enhanced macrophage uptake of low density lipoprotein after self-aggregation. *Arteriosclerosis*, **8**(4), 348-58.

Kinscherf, R., Claus, R., Wagner, M., Gehrke, C., Kamencic, H., Hou, D., Nauen, O., Schmiedt, W., Kovacs, G., Pill, J., Metz, J. & Deigner, H. P. (1998). Apoptosis caused by oxidized LDL is manganese superoxide dismutase and p53 dependent. *Faseb J*, **12**(6), 461-7.

Kirsch, D. G., Doseff, A., Chau, B. N., Lim, D.-S., de Souza-Pinto, N. C., Hansford, R., Kastan, M. B., Lazebnik, Y. A. & Hardwick, J. M. (1999). Caspase-3-dependent cleavage of Bcl-2 promotes release of cytochrome c. *J Biol Chem*, **274**(30), 21155-61.

Kluck, R. M., Esposti, M. D., Perkins, G., Renken, C., Kuwana, T., Bossy-Wetzel, E., Goldberg, M., Allen, T., Barber, M. J., Green, D. R. & Newmeyer, D. D. (1999). The pro-apoptotic proteins, Bid and Bax, cause a limited permeabilization of the mitochondrial outer membrane that is enhanced by cytosol. *J Cell Biol*, **147**(4), 809-22.

Knott, H. M., Baoutina, A., Davies, M. J. & Dean, R. T. (2002). Comparative time-courses of copper-ion-mediated protein and lipid oxidation in low-density lipoprotein. *Arch Biochem Biophys*, **400**(2), 223-32.

Kojima, S., Nomura, T., Icho, T., Kajiwara, Y., Kitabatake, K. & Kubota, K. (1993). Inhibitory effect of neopterin on NADPH-dependent superoxide-generating oxidase of rat peritoneal macrophages. *FEBS Lett*, **329**(1-2), 125-8.

Kojima, S., Icho, T., Mori, H. & Arai, T. (1995). Enhancing potency of neopterin toward B-16 melanoma cell damage induced by UV-A irradiation and its possible application for skin tumor treatment. *Anticancer Res*, **15**(5B), 1975-80.

Kolodgie, F. D., Narula, J., Burke, A. P., Haider, N., Farb, A., Hui-Liang, Y., Smialek, J. & Virmani, R. (2000). Localization of apoptotic macrophages at the site of plaque rupture in sudden coronary death. *Am J Pathol*, **157**(4), 1259-68.

Kosaka, S., Takahashi, S., Masamura, K., Kanehara, H., Sakai, J., Tohda, G., Okada, E., Oida, K., Iwasaki, T., Hattori, H., Kodama, T., Yamamoto, T. & Miyamori, I. (2001). Evidence of macrophage foam cell formation by very low-density lipoprotein receptor: interferon-gamma inhibition of very low-density lipoprotein

receptor expression and foam cell formation in macrophages. *Circulation*, **103**(8), 1142-7.

Krieger, M. & Herz, J. (1994). Structures and functions of multiligand lipoprotein receptors: Macrophage scavenger receptors and LDL receptor-related protein (LRP). *Ann Rev Biochem*, **63**, 601-37.

Krieger, M. & Kozarsky, K. (1999). Influence of the HDL receptor SR-BI on atherosclerosis. *Curr Opin Lipidol*, **10**(6), 491-7.

Kritharides, L., Jessup, W., Gifford, J. & Dean, R. T. (1993). A method for defining the stages of low-density lipoprotein oxidation by the separation of cholesterol- and cholesteryl ester-oxidation products using HPLC. *Anal Biochem*, **213**, 79-89.

Kroemer, G. & Reed, J. C. (2000). Mitochondrial control cell death. *Nat Med*, **6**(5), 513-9.

Kroemer, G. & Martin, S. J. (2005). Caspase-independent cell death. *Nat Med*, **11**(7), 725-30.

Kruth, H. S., Jones, N. L., Huang, W., Zhao, B., Ishii, I., Chang, J., Combs, C. A., Malide, D. & Zhang, W. Y. (2005). Macropinocytosis is the endocytic pathway that mediates macrophage foam cell formation with native low density lipoprotein. *J Biol Chem*, **280**(3), 2352-60.

Kulkarni, G. V. & McCulloch, C. A. (1994). Serum deprivation induces apoptotic cell death in a subset of Balb/c 3T3 fibroblasts. *J Cell Sci*, **107**(5), 1169-79.

Kunjathoor, V. V., Febbraio, M., Podrez, E. A., Moore, K. J., Andersson, L., Koehn, S., Rhee, J. S., Silverstein, R., Hoff, H. F. & Freeman, M. W. (2002). Scavenger receptors class A-I/II and CD36 are the principal receptors responsible for the uptake of modified low density lipoprotein leading to lipid loading in macrophages. *J Biol Chem*, **277**(51), 49982-8.

LaMarre, J., Wolf, B. B., Kittler, E. L., Quesenberry, P. J. & Gonias, S. L. (1993). Regulation of macrophage alpha 2-macroglobulin receptor/low density lipoprotein receptor-related protein by lipopolysaccharide and interferon-gamma. *J Clin Invest*, **91**(3), 1219-24.

Lamb, D. J. & Leake, D. S. (1994a). Iron released from transferrin at acidic pH can catalyse the oxidation of low density lipoprotein. *FEBS Lett*, **352**, 15-18.

Lamb, D. J. & Leake, D. S. (1994b). Acidic pH enables caeruloplasmin to catalyse the modification of low-density lipoprotein. *FEBS Lett*, **338**(2), 122-6.

Lawen, A. (2003). Apoptosis-an introduction. *Bioessays*, **25**(9), 888-96.

Lee, T.-S. & Chau, L.-Y. (2001). Fas/Fas ligand-mediated death pathway is involved in oxLDL-induced apoptosis in vascular smooth muscle cells. *Am J Physiol Cell Physiol*, **280**(3), C709-18.

Lehtolainen, P., Takeya, M. & Ylä-Herttuala, S. (2000). Retrovirus-mediated, stable scavenger-receptor gene transfer leads to functional endocytotic receptor expression, foam cell formation, and increased susceptibility to apoptosis in rabbit aortic smooth muscle cells. *Arterioscler Thromb Vasc Biol*, **20**, 52-60.

Lelli, J. L., Jr., Becks, L. L., Dabrowska, M. I. & Hinshaw, D. B. (1998). ATP converts necrosis to apoptosis in oxidant-injured endothelial cells. *Free Radic Biol Med*, **25**(6), 694-702.

Leon, M. L. & Zuckerman, S. H. (2005). Gamma interferon: a central mediator in atherosclerosis. *Inflamm Res*, **54**(10), 395-411.

Leonarduzzi, G., Vizio, B., Sottero, B., Verde, V., Gamba, P., Mascia, C., Chiarpotto, E., Poli, G. & Biasi, F. (2006). Early involvement of ROS overproduction in apoptosis induced by 7-Ketocholesterol. *Antioxid Redox Signaling*, **8**(3-4), 375-80.

Lesauskaite, V., Ivanoviene, L. & Valenciute, A. (2003). Programmed cellular death and atherogenesis:from molecular mechanisms to clinical aspects. *Medicina*, **39**(6), e353-7.

Li, D., Yang, B. & Mehta, J. L. (1998). Oxidized LDL induces apoptosis in human coronary artery endothelial cells: role of PKC, PTK, bcl-2, and Fas. *Am J Physiol*, **275**(2 Pt 2), H568-76.

Li, D., Saldeen, T. & Mehta, J. L. (1999). [gamma]-Tocopherol decreases ox-LDL-mediated activation of nuclear factor-[kappa]B and apoptosis in human coronary artery endothelial cells. *Biochem Biophys Res Commun*, **259**(1), 157-61.

Li, H. L., Wang, A., Zhang, R., Wei, Y., Chen, H., She, Z., Huang, Y., Liu, D. & Liang, C. (2006). A20 inhibits oxidized low-density lipoprotein-induced apoptosis through negative Fas/Fas ligand-dependent activation of caspase-8 and mitochondrial pathways in murine Raw264.7 macrophages. *J Cellular Physiol*, **208**, 307–18.

Li, Y., Higashi, Y., Itabe, H., Song, Y.-H., Du, J. & Delafontaine, P. (2003). Insulin-like growth factor-1 receptor activation inhibits oxidized LDL-induced cytochrome c release and apoptosis via the phosphatidylinositol 3 kinase/Akt signaling pathway. *Arterioscler Thromb Vasc Biol*, **23**(12), 2178-84.

Liao, H. S., Kodama, T. & Geng, Y. J. (2000). Expression of class A scavenger receptor inhibits apoptosis of macrophages triggered by oxidised low density lipoprotein and oxysterols. *Arterioscler Thromb Vasc Biol*, **20**, 1968-75.

Libby, P. & Hansson, G. K. (1991). Involvement of the immune system in human atherogenesis: current knowledge and unanswered questions. *Lab Invest*, **64**(1), 5-15.

Libby, P. (1995). Molecular bases of the acute coronary syndromes. *Circulation*, **91**(11), 2844-50.

Libby, P. (2002). Atherosclerosis: the new view. *Sci Am*, **286**(5), 46-55.

Libby, P., Ridker, P. M. & Maseri, A. (2002). Inflammation and Atherosclerosis. *Circulation*, **105**(9), 1135-43.

Lipton, B. A., Parthasarathy, S., Ord, V. A., Clinton, S. K., Libby, P. & Rosenfeld, M. E. (1995). Components of the protein fraction of oxidized low density lipoprotein stimulate interleukin-1 alpha production by rabbit arterial macrophage-derived foam cells. *J Lipid Res*, **36**(10), 2232-42.

Littlewood, T. D. & Bennet, M. R. (2003). Apoptotic cell death in atherosclerosis. *Curr Opin Lipidol*, **14**, 468-75.

Liu, J., Thewke, D. P., Su, Y. R., Linton, M. F., Fazio, S. & Sinensky, M. S. (2005). Reduced macrophage apoptosis is associated with accelerated atherosclerosis in low-density lipoprotein receptor-null mice. *Arterioscler Thromb Vasc Biol*, **25**(1), 174-9.

Liu, W.-L., Guo, X. & Guo, Z.-G. (1998). Oxidized low-density lipoproteins induce apoptosis in vascular smooth muscle cells. *Acta Pharmacol Sinica*, **19**(3), 245-7.

Liu-Wu, Y., Svenningsson, A., Stemme, S., Holm, J. & Wiklund, O. (1997). Identification and analysis of macrophage-derived foam cells from human atherosclerotic lesions by using a "mock" FL3 channel in flow cytometry. *Cytometry*, **29**(2), 155-64.

Liu, X., Kim, C., Yang, J., Jemmerson, R. & Wang, X. (1996). Induction of apoptotic program in cell-free extracts: Requirement for dATP and cytochrome c. *Cell*, **86**(1), 147-57.

Liuzzo, G., Biasucci, L. M., Gallimore, J. R., Grillo, R. L., Rebuzzi, A. G., Pepys, M. B. & Maseri, A. (1994). The Prognostic Value of C-Reactive Protein and Serum Amyloid A Protein in Severe Unstable Angina. *N Engl J Med*, **331**, 417-24.

Lizard, G., Gueldry, s., Sordet, O., Monier, S., Athias, A., Miguet, C., Bessede, G., Lemaire, S., Solary, E. & Gambert, P. (1998). Glutathione is implied in the control of 7-ketocholesterol-induced apoptosis, which is associated with radical oxygen species production. *FASEB J*, **12**(15), 1651-63.

Lizard, G., Monier, S., Cordelet, C., Gesquiere, L., Deckert, V., Gueldry, S., Lagrost, L. & Gambert, P. (1999). Characterization and comparison of the mode of cell death,

apoptosis versus necrosis, induced by 7ß-Hydroxycholesterol and 7-Ketocholesterol in the cells of the vascular wall. *Arterioscler Thromb Vasc Biol*, **19**(5), 1190-200.

Lizard, G., Miguet, C., Bessede, G., Monier, S., Gueldry, S., Neel, D. & Gambert, P. (2000). Impairment with various antioxidants of the loss of mitochondrial transmembrane and of the cytosolic release of cytochrome c occuring during 7-ketocholesterol-induced apoptosis. *Free Radic Biol Med*, **28**(4), 743-53.

Lougheed, M. & Steinbrecher, U. P. (1996). Mechanism of uptake of copper-oxidized low density lipoprotein in macrophages is dependent on its extent of oxidation. *J Biol Chem*, **271**(20), 11798-805.

Lougheed, M., Moore, E. D., Scriven, D. R. & Steinbrecher, U. P. (1999). Uptake of oxidized LDL by macrophages differs from that of acetyl LDL and leads to expansion of an acidic endolysosomal compartment. *Arterioscler Thromb Vasc Biol*, **19**(8), 1881-90.

Lundberg, G. A., Kellin, A., Samnegard, A., Lundman, P., Tornwall, P., Dimmeler, S., Zeiher, A. M., Hamsten, A., Hansson, G. K. & Eriksson, P. (2005). Severity of coronary artery stenosis is associated with a polymorphism in the CXCL16/SR-PSOX gene. *J Intern Med,* **257**, 415-22.

Luo, X., Budihardjo, I., Zou, H., Slaughter, C. & Wang, X. (1998). Bid, a Bcl2 interacting protein, mediates cytochrome c release from mitochondria in response to activation of cell surface death receptors. *Cell*, **94**(4), 481-90.

Lusis, A. J. (2000). Atherosclerosis. *Nature*, **407**(6801), 233-41.

Ly, J. D., Grubb, D. R. & Lawen, A. (2003). The mitochondrial membrane potential (deltapsi(m)) in apoptosis; an update. *Apoptosis*, **8**(2), 115-28.

Mach, F., Schonbeck, U. & Libby, P. (1998). CD40 signaling in vascular cells: A key role in atherosclerosis? *Atherosclerosis*, **137**(Supplement 1), S89-S95.

Maddipati, K. R. & Marnett, L. (1987). Characterization of the major hydroperoxide-reducing activity of human plasma *J Biol Chem*, **262**(36), 17398-403.

Madesh, M. & Hajnoczky, G. (2001). VDAC-dependent permeabilization of the outer mitochondrial membrane by superoxide induces rapid and massive cytochrome c release. *J Cell Biol*, **155**(6), 1003-16.

Maerker, G., Nungesser, E. H. & Zulak, I. M. (1988). HPLC separation and quantitation of cholesterol oxidation products with flame ionization detection. *J Agric Food Chem* **36**, 61-3.

Malavasi, B., Rasetti, M. F., Roma, P., Fogliatto, R., Allevi, P., Catapano, A. L. & Galli, G. (1992). Evidence for the presence of 7-hydroperoxylcholest-5-e-3beta-ol in oxidized human LDL. *Chem and Phys of Lipids*, **62**, 209-14.

Mallat, Z., Nakamura, T., Ohan, J., Leseche, G., Tedgui, A., Maclouf, J. & Murphy, R. C. (1999). The relationship of hydroxyeicosatetraenoic acids and F2-isoprostanes to plaque instability in human carotid atherosclerosis. *J Clin Invest*, **103**(3), 421-7.

Maor, I., Hayek, T., Coleman, R. & Aviram, M. (1997). Plasma LDL oxidation leads to its aggregation in the atherosclerotic apolipoprotein E-deficient mice. *Arterioscler Thromb Vasc Biol*, **17**(11), 2995-3005.

Marleau, S., Harb, D., Bujold, K., Avallone, R., Iken, K., Wang, Y., Demers, A., Sirois, M. G., Febbraio, M., Silverstein, R. L., Tremblay, A. & Ong, H. (2005). EP 80317, a ligand of the CD36 scavenger receptor, protects apolipoprotein E-deficient mice from developing atherosclerotic lesions. *FASEB J*, **19**(13),1869-71.

Marzo, I., Pérez-Galán, P., Giraldo, P., Rubio-Félix, D., Anel, A. & Naval, J. (2001). Cladribine induces apoptosis in human leukaemia cells by caspase-dependent and -independent pathways acting on mitochondria. *Biochem J*, **359**(3), 537-46.

Mathews, C. K. & van Holde, K. E. (1996). *Biochemistry. Second edition ed.* The Benjamin/Cummings Publishing Company, Inc., California.

Mattsson, L., Johansson, H., Ottosson, M. & Wiklund, O. (1993). Expression of lipoprotein lipase mRNA and secretion in macrophages isolated from human atherosclerotic aorta. *J Clin Invest*, **92**(4), 1759-65.

Maziere, C., Conte, M. A., Dantin, F. & Maziere, J. C. (1999). Lipopolysaccharide enhances oxidative modification of low density lipoprotein by copper ions, endothelial and smooth muscle cells. *Atherosclerosis*, **143**(1), 75-80.

Mazumder, B., Mukhopadhyay, C. K., Prok, A., Cathcart, M. K. & Fox, P. L. (1997). Induction of ceruloplasmin synthesis by IFN-gamma in human monocytic cells. *J Immunol*, **159**(4), 1938-44.

Meyer, D. F., Mayans, M. O., Groot, P. H. E., Suckling, K. E., Bruckdorfer, K. R. & Perkins, S. J. (1995). Time-course studies by neutron solution scattering and biochemical assays of the aggregation of human low-density lipoprotein during Cu2+-induced oxidation. *Biochem J*, **310**(2), 417-26.

Miller, M. & Hutchins, G. M. (1994). Hemochromatosis, multiorgan hemosiderosis, and coronary artery disease. *JAMA*, **272**(3), 231-3.

Mirkovic, N., Voehringer, D. W., Story, M. D., McConkey, D. J., McDonnell, T. J. & Meyn, R. E. (1997). Resistance to radiation-induced apoptosis in Bcl-2-expressing cells is reversed by depleting cellular thiols. *Oncogene*, **15**, 1461-70.

Moldeus, P., Hogberg, J. & Orrenius, S. (1978). Isolation and use of liver cells. *Methods Enzymol*, **52**, 60-71.

Moore, K. J., Kunjathoor, V. V., Koehn, S. L., Manning, J. J., Tseng, A. A., Silver, J. M., McKee, M. & Freeman, M. W. (2005). Loss of receptor-mediated lipid uptake via scavenger receptor A or CD36 pathways does not ameliorate atherosclerosis in hyperlipidecic mice. *J Clin Invest*, **115**(8), 2192-201.

Moore, K. J. & Freeman, M. W. (2006). Scavenger receptors in atherosclerosis beyond lipid uptake. *Arterioscler Thromb Vasc Biol*, **26**, 1702-11.

Mosmann, T. (1983). Rapid colorimetric assay for cellular growth and survival: application to proliferation and cytotoxicity assays. *J Immunol Methods*, **65**(1-2), 55-63.

Munteanu, A., Zingg, J.-M., Ricciarelli, R. & Azzi, A. (2005). CD36 overexpression in ritonavir-treated THP-1 cells is reversed by a-tocopherol. *Free Radic Biol Med*, **38**, 1047– 56.

Muralidhar, B., Carpenter, K. L., Muller, K., Skepper, J. N. & Arends, M. J. (2004). Potency of arachidonic acid in polyunsaturated fatty acid-induced death of human monocyte-macrophages: implications for atherosclerosis. *Prostaglandins Leukot Essent Fatty Acids*, **71**(4), 251-62.

Murphy, J. E., Tacon, D., Tedbury, P. R., Hadden, J. M., Knowling, S., Sawamura, T., Peckham, M., Phillips, S. E., Walker, J. H. & Ponnambalam, S. (2006). LOX-1 scavenger receptor mediates calcium-dependent recognition of phosphatidylserine and apoptotic cells. *Biochem J*, **393**(1), 107-15.

Murr, C., Fuchs, D., Gossler, W., Hausen, A., Reibnegger, G., Werner, E. R., Werner-Felmayer, G., Esterbauer, H. & Wachter, H. (1994). Enhancement of hydrogen peroxide-induced luminol-dependent chemiluminescence by neopterin depends on the presence of iron chelator complexes. *FEBS Lett*, **338**(2), 223-6.

Murr, C., Baier-Bitterlich, G., Fuchs, D., Werner, E. R., Esterbauer, H., Pfleiderer, W. & Wachter, H. (1996). Effects of neopterin-derivatives on H2O2-induced luminol chemiluminescence: mechanistic aspects. *Free Radic Biol Med*, **21**(4), 449-56.

Nagy, L., Tontonoz, P., Alvarez, J. G., Chen, H. & Evans, R. M. (1998). Oxidized LDL regulates macrophage gene expression through ligand activation of PPARgamma. *Cell*, **93**(2), 229-40.

Naito, M., Nomura, H., Esaki, T. & Iguchi, A. (1997). Characteristics of macrophage-derived foam cells isolated from atherosclerotic lesions of rabbits. *Atherosclerosis*, **135**(2), 241-7.

Nakagawa, T., Nozaki, S., Nishida, M., Yakub, J. M., Tomiyama, Y., Nakata, A., Matsumoto, K., Funahashi, T., Kameda-Takemura, K., Kurata, Y., Yamashita, S. & Matsuzawa, Y. (1998). Oxidized LDL increases and interferon-gamma decreases expression of CD36 in human monocyte-derived macrophages. *Arterioscler Thromb Vasc Biol*, **18**(8), 1350-7.

Napoli, C., Quehenberger, O., De Nigris, F., Abete, P., Glass, C. K. & Palinski, W. (2000). Mildly oxidized low density lipoprotein activates multiple apoptotic signaling pathways in human coronary cells. *FASEB J* **14**(13), 1996-2007.

Nardini, M., Pisu, P., Gentili, V., Natella, F., Di Felice, M., Piccolella, E. & Scaccini, C. (1998). Effect of caffeic acid on tert-butyl hydroperoxide-induced oxidative stress in U937. *Free Radic Biol Med*, **25**(9), 1098-105.

Nathan, C. F. (1986). Peroxide and pteridine: a hypothesis on the regulation of macrophage antimicrobial activity by interferon gamma. *Interferon*, **7**, 125-43.

Newman, H. A. I., Murad, T. M. & Geer, J. C. (1971). Foam cell of rabbit atheromatous lesions: identifications and cholesterol uptake in isolated cells. *Lab Invest*, **25**(6), 586-95.

Nguyen-Khoa, T., Massy, Z. A., Witko-Sarsat, V., Canteloup, S., Kebede, M., Lacour, B., Drueke, T. & Descamps-Latscha, B. (1999). Oxidized low-density lipoprotein induces macrophage respiratory burst via its protein moiety: A novel pathway in atherogenesis? *Biochem Biophys Res Commun*, **263**(3), 804-9.

Nieminen, A. L., Byrne, A. M., Herman, B. & Lemasters, J. J. (1997). Mitochondrial permeability transition in hepatocytes induced by t-BuOOH: NAD(P)H and reactive oxygen species. *Am J Physiol Cell Physiol*, **272**(4), C1286-94.

Niu, X., Zammit, V., Upston, J. M., Dean, R. T. & Stocker, R. (1999). Coexistence of oxidized lipids and alpha-tocopherol in all lipoprotein density fractions isolated from advanced human atherosclerotic plaques. *Arterioscler Thromb Vasc Biol*, **19**(7), 1708-18.

Niu, X. L., Zhang, X. W. & Guo, Z. G. (1996). Oxidized low-density lipoproteins induce apoptosis in macrophages. *Acta Pharmacol Sinica*, **17** (5), 467-70

Nur-E-Kamal, A., Gross, S.R.,Pan, Z.,Balklava, Z.,Ma, J. & Liu, L.F. (2004). Nuclear translocation of cytochrome c during apoptosis. *J Biol Chem*, **279**(24), 24911-4.

Oettl, K., Dikalov, S., Freisleben, H. J., Mlekusch, W. & Reibnegger, G. (1997). Spin trapping study of antioxidant properties of neopterin and 7,8-dihydroneopterin. *Biochem Biophys Res Commun*, **234**(3), 774-8.

Oettl, K. & Reibnegger, G. (1999). Pteridines as inhibitors of xanthine oxidase: structural requirements. *Biochim Biophys Acta*, **1430**(2), 387-95.

Oettl, K., Wirleitner, B., Baier-Bitterlich, G., Grammer, T., Fuchs, D. & Reibnegger, G. (1999). Formation of oxygen radicals in solutions of 7,8-dihydroneopterin. *Biochem Biophys Res Commun*, **264**(1), 262-7.

Okado, A., Kawasaki, Y., Hasuike, Y., Takahashi, M., Teshima, T., Fujii, J. & Taniguchi, N. (1996). Induction of apoptotic cell death by methylglyoxal and 3-deoxyglucosone in macrophage-derived cell lines. *Biochem Biophys Res Commun*, **225**(1), 219-24.

Okura, Y., Brink, M., Itabe, H., Scheidegger, K. J., Kalangos, A. & Delafontaine, P. (2000). Oxidized low-density lipoprotein is associated with apoptosis of vascular smooth muscle cells in human atherosclerotic plaques. *Circulation*, **102**(22), 2680-6.

Osterud, B. & Bjorklid, E. (2003). Role of monocytes in atherogenesis. *Physiol Rev*, **83**(4), 1069-112.

Panini, S. R., Yang, L., Rusinol, A. E., Sinensky, M. S., Bonventre, J. V., & Leslie,C. C. (2001). Arachidonate metabolism and the signaling pathway of induction of apoptosis by oxidized LDL/oxysterol. *J Lipid Res*, 42, 1678–86.

Panousis, C. G. & Zuckerman, S. H. (2000). Interferon-{gamma} induces downregulation of tangier disease gene (ATP-Binding-Cassette Transporter 1) in macrophage-derived foam cells. *Arterioscler Thromb Vasc Biol*, **20**(6), 1565-71.

Parhami, F., Fang, Z. T., Fogelman, A. M., Andalibi, A., Territo, M. C. & Berliner, J. A. (1993). Minimally modified low density lipoprotein-induced inflammatory responses in endothelial cells are mediated by cyclic adenosine monophosphate. *J Clin Invest*, **92**(1), 471-8.

Parthasarathy, S., Santanam, N., Ramachandran, S. & Meilhac, O. (1999). Oxidants and antioxidants in atherogenesis: an appraisal. *J Lipid Res*, **40**, 2143-57.

Patrick, L. & Uzick, M. (2001). Cardiovascular disease: C-reactive protein and the inflammatory disease paradigm: HMG-CoA reductase inhibitors, alpha-tocopherol, red yeast rice, and olive oil polyphenols. A review of the literature. *Altern Med Rev*, **6**(3), 248-71.

Pentikainen, M. O., Oorni, K., Ala-Korpela, M. & Kovanen, P. T. (2000). Modified LDL - trigger of atherosclerosis and inflammation in the arterial intima. *J Intern Med*, **247**(3), 359-70.

Petrosillo, G., Ruggiero, F. M. & Paradies, G. (2003). Role of reactive oxygen species and cardiolipin in the release of cytochrome c from mitochondria. *FASEB J*, **17**(15), 2202-8.

Pifat, G., Brnjas-Kraljević, J., Jürgens, G., Herak-Kramberger, C. M. & Herak, J. N. (1992). Chemical modification of low-density lipoprotein enhances the number of binding sites for divalent cations. *Chem Phys Lipids*, **63**(3), 159-67.

Podrez, E. A., Schmitt, D., Hoff, H. F. & Hazen, S. L. (1999). Myeloperoxidase-generated reactive nitrogen species convert LDL into an atherogenic form *in vitro*. *J Clin Invest*, **103**(11), 1547-60.

Porn-Ares, M. I., Saido, T. C., Andersson, T. & Ares, M. P. S. (2003). Oxidized low-density lipoprotein induces calpain-dependent cell death and ubiquitination of caspase 3 in HMEC-1 endothelial cells. *Biochem J*, **374**(2), 403-11.

Post, S. R., Gass, C., Rice, S., Nikolic, D., Crump, H. & Post, G. R. (2002). Class A scavenger receptors mediate cell adhesion via activation of Gi/o and formation of focal adhesion complexes. *J Lipid Res*, **43**(11), 1829-36.

Rajavashisth, T. B., Andalibi, A., Territo, M. C., Berliner, J. A., Navab, M., Fogelman, A. M. & Lusis, A. J. (1990). Induction of endothelial cell expression of granulocyte and macrophage colony-stimulating factors by modified low-density lipoproteins. *Nature*, **344**(6263), 254-7.

Ramprasad, M. P., Fisher, W., Witztum, J. L., Sambrano, G. R., Quehenberger, O. & Steinberg, D. (1995). The 94- to 97-kDa mouse macrophage membrane protein that recognizes oxidized low density lipoprotein and phosphatidylserine-rich liposomes is identical to macrosialin, the mouse homologue of human CD68. *Proc Nat Acad Sc USA*, **92**(21), 9580-4.

Razumovitch, J. A., Semenkova, G. N., Fuchs, D. & Cherenkevich, S. N. (2003). Influence of neopterin on the generation of reactive oxygen species in human neutrophils. *FEBS Lett*, **549**(1-3), 83-6.

Reiss, A. B., Patel, C. A., Rahman, M. M., Chan, E. S., Hasneen, K., Montesinos, M. C., Trachman, J. D. & Cronstein, B. N. (2004). Interferon-gamma impedes reverse cholesterol transport and promotes foam cell transformation in THP-1 human monocytes/macrophages. *Med Sci Monit*, **10**(11), BR420-5.

Ricci, R., Sumara, G., Sumara, I., Rozenberg, I., Kurrer, M., Akhmedov, A., Hersberger, M., Eriksson, U., Eberli, F. R., Becher, B., Borén, J., Chen, M., Cybulsky, M. I., Moore, K. J., Freeman, M. W., Wagner, E. F., Matter, C. M. & Lüscher, T. F. (2004). Requirement of JNK2 for scavenger receptor A-mediated foam cell formation in atherogenesis. *Science*, **306**(5701), 1558-61.

Ricciarelli, R., Zingg, J.-M. & Azzi, A. (2000). Vitamin E reduces the uptake of oxidized LDL by inhibiting CD36 scavenger receptor expression in cultured aortic smooth muscle cells. *Circulation*, **102**(1), 82-7.

Rippin, J. J. (1992). Analysis of fully oxidised neopterin in serum by high-performance liquid chromatography. *Clin Chem*, **38**(9), 1722-4.

Rohrer, L., Freeman, M., Kodama, T., Penman, M. & Krieger, M. (1990). Coiled-coil fibrous domains mediate ligand binding by macrophage scavenger receptor type II. *Nature*, **343**(6258), 570-2

Roland, A., Patterson, R. A. & Leake, D. S. (2001). Measurement of copper-binding sites on low density lipoprotein. *Arterioscler Thromb Vasc Biol*, **21**(4), 594-602.

Ross R. (1986). The pathogenesis of atherosclerosis--an update. *N Engl J Med.* **314**(8), 488-500.

Ross, R. (1993). The pathogenesis of atherosclerosis: a perspective for the 1990s. *Nature*, **362**(6423), 801-9.

Rubic, T. & Lorenz, R. L. (2006). Downregulated CD36 and oxLDL uptake and stimulated ABCA1/G1 and cholesterol efflux as anti-atherosclerotic mechanisms of interliukin-10. *Cardiovas Res*, **69**, 527-35.

Rudzite, V., Jurika, E., Fuchs, D., Kalnins, U., Erglis, A. & Trusinskis, K. (2003). Serum concentration of C-reactive protein, neopterin and phospholipids in patients with different grade of coronary heart disease. *Pteridines*, **14**(4), 133-7.

Rusinol, A. E., Yang, L., Thewke, D., Panini, S. R., Kramer, M. F. & Sinensky, M. S. (2000). Isolation of a somatic cell mutant resistant to the induction of apoptosis by oxidized low density lipoprotein. *J Biol Chem*, **275**(10), 7296–303.

Rusiñol, A. E., Thewke, D., Liu, J., Freeman, N., Panini, S. R. & Sinensky, M. S. (2004). AKT/Protein kinase B regulation of Bcl family members during oxysterol-induced apoptosis. *J Biol Chem*, **279**(2), 1392-9

Sakaguchi, H., Takeya, M., Suzuki, H., Hakamata, H., Kodama, T., Horiuchi, S., Gordon, S., van der, L. L. J., Kraal, G., , , Ishibashi, S., Kitamura, N. & Takahashi, K. (1998). Role of macrophage scavenger receptors in diet-induced atherosclerosis in mice. *Lab Invest*, **78**(4), 423-34.

Salonen, J. T., Yla-Herttuala, S., Yamamoto, R., Butler, S., Korpela, H., Salonen, R., Nyyssonen, K., Palinski, W. & Witztum, J. L. (1992). Autoantibody against oxidised LDL and progression of carotid atherosclerosis. *Lancet*, **339**(8798), 883-7.

Salvayre, R., Auge, N., Benoist, H. & Negre-Salvayre, A. (2002). Oxidized low-density lipoprotein-induced apoptosis. *Biochim et Biophys Acta*, **1585**(2-3), 213-21.

Sata, M. & Walsh, K. (1998a). Endothelial cell apoptosis induced by oxidized LDL is associated with the down-regulation of the cellular caspase inhibitor FLIP. *J Biol Chem,* **273**(50), 33103-6.

Sata, M. & Walsh, K. (1998b). Oxidized LDL activates fas-mediated endothelial cell apoptosis. *J Clin Invest*, **102**(9), 1682-9.

Savenkova, M. L., Mueller, D. M. & Heinecke, J. W. (1994). Tyrosyl radical generated by myeloperoxidase is a physiological catalyst for the initiation of lipid peroxidation in low density lipoprotein. *J Biol Chem*, **269**(32), 20394-400.

Schafer, F. Q. & Buettner, G. R. (2001). Redox environment of the cell as viewd through the redox state of the glutathione/glutathione couple. *Free Radic Biol Med*, **30**, 1191-212.

Schaffner, T., Taylor, K., Bartucci, E. J., Fischer-Dzoga, K., Beeson, J. H., Glagov, S. & Wissler, R. W. (1980). Arterial foam cells with distinctive immunomorphologic and histochemical features of macrophages. *Am J Pathol*, **100**(1), 57-80.

Schobersberger, W., Hoffmann, G., Grote, J., Wachter, H. & Fuchs, D. (1995). Induction of inducible nitric oxide synthase expression by neopterin in vascular smooth muscle cells. *FEBS Lett*, **377**(3), 461-4.

Schobersberger, W., Hoffmann, G., Hobisch-Hagen, P., Bock, G., Volkl, H., Baier-Bitterlich, G., Wirleitner, B., Wachter, H. & Fuchs, D. (1996). Neopterin and 7,8-dihydroneopterin induce apoptosis in the rat alveolar epithelial cell line L2. *FEBS Lett*, **397**(2-3), 263-8.

Schroder, K., Hertzog, P. J., Ravasi, T. & Hume, D. A. (2004). Interferon-gamma: an overview of signals, mechanisms and functions. *J Leukoc Biol*, **75**, 163-89.

Schroecksnadel, K., Murr, C., Winkler, C., Wirleitner, B., Fuith, L. C. & Fuchs, D. (2004). Neopterin to monitor clinical pathologies involving interferon-γ production. *Pteridines*, **15**(3), 75-90

Schumacher, M., Eber, B., Tatzber, F., Kaufmann, P., Esterbauer, H. & Klein, W. (1992). Neopterin levels in patients with coronary artery disease. *Atherosclerosis*, **94**(1), 87-8.

Schumacher, M., Halwachs, G., Tatzber, F., Fruhwald, F. M., Zweiker, R., Watzinger, N., Eber, B., Wilders-Truschnig, M., Esterbauer, H. & Klein, W. (1997). Increased neopterin in patients with chronic and acute coronary syndromes. *J Am Coll Cardiol*, **30**(3), 703-7.

Schuster, B., Prassl, R., Nigon, F., Chapman, M. J. & Laggner, P. (1995). Core lipid structure is a major determinant of the oxidative resistance of low density lipoprotein *Proc Nat Acad Sc*, **92** (7), 2509-13.

Scott, J. (2004). Pathophysiology and biochemistry of cardiovascular disease. *Curr Opin Genet Dev*, **14**(3), 271-9.

Sell, C., Baserga, R. & Rubin, R. (1995). Insulin-like Growth Factor I (IGF-I) and the IGF-I receptor prevent etoposide-induced apoptosis. *Cancer Res*, **55**(2), 303-6.

Sevanian, A., Seraglia, R., Traldi, P., Rossato, P., Ursini, F. & Hodis, H. (1994). Analysis of plasma cholesterol oxidation products using gas- and high-performance liquid chromatography/mass spectrometry. *Free Rad Biol Med*, **17**(5), 397-409.

Shashkin, P., Dragulev, B. & Ley, K. (2005). Macrophage differentiation to foam cells. *Curr Pharmaceutical Design*, **11**(23), 3061-72.

Shaw, P. X., Horkko, S., Tsimikas, S., Chang, M. K., Palinski, W., Silverman, G. J., Chen, P. P. & Witztum, J. L. (2001). Human-derived anti-oxidized LDL autoantibody blocks uptake of oxidized LDL by macrophages and localizes to atherosclerotic lesions *in vivo*. *Arterioscler Thromb Vasc Biol*, **21**(8), 1333-9.

Shen, L. & Sevanian, A. (2001). OxLDL induces macrophage {{gamma}}-GCS-HS protein expression: a role for oxLDL-associated lipid hydroperoxide in GSH synthesis. *J Lipid Res*, **42**(5), 813-23.

Shen, R. S. (1994). Inhibition of luminol-enhanced chemiluminescence by reduced pterins. *Arch Biochem Biophys*, **310**(1), 60-3.

Shidoji, Y., Hayashi, K., Komura, S., Ohishi, N. & Yagi, K. (1999). Loss of molecular interaction between cytochrome *c* and cardiolipin due to lipid peroxidation. *Biochem Biophys Res Commun*, **264**(2), 343-7.

Shige, H., Ishikawa, T., Suzukawa, M., Nishiwaki, M. & Yamashita, T. (1998). Vitamin E reduces cholesterol esterification and uptake of Ac-LDL in macrophages. *Lipids*, **33**, 169-75.

Shih, P. T., Brennan, M.-L., Vora, D. K., Territo, M. C., Strahl, D., Elices, M. J., Lusis, A. J. & Berliner, J. A. (1999). Blocking Very Late Antigen-4 Integrin decreases leukocyte entry and fatty streak formation in mice fed an atherogenic diet. *Circ Res*, **84**(3), 345-51.

Shimaoka, T., Kume, N., Minami, M., Hayashida, K., Kataoka, H., Kita, T. & Yonehara, S. (2000). Molecular cloning of a novel scavenger receptor for oxidized low density lipoprotein, SR-PSOX, on macrophages. *J Biol Chem*, **275**(52), 40663-6.

Shio, H., Haley, N.J. & Fowler, S. (1978). Characterisation of lipid-laden aortic cells from cholesterol-fed rabbits, II. Morphometric analysis of lipid-filled lysosomes and lipid droplets in aortic cell populations. *Lab Invest*, **39**(4), 390-7.

Sigma Product Information. RPMI-1640 Medium. http://www.sigmaaldrich.com/catalog /search/ProductDetail?ProdNo=R6504&Brand=SIGMA

Singh, I., Pahan, K., Khan, M. & Singh, A. K. (1998). Cytokine-mediated induction of ceramide production is redox-sensitive. Implications to proinflammatory cytokine-mediated apoptosis in demyelinating diseases. *J Biol Chem*, **273**(32), 20354-62.

Siow, R. C., Richards, J. P., Pedley, K. C., Leake, D. S. & Mann, G. E. (1999). Vitamin C protects human vascular smooth muscle cells against apoptosis induced by moderately oxidized LDL containing high levels of lipid hydroperoxides. *Arterioscler Thromb Vasc Biol*, **19**(10), 2387-94.

Skepper, J. N., Karydis, I., Garnett, M. R., Hegyi, L., Hardwick, S. J., Warley, A., Mitchinson, M. J. & Cary, N. R. B. (1999). Changes in elemental concentrations are associated with early stages of apoptosis in human monocyte-macrophages exposed to oxidized low-density lipoprotein: An x-ray microanalytical study. *J Pathol*, **188**(1), 100-6.

Skiba, P. J., Keesler, G. A. & Tabas, I. (1994). Interferon-gamma down-regulates the lipoprotein(a)/apoprotein(a) receptor activity on macrophage foam cells. Evidence for disruption of ligand-induced receptor recycling by interferon-gamma. *J Biol Chem*, **269**(37), 23059-67.

Smith, C., Mitchinson, M. J., Aruoma, O. I. & Halliwell, B. (1992). Stimulation of lipid peroxidation and hydroxyl-radical generation by the contents of human atherosclerotic lesions. *Biochem J*, **286 (Pt 3)**, 901-5.

Smith, J. D., Trogan, E., Ginsberg, M., Grigaux, C., Tian, J. & Miyata, M. (1995). Decreased atherosclerosis in mice deficient in both macrophage colony-stimulating factor (op) and apolipoprotein E. *Proc Natl Acad Sci USA*, **92**(18), 8264-8.

Song, L., Leung, C. & Schindler, C. (2001). Lymphocytes are important in early atherosclerosis. *J Clin Invest*, **108**(2), 251-9.

Spottl, N., Wirleitner, B., Bock, G., Widner, B., Fuchs, D. & Baier-Bitterlich, G. (2000). Reduced pteridine derivatives induce apoptosis in human neuronal NT2/HNT cells. *Immunobiology*, **201**(3-4), 478-91.

Stadler, N., Lindner, R. A. & Davies, M. J. (2004). Direct detection and quantification of transition metal ions in human atherosclerotic plaques: Evidence for the presence of elevated levels of iron and copper. *Arterioscler Thromb Vasc Biol*, **24**(5), 949-54.

Stary, H. C., Chandler, A. B., Dinsmore, R. E., Fuster, V., Glagov, S., Insull, W., Jr., Rosenfeld, M. E., Schwartz, C. J., Wagner, W. D. & Wissler, R. W. (1995). A definition of advanced types of atherosclerotic lesions and a histological classification of atherosclerosis. A report from the Committee on Vascular Lesions of the Council on Arteriosclerosis, American Heart Association. *Arterioscler Thromb Vasc Biol*, **15**(9), 1512-31.

Steinberg, D., Parthasarathy, S., Carew, T. E., Khoo, J. C. & Witztum, J. L. (1989). Beyond cholesterol. Modifications of low-density lipoprotein that increase its atherogenicity. *N Engl J Med*, **320**(14), 915-24.

Steinbrecher, U. P., Parthasarathy, S., Leake, D. S., Witztum, J. L. & Steinberg, D. (1984). Modification of low density lipoprotein by endothelial cells involves lipid peroxidation and degradation of low density lipoprotein phospholipids. *Proc Nat Acad Sc USA*, **81**(12), 3883-7.

Steinbrecher, U. P. (1987). Oxidation of human low density lipoprotein results in derivatization of lysine residues of apolipoprotein B by lipid peroxide decomposition products. *J Biol Chem*, **262**(8), 3603-8.

Steinbrecher, U. P., Zhang, H. & Lougheed, M. (1990). Role of oxidatively modified LDL in atherosclerosis. *Free Rad Biol Med*, **9**(2), 155-68.

Stephan, Z. F. & Yurachek, E. C. (1993). Rapid fluorometric assay of LDL receptor activity by DiI-labeled LDL. *J Lipid Res*, **34**(2), 325-30.

Stocker, R., Glazer, A. N. & Ames, B. N. (1987). Antioxidant activity of albumin-bound bilirubin (reactive oxygen species/plasma antioxidants/biliverdin/evolution). *Proc Natl Acad Sci USA*, **84**, 5918-22.

Stocker, R. & Keaney Jr, J. F. (2004). Role of oxidative modifications in atherosclerosis. *Physiol Rev*, **84**(4), 1381-478.

Stridth, H., Kimland, M., Jones, D. P., Orennius, S. & Hampton, M. B. (1998). Cytochrome c release and caspase activation in hydrogen peroxide- and tributylin-induced apoptosis. *FEBS Lett*, **429**, 351-5.

Sugiyama, S., Kugiyama, K., Aikawa, M., Nakamura, S., Ogawa, H. & Libby, P. (2004). Hypochlorous acid, a macrophage product, induces endothelial apoptosis and tissue factor expression: involvement of myeloperoxidase-mediated oxidant in plaque erosion and thrombogenesis. *Arterioscler Thromb Vasc Biol*, **24**(7), 1309-14.

Sukhanov, S., Higashi, Y., Shai, S.-Y., Itabe, H., Ono, K., Parthasarathy, S. & Delafontaine, P. (2006). Novel effect of oxidized low-density lipoprotein: Cellular ATP depletion via downregulation of glyceraldehyde-3-phosphate dehydrogenase. *Circ Res*, **99**(2), 191-200.

Suzuki, H., Kurihara, Y., Takeya, M., Kamada, N., Kataoka, M., Jishage, K., Ueda, O., Sakaguchi, H., Higashi, T., Suzuki, T., Takashima, Y., Kawabe, Y., Cynshi, O., Wada, Y., Honda, M., Kurihara, H., Aburatani, H., Doi, T., Matsumoto, A., Azuma, S., Noda, T., Toyoda, Y., Itakura, H., Yazaki, Y., Kodama, T. & *et al*. (1997). A role for macrophage scavenger receptors in atherosclerosis and susceptibility to infection. *Nature*, **386**(6622), 292-6.

Tabas, I., Weiland, D. A. & Tall, A. R. (1985). Unmodified low density lipoprotein causes cholesteryl ester accumulation in J774 macrophages. *Proc Nat Acad Sc*, **82**(2), 416-20.

Tabas, I. (2005). Consequences and therapeutic implications of macrophage apoptosis in atherosclerosis: The importance of lesion stage and phagocytic efficiency *Arterioscler Thromb Vasc Biol*, **25**, 2255-64.

Takahashi, K., Takeya, M. & Sakashita, N. (2002). Multifunctional roles of macrophages in the development and progression of atherosclerosis in humans and experimental animals. *Med Electron Microsc* **35**, 179-203.

Tashiro, K., Makita, Y., Shike, T., Shirato, I., Sato, T., Cynshi, O. & Tomino, Y. (1999). Detection of cell death of cultured mouse mesangial cells induced by oxidized low-density lipoprotein. *Nephron*, **82** (1), 51-8.

Tatzber, F., Rabl, H., Koriska, K., Erhart, U., Puhl, H., Waeg, G., Krebs, A. & Esterbauer, H. (1991). Elevated serum neopterin levels in atherosclerosis. *Atherosclerosis*, **89**(2-3), 203-8.

Tedgui, A. & Mallat, Z. (2006). Cytokines in atherosclerosis: Pathogenic and regulatory pathways. *Physiol Rev*, **86**(2), 515-81.

Teupser, D., Thiery, J. & Seidel, D. (1999). Alpha-tocopherol down-regulates scavenger receptor activity in macrophages. *Atherosclerosis*, **144**, 109-115.

Torgano, G., Cosentini, R., Mandelli, C., Perondi, R., Blasi, F., Bertinieri, G., Tien, T. V., Ceriani, G., Tarsia, P., Arosio, C. & Ranzi, M. L. (1999). Treatment of Helicobacter pylori and Chlamydia pneumoniae infections decreases fibrinogen plasma level in patients with ischemic heart disease. *Circulation*, **99**(12), 1555-9.

Tribble, D. L., Chu, B. M., Levine, G. A., Krauss, R. M. & Gong, E. L. (1996). Selective resistance of LDL core lipids to iron-mediated oxidation. Implications for the

biological properties of iron-oxidized LDL. *Arterioscler Thromb Vasc Biol*, **16**(12), 1580-7.

Tyurina, Y. Y., Shvedova, K. K., Kawai, K., Tyurin, V. A., Kommineni, C., Quinn, P. J., Gfabisiak, J. P. & Kagan, V. E. (2000). Phospholipid signaling in apoptosis: peroxidation and externalisation of phosphatidylserine. *Toxicology*, **148**, 93-101.

Uberall, F., Werner-Felmayer, G., Schubert, C., Grunicke, H. H., Wachter, H. & Fuchs, D. (1994). Neopterin derivatives together with cyclic guanosine monophosphate induce c-fos gene expression. *FEBS Lett*, **352**(1), 11-4.

Upston, J. M., Niu, X., Brown, A. J., Mashima, R., Wang, H., Senthilmohan, R., Kettle, A. J., Dean, R. T. & Stocker, R. (2002). Disease stage-dependent accumulation of lipid and protein oxidation products in human atherosclerosis. *Am J Pathol*, **160**(2), 701-10.

van den Dobbelsteen, D. J., Nobel, C. S., Schlegel, J., Cotgreave, I. A., Orrenius, S. & Slater, A. F. (1996). Rapid and specific efflux of reduced glutathione during apoptosis induced by anti-Fas/APO-1 antibody. *J Biol Chem*, **271**(26), 15420-7.

van der Wal, A. C., Becker, A. E., van der Loos, C. M. & Das, P. K. (1994). Site of intimal rupture or erosion of thrombosed coronary atherosclerotic plaques is characterized by an inflammatory process irrespective of the dominant plaque morphology. *Circulation*, **89**(1), 36-44.

Van Eck, M., Bos, I., T., S., Hildebrand, R. B., Van Rij, B. T. & Van Berkel, T. J. C. (2004). Dual role for scavenger receptor class B, type I on bone marrow-derived cells in atherosclerotic lesion development. *Am J Pathol*, **165**(3), 785-94.

Van Eck, M., De Winther, M. P. J., Herijgers, N., Havekes, L. M., Hofker, M. H., Groot, P. H. E. & Van Berkel, T. J. C. (2000). Effect of human scavenger receptor class A overexpression in bone marrow-derived cells on cholesterol levels and atherosclerosis in apoE-deficient mice. *Arterioscler Thromb Vasc Biol*, **20**(12), 2600-6.

Van Engeland, M., Ramaekers, F. C. S., Schutte, B. & Reutelingsperger, C. P. M. (1996). A novel assay to measure loss of plasma membrane asymmetry during apoptosis of adherent cells in culture. *Cytometry,* **24** (2), 131-9.

Van Engeland, M., Nieland, L. J. W., Ramaekers, F. C. S., Schutte, B. & Reutelingsperger, C. P. M. (1998). Annexin V-affinity assay: A review on an apoptosis detection system based on phosphatidylserine exposure. *Cytometry*, **31**(1), 1-9.

Van Lente, F. (2000). Markers of inflammation as predictors in cardiovascular disease. *Clin Chim Acta*, **293**(1-2), 31-52.

van Reyk, D. M. & Jessup, W. (1999). The macrophage in atherosclerosis: modulation of cell function by sterols. *J Leukoc Biol*, **66**(4), 557-561.

Verhagen, A. M., Ekert, P. G., Pakusch, M., Silke, J., Connolly, L. M., Reid, G. E., Moritz, R. L., Simpson, R. J. & Vaux, D. L. (2000). Identification of DIABLO, a mammalian protein that promotes apoptosis by binding to and antagonizing IAP proteins. *Cell*, **102**(1), 43-53.

Vicca, S., Hennequin, C., Nguyen-Khoa, T., Massy, Z. A., Descamps-Latscha, B., Drueke, T. B. & Lacour, B. (2000). Caspase-dependent apoptosis in THP-1 cells exposed to oxidized low-density lipoproteins. *Biochem Biophys Res Commun*, **273**(3), 948-54.

Vindis, C., Elbaz, M., Escargueil-Blanc, I., Auge, N., Heniquez, A., Thiers, J.-C., Negre-Salvayre, A. & Salvayre, R. (2005). Two distinct calcium-dependent mitochondrial pathways are involved in oxidized LDL-induced apoptosis. *Arterioscler Thromb Vasc Biol*, **25**(3), 639-45.

Vissers, M. C. M., Lee, W.-G. & Hampton, M. B. (2001). Regulation of apoptosis by vitamin C. Specific protection of the apoptotic machinery against exposure to chlorinated oxidants. *J Biol Chem*, **276**(50), 46835-40.

Volf, I., Roth, A., Cooper, J., Moeslinger, T. & Koller, E. (2000). Hypochlorite modified LDL are a stronger agonist for platelets than copper oxidized LDL. *FEBS Lett*, **483**(2-3), 155-9.

Wachter, H., Fuchs, D., Hausen, A., Reibnegger, G. & Werner, E. R. (1989). Neopterin as marker for activation of cellular immunity: immunologic basis and clinical application. *Adv Clin Chem*, **27**, 81-141.

Wachter, H., Fuchs, D., Hausen, A., Reibnegger, G., Weiss, G., Werner, E. R. & Werner-Felmayer, G. (1992). *Neopterin: Biochemistry-Methods-Clinical Application*. Walter de Gruyter, New York.

Wagner, P. & Heinecke, J. W. (1997). Copper ions promote peroxidation of low density lipoprotein lipid by binding to histidine residues of apolipoprotein B100, but they are reduced at other sites on LDL. *Arterioscler Thromb Vasc Biol*, **17**(11), 3338-46.

Walter, D. H., Haendeler, J., Galle, J., Zeiher, A. M. & Dimmeler, S. (1998). Cyclosporin A inhibits apoptosis of human endothelial cells by preventing release of cytochrome c from mitochondria. *Circulation*, **98**(12), 1153-7.

Walter, R., Schaffner, A. & Schoedon, G. (2001). Tetrahydrobiopterin in the vascular system. *Pteridines*, **12**, 93-120.

Wang, Y., Qiao, M., Mieyal, J. J., Asmis, L. M. & Asmis, R. (2006). Molecular mechanism of glutathione-mediated protection from oxidized low-density

lipoprotein-induced cell injury in human macrophages: Role of glutathione reductase and glutaredoxin. *Free Radic Biol and Med,* **41**(5), 775-85.

Warner, G. J., Stoudt, G., Bamberger, M., Johnson, W. J. & Rothblat, G. H. (1995). Cell toxicity induced by inhibition of acyl coenzyme A:cholesterol acyltransferase and accumulation of unesterified cholesterol. *J Biol Chem*, **270**(11), 5772-8.

Waterhouse, N. J., Ricci, J. E. & Green, D. R. (2002). And all of a sudden it's over: mitochondrial outer-membrane permeabilization in apoptosis. *Biochimie*, **84**(2-3), 113-21.

Wayner, D. D. M., Burton, G. W., Ingold, K. U., Barclay, L. R. C. & Locke, S. J. (1987). The relative contribution of vitamin E, urate, ascorbate and proteins to the total peroxyl radical-trapping antioxidant activity of human plasma. *Biochem Biophys Acta*, **924**, 408-419.

Wede, I., Widner, B. & Fuchs, D. (1999). Neopterin derivatives modulate toxicity of reactive species on Escherichia coli. *Free Radic Res*, **31**(5), 381-8.

Weiss, G., Fuchs, D., Hausen, A., Reibnegger, G., Werner, E. R., Werner-Felmayer, G., Semenitz, E., Dierich, M. P. & Wachter, H. (1993). Neopterin modulates toxicity mediated by reactive oxygen and chloride species. *FEBS Lett*, **321**(1), 89-92.

Werner, E. R., Fuchs, D., Hausen, A., Reibnegger, G. & Wachter, H. (1987). Simultaneous determination of neopterin and creatinine in serum with solid-phase extraction and on-line elution liquid chromatography. *Clin Chem*, **33**(11), 2028-33.

Werner, E. R., Werner-Felmayer, G., Fuchs, D., Hausen, A., Reibnegger, G., Yim, J. J., Pfleiderer, W. & Wachter, H. (1990). Tetrahydrobiopterin biosynthetic activities in human macrophages, fibroblasts, THP-1, and T 24 cells. GTP-cyclohydrolase I is stimulated by interferon-gamma, and 6-pyruvoyl tetrahydropterin synthase and sepiapterin reductase are constitutively present. *J Biol Chem*, **265**(6), 3189-92.

Westermann, J., Thiemann, F., Gerstner, L., Tatzber, F., Kozak, I., Bertsch, T. & Kruger, C. (2000). Evaluation of a new simple and rapid enzyme-linked immunosorbent assay kit for neopterin determination. *Clin Chem Lab Med*, **38**(4), 345-353.

Whatling, C., Bjork, H., Gredmark, S., Hamsten, A. & Eriksson, P. (2004). Effect of macrophage differentiation and exposure to mildly oxidized LDL on the proteolytic repertoire of THP-1 monocytes. *J Lipid Res*, **45**(9), 1768-76.

Whitman, S. C., Ravisankar, P., Elam, H. & Daugherty, A. (2000). Exogenous interferon-gamma enhances atherosclerosis in apolipoprotein E-/- mice. *Am J Pathol*, **157**(6), 1819-24.

Whitman, S. C., Sawyez, C. G., Miller, D. B., Wolfe, B. M. & Huff, M. W. (1998). Oxidized type IV hypertriglyceridemic VLDL-remnants cause greater macrophage cholesteryl ester accumulation than oxidized LDL. *J Lipid Res*, **39**(5), 1008-20.

Widner, B., Baier-Bitterlich, G., Wede, I., Wirleitner, B. & Fuchs, D. (1998). Neopterin derivatives modulate the nitration of tyrosine by peroxynitrite. *Biochem Biophys Res Commun*, **248**(2), 341-6.

Widner, B., Mayr, C., Wirleitner, B. & Fuchs, D. (2000). Oxidation of 7,8-dihydroneopterin by hypochlorous acid yields neopterin. *Biochem Biophys Res Commun*, **275**(2), 307-11.

Wilcox, J. N., Smith, K. M., Schwartz, S. M. & Gordon, D. (1989). Localization of tissue factor in the normal vessel wall and in the atherosclerotic plaque. *Proc Natl Acad Sci USA*, **86**(8), 2839-43.

Wilson, A. M., Ryan, M. C. & Boyle, A. J. (2006). The novel role of C-reactive protein in cardiovascular disease: risk marker or pathogen. *Int J Cardiol*, **106**(3), 291-7.

Wintergerst, E. S., Jelk, J., Rahner, C. & Asmis, R. (2000). Apoptosis induced by oxidized low density lipoprotein in human monocyte-derived macrophages involves CD36 and activation of caspase-3. *Eur J Biochem*, **267**(19), 6050-9.

Wirleitner, B., Baier-Bitterlich, G., Bock, G., Widner, B. & Fuchs, D. (1998). 7,8-Dihydroneopterin-induced apoptosis in Jurkat T lymphocytes: a comparison with anti-Fas- and hydrogen peroxide-mediated cell death. *Biochem Pharmacol*, **56**(9), 1181-7.

Wirleitner, B., Czaputa, R., Oettl, K., Bock, G., Widner, B., Reibnegger, G., Baier, G., Fuchs, D. & Baier-Bitterlich, G. (2001). Induction of apoptosis by 7,8-dihydroneopterin: involvement of radical formation. *Immunobiology*, **203**(4), 629-41.

Wirleitner, B., Schroecksnadel, K., Winkler, C. & Fuchs, D. (2005). Neopterin in HIV-1 infection. *Mol Immunol*, **42**(2), 183-94.

Woll, E., Weiss, G., Fuchs, D., Lang, F. & Wachter, H. (1993). Effect of pteridine derivatives on intracellular calcium concentration in human monocytic cells. *FEBS Lett*, **318**(3), 249-52.

Wu, J. T. & Wu, L. L. (2006). Linking inflammation and atherogenesis: Soluble markers identified for the detection of risk factors and for early risk assessment. *Clin Chim Acta*, **366**(1-2), 74-80.

Wuttge, D. M., Zhou, X., Sheikine, Y., Wagsater, D., Stemme, V., Hedin, U., Stemme, S., Hansson, G. K. & Sirsjo, A. (2004). CXCL16/SR-PSOX is an interferon-gamma-

regulated chemokine and scavenger receptor expressed in atherosclerotic lesions. *Arterioscler Thromb Vasc Biol*, **24**(4), 750-5.

Xu, X.-P., Meisel, S. R., Ong, J. M., Kaul, S., Cercek, B., Rajavashisth, T. B., Sharifi, B. & Shah, P. K. (1998). Oxidized low-density lipoprotein regulates matrix metalloproteinase-9 and its tissue inhibitor in human monocyte-derived macrophages. *Circulation*, **99**, 993-998.

Yan, L. J., Lodge, J. K., Traber, M. G. & Packer, L. (1997). Apolipoprotein B carbonyl formation is enhanced by lipid peroxidation during copper-mediated oxidation of human low-density lipoproteins. *Arch Biochem Biophys*, **339**(1), 165-71.

Yancey, P. G. & St Clair, R. W. (1992). Cholesterol efflux is defective in macrophages from atherosclerosis-susceptible white Carneau pigeons relative to resistant Show Racer pigeons. *Arterioscler Thromb Vasc Biol*, **12**, 1291-1304.

Yu, A., Byers, D. M., Ridgway, N. D., McMaster, C. R. & Cook, H. W. (2000). Preferential externalization of newly synthesized phosphatidylserine in apoptotic U937 cells is dependent on caspase-mediated pathways. *Biochim Biophys Acta*, **1487**(2-3), 296-308.

Yuan, X. M., Li, W., Brunk, U. T., Dalen, H., Chang, Y. H. & Sevanian, A. (2000). Lysosomal destabilization during macrophage damage induced by cholesterol oxidation products. *Free Radic Biol Med*, **28**(2), 208-18.

Zamzami, N., Hirsch, T., Dallaporta, B., Petit, P. X. & Kroemer, G. (1997). Mitochondrial implication in accidental and programmed cell death: apoptosis and necrosis. *J Bioenerg Biomembr* **29**(2), 185-93.

Zhang, H., Yang, Y. & Steinbrecher, U. P. (1993). Structural requirements for the binding of modified proteins to the scavenger receptor of macrophages. *J Biol Chem*, **268**(8), 5535-2.

Zhang, H. F., Basra, H. J. & Steinbrecher, U. P. (1990). Effects of oxidatively modified LDL on cholesterol esterification in cultured macrophages. *J Lipid Res*, **31**(8), 1361-9.

Zhang, W., Li, D. & Mehta, J. L. (2004). Role of AIF in human coronary artery endothelial cell apoptosis. *Am J Physiol Heart Circ Physiol*, **286**, H354-8.

Zhao, B., Li, Y., Buono, C., Waldo, S. W., Jones, N. L., Mori, M. & Kruth, H. S. (2006). Constitutive receptor-independent low density lipoprotein uptake and cholesterol accumulation by macrophages differentiated from human monocytes with macrophage-colony-stimulating factor (M-CSF). *J Biol Chem*, **281**(23), 15757-62.

Zhou, X., Paulsson, G., Stemme, S. & Hansson, G. K. (1998). Hypercholesterolemia is associated with a T helper (Th) 1/Th2 switch of the autoimmune response in atherosclerotic apo E-knockout mice. *J Clin Invest*, **101**(8), 1717-25.

Ziouzenkova, O., Sevanian, A., Abuja, P. M., Ramos, P. & Esterbauer, H. (1998). Copper can promote oxidation of LDL by markedly different mechanisms. *Free Radic Biol Med*, **24**(4), 607-23.

Zmijewski, J. W., Moellering, D. R., Goffe, C. L., Landar, A., Ramachandran, A. & Darley-Usmar, V. M. (2005a). Oxidized LDL induces mitochondrially associated reactive oxygen/nitrogen species formation in endothelial cells. *Am J Physiol Heart Circ Physiol*, **289**(2), H852-61.

Zmijewski, J. W., Landar, A., Watanabe, N., Dickinson, D. A., Noguchi, N. & Darley-Usmar, V. M. (2005b). Cell signalling by oxidized lipids and the role of reactive oxygen species in the endothelium. *Biochem Soc Trans*, **33**(6), 1385-9.

Zou, H., Li, Y., Liu, x. & Wang, X. (1999). An APAF-1 cytochrome c multimeric complex is a functional apoptosome that activates procaspase-9. *J Biol Chem*, **274**(17), 11549-65.

ACKNOWLEDGEMENTS

Thanks to my supervisor, Dr. Steven Gieseg, for the constant guidance and support throughout my PhD. I am also grateful to my two co-supervisors, Associate Professor Frank Sin and Dr Drusilla Mason for their advice and support.

Thanks to all the technical staff and secretaries of the School of Biological Sciences. Special thanks in particular to: Ms Jan McKenzie for the supervision of the fluorescence microscope work, Mrs Jackie Healy for assistance with the ultracentrifuge, Mrs Claire Galilee for keeping the lab running smoothly, Mr. Franz Ditz and Mr. Nick Etheridge for maintaining the laboratory equipment, Mr. Gavin Robinson for keeping the laboratory's gas cylinders well stocked and Mr. John Scott for maintaining the computers.

Thank you to the haemochromatosis patients from the New Zealand Blood Service (Riccarton branch) and blood donors at the University of Canterbury. My research will not be possible without the constant blood supply from these two groups. Special thanks to Dr Jinny Willis and Mrs Theresa Madden for bleeding the university blood donors. Thank you to Dr. Mark Hampton and Sarah Cuddihy of the Free Radical Research Laboratory of the Christchurch School of Medicine for the β-actin antibody. Thank you also to Dr Barry Hock of the Department of Hematology for the GM-CSF.

Thanks to all the members or the Free Radical Biochemistry Laboratory especially Linzi, Carole, Anna, Nick, Tina, Hanadi and Elizabeth for the warm encouragement and support through all the good and bad time. Special thanks to Tina and Hanadi for helping me with my works and keeping me accompanied during late night experiments. I really appreciate it and I will treasure our friendship. Thanks also to Professor Barry Hick and Associate Professor Matt Whiteman for the valuable advice.

I express love and thanks to my wonderful families for always believing in me and giving me a moral suppot to go through my PhD. I am so grateful to my husband, Noreffendi, for being patience, supportive and tolerance. I wouldn't be able to go through my PhD without your support throughout the years. My beloved children, Abdul, Aiman, Nadhrah, Iman and Husna, you guys are my inspiration.

Lastly, I am grateful to Tunku Abdul Rahman Sarawak Scholarship Foundation and Univeristi Malaysia Sarawak for financing my PhD studies.

Appendix I

Total mass of LDL = 3 mg /ml which is equivalent to 3 g/L

Molecular weight of LDL = 2.5×10^6 dalton

Therefore [LDL]= $3 / 2.5 \times 10^6 = 1.2 \times 10^{-6}$ M = 1.2 µM

Copper concentration used to oxidize LDL = 300 µM

Therefore, 300/1.2 = 250 Cu/LDL

Total mass of LDL = 0.5 mg /ml which is equivalent to 0.5 g/L

Molecular weight of LDL = 2.5×10^6 dalton

Therefore [LDL]= $0.5 / 2.5 \times 10^6 = 0.2 \times 10^{-6}$ M = 0.2 µM

Copper concentration used to oxidize LDL = 50 µM

Therefore, 50/0.2 = 250 Cu/LDL